



Degree Project in Energy and Climate Studies

Second cycle, 30 credits

Tool to assess the cost of hydrogen considering its supply chain

A case study of Germany, France and Spain until 2030

AFONSO NOLAN RUAS REGO CANHA

PIETRO DOGLIANI



**KTH Industrial Engineering
and Management**

**Master of Science Thesis
Department of Energy Technology
KTH**

**Tool to assess the cost of hydrogen considering its
supply chain: A case study of Germany, France and
Spain until 2030**

TRITA: TRITA-ITM-EX 2022:495 Afonso Canha / Pietro
Dogliani

Afonso Nolan Ruas Rego Canha
Pietro Dogliani

Approved	Examiner Prof. Viktoria Martin	Supervisor Main supervisor: Jagruti Thakur, Phd Co-supervisor: Ahmed Elberry
	Industrial Supervisor Antonius Kies, Magnus Fröberg	Contact person Jagruti Thakur, Phd

Abstract

Hydrogen is envisioned to become a fundamental energy vector within the decarbonization of the energy systems. Despite already being employed in several industries, its production comes almost completely from processes based on fossil fuels. The upcoming challenge towards a hydrogen economy includes the development of low- and zero-carbon processes, the creation of an adequate infrastructure, and the diffusion of new, hydrogen-based applications. Two key factors that will define the success of hydrogen are its sustainability and competitiveness with alternative solutions, e.g., electrification. This study therefore aims at assessing the economic feasibility of hydrogen supply chains, with a focus on their final use in Germany, Spain, and France. The different production methods for each stage (production, transmission and distribution, storage) are discussed and evaluated. Consequently, the entire supply chains are analyzed, comparing domestic production with hydrogen imports from favorable locations. The economic assessment is based on an indicator, the levelized cost of hydrogen, the LCOH.

The study results in an Excel-based tool calculating the LCOH for different supply chains. Different scenarios are developed for each end-use country. In Germany, domestic production is compared with imports, also addressing the need for adequate storage. Blue hydrogen imports from close locations present the lowest LCOH, with values as low as 2.1 €/kg in 2030. This requires pipeline transmission and a monthly storage in depleted natural gas or oil reservoirs. Longer storage durations increase the supply security but also the related costs. In Spain, local, small-scale supply chains are evaluated in opposition to central, larger-scale alternatives. Both configurations are competitive with costs around 3.6 €/kg, suggesting that both supply pathways are feasible. This can spark competition between different players towards a hydrogen economy. In France, domestic hydrogen production via electrolysis is studied, considering different electricity sources, such as the power grid, electricity from nuclear plants and from renewable energy sources. Despite the high interest of France in pink hydrogen, renewables produce the cheapest product, at an LCOH of 4.4 €/kg for onshore wind. If this result is compared to the other two countries, French hydrogen is not competitive. However, the focus on solid oxide electrolysis and novel nuclear technologies might determine a decline in hydrogen costs.

Keywords: Hydrogen, Hydrogen supply chain, LCOH, Hydrogen production, Hydrogen storage, Hydrogen transportation

Sammanfattning

Vätgas är tänkt att bli en grundläggande energivektor i samband med avkolning av energisystemen. Trots att vätgas redan används i flera industrier kommer produktionen av vätgas nästan helt och hållet från processer som bygger på fossila bränslen. Den kommande utmaningen mot en vätgasekonomi inbegriper utveckling av processer med låga eller inga koldioxidutsläpp, skapande av en lämplig infrastruktur och spridning av nya vätgasbaserade tillämpningar. Två nyckelfaktorer som kommer att avgöra vätgasens framgång är dess hållbarhet och konkurrenskraft i förhållande till alternativa lösningar, t.ex. elektrifiering. Denna studie syftar därför till att bedöma den ekonomiska genomförbarheten av vätgasförsörjningskedjor, med fokus på slutanvändning i Tyskland, Spanien och Frankrike. De olika produktionsmetoderna för varje steg (produktion, överföring och distribution, lagring) diskuteras och utvärderas. Följaktligen analyseras hela försörjningskedjorna genom att jämföra inhemsk produktion med import av vätgas från gynnsamma platser. Den ekonomiska bedömningen baseras på en indikator, den genomsnittliga nuvärdesberäknade kostnaden för vätgas, LCOH.

Studien resulterar i ett Excel-verktyg som beräknar LCOH för olika försörjningskedjor. Olika scenarier utvecklas för varje slutanvändarland: i Tyskland jämförs inhemsk produktion med import, där man också tar hänsyn till behovet av lämplig lagring. Import av blå väte från närliggande platser ger de lägsta LCOH-värdena, med värden så låga som 2.1 €/kg år 2030. Detta kräver överföring via rörledningar och en månatlig lagring i uttömda naturgas- eller oljereserver. Längre lagringstider ökar försörjningstryggheten men också de relaterade kostnaderna. I Spanien utvärderas lokala, småskaliga försörjningskedjor i motsats till centrala, storskaliga alternativ. Båda konfigurationer är konkurrenskraftiga med kostnader på omkring 3.6 €/kg, vilket tyder på att båda försörjningsvägarna är genomförbara. Detta kan utlösa konkurrens mellan olika aktörer i riktning mot en vätgasekonomi. I Frankrike studeras inhemsk vätgasproduktion via elektrolys med hänsyn till olika elkällor, t.ex. elnätet, el från kärnkraftverk och förnybara energikällor. Trots Frankrikes stora intresse för rosa vätgas är det förnybara energikällor som producerar den billigaste produkten, med en LCOH på 4.4 €/kg för landbaserad vindkraft. Om detta resultat jämförs med de andra två länderna är fransk vätgas inte konkurrenskraftig. Fokuseringen på SOEC-teknik och ny kärnkraftsteknik kan dock leda till att vätgaskostnaderna sjunker.

Nyckelord: Vätgas, Vätgas försörjningskedjan, LCOH, Vätgasproduktion, Vätgaslagring, Vätgastransport

Acknowledgements

We would like to thank our KTH supervisor Jagruti Thakur for her help and guidance throughout this thesis. We would also like to express our gratitude to Ahmed Elberry, who was a fundamental addition and supported us with insightful help and tips. Thanks also to Viktoria Martin for being the examiner of this thesis.

We would also like to thank Antonius Kies and Magnus Fröberg, our supervisors at Scania. Their guidance was essential to push us to realize this work. Our exposure in the company was vital: the frequent presentations motivated us to give our best, so we would also like to extend our gratitude to all the people at Scania that always provided us with valuable feedback.

Last but not least, we would like to thank our families and friends, who always supported us during our Master, especially in this hectic last semester.

List of abbreviations

AEL	Alkaline Electrolyzer
AEM	Anion Exchange Membrane
AGR	Annual Growth Rate
AWE	Alkaline Water Electrolysis
BEV	Battery Electric Vehicle
BoP	Balance Of Plant
CAPEX	Capital Expenses
CCS	Carbon Capture and Storage
EPR	European Pressurized Reactor
ETS	Emission Trading System
EU	European Union
FCEV	Fuel-Cell Electric Vehicle
gH₂	Gaseous Hydrogen
GHG	Greenhouse Gases
HDV	Heavy-Duty Vehicles
HHV	Higher Heating Value
HRS	Hydrogen Refueling Station
HTGR	High Temperature Gas Reactor
LCOE	Levelized Cost Of Electricity
LCOH	Levelized Cost Of Hydrogen
LH₂	Liquid Hydrogen
LHV	Lower Heating Value
LNG	Liquid Natural Gas
LOHC	Liquid Organic Hydrogen Carriers
LR	Learning Rate
MoU	Memorandum Of Understanding
NG	Natural Gas
NH₃	Ammonia
OPEX	Operating Expenses
PEM	Proton Exchange Membrane
PSA	Pressure Swing Adsorption
RE	Renewable Energy
SEC	Specific Energy Consumption
SMR	Steam Methane Reforming
SOE	Solid Oxide Electrolysis
SOEC	Solid Oxide Electrolyzer Cell
STP	Standard Temperature and Pressure
TCO	Total Cost of Ownership
T&D	Transmission And Distribution

Table of contents

Abstract	ii
Sammanfattning	iii
Acknowledgements	iv
List of abbreviations	v
List of Tables.....	vii
List of Figures.....	viii
1. Introduction	12
2. Literature review.....	13
3. Research objective and questions	16
3.1 Scope and limitations.....	16
4. Background.....	18
4.1 Production	19
4.2 Storage.....	25
4.3 Conversion.....	33
4.4 Transmission and distribution	34
4.5 Hydrogen economy and policy framework	36
5. Methodology	42
5.1 Definition of Levelized Cost of Hydrogen.....	42
5.2 The Excel tool.....	43
5.3 Other key concepts	44
5.4 Production	47
5.5 Storage.....	58
5.6 Conversion.....	72
5.7 Transmission and distribution	95
5.8 Scenarios	101
6. Results and discussion	104
6.1 Production	104
6.2 Transmission and distribution	114
6.3 Storage.....	116
6.4 Conversion and reconversion	128
6.5 Overall supply chain	130
7. Contribution to sustainability	142
8. Conclusion	143
9. Bibliography.....	145
Appendix	163
Appendix I.....	163

Appendix II.....	164
Appendix III.....	165
Appendix IV.....	166
Estimates for gas well upstream cost.....	166
Appendix V.....	171
Appendix VI.....	173
Appendix VII.....	174
Appendix VIII.....	175

List of Tables

Table 1: Advantages and disadvantages of diesel, battery, and fuel cell powertrains. Adapted from [7].....	19
Table 2: Color codes for hydrogen production. Adapted from [42].	19
Table 3: Summary of the main technical parameters, maturity level, advantages and disadvantages of four different electrolyzer technologies. Adapted from [13], [47].	22
Table 4: Thermochemical properties of different fuels.	25
Table 5: Operational geological reservoirs for NG storage.	32
Table 6: Repurposing potential of geological storage for H2 storage (NG->H2).....	32
Table 7: Exchange rate for currencies found in literature, 2021 average, quoted against the euro [157].	45
Table 8: Electrical efficiency for different electrolyzer technologies [47]. Similar values can be found in [3], [162].....	48
Table 9: Electrolyzer costs in 2021, 1 MW capacity [164]. Similar values can be found in [3], [47], [165].	49
Table 10: Learning rates and indexes for different electrolyzer technologies [164].....	49
Table 11: Main parameters to assess economy-of-scale effects on electrolyzer CAPEX [160].	51
Table 12: Stack lifetime for different electrolyzer technologies [3], [162].....	51
Table 13: Renewable electricity sources, general data [171]. Similar values can be found in [172]. ..	52
Table 14: Renewable electricity sources, learning effect data concerning capital costs. Own elaboration from [173]–[175].	52
Table 15: Capital expenses for a SMR reference plant (300 MW _{H₂,LHV} in 2021) [9]. Similar values in [3], [180], [181].	54
Table 16: Learning and scaling factors for different components of a SMR plant.	54
Table 17: CO ₂ transportation-and-storage costs for different locations [183]. Similar values in [184], [185].	56
Table 18: Electricity consumption of a SMR plant, for the three different modes considered [9]. ..	56
Table 19: Hydrogen storage for different time durations.....	59
Table 20: Hydrogen gas density per type of storage tank.....	60
Table 21: Hydrogen gas density per type of geological reservoir.	60
Table 22: Maximum design volume per type of storage tank [193].	61
Table 23: Economic parameters for each type of storage tank.	62
Table 24: Cost performance of tank storage.	62
Table 25: Minimum and maximum design volume per type of geological reservoir.....	63
Table 26: Fixed operating costs per type of storage tank.....	64
Table 27: Fixed operating costs per type of geological reservoir.....	64
Table 28: Financial parameters for each type of storage tank.....	65
Table 29: Financial parameters for each type of geological reservoir.	66

Table 30: Maximum design capacity per type of cryogenic tank	68
Table 31: Economic parameters for each type of cryogenic tank located in the export terminal.	69
Table 32: Economic parameters for each type of cryogenic tank located in the import terminal. ...	69
Table 33: Fixed operating costs per type of cryogenic tank located in the export terminal.	70
Table 34: Fixed operating costs per type of cryogenic tank located in the import terminal.	70
Table 35: Relation between the number of cycles per year in the tank and the storage time duration at the harbor.	71
Table 36: Financial parameters for each type of cryogenic tank for the export and import terminal.	72
Table 37: Capacity flow rate of the compression station per type of application.	73
Table 38: Economic parameters for a generalized multi-stage compressor.	75
Table 39: Financial parameters for a generalized multi-stage compressor.	78
Table 40: Economic parameters for each type of liquefaction plant.	81
Table 41: Collected data for hydrogen liquefaction plant's specific energy consumption (SEC) for different plant sizes.....	82
Table 42: Thermophysical properties of hydrogen at the beginning and end of the hydrogen liquefaction plant [214].....	83
Table 43: Financial parameters for each hydrogen liquefaction plant.....	84
Table 44. Collected data on the uninstalled cost of the hydrogen regasification plant with varying plant capacities [89].....	85
Table 45: Economic parameters for the hydrogen regasification plant.	86
Table 46: Financial parameters for a hydrogen regasification plant.	87
Table 47: Equilibrium percent concentrations of ammonia at various temperatures and pressures [225].	89
Table 48: Economic parameters for the ammonia production plant.	90
Table 49: <i>Specific energy consumption in the ammonia production plant.</i>	91
Table 50: Fixed operating costs of the ammonia production plant.....	91
Table 51: Financial parameters for the ammonia production plant.	92
Table 52: Economic parameters for the ammonia reconversion plant.	93
Table 53: Specific energy consumption in each stage of the ammonia reconversion plant.	94
Table 54: Technical and financial parameters for the ammonia reconversion plant.	95
Table 55: New and repurposed (rep.) onshore pipeline parameters. Data from [94], [108] and own calculations.	96
Table 56: General parameters for pipelines.	96
Table 57: General shipping parameters.....	99
Table 58: General truck parameters. Internal assumptions and [100], [237], [238].	100
Table 59: Truck parameters dependent on the annual mileage. Internal assumptions.....	100
Table 60: RE locations and corresponding capacity factors.	163
Table 61: Projection of commodity prices until 2030.....	165
Table 62: Economic parameters for each type of geological reservoir.	171
Table 63: Pressure and temperature for each type of applications.	173
Table 64: Transmission by ship, in km [233], [234].	174
Table 65: Transmission by offshore pipeline, in km [231], [232].	174
Table 66: Transmission by onshore pipeline, in km [231], [232].	174

List of Figures

Figure 1: Tool scope and possible hydrogen supply pathways.	16
Figure 2: Countries considered in the research with related hydrogen-production methods.....	17
Figure 3: Hydrogen demand mix in 2020. Elaboration from [39].	18

Figure 4: Conventional SMR plant layout [9].	20
Figure 5: Simplified SMR plant layout, with three feasible CO ₂ capture locations [9].	21
Figure 6: Scheme of the operating principle of an alkaline electrolysis cell [46].	23
Figure 7: Scheme of the operating principle of a PEM electrolysis cell [46].	23
Figure 8: Scheme of the operating principle of an AEM electrolysis cell [47].	24
Figure 9: Scheme of the operating principle of a solid oxide electrolysis cell [46].	24
Figure 10: Hydrogen supply chain in the transportation sector [52].	25
Figure 11: Schematic views of a) direct brine circulation method and, b) reverse brine circulation method [76].	29
Figure 12: Hydrogen storage potential of salt caverns in Europe [80].	31
Figure 13: Snapshot of the top part of the Home sheet in the Excel tool.	44
Figure 14: Electrolyzer global capacity projections. Own elaboration based on [47], [105], [166]–[168].	50
Figure 15: SMR modes, with related CO ₂ emissions and natural gas need. Own elaboration, data from [9]. Similar data and configurations in [180], [181].	53
Figure 16: Classification of the different cases with respect to their capacity and time duration of each cycle.	58
Figure 17: General diagram representing the relation between loading time and the storage time duration in the tank/reservoir.	59
Figure 18: General diagram of intermediate storage in the hydrogen supply chain.	67
Figure 19: Considered end use applications that integrate a compressor station.	72
Figure 20: Type of compressor selection based on mass flow rate and discharge pressure [205].	73
Figure 21: General diagram of a conventional liquefaction plant [210].	79
Figure 22: General diagram of the proposed liquefaction plant [210], [214].	80
Figure 23: Liquefaction plant performance: SEC as a function of the liquefaction plant capacity.	82
Figure 24: Ideal liquefaction temperature-entropy diagram [192].	83
Figure 25: Block diagram of a general hydrogen regasification plant.	85
Figure 26: Hydrogen regasification plant uninstalled cost as a function of the respective plant capacity.	85
Figure 27: General diagram of the ammonia production plant.	88
Figure 28: Detailed overview of the ammonia production plant.	88
Figure 29: Detailed overview of the H-B process.	88
Figure 30: General diagram of the ammonia reconversion plant.	93
Figure 31: Scenario flowchart for Germany.	102
Figure 32: Scenario flowchart for Spain.	102
Figure 33: Scenario flowchart for France.	103
Figure 34: Levelized cost of electricity from solar PV in 2022 and 2030, for selected locations.	104
Figure 35: Levelized cost of electricity from onshore wind in 2022 and 2030, for selected locations.	105
Figure 36: Levelized cost of electricity from offshore wind in 2022 and 2030, for selected locations.	105
Figure 37: Comparison between the calculated LCOE in Germany and values from the literature, for different RES [15], [171], [172], [242].	105
Figure 38: Impact of scaling effects on the CAPEX of an electrolyzer system (stack + auxiliary components) in 2022.	106
Figure 39: Impact of learning effects on the CAPEX of a 1 MW electrolyzer system (stack + auxiliary components).	107
Figure 40: LCOH _p via electrolysis (1-MW _{el} system) with varying electricity price in 2022 and 2030.	108
Figure 41: LCOH _p via electrolysis with fixed electricity price at 8 c€/kWh _{el} .	108
Figure 42: SMR configuration comparison in 2022 with varying gas and carbon prices. Cheapest configuration (left) and its LCOH isolines (left).	109

Figure 43: SMR configuration comparison in 2030 with varying gas and carbon prices. Cheapest configuration (left) and its LCOH isolines (left).....	109
Figure 44: Levelized cost of hydrogen production for different SMR configurations and pyrolysis in 2022 and in 2030. If not indicated otherwise, carbon price fixed at 100 €/t _{CO2}	110
Figure 45: Levelized cost of hydrogen production in Germany, from 2022 to 2030.	111
Figure 46: Levelized cost of hydrogen production via electrolysis from solar PV electricity in Spain. Comparison between a small-scale (1 MW _{el}) and a large-scale (100 MW _{el}) plant.	111
Figure 47: Levelized cost of hydrogen production via electrolysis in France, from 2022 to 2030..	112
Figure 48: LCOH _p for green hydrogen production in different countries, with reference to a 100-MW PEM electrolyzer in 2022 and in 2030.	112
Figure 49: Gas and carbon prices (left) and LCOH _p for SMR by component in Europe.	113
Figure 50: LCOH _p for SMR in Europe and gas-producing countries.	113
Figure 51: LCOH _p for pyrolysis in Europe and gas-producing countries.	114
Figure 52: Comparison between LCOH _p for SMR and for pyrolysis in Europe and in Qatar.	114
Figure 53: Comparison of transmission options with varying route distance.	115
Figure 54: Comparison of distribution options with varying route distance.	116
Figure 55: Variation of the levelized cost of hydrogen final storage with respect to the production plant's capacity.	117
Figure 56: Variation of the CAPEX with respect to the production plant's capacity.	117
Figure 57: Compilation of three graphs representing the variation of the levelized cost of hydrogen final storage, CAPEX, and number of geological reservoirs in the considered underground storage facility with maximum design volume with respect to the desired volume of the reservoir, in other words the total volume of hydrogen to be stored. Case of seasonal storage in salt caverns.	119
Figure 58: Compilation of three graphs representing the variation of the levelized cost of hydrogen final storage, CAPEX, and number of geological reservoirs in the considered underground storage facility with maximum design volume with respect to the desired volume of the reservoir, in other words the total volume of hydrogen to be stored. Case of seasonal storage in depleted NG or oil reservoirs.....	120
Figure 59: Compilation of three graphs representing the variation of the levelized cost of hydrogen final storage, CAPEX, and number of geological reservoirs in the considered underground storage facility with maximum design volume with respect to the desired volume of the reservoir, in other words the total volume of hydrogen to be stored. Case of seasonal storage in lined rock caverns.	121
Figure 60: CAPEX versus volume storage in salt caverns.	122
Figure 61: a) Top graph shows the CAPEX variation of hydrogen storage in salt caverns with the hydrogen production plant capacity. b) Bottom graph shows the variation of the levelized cost of final storage of hydrogen in salt caverns with the hydrogen production plant.....	123
Figure 62: a) Top graph shows the CAPEX variation of hydrogen storage in lined rock caverns with the hydrogen production plant capacity. b) Bottom graph shows the variation of the levelized cost of final storage of hydrogen in lined rock caverns with the hydrogen production plant capacity.	124
Figure 63: Amount of hydrogen that it is being stored in the pressurized tanks for the case of daily, weekly, and monthly storage for each of the hydrogen production plant's capacity considered.	125
Figure 64: Volume of hydrogen that it is being stored in each type of pressurized tank for the case of daily, weekly, and monthly storage for each of the hydrogen production plant's capacities considered.....	125
Figure 65: Impact of the amount of hydrogen to be stored on the levelized cost of hydrogen storage in each type of storage tank for the case of daily, weekly, and monthly storage.	127
Figure 66: Variation of the levelized cost of (re)conversion processes with respect to different plant's size capacities.	129

Figure 67: Variation of the cost of initial capital expenditures for each considered hydrogen conversion and reconversion process with respect to different plant's size capacities.	129
Figure 68: Variation of the specific energy consumption (SEC) of each (re)conversion process with respect to different plant's size capacities.....	129
Figure 69: Relation between hydrogen liquefaction plant capacities and respective plant's efficiency.	130
Figure 70: Levelized cost of hydrogen compression a) with varying compressor's discharge pressure (left graph) and b) with varying compressor's capacity flow rate (right graph).	130
Figure 71: Levelized cost of hydrogen for domestic supply chains in Germany, in 2022.	131
Figure 72: Levelized cost of hydrogen for domestic supply chains in Germany, in 2022.	132
Figure 73: Levelized cost of hydrogen for green hydrogen imports to Germany, in 2022.	133
Figure 74: Levelized cost of hydrogen for green hydrogen imports to Germany, in 2030.	134
Figure 75: Levelized cost of hydrogen for blue hydrogen imports to Germany, in 2022.	135
Figure 76: Levelized cost of hydrogen for blue hydrogen imports to Germany, in 2030.	135
Figure 77: Levelized cost of hydrogen for relevant scenarios in Germany, in 2022 and in 2030....	136
Figure 78: Levelized cost of hydrogen domestically produced in Germany and distribution by truck, in 2030.	137
Figure 79: Levelized cost of hydrogen imported from Algeria, transmission by pipeline and distribution by truck, in 2030.....	138
Figure 80: Levelized cost of hydrogen from electrolysis powered with solar electricity in Spain, in 2022.....	139
Figure 81: Levelized cost of hydrogen from electrolysis powered with solar electricity in Spain, in 2030.....	139
Figure 82: Levelized cost of hydrogen domestically produced via electrolysis in France and delivered by truck, in 2022.	140
Figure 83: Levelized cost of hydrogen domestically produced via electrolysis in France and delivered by truck, in 2030.....	141
Figure 84: Graphical description of the Excel tool.	164
Figure 85: Comparison between own LCOE in France and values from the literature, for different RES [15], [171], [172], [256].....	175
Figure 86: Comparison between own LCOE in Spain and values from the literature, for different RES [15], [172].	175
Figure 87: Comparison between own CAPEX projections for alkaline electrolyzer and values from the literature [3], [47], [162], [165], [257]–[259].....	176
Figure 88: Comparison between own CAPEX projections for PEM electrolyzer and values from the literature [3], [47], [162], [165], [257]–[261].....	176
Figure 89: Comparison between own CAPEX projections for PEM electrolyzer and values from the literature [3], [165], [257].....	176
Figure 90: Comparison between own LCOH _p in Germany and values from the literature, for electrolysis and different RES [2], [37], [262], [263].	177
Figure 91: Comparison between own LCOH _p in France and values from the literature, for electrolysis and different RES [37], [262], [263].	177
Figure 92: Comparison between own LCOH _p in Spain and values from the literature, for electrolysis and different RES [37], [262], [263].	178
Figure 93: Comparison between own LCOH _p in Algeria and values from the literature, for electrolysis and different RES [3], [37], [132], [264].	178
Figure 94: Comparison between own LCOH _p in Chile and values from the literature, for electrolysis and different RES [2], [37], [93], [263], [265].	178
Figure 95: Comparison between own LCOH _p in Australia and values from the literature, for electrolysis and different RES [2], [37], [263], [266].	179
Figure 96: Comparison between own LCOH _p in Saudi Arabia and values from the literature, for electrolysis and different RES [2], [37].	179

1. Introduction

With the rising concern to limit global warming to 1.5°C, countries around the world are facing an unprecedented challenge. To fulfill their commitments in the framework of the Paris agreement, a deep and fast transition is needed, involving all sectors and systems [1]. A multidimensional approach is thus needed, and the interest in alternative solutions to fossil fuels has been rapidly growing. High hopes have been put in hydrogen as an energy carrier that can easily adapt to the flexible needs of different applications and can be produced from zero- and low-carbon sources. Specifically, its potential to decarbonize hard-to-abate sectors gives it a central role in the efforts toward decarbonized energy systems. Despite technological advances and cost reductions, the path to its competitiveness and large-scale deployment remains unclear [2].

Nowadays, hydrogen is mainly used as a reagent in several industrial processes. The demand for its pure form is around 90 Mt per year, with its two largest uses being ammonia production and fossil fuel refining [3]. Current hydrogen production is mainly based on fossil fuels: 49% of global hydrogen is derived from natural gas; 28% from oil; 18% from coal; only 4% via water electrolysis [4]. This translates into 900 Mt of carbon dioxide (CO₂) emitted per year [3]. The future increase in hydrogen demand requires a shift of its production to cleaner processes. Namely, water electrolysis powered with renewable electricity, pyrolysis, and conventional methods coupled with carbon capture and storage (CCS) technologies have the largest potential. Biomass-based and biological methods are still in earlier phases but might also be promising alternatives [3].

Low- and zero-carbon hydrogen is seen as a plausible alternative to fossil fuels in many hard-to-abate and carbon-intensive sectors. Among these, transportation became the largest energy-consuming end-use sector in 2017, with its CO₂ emissions contributing to almost one quarter of the total GHG emissions [5]. The challenge to decarbonize this sector lies in implementing innovative and renewable technologies that are economically and operationally feasible. It has been demonstrated that hydrogen can be particularly interesting for the heavy transportation segments, given its technical properties. With reference to road transportation, several factors (e.g., vehicle performance, infrastructure size, traditional pollutants) suggest the importance to prioritize heavy-duty vehicles (HDVs) in the first phases of the hydrogen deployment [6]. Within this segment, hydrogen fuel-cell electric vehicles (FCEVs) will compete with conventional diesel engine vehicles and battery electric vehicles (BEVs). In the short term, diesel HDVs will still dominate the market. However, FCEVs and BEVs can gradually replace the conventional fleet due to their low or zero emissions. BEVs have a high efficiency but lack in energy density; FCEVs have higher specific energy but lack in existing infrastructure and require a high capital [7].

Since HDVs are usually considered as working equipment, the total cost of ownership (TCO; sum of investment and operational costs) is a common term of comparison among different options. The energy component has a significant weight in the TCO, and its detailed study has primary importance in properly assessing and planning the current and future hydrogen economy. This thesis hence aims at investigating the hydrogen cost throughout its whole supply chain in Germany, France, and Spain.

2. Literature review

Hydrogen is an energy vector with important properties that make it a key prospect in future energy systems. It can be produced from zero- and low-carbon sources, then stored, transported, used as a fuel, and/or converted to electricity. This and other properties make it the logical replacement for fossil fuels, and the ideal complementary carrier to electricity [8]. Currently, the potential of hydrogen in many applications is well-known. However, their actual implementation on a large scale is still in the early phases. In fact, hydrogen is still not competitive with the conventional alternatives. For this reason, the literature often focused on the supply side, from production to distribution, analyzing the technical, economic, and environmental aspects. The creation of an optimal, reliable supply chain is paramount to establish a clean hydrogen market.

Starting from the production side, Kayfeci *et al.* [4] give a detailed overview of hydrogen production methods, dividing them into five large categories:

- Hydrogen from fossil fuels (e.g., coal gasification, steam reforming)
- Hydrogen from water splitting (e.g., electrolysis, thermolysis)
- Biomass-based hydrogen
- Biological hydrogen
- Hydrogen recovery from waste gas stream

It is worth mentioning that these production methods are at very different levels of maturity: some are established industrial processes, while others are in very early phases. As stated earlier, 96% of the global hydrogen is derived from fossil fuels [4]. The necessity to switch to cleaner methods of production has been supported by a wide literature. Two main fields of research can be identified: improvements to conventional production processes, and the development of alternative methods. In the first category, the focus has been on the possibility to couple the leading technology for H₂ production, steam methane reforming (SMR), with carbon capture and storage (CCS). Collodi *et al.* [9], Roussanaly *et al.* [10], and Meerman *et al.* [11] carry out techno-economic analyses that show the technical feasibility of SMR and CCS coupling. However, they also show the current economic disadvantages of this production method. In particular, Collodi *et al.* [9] conclude that, depending on the CCS technology, a capture rate ranging between 53% and 90% translates into a LCOH increase between 18% and 45%, and a CO₂ emission avoidance cost between 47 and 70 €/t_{CO2}. Despite the high production costs, Navas-Anguita *et al.* [12] show how SMR with CCS can be a short-medium term solution before the uptake of electrolysis methods. Specifically, the authors examine the hydrogen demand for Spanish transportation, demonstrating that SMR with CCS could satisfy a similar market in a transitory period.

Among the alternative H₂ production methods, only water electrolysis achieved an advanced readiness level. Chi and Yu [13] compare the different water electrolysis processes from a technical standpoint: alkaline water electrolysis (AWE), anion exchange membrane (AEM) electrolysis, solid oxide electrolysis (SOE), and proton exchange membrane (PEM) electrolysis. Saba *et al.* [14] instead analyze alkaline and PEM electrolyzer systems from an economic perspective, examining their capital expenses (CAPEX) and their learning curves. The currently more expensive PEM electrolyzers are approaching the alkaline costs: estimations of investment costs in 2030 are within a range of 397-955 €/kW for PEM, 787-906 €/kW for alkaline. Janssen *et al.* [15] show that a reduction in electrolyzer cost is vital for PV-hydrogen projects: they focus on off-grid electricity systems for hydrogen production across Europe. Hybrid solar-wind systems have the lowest production costs in Europe, followed by onshore wind. The study also shows that a reduction in electrolyzer cost is vital for PV-hydrogen projects. In general, the current LCOH (2.1-15 €/kg_{H2}) is forecasted to rapidly decrease to 1.6-8.4 €/kg_{H2} in 2050.

The transportation of hydrogen is often regarded as the most challenging part of its supply chain: its physical properties lead to engineering, safety, and monetary complexity. In fact, its inherent low density

(0.09 kg/m³ at Standard Temperature and Pressure, STP, conditions¹) requires large volumes for its transportation. Compared to natural gas (0.7-0.9 kg/m³ at STP), it requires a volume about 9 times larger to transport the same mass. This translates to hydrogen having around 30% of the volumetric energy content of natural gas [16], [17]. Additionally, hydrogen causes embrittlement in high strength materials, leading to a decrease in their mechanical properties, and its low molecular density can lead to leakages in regular metal containers [18]. For these reasons, the conversion of hydrogen to different states of matter or even different molecules has been considered as a possible solution to its transportation difficulties. In literature there has been an extensive assessment of several mediums, namely liquified hydrogen (LH₂), ammonia (NH₃), and liquid organic hydrogen carriers (LOHC). LH₂ has a high volumetric energy density (0.08-0.09 MJ/m³), about twice higher than compressed hydrogen at 700 bar (0.04-0.05 MJ/m³). However, the main constraint is the extremely low temperature needed, below -253°C [19]. Ammonia has instead a much higher liquefaction temperature, around -33°C, which makes it more efficient and cheaper to maintain in a liquid state. Moreover, ammonia supply chains have been well proven and consolidated, given its wide use in the fertilizer industry [20]. LOHCs have also been investigated as a feasible option, given their stability at standard conditions and their compatibility with current fuel infrastructure [21].

In addition to the physical and technical studies of these options, researchers also compared their economies to determine the most cost-effective and advantageous solution. The distance and volume usually influence the choice of the analyzed transportation methods: for transmission (longer distances and larger volumes), shipping and pipelines; for distribution, trucks and pipelines. The International Energy Agency (IEA) [3] compares different transmission carriers and modes, concluding that the cheapest option is highly dependent on the distance, and even more importantly, on the additional costs of conversion and reconversion. Over shorter distances, Demir and Dincer [22] determine that pipelines are a feasible solution with larger hydrogen quantities, while compressed gas delivery by truck becomes more attractive with lower volumes. Some authors took their work even further, comparing energy transportation via hydrogen and electricity [23]–[25]. The conclusions are not univocal, but they all emphasize the necessity for the development of both ones to achieve lower carbon-intensive energy systems.

In literature, hydrogen storage is studied either as part of the hydrogen supply chain or, more often, as individual techno-economic investigations, given the high level of complexity of energy storage systems. An IEA hydrogen working group developed an important study on the hydrogen value chain [3]. Variables such as volume, duration of storage, speed of discharge, and geographic availability usually determine the type of storage technology most suitable for a certain application [3]. Due to the very low density of hydrogen at STP conditions (0.09 kg/m³), hydrogen is often considered to be stored by increasing its pressure or by changing it from gaseous form to liquid form [26]. Moreover, the conversion of hydrogen into other chemical compounds with better chemical properties such as ammonia and LOHCs has often been analyzed [3]. Abdin *et al.* [27] point out the fact that converting hydrogen to ammonia and methanol can be a good opportunity to reduce infrastructure costs given the already existing liquid fuel infrastructure that can be easily adapted to accommodate such energy mediums. The same reasoning works for the case of LOHCs [3].

For large-scale and long-term storage applications, hydrogen is often considered to be optimally stored in geological reservoirs [3]. Tietze *et al.* [28] have performed a technical study on the gaseous storage of hydrogen and natural gas in salt caverns by performing a thermodynamic simulation. They concluded that there are no obstacles in storing hydrogen in salt caverns from the perspective of thermodynamics. The HyUnder project, a million euro investigation project supported by the European Union, looked into the feasibility of storing gaseous hydrogen in salt caverns [29]. The methodology used for this work is based on two modules, a static module, and a dynamic module. The static module assesses the operating feasibility of salt caverns based on annual values, whereas the dynamic module considered an hourly framework for the feasibility study [30]. The study delivers valuable results when considering economic

¹ STP conditions: 0°C, 1 atm

analysis of underground storage facilities. However, it also concludes that underground hydrogen storage is still not economically attractive for energy produced from renewable sources [31].

Van Leeuwen *et al.* [32, p. 3] mention that aboveground storage is fifty times more expensive than underground storage, with cost estimates ranging respectively around 15 and 0.3 \$/kWh. R. Tarkowski [31] ranks the main underground hydrogen storage technologies in terms of initial capital expenditures. The depleted natural gas or oil reservoirs are the cheapest technology with a specific cost of 1.23 \$/kg. They are followed by aquifers, at 1.29 \$/kg, then salt caverns, at 1.61 \$/kg, and, finally, hard rock caverns at 2.77 \$/kg. In general however, it is very difficult to make a direct comparison between results of different studies on the specific costs of underground hydrogen storage, because they tend to differ a lot on the assumptions considered and the data and methodologies used [30] [33]. Mayer *et al.* [34] suggest that there is no standard metric for calculating the levelized cost of energy storage contrasting with energy generation technologies that are commonly assessed by the levelized cost of energy.

Some studies also tried to investigate the supply chain as a whole, combining the different stages just described. Two different approaches have been usually employed: optimization and linear modelling. Stockl *et al.* [35] optimize and compare large- and small-scale hydrogen production with grid electricity. The study shows that small-scale on-site electrolysis is the most beneficial with low shares of renewable energy in the electricity mix and low hydrogen demand. For higher renewable shares or higher hydrogen demand, large-scale production becomes more interesting. In particular, LH₂ results to be the best solution with these settings, thanks to favorable efficiency, flexibility, and investment costs. Almansoori and Shah [36] set up a similar optimization problem, although considering only conventional methods for hydrogen production. The optimal supply chain results in the combination of the following steps: medium-to-large, centralized SMR plants, distributed via LH₂ tanker trucks and stored in centralized storage sites. A linear approach is instead followed by Brändle *et al.* [37], that estimate the hydrogen supply cost until 2050. They conclude that in the medium term SMR will be the cheapest option. However, hydrogen from electrolysis could become competitive in the long term, with production cost below 1 \$/kg in some regions. To transport such hydrogen to Europe, retrofitting natural gas pipelines would provide the opportunity for a low-cost transportation method, especially compared to shipping options. The authors conclude that these would lead to the development of a regional market, rather than a global exchange.

3. Research objective and questions

This research aims at investigating the future hydrogen cost, considering its whole supply chain, from production to final distribution. The study focuses on Germany, France, and Spain, studying different options and locations to produce, store, and transport hydrogen.

The following research questions are identified:

- What is the cost range for each stage (production, transportation, storage) of the hydrogen supply chain?
- What is the cost range for the different hydrogen supply pathways, considering a final use for transportation in Germany, France, and Spain?
- What is the comparative advantage in terms of cost while producing locally versus importing hydrogen?
- What is the cost impact of some critical factors (learning effects; production capacity; electricity, gas, and carbon prices; transportation distances; storage size) in the hydrogen supply chain and its different stages?

3.1 Scope and limitations

The study investigates the current and future hydrogen supply chain by developing an Excel tool, then applying it to specific case studies. To discuss the scope and limitations of the research, it is hence essential to make a distinction between those for the general Excel tool, and those for the specific pathways of interest. Starting with the former, the geographical scope is undefined, given the universality of the tool. In fact, only the input parameters influence the result with information about the location, not the structure and the formulas, which are instead geographically neutral. The tool considers an 8-year timespan, from 2022 to 2030. The technologies and the possible pathways that the tool encompasses are depicted in Figure 1. The final state of hydrogen can either be gaseous hydrogen (gH₂) at a set pressure (300 bar in this analysis), liquid hydrogen (LH₂), or ammonia (NH₃). The specific discussion about the single stages and the combination of different technologies is presented in Section 4 and its subsections.

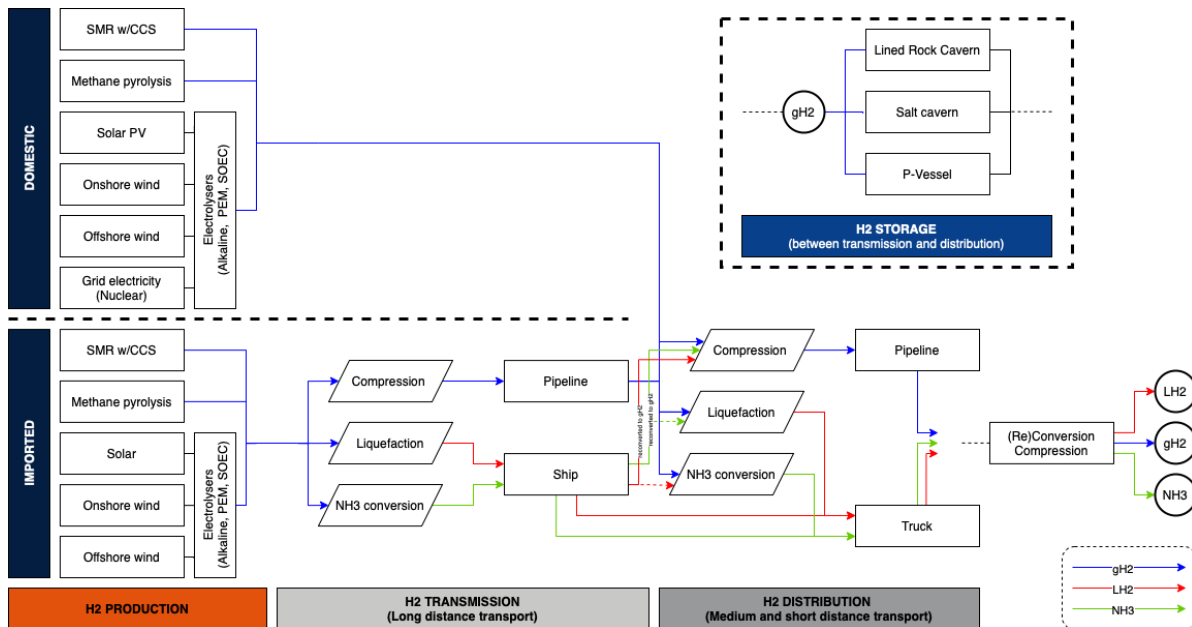


Figure 1: Tool scope and possible hydrogen supply pathways.

The proposed model does not provide a clear indication of the forecasted hydrogen price since it considers only the supply side. The main limitation concerns therefore uncertainty about economy of scale considerations: without a defined demand side, the sizing and typology of the infrastructure are not

optimized. In fact, the type of final use and its extent influence investment decisions and costs. To partially overcome this limitation, some assumptions and educated guesses are introduced, considering country-specific strategies, targets, and demand forecasts. Moreover, given the quasi-static nature of the research (i.e., no hourly resolution, no dynamic analysis of the supply chain), the sizing of the storage cannot be directly calculated. However, the storage size can be approximated based on demand projections, and national and commercial plans.

The model is then applied to three specific countries: Germany, France, and Spain. These three European countries have been selected since their energy and electricity mixes have some major differences [5], as also their natural resource availability and their future hydrogen strategies. However, it is paramount to highlight that these three countries are only the destination of the hydrogen supply chain. For this reason, production and transmission in other countries, also outside the European borders, are considered. Some announced production and transmission projects are considered, and their details are studied with reference to their precise location. Figure 2 summarizes the hydrogen production countries considered in the tool. Besides the destination countries, where every hydrogen production method is modelled, the other countries can be divided into two categories: natural gas producers and regions with great solar and wind potential. The first category includes Norway, Algeria, and Qatar, which were respectively second, third, and fourth largest gas exporters in 2020 [38]. In the second category, countries with large solar and wind potential, and announced green hydrogen projects, are chosen: Saudi Arabia, Chile, Australia, and again Algeria. Each one of these countries is in a different continent, so they are selected as representative of their region. A detailed outline of these countries' strategies and projects is carried out in Section 4.5, while the precise locations considered are summarized in Appendix I. The study covers hydrogen supply chain costs from 2022 to 2030. The timeframe was chosen to avoid the high uncertainties of hydrogen technology costs in the future.

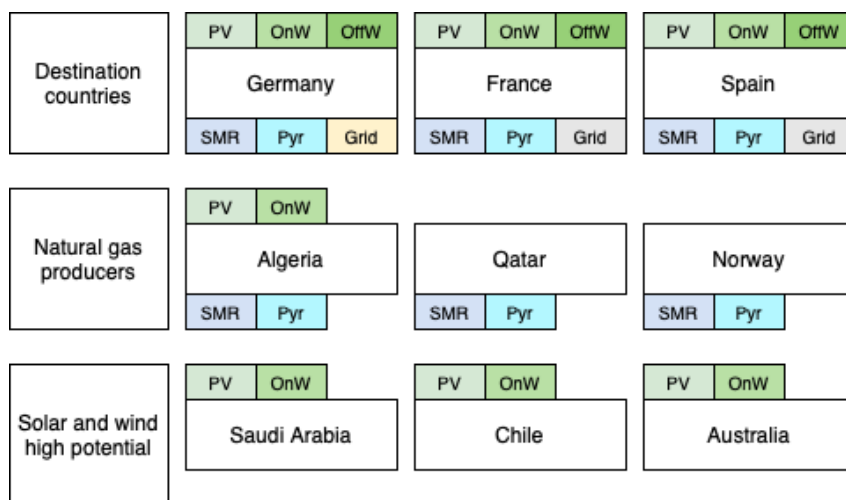


Figure 2: Countries considered in the research with related hydrogen-production methods².

Analyzing specific countries as case studies entails some inherent limitations. First, many relevant parameters need to be approximated to a national average. Making some examples, for the distributed hydrogen production from electrolysis in Europe, average wind and solar data for the whole country are used. Similarly, average distances from arrival/production hub to end-use location are calculated for hydrogen transmission. The final outputs refer therefore to a national average and may not reflect the specificity of single projects. A second limitation concerns the number of pathways considered in each country: due to time constraints, only the main, most promising and announced projects are considered, neglecting other possible pathways. However, the universality of the Excel tool gives the possibility to update the cost calculation in future work.

² OnW: Onshore wind; OffW: Offshore wind; Pyr: Pyrolysis.

4. Background

Hydrogen is expected to have a central role in future energy systems. Yet, it is already today an important commodity, used and traded globally. Its consumption reached 90 Mt in 2020 [39], with a generation market size of \$220bn [40]. Current hydrogen production relies almost entirely on fossil fuels, with this having a discreet impact on their annual consumption: around 6% of the global natural gas demand and 2% of coal are employed to generate hydrogen [3]. This translated to 900 Mton of CO₂ emissions in 2021 [39]. Two sectors widely employ hydrogen: the refining and the chemical industry, with respectively 40 and 46 Mtpa. The former uses it for its hydrodesulfurization process, to decrease the sulphur content in fossil fuels. In the chemical sector, hydrogen is the main feedstock to produce ammonia and methanol. The remaining 6% of the total hydrogen demand is consumed for the direct reduced iron process in steelmaking [39].

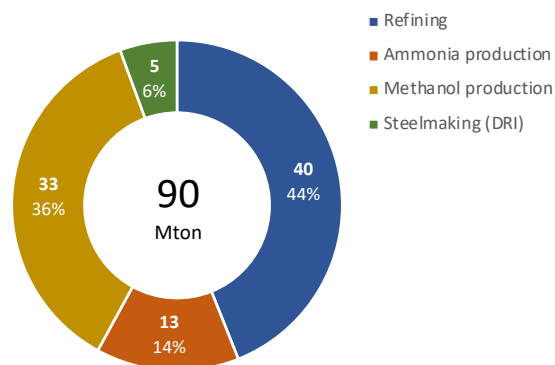


Figure 3: Hydrogen demand mix in 2020. Elaboration from [39].

Similarly to electricity, hydrogen has the great advantage of not releasing any pollutant and greenhouse gas at the point of use. However, the related emissions mainly come from its production phase. Compared to electricity, it can replace fossil fuels in several hard-to-abate industrial processes, and it can be stored with comparatively higher energy densities. Therefore, if its production shifts to cleaner methods, hydrogen has the potential to become an essential molecule towards the decarbonization of the energy systems, complementarily to electricity. The applications where clean hydrogen is an attractive solution can be divided into two categories: existing processes and new uses. The decarbonization of the current market presents fewer challenges and barriers, giving an ideal opportunity to develop a cleaner supply. Moreover, hydrogen can also play an essential role in applications where electricity, or other low-carbon options, are not competitive to replace the conventional processes. Some examples are the steel industry, heavy-duty vehicles, and long-term storage [3]. The potential hydrogen demand in 2050 could then range between 190 and 700 Mt [41].

Its capacity as alternative fuel is particularly significant for the transport sector, currently dominated by fossil fuels. Its heavy-duty segment can be seen as a protected niche giving the perfect launching pad for a larger hydrogen deployment, given its limited number of vehicles, owned by relatively small and advanced firms, operated by professional crews, and used in predetermined routes [6]. Despite the decarbonization ambitions, diesel HDVs will still dominate the market in the short term, due to their already existing infrastructure. Gradually, BEVs and FCEVs will replace the conventional fleet [7]. The prevalence of one on the other is still uncertain, given their advantages and disadvantages. Table 1 summarizes the main pros and cons of each vehicle option.

Table 1: Advantages and disadvantages of diesel, battery, and fuel cell powertrains. Adapted from [7].

Technology	Advantages	Disadvantages
Diesel	<ul style="list-style-type: none"> Lower vehicle cost No infrastructure investment required Long range and high payload Faster refueling time Large market 	<ul style="list-style-type: none"> High GHG emissions Source of local air pollution High refueling costs Low energy efficiency
Battery	<ul style="list-style-type: none"> Low GHG emissions and no local air pollution Potentially lower refueling and maintenance costs Higher energy efficiency 	<ul style="list-style-type: none"> Infrastructure investment required Higher vehicle cost than diesel Long recharging time Trade-off between range and payload
Fuel cell	<ul style="list-style-type: none"> Low GHG emission and no local air pollution Regenerative braking possible Faster refueling time than BEVs 	<ul style="list-style-type: none"> High hydrogen fuel cost Heavy infrastructure development required Higher vehicle cost Slow technology development

Hydrogen is now receiving unprecedented attention, both in terms of political support and investor interest. However, it still presents several technical and economic hurdles, especially concerning the creation of a supply chain. In the following sections, the production, transportation, and storage of hydrogen are reviewed, presenting the current state and future possibilities.

4.1 Production

Hydrogen can originate from different molecules, such as water and hydrocarbons. Together with hydrogen, the reaction generates different by-products, depending on the process adopted: oxygen, CO, CO₂, and solid carbon are some of the examples. Hydrogen production is currently based on fossil fuels in almost its entirety. Half of it comes from natural gas, mainly employed in the SMR process. Oil is responsible for 30% of the production, with its partial oxidation and subsequent use in petroleum refineries. Coal adds a 19%, providing hydrogen through its gasification. The remaining 4% is hydrogen from the electrolysis of water. Other methods have been studied, both from fossil fuels and alternative feedstock. In the first category, autothermal reforming and pyrolysis are found. Particular interest has also been put into combining CCS with conventional practices. Moreover, some of the processes based on fossil fuels can potentially use biomass and biofuels as feedstock, such as gasification and pyrolysis. Hydrogen can also have a biological origin, e.g., bacteria and microalgae. Last, in alternative to water electrolysis, thermal and thermochemical methods to split water are being researched [4]. Hydrogen production methods are often labelled with a specific color. Since this color convention is sometimes used in this work, the codes are reported in Table 2. To limit the review to the scope of the research, the next sections will focus on few processes: steam methane reforming, natural gas pyrolysis, and water electrolysis.

Table 2: Color codes for hydrogen production. Adapted from [42].

Color	Process	Carbon intensity
Brown	Gasification of fossil fuel feedstock (e.g., coal)	High
Grey	Natural gas SMR	High
Blue	Natural gas SMR with CCS	Low
Turquoise	Methane pyrolysis	Low (solid carbon)
Green	Electrolysis with electricity from renewables	Zero
Yellow	Electrolysis with grid electricity	Depends on grid carbon intensity
Pink	Electrolysis with energy from nuclear	Zero

4.1.1 Steam methane reforming

The steam reforming process is based on the endothermic reaction of steam and hydrocarbons to produce hydrogen and carbon oxides, in presence of a Co-Ni catalyst. In an SMR facility, natural gas is the process feedstock. A conventional plant configuration is represented in Figure 4. A pre-treatment unit initially removes any sulphur and chlorine present in the natural gas, to avoid catalyst poisoning downstream. The reformer is fed with the treated feedstock and high-pressure steam at 700-1000°C [4]. In the catalyzed reactor, at a pressure in the range of 3-25 bar [4], the conversion reactions are:



The carbon monoxide contained in the reformed syngas is converted to H₂ and CO₂ in a shift reactor. The shift reaction to reduce the CO level to around 2.5-3%_v is:



The shifted stream is fed to a pressure swing adsorption (PSA) unit, where residual impurities (e.g., CO, CO₂, CH₄, N₂) are removed and 90% of the hydrogen is recovered with a purity higher than 99.9%. The by-product of this section, the PSA tail gas, is the primary fuel of the SMR plant. Natural gas is also used as process fuel. The process usually has excessive steam, that can be used to produce electricity in a combined steam turbine [9], [11].

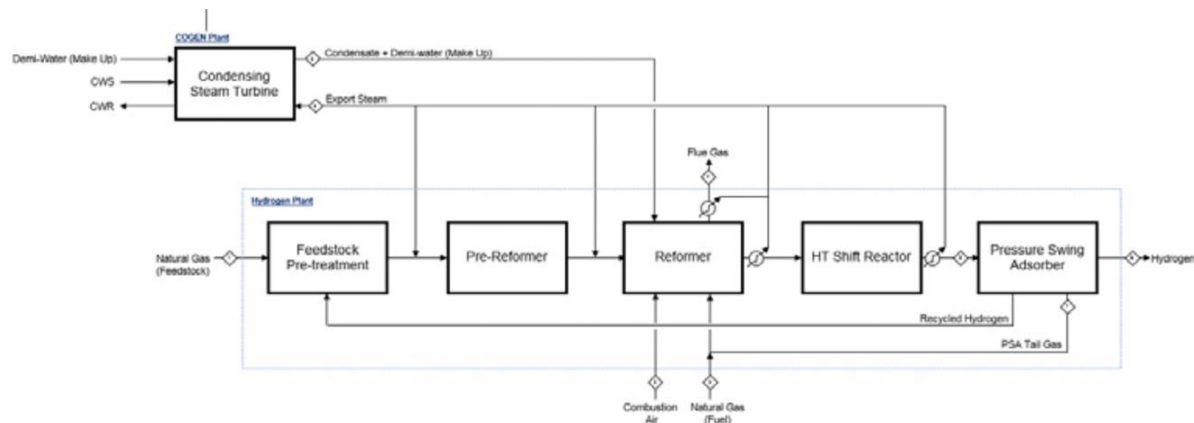


Figure 4: Conventional SMR plant layout [9].

The conventional SMR process has already achieved very high efficiency levels (3.4 kg_{ng}/kg_{H₂}, [9]), with CO₂ production close to the theoretical minimum. Therefore, only CCS could further reduce the CO₂ emissions [9]. The application of carbon capture to SMR presents some advantages, especially in the first stages of CCS development. First, an SMR plant is a large, stationary emitter of CO₂. Second, the process streams have high pressures and high carbon content, increasing the capture efficiency. Third, the SMR excess heat can reduce the capture energy penalty and decrease its costs. Last, the suitable CO₂ separation technologies for SMR are already widely used. In fact, the preferred option for SMR is gas absorption with amine-based solvents (MEA, MDEA). Other techniques are either inefficient (adsorption; the other residual particles, such as CO and CH₄, have similar adsorption forces), energy-intensive (cryogenic separation), or not commercially available (membrane separation) [11].

CO₂ can be captured from three different locations in a SMR plant: after the shift section, from the PSA tail gas, and from the SMR flue gases. Figure 5 shows another SMR diagram, this time highlighting the three possible capture sites. Collodi *et al.* [9] study the avoided CO₂ emissions in different cases, compared to the conventional process: 54% from the shifted stream; 52% from the PSA tail gas, and 89% from the flue gas. An attractive alternative involves the use of a H₂-rich fuel, avoiding any natural gas consumption as fuel, and the carbon capture from the shifted gas. This would lead to 64% avoided emissions. In almost

every case, the excess steam would fully cover the energy demand for the carbon removal, not requiring any external heat and electricity but only partially reducing the export of electricity.

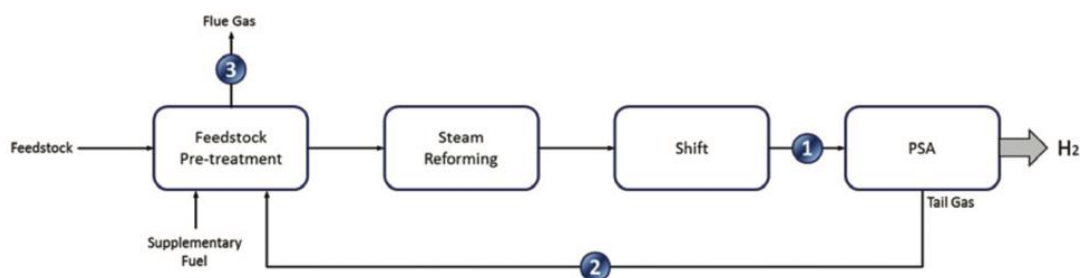


Figure 5: Simplified SMR plant layout, with three feasible CO₂ capture locations [9].

4.1.2 Pyrolysis

The pyrolysis is the thermal decomposition of a substance at elevated temperatures, in complete absence of an oxidizing agent (e.g., oxygen). The pyrolysis of methane from natural gas is a relevant process to produce hydrogen, since the element is the only product together with carbon [43]:

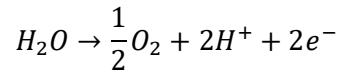


Both methane and hydrogen are in a gaseous state, while carbon is in its solid phase, which makes pyrolysis an appealing solution for hydrogen production. In fact, the absence of oxygen in the reaction entails that neither CO nor CO₂ are generated, and no additional carbon separation units are needed. The solid carbon can then be either stored or used as a raw material. The sale of solid carbon can improve the economics of the plant. However, the current market is very modest, therefore new applications are needed if a larger hydrogen demand will come for pyrolysis. An example of novel adoption would be soil and environmental restoration [44]. At the same time, the large-scale development of pyrolysis might result in the oversupply of the solid carbon market. This would lead to additional cost related to solid carbon disposal. A disadvantage of pyrolysis is its lower efficiency compared to SMR: its endothermic reaction has a theoretical efficiency of 59% (4.9 kg_{NG}/kg_{H₂}) versus a 75% for SMR. However, the efficiencies are similar when CCS is considered with SMR [44], [45]. Overall, the greater simplicity and the CO₂-free nature give pyrolysis unique advantages compared to conventional methods, suggesting its development as an important bridging technology.

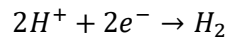
Despite its benefits, pyrolysis is still not competitive with more mature processes [44]. Different configurations have been studied, with few of them reaching a commercial scale [45]. The main distinctions pertain to the reactor design, the fuel supply, and the catalyst. Three main layouts can be identified: molten metal, plasma, and gas reactors. In the first configuration, the reactor contains liquid metal at high temperatures. Methane is injected at the bottom of the reactor, with hydrogen and carbon black leaving at the top. The process heat can come from different sources: natural gas, recirculated hydrogen, or electricity by resistant, inductive, or electric arc heating. The molten metal enables an efficient heat transfer and a natural separation from solid carbon, allowing for its simple removal. In the second configuration, the methane in a plasma state is decomposed, usually without a catalyst. The plasma state also decreases the methane purification need. Based on the plasma type, two processes are studied: a hot plasma reactor, where the temperature is higher than 1000 K and uniformly distributed; and a cold plasma reactor, with electrons at a higher temperature than neutrons and protons. Hot plasma processes have higher conversion efficiencies but lower selectivity than their cold alternatives. In general, plasma processes have a low inertia, also meaning a rapid ramp-up time. This allows their combination with an electricity supply from intermittent renewable energy sources. In the third configuration, conventional gas reactors (e.g., tubular fixed-bed and fluidized-bed) are used for methane decomposition. Despite the use of a mature technology, the process presents a substantial disadvantage: the catalyst is subject to a fast deactivation due to the accumulation of solid carbon on its surface [45].

4.1.3 Electrolysis

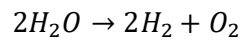
Water electrolysis is a process where water splits into hydrogen and oxygen under the influence of direct current. It is an endothermic process, with the necessary energy coming from electricity. In other words, electric and thermal energy are converted into chemical energy contained in a fuel, hydrogen. An electrolysis module presents two electrodes (anode and cathode) immersed in an electrolyte to raise the ionic conductivity. In a general case, water splits with the application of a direct current, so oxygen is produced at the anode:



and hydrogen at the cathode:



The overall reaction is therefore:



A diaphragm impedes the recombination of the two elements. This separator must have both high ionic conductivity and electric resistance to avoid the electrodes from short-circuiting. The produced hydrogen has usually a high purity (99.999 %_v) that allows its safe use in low-temperature fuel cells [4], [13], [46]. The electrodes, the electrolyte, and the diaphragm are the central elements of an electrolyzer cell. Multiple cells in series constitute the electrolyzer stack. The balance of plant (BoP) complements the stack and includes components for cooling, converting the electricity input (e.g., transformer, rectifier), and water, hydrogen, and oxygen processing (e.g., purification) [47]. Despite sharing the same operating principle, different electrolyzer systems have been developed, such as alkaline electrolyzers (AEL), proton exchange membranes (PEM), anion exchange membranes (AEM), and solid oxide electrolyzer cells (SOEC). Table 3 compares the different technologies and their main parameters.

Table 3: Summary of the main technical parameters, maturity level, advantages and disadvantages of four different electrolyzer technologies. Adapted from [13], [47].

	AEL	PEM	AEM	SOEC
Temperature	70-90 °C	50-80 °C	40-60 °C	700-850 °C
Pressure	1-30 bar	< 70 bar	< 35 bar	1 bar
Electrolyte	Liquid	Solid, polymeric	Solid, polymeric	Solid, ceramic
Stack efficiency	59-70%	65-82%	-	Up to 100%
Maturity level	Commercial	Near-term commercialization	Laboratory scale	Laboratory scale
Advantages	Low CAPEX, relatively stable, mature technology	Compact design, fast start-up, high-purity H ₂	Combination of AEL and PEM electrolysis	Enhanced kinetics and thermodynamics, lower energy demand
Disadvantages	Corrosive electrolyte, gas permeation, slow dynamics	High-cost polymeric membranes	Low OH ⁻ conductivity in polymeric membranes	Mechanically unstable electrodes, safety issues

Alkaline electrolysis is a well-established technology, currently dominating the electrolyzer market [46]. AELs are characterized by an electrolyte consisting of an aqueous caustic potash solution, with a KOH concentration of 20-30%. The electrodes are in nickel materials while the diaphragm is asbestos. The cell operates at low temperatures, around 20-80°C [13]. Despite its high maturity level, AWE presents several operational limitations and issues. First, an alkali fog is present in the gas. To produce high purity hydrogen, the contaminant is removed through desorption [13]. Second, the diaphragm does not completely avoid the recirculation of H₂ and O₂. To prevent this, the pressure between the electrodes

needs always to be balanced. However, the phenomenon becomes more severe at low loads (<40%) with an inherent explosion risk. This is caused by the low oxygen production at a low load, with the hydrogen reaching dangerous levels (lower explosion limit at H₂ concentrations >4%_{mol}). Consequently, a steady power input is usually preferred to the direct feed of intermittent renewable energy sources [13], [48]. Third, due to the high ohmic losses, the current density is limited to less than 400 mA/cm² [13]. Last, AELs cannot be operated at high pressures, preventing the realization of bulkier stack systems. However, the pressure is usually around 25-30 bar, sufficient to avoid the first compression stage in most applications [46], [48].

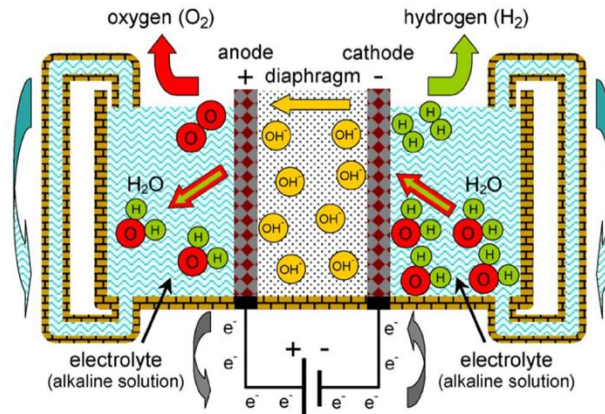


Figure 6: Scheme of the operating principle of an alkaline electrolysis cell [46].

PEM systems have been developed to overcome some of the limitations of AEL. Their main characteristic is the solid polymer electrolyte, which also acts as a separator. The polymeric membrane presents functional groups of the sulfonic acid (-SO₃H) type, allowing the conduction of protons through an ion exchange mechanism. The solid nature of the electrolyte translates into a more compact system with resistant structural properties. Among other advantages, this gives the possibility to reach higher operational pressures, either equal or differential. In the second configuration, high pressures are only located in the cathode side. This saves some hydrogen compression stages, while oxygen is not pressurized, facilitating its handling, and lowering the explosion risks [46], [48]. The risk is also decreased by the lower gas permeability of the polymeric membrane [13]. The alkaline fog is not generated and a higher hydrogen purity can be reached without the need for auxiliary components [13], [46]. Moreover, higher current densities can be achieved, above 2000 mA/cm². One of the key advantages of PEM over alkaline is the much quicker response to a varying electricity input, facilitating their combination with variable renewable energy sources. This is due to the rapid reaction time of proton transport through the membrane [48]. Despite many benefits, PEM electrolyzers are still in the early phases of their commercialization, with some issues to overcome: the higher cost, partly due to the membranes and the noble-metal electrodes; the shorter lifetime; and the scalability of both its system and its manufacturing capacity [14], [46], [47].

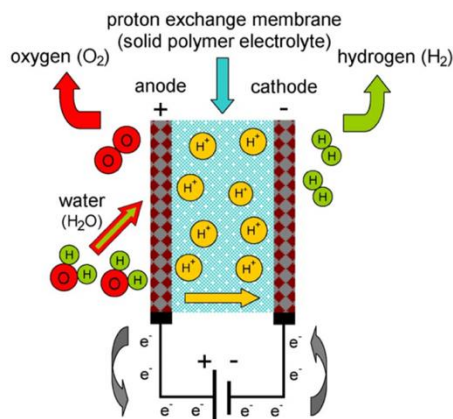


Figure 7: Scheme of the operating principle of a PEM electrolysis cell [46].

Anion exchange membrane electrolyzers have similar design concepts to PEM systems, but an inverted ion flow, with anions (OH^-) moving from the cathode to the anode. AEM electrolysis tries to combine the advantages of AWE with the ones of PEM electrolysis. Non-noble electrocatalysts can be used due to the less acid and harsh character of the membrane, compared to PEM. However, the simplicity and efficiency of PEM electrolysis is kept, also allowing operations under differential pressures. Despite the announced benefits, AEM is still in its early phases, with many issues to solve: for instance, its current chemical and mechanical instability; lower-than-expected performances; and low intrinsic anion conductivity [47].

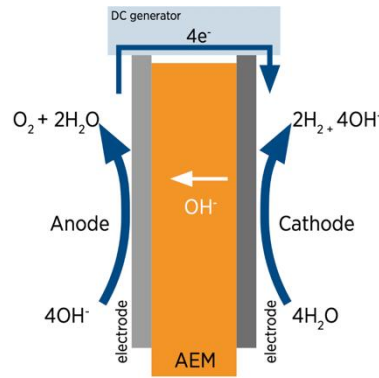


Figure 8: Scheme of the operating principle of an AEM electrolysis cell [47].

Solid oxide electrolyzers differ from the other configurations for the physical state of split water. In fact, steam is electrolyzed at high temperatures ($700\text{--}850^\circ\text{C}$), enabling higher efficiencies. Steam and recirculated hydrogen are injected into the cathode, where hydrogen and oxide anions (O^{2-}) are produced. The anions then flow towards the anode where the circuit closes, and oxygen is formed. The process is thermodynamically advantageous: despite a slightly higher reaction energy demand, the electrical energy demand significantly decreases, shifting the proportion to a larger heat supply. This explains the interest in this technology in industries with large heat availability. For instance, the combination of nuclear energy plants, in particular high-temperature gas-cooled reactors (HTGR), with SOEs has many economic and operational advantages [46]. The SOEC electrodes present a porous structure to optimize the interfacial contact area between the electrodes and the chemical species. However, the high temperature also causes some issues, especially in terms of material degradation and stack lifetime. Moreover, the outlet stream is a mixture of hydrogen and steam, requiring additional purification steps, and thus costs, to obtain a high purity product [13].

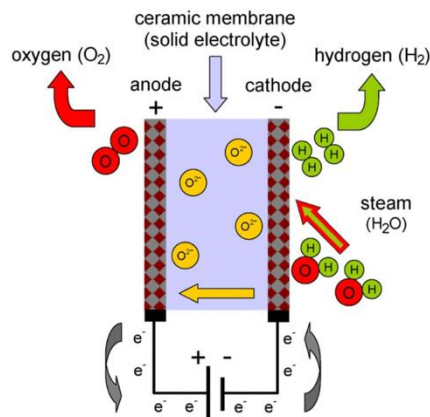


Figure 9: Scheme of the operating principle of a solid oxide electrolysis cell [46].

4.2 Storage

One of the most important stages of any supply chain is the storage stage, in particular when designing an energy commodity supply chain. Storage helps supply and demand balancing. In other words, with storage it becomes easier to deliver the energy at the exact time the customer wants. Over the past years, with increased production of renewable energy from solar and wind, two intermittent sources of electricity production, energy producers have been raising concerns to the fact that a lot of energy is being wasted due to difficulties in meeting the time of production with the time of demand. Several industry players and scientific researchers suggest hydrogen to be a great energy carrier to store the energy produced from these intermittent sources [49] [50]. At the same time, hydrogen storage guarantees that in case of any supply chain disruption, there is enough hydrogen to meet delivery needs [51]. The design of a hydrogen supply chain varies a lot depending on its final use [52]. In this study the focus has been put on correctly selecting the best technological options for each supply chain stage that meets the requirements of supplying hydrogen to hydrogen refueling stations (HRS). Without exceptions, the stationary storage options were chosen to take in consideration this specific supply chain. The storage stage is a terminal located in between the production site and the HRS, crossing at one point with the transportation stage, as it is shown in Figure 10.

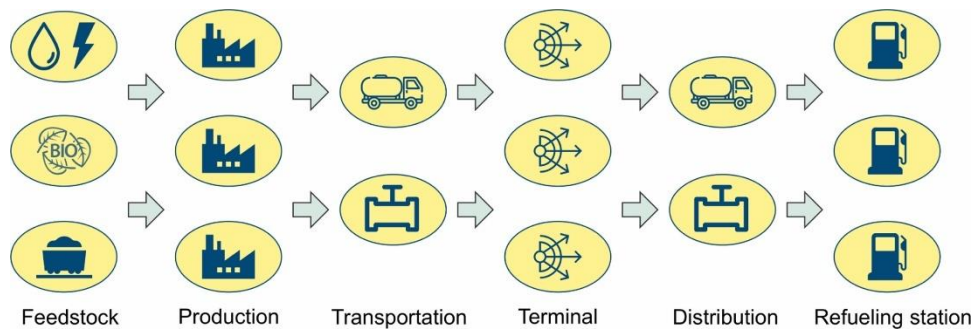


Figure 10: Hydrogen supply chain in the transportation sector [52].

However, the thermophysical properties of hydrogen are common for every type of supply chain. Storing hydrogen is particularly difficult because of its chemical characteristics (Table 4).

Table 4: Thermochemical properties of different fuels.

	Hydrogen, H_2	Methane, CH_4	Propane, C_3H_8	Ammonia, NH_3	Toluene, C_7H_8
Molecular weight [kg/kmol]	2.02	16.04	44.09	17.03	92.14
Boiling point [°C], at atm. pressure	-252.7	-161.5	-42.1	-33	110.6 [53]
Density [kg/m ³], at NTP conditions (1 atm and 20°C)	0.0837 [53]	0.668 [53]	1.8650 [53]	0.716 [53]	866.89 [53]
Gravimetric energy density, (LHV) [kWh/kg]	33.3 [54]	13.89 [54]	12.88 [54]	5.22 [55]	11.3
Volumetric energy density, at NTP conditions (1 atm and 20°C) [kWh/m ³]	2.787	9.279	24.02	3.74	9774

By comparing the volumetric energy density of hydrogen, methane, and propane, it is easily possible to conclude that much larger reservoirs are required to store the same amount of energy with hydrogen than with any other considered fuels at normal temperature and pressure (NTP) conditions. In one cubic meter of methane, there is 3.3 times more energy stored than in one cubic meter of hydrogen, while in one cubic meter of propane, even 8.6 times more. However, the gravimetric energy density, i.e., lower heating value (LHV), of hydrogen is the highest of them all. In one kilogram of hydrogen, there is 2.4 times more energy than in one kilogram of methane and 2.6 times more energy than in one kilogram of propane. Having said

that, by changing the temperature and pressure conditions of hydrogen, it is possible to store more or less hydrogen in the same reservoir. For example, by increasing the pressure of the hydrogen stored in a fixed volume tank, the amount of energy stored per unit of volume can be immediately increased.

The thermochemical properties of hydrogen presented above have led to a thorough research work on improving the storage potential of hydrogen. One other obvious way of improving the storage potential of hydrogen is to change its physical properties. For example, by liquefying hydrogen at atmospheric pressure. One least obvious way of improving the storage potential of hydrogen is instead making it react with other molecules to form chemical compounds with better characteristics for storage purposes. For instance, to convert hydrogen into ammonia or in a liquid organic hydrogen carrier (LOHC) such as toluene [3].

Many hydrogen storage technologies have been researched over the last years for stationary and mobile applications. Numerous scientific books and papers have been published on investigating new materials that can store hydrogen in the molecular form [56], without dissociating, on the surface of a solid material, with a mechanism known as physical adsorption, and materials that can store the hydrogen within solids, which is referred to as physical absorption. A product of this last mechanism are the well-known metal hydrides. Metal hydrides are metals that host hydrogen interstitially over a hydrogenation process. These have had special attention recently because of their high volumetric energy densities, even higher than liquid hydrogen [56], and the fact that hydrogenation and dehydrogenation occur with small change in hydrogen pressure [56]. One different hydrogen storage material, but also with very high volumetric energy density are complex hydrides. Abdin *et al.* [57] go even further and state that “complex metal hydrides typically have higher hydrogen gravimetric storage capacities and volumetric densities than simple hydrides”.

Various hydrogen storage materials have been investigated in the last years not only to find ways to store hydrogen in a more densified way, but also due to safety issues that come up with storing gaseous hydrogen at very high pressures [56]. One first problem is hydrogen embrittlement [51], which is a complex process that weakens the mechanical properties of a metal. Particularly, it reduces its ductility making it easier to fracture [58]. This process then leads to hydrogen leakage from the storage tanks, valves, pipes, or other metallic infrastructure used to handle the high-pressure hydrogen. Zheng *et al.* [59] stress the fact that with increased operating pressures in seamless metal hydrogen storage vessels, they become more susceptible to hydrogen embrittlement. Another safety parameter, but by any means less important, is the autoignition temperature, which is the temperature at which the material will ignite without any external ignition source. An advantage of hydrogen over other fuels is its high autoignition temperature (585 °C) when compared to methane (540°C) and propane (490 °C) [60].

As it was explained previously, there are multiple hydrogen storage technologies, however some of them can be disregarded when considering a supply chain for hydrogen refueling stations (HRSs) where compressed or liquified hydrogen is usually discharged to vehicles [49]. Chen *et al.* [61] considered that using alternative hydrogen carriers such as LOHCs and metal hydrides in a such supply chain offers no advantages for the decrease of hydrogen costs. For this reason, the upcoming sections describe pressure tanks for hydrogen storage, cryogenic tanks for liquid hydrogen and liquid ammonia storage. Also, a detailed overview is carried out for salt caverns, depleted NG or oil reservoirs, aquifers, and lined rock caverns for hydrogen storage.

4.2.1 Storage tanks

The required properties of a gas storage tank can vary a lot depending on the type of gas, and most importantly on its physical properties. In other words, the design requirements for storing hydrogen are different from storing ammonia or any other chemical substance. As explained in Section 4.2, the different chemical properties of gases can lead to distinct interactions with materials, particularly metals or composite materials that are commonly used in storage tanks, needing specific safety requirements. Additionally, a storage tank design varies significantly if the hydrogen is in gaseous form or liquid form. For example, when designing a vessel for gaseous hydrogen storage at high pressure it is significantly more

important to take into consideration mechanical properties such as strength, ductility, and fracture toughness. While, for liquid hydrogen storage, where the hydrogen temperature is below its boiling point, thermophysical properties such as thermal conductivity are relatively more important.

In the end, the type of storage tank will be dependent on the final use application. For instance, the required characteristics of a hydrogen vessel for a fuel cell electric vehicle (FCEV) should be low weight and high volumetric energy density. In fact, the European target weight efficiency for onboard storage in vehicles is set at 4.8 wt% of hydrogen in a system [58]. For industrial purposes, the weight factor of the tank is not as important as for the vehicle application, however hydrogen tanks should be of high energy density and low cost. These characteristics are of increased importance for stationary storage applications, such as for long-term and large-scale storage.

4.2.1.1 Storage tank for high-pressure gaseous hydrogen

Undoubtedly, compressed hydrogen storage has been the preferred method to store hydrogen [62]. Considering hydrogen storage for stationary applications, hydrogen can be stored in pressure tanks for small and medium scale [63]. Compressed hydrogen has been stored in steel tanks for pressures ranging between 200 and 350 bar [56]. However, more recently higher storage pressures, equal or higher to 700 bar [56] have been considered to fulfill specific requirements of the transportation sector. For stationary applications, composite tanks have been under trial to store higher capacities at higher pressures of hydrogen [27] since these types of tanks can provide sufficiently high strength and manage some safety issues such as fatigue and corrosion [63].

Type I

Type I tanks are metal tanks, more often steel tanks [64, p. 27] [63] [62], used for stationary storage in industry [62, p. 13] [64, p. 27]. Even though they have a poor weight performance and can operate at limited pressures up to 300 bar [62, p. 13] [64, p. 27], some references state 500 bar [63], they benefit from low cost [64, p. 27].

Type II

Type II tanks are metal liner hoop-wrapped composite tanks [62, p. 13] [64] [63]. They can be used for stationary applications which require high storing pressures [63] [64, p. 27]. They have been indicated to meet the requirements for buffer hydrogen storage in hydrogen refueling stations [65]. However, these tanks do not hugely benefit from a weight reduction when compared to type I tanks, they can operate at very high pressures. This type of tanks have already reach a good technological development level while operating at very different pressures [63] [64, p. 27]. They have slightly higher costs than type I tanks [64, p. 27].

Type III

Type III tanks are fully metallic composite overwrapped with a metallic liner [62] [63]. The metal liner is often aluminium which helps with issues such as hydrogen embrittlement, and it is used for making the tank impermeable [62]. These tanks are more advantageous in terms of weight performance than type I and II tanks, benefitting mobile applications [62] [65]. Also, they can be used for industrial applications [63] [64, p. 27]. The technology is mature for pressure equal to or lower than 350 bar and there are some barriers to overcome when it comes to 700 bar operating pressure [62] [64, p. 27]. Unlike type I and II tanks, these tanks are more expensive.

Type IV

Type IV tanks are fully composite and metallic liner overwrapped with a polymer liner [63] [64, p. 27]. The polymer liner helps solely with permeation problems [62, p. 13] whereas the fully composite overwrap deals with supporting the tensile strengths in the tank [62, p. 13]. These tanks can even register a lower weight than type III tanks [64, p. 27] [62] and benefit from technology maturity for higher operating pressures, up to 1000 bar [62, p. 13]. Making them a good application for mobility purposes [64, p. 27].

for example using this type of tanks for hydrogen transportation in tube trailers [65]. The biggest barrier attached to this technology is the very poor cost performance [64, p. 27].

Type V

Type V tanks are fully composite tanks without any liner [62, p. 13] [63]. These tanks can have a very low weight even more than type IV tanks [62, p. 13]. However, this technology is very premature and is still under a lot of technical improvements [63].

4.2.1.2 Storage tank for liquid hydrogen

Liquid hydrogen is often stored in cryogenic tanks at atmospheric pressure [62, p. 13]. Storing hydrogen in this type of tank benefits from the increase of hydrogen's volumetric energy density, also it is considered to be a safer technology [63] since it operates at lower pressures. However, their biggest issue is the hydrogen boil-off losses. Hydrogen boil-off is the process of hydrogen's phase changing from liquid form to gaseous form due to heat exchanges between the liquid hydrogen and the environment [62, p. 13]. This issue is of particular importance for liquid hydrogen storage in cryogenic tanks because of hydrogen's very low boiling point [58]. The boil-off rate depends on the amount of hydrogen to be stored [62, p. 13]. As the cryogenic tank volume increases, the boil-off rate decreases [56], [62], [64, p. 27], [65]. It can vary from 0.03%/day for large spherical tanks to 1%/day for small cylindrical tanks [65]. M. Al-Breiki *et al.* [66] mentioned an additional hydrogen mass loss when charging and discharging the tank. At the same time, it also depends on the shape of the tank [62, p. 13]. So, hydrogen tanks usually have a spherical shape so it reduces the surface contact area between the liquid hydrogen and the tank [27], [62, p. 13]. The cryogenic tanks usually have a double wall where the vacuum between walls reduces the heat losses [62, p. 13]. In recent years, space exploration institutes have been focusing on reducing the boil-off effect from cryogenic storage tanks for both mobile applications [67] and stationary applications [68] [69]. Several engineering concepts have been studied to develop these zero boil-off (ZBO) systems which the concept is based on passive insulation and active cooling at the same time [67]. NASA has developed a method called Integrated Refrigeration and Storage (IRAS) that uses a Brayton cycle cryogenic refrigerator coupled to an immersed internal heat exchanger [68]. A series of tests have demonstrated the feasibility of the method where zero boil-off operations were conducted on large quantities of liquid hydrogen for over 13 months [68]. Finally, it is possible to increase even more the hydrogen storage density by elevating the pressure in the cryogenic tanks, these tanks are called cryo-compressed hydrogen tanks [63].

4.2.1.3 Storage tank of liquid ammonia

Ammonia has been stored in large capacities for many years at atmospheric pressure and -33°C in big cylindrical storage tanks [70]. In the same way as liquid hydrogen storage, liquid ammonia suffers boil-off losses due to heat transfer from the tank to the surroundings [66]. Typically, a boil-off rate assumed for low temperature ammonia storage is 0.04%/day [66]. On the contrary of hydrogen, ammonia is considered one of the biggest chemical markets in the world [70, p. 5]. As a consequence, a well-established ammonia supply chain is already in operation, with multiple production and consumption points in the world. For these reasons, the technology readiness level for liquid ammonia storage is higher than for liquid hydrogen storage [71]. Verifying stronger developments of low temperature ammonia storage at import and export terminal for transportation purposes [70, p. 5]. DNV GL has developed a project named "Study on the Import of Liquid Renewable Energy: Technology Cost Assessment" [71]. The result of this project was the development of a database with techno-economic data for the import of liquid renewable energy carriers. Ammonia is one of the energy carriers evaluated. The investment cost of capital expenditures of liquid ammonia storage range from 115 EUR/MWh_{(LHV)NH₃} to 337 EUR/MWh_{(LHV)NH₃} [71], whereas the cost of capital expenditures of liquid hydrogen storage range from 717 EUR/MWh_{(LHV)H₂} to 3935 EUR/MWh_{(LHV)H₂} [71]. Comparing the cost range between each tank technology, it is possible to conclude that storing hydrogen in form of liquid ammonia is more competitive than liquid hydrogen. Indeed, A. Patonia *et al.* [72] refers to the costs of low temperature storage of ammonia being significantly lower than low temperature hydrogen. At the same time, it must be highlighted that conversion and reconversion costs are not included.

4.2.2 Geological reservoirs

When it comes to large-scale hydrogen storage, storing hydrogen in geological reservoirs can be economically advantageous [51] because of the huge storage capacities of this type of underground storage. Gaseous hydrogen directly benefits from this characteristic because of its very low volumetric energy density. Also, there is some transfer of technology know-how from storing natural gas which can help a faster deployment of the hydrogen storage technologies [50, p. 26]. However, the chemical behavior of hydrogen inside geological reservoirs differs a lot from natural gas. For example, the high diffusivity of hydrogen, higher capability of mass transfer in a material, can lead to measurable losses in porous media [65]. The main geological storage reservoirs considered in the literature are porous media, meaning aquifers and depleted natural gas (NG) or oil reservoirs, and caverns, meaning salt caverns and lined rock caverns [50] [51] [73] [74, p. 1]. It is relevant to argue that every geological reservoir depends on its site location, characteristics such as maximum geometrical volume [73], the reservoirs injection and withdrawal rates, and leakage potential, can be very different from one site to another, leading to difficulties in generalization of each geological reservoir technology [73].

4.2.2.1 Salt cavern

Salt caverns are either constructed in salt diapirs or in bedded salt [50, p. 26]. In salt diapirs, salt caverns assuming a cylindrical shape are made vertically whereas, in bedded salt, these are made horizontally [50, p. 26]. This variation happens because of the shape of these two geological structures [50, p. 26]. The construction of a salt cavern is preferred out of the other three caverns because of the fact that construction and further operation is made through a well bore [74], the hole drilled in the cavern. The salt cavern is formed by a mechanical process called leaching [75] [74] [51]. In this process water is injected into the excavated well where it dissolves the rock salt turning into a brine solution. The brine is then discharged from well until it is fully emptied. After this process, the salt cavern is ready to cycle the hydrogen [74], as it can be seen in Figure 11. Figure 11 represents the two ways of building the salt cavern, it is either possible to inject the water through the inner hole and discharge the brine solution from the annular space (sketch on the left) or vice versa (sketch on the right) [76].

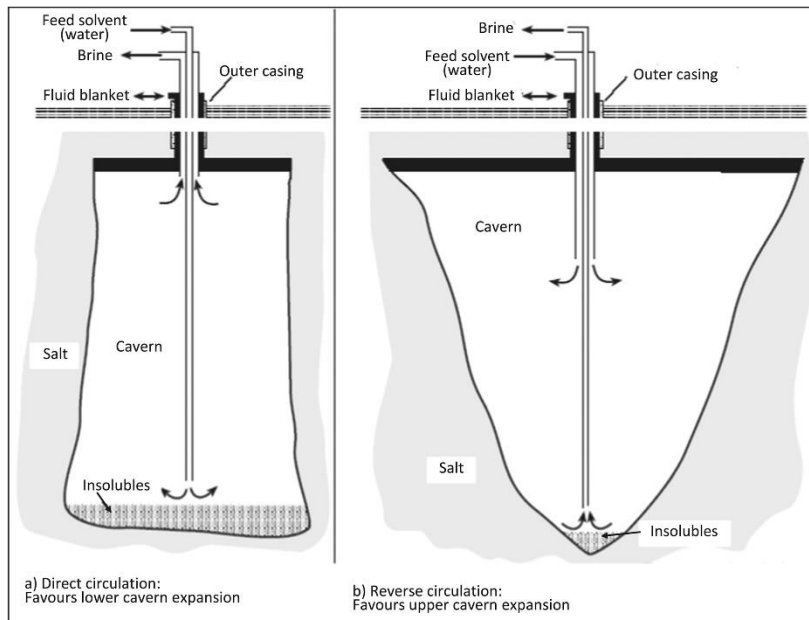


Figure 11: Schematic views of a) direct brine circulation method and, b) reverse brine circulation method [76].

Salt caverns are the only type of reservoirs currently storing 100% hydrogen. These salt caverns are located in Teesside, United Kingdom, in Moss Bluff, Texas, USA, and in Clemens Dome, Texas, USA [65] [50]. They store 210000 m³ [50, p. 26], 566000 m³ [65], and 580000 m³ [50, p. 26], respectively. These particular caverns have proven the feasibility of hydrogen storage, having the desired tightness to store large volumes of hydrogen [63] [65]. The low permeability characteristic of salt caverns allows them to have extra cycling

[51] registering up to ten charge and discharge cycles in a year [73]. This is why salt caverns are considered to be the type of reservoir with higher technical readiness level (TRL) out of the other three reservoirs, with a rating of 8 out of 10 [73]. In order to operate a salt cavern, a certain amount of hydrogen has to be kept in the reservoir since the beginning and until the end of its lifetime. This amount is called cushion gas and makes sure that the operating pressure inside the reservoir does not get lower than the minimum allowable pressure [75] [51] avoiding salt creep inside the cavern, and this way preventing an eventual structural degradation [75]. The cushion gas value is about 30% in salt caverns [73] [51]. The operating pressure of the cavern typically ranges from a minimum and a maximum pressure. It is important to say that the operating pressure is dependent on the cavern location as well as its depth. The maximum operating pressure increases with the increased depth of the reservoir. An operating pressure exceeding 200 bar is possible for cavern depths above 1000 meters [75]. Olaf Kruck *et al.* [74, p. 1] says that typical investment costs for this type of caverns are 55 €/m³ for hydrogen storage whereas M. Reuß *et al.* [49] assumes a cost of 162 €/m³ cavern. It is important to mention that the salt caverns tend to scale better than lined rock caverns, because these have a “higher maximum storage capacity” [65].

4.2.2.2 Lined rock cavern

A lined rock cavern (LRC) is a hard rock cavern with an enforced liner made of a polymer or steel [65] [51]. The hosting rock is supposed to have sufficient mechanical stability to support the stresses during the caverns’ cycling [74]. However, sometimes a layer of cement, in between the rock and the lining, is added to the cavern so it can withstand the pressure forces [74]. One of the advantages of LRCs is that the hydrogen operating pressure can achieve much higher values than in normal hard rock caverns, because of the lower permeability achieved by the polymer or steel liners [51], [65]. Like salt caverns, the LRCs benefit from low mass losses [77]. In fact, most of the hard rock caverns do not offer the sufficient tightness to store hydrogen [74]. An attractive aspect of this type of cavern is the fact that they operate in a similar way to salt caverns [51]. J. Cihlar *et al.* [73] classifies the TRL of LRC to be in the range of 5 to 6 points out of 10 which shows the low technology development of this type of technology even for natural gas storage. When it comes to the cushion gas requirements, LRCs can achieve quite low percentages of the cavern total volume [51] [73]. The operating pressure inside these caverns usually can achieve the lowest minimum operating pressure as well as the highest operating pressure of all types of caverns, because the stress tensions only affect the hosting rock cavern and not the lining that is in contact with the hydrogen [74]. As for salt caverns, the operating pressure inside the reservoir is dependent on the depth, however not as much. L. Londe *et al.* [75] refers that for operating pressures of 100 bar to 200 bar, LRCs can be at depths of 100 to 200 meters. For example, a LRC has been built in Skallen, Sweden, to store natural gas [74]. The cavern has 40,000 m³ of geometrical volume and a maximum pressure of 230 bar [74]. Finally, the costs of LRC are particularly high because of the expensive mining procedures required to construct the cavern [74]. The mentioned LRC in Sweden registered a total investment cost of 675 €/m³ [74].

4.2.2.3 Depleted natural gas or oil reservoir

Depleted natural gas (NG) or oil reservoirs are geological structures that previously stored hydrocarbons. The sedimentary rocks are characteristic of this type of fields, which have a certain porosity [75]. Usually, it is preferred to choose depleted natural gas reservoirs over depleted oil reservoirs for hydrogen storage, because the operating pressure of the previous natural gas fields was much higher (proximate to the hydrogen storage requirements) than oil fields [78], meaning less uncertainty on the viability of storing hydrogen in these fields [78]. At the same time, residual oil left in the depleted field can lead to hard contamination of the hydrogen resulting in an additional separation process after the hydrogen is withdrawn [74]. J. Cihlar *et al.* [73] classifies the TRL of depleted NG or oil reservoirs to be in the range of 3 to 6 points out of 10. The cushion gas requirements for depleted NG or oil reservoirs can be relatively high. Lord *et al.* [51] indicates a cushion gas percentage of 50%. In the same range are the cushion gas values presented by J. Cihlar *et al.* [73], 50% to 60%. It should be highlighted that the natural gas or oil previously present in the depleted reservoir can contribute to the needed cushion gas [51], [74]. This type of reservoirs are characterized to have high leakage risk potential [77] due to leaky wells [51] and proven

microbial activity inside the reservoirs. B. Bourgeois *et al.* [78] clearly enhance the propensity of porous media to have higher hydrogen mass losses than caverns. The main reason is that both depleted NG or oil reservoirs and aquifers use water to tighten the hydrogen inside the reservoir, and the contact between the water and the reservoir intensifies the microbial activity [78]. It has been proven over time loss of town gas, which is constituted by 50% NG and the other 50% by hydrogen, stored in a depleted field because of reactions between hydrogen and carbon monoxide as well as carbon dioxide to originate methane [74]. Also, remaining sulfates in the depleted field can react with hydrogen and originate hydrogen sulfide [65] [75]. The operating pressure in the reservoirs is dependent on the previous natural gas field. L. Londe *et al.* [75] states that pressures of 200 bar are common. In [73], the operating pressure for hydrogen storage in these fields range between a minimum pressure of 15 bar and a maximum pressure of 285 bar. Low costs are the biggest advantage of this type of reservoir. A. V. Lejarreta *et al.* [79] indicate an investment cost ranging between 280 €₂₀₁₉/MWh_{H2} and 424 €₂₀₁₉/MWh_{H2}. Lord *et al.* [51] and J. Cihlar *et al.* [73] indicate the same cost of capital expenditures to be 17.41 €/kg.

4.2.2.4 Aquifer

Aquifers have the same structure as depleted NG or oil reservoirs [74] [51]. The main difference is that these last reservoirs hosted hydrocarbons whereas aquifers hosted liquid water [74]. J. Cihlar *et al.* [73] classifies the TRL of aquifers to be in the range of 3 points out of 10. The low TRL is justified by uncertainties related to sufficient gas tightness, due to the lack of geological tests performed in this type of reservoir. Aquifers are the type of reservoirs that require a larger amount of cushion gas, typically ranging from 50% [73] and 80% [51] depending on the depth [73]. The potential hydrogen loss rate in aquifers is justified by the same reasons presented for depleted NG or oil reservoirs since they are both porous media [75]. It is relevant to say that hydrogen losses can happen due to the contact of hydrogen with the water used inside the reservoir, this issue can be aggravated by increased temperatures and pressures [65]. The operating pressure in these reservoirs can range from 30 to 350 bar.

4.2.2.5 Hydrogen underground storage across Europe, special focus to Germany, France and Spain

As explained in Section 4.2.2, the availability of geological storage is highly dependent on the location [32, p. 3]. For this reason, the geological storage potential across Europe shows an irregular distribution [32, p. 3]. From Figure 12, this irregularity in the case of salt caverns can be verified. With a higher potential in the north of Germany, and the Netherlands. France and Spain show a low potential for hydrogen storage in salt caverns.

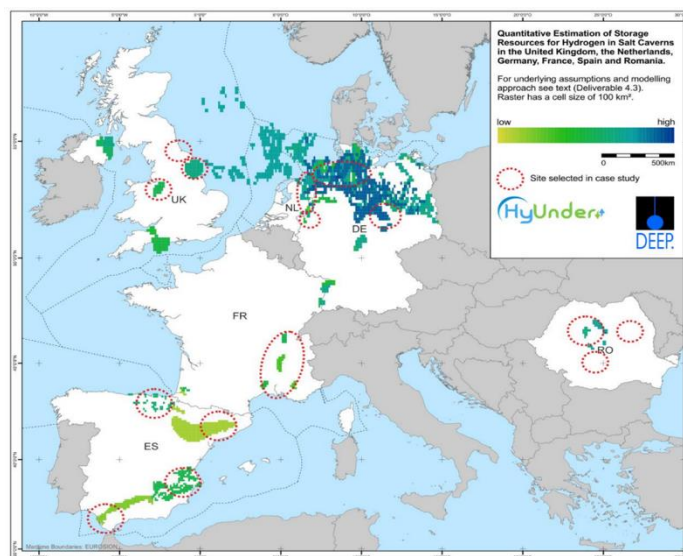


Figure 12: Hydrogen storage potential of salt caverns in Europe [80].

As part of the HYdrogen STORAge In European Subsurface (Hystories) project, an extensive database collating different data about geological availability for hydrogen storage throughout Europe as well as their respective petrophysical and geochemical data will be accessible to the public in the near future [80, p. 2]. For example, this database will provide additional information on microbial activity in geological reservoirs helping to interpret the impact on hydrogen underground storage [80]. The Hystories database is being built on top of two main projects, Energy Storage Mapping and Planning (ESTMAP) and CO2 Storage Potential in Europe (CO2StoP) [80].

Geological storage similarities between natural gas and hydrogen allow us to establish a comparison between the current operational storage facilities of natural gas and the potential hydrogen storage facilities. The values in Table 5 were obtained from the Gas Infrastructure Europe (GIE) Storage Map 2021 database. In Table 5, it can be seen that Germany has the biggest number of geological storage facilities when compared to France and Spain registering a number of 60 facilities out of 196 European facilities. While France and Spain have 17 and 4 facilities, respectively. Clearly, showing the bigger interest of Germany in storing large quantities of fuel in this type of underground storage. The most used type of geological storage for NG in Germany is the salt cavern, whereas for France is the aquifer and for Spain the depleted NG or oil reservoir.

Table 5: Operational geological reservoirs for NG storage.

	Europe		Germany		France		Spain		
	N° of facilities	WGV ** (TWh)	N° of facilities	WGV (TWh)	N° of facilities	WGV (TWh)	N° of facilities	WGV (TWh)	
Salt Cavern	68.00	307.54	44.00	153.82	4.00	14.40	-	-	
Depleted NG and Oil Reservoir	99.00	837.33	10.00	86.49	2.00	N/D	3.00	N/D	
Types of geological storage	Rock Caverns	2.00	0.09	-	-	-	-	-	-
	Aquifer	27.00	88.65	6.00	4.41	11.00	26.90	1.00	N/D
	VGS * - multiple types		518.44		21.71		95.10		34.25
	Total	196.00	1752.05	60.00	266.42	17.00	136.40	4.00	34.25

* "Virtual Gas Storage (VGS)-multiple types" includes cumulated WGV for storage sites of different type of geological storages (aquifer, depleted fields, salt caverns, etc.). GIE values are provided based on the territorial location of storages.

** Technical Working Gas Volume

In fact, the higher volume of NG storage in geological reservoirs in Germany is interpreted as having a higher repurposing potential of NG reservoirs into hydrogen reservoirs, as it is shown in Table 8. The values in Table 6 were collected from [73].

Table 6: Repurposing potential of geological storage for H2 storage (NG->H2).

	Europe 21 countries covered by EHB **		Germany	France	Spain
	Total Capacity (TWh)	Total Capacity (TWh)	Total Capacity (TWh)	Total Capacity (TWh)	Total Capacity (TWh)
Types of geological storage	Salt Cavern	50.00	39.50	2.50	0.00
	All storage types *	265.00	61.40	31.90	8.20
	Total	315.00	100.90	34.40	8.20

* Depleted NG or Oil Reservoir, Rock Cavern, and Aquifer

** EHB, European Hydrogen Backbone

Finally, future pilot projects in Europe are mainly investing in salt caverns based on the viability demonstrated by past projects, such as the ones referred in Section 4.2.2.1.

4.3 Conversion

The conversion stage on the hydrogen supply chain represents the necessary stage to transform hydrogen, either through a physical change with hydrogen compression or liquefaction, or chemical change with ammonia production. Additionally, reconversion steps are necessary in order to supply hydrogen in gaseous form at the end point. These processes can register high energy consumption and possible hydrogen losses. These are the two main variables evaluated to correctly assess the cost in this stage of the supply chain.

4.3.1 Compression

A compression stage is characterized by elevating the pressure of a gas. In the hydrogen supply chain, the hydrogen is compressed to densify it for transportation or storage reasons. A compression station is constituted by either one or multiple compressors. Its final purpose is to provide the necessary energy to hydrogen so it can meet the required pressure levels established for a certain mass flow rate.

To assess the real power required for compression, it is needed to first calculate the isentropic power. For this reason, defining the pressure ratio, mass flow rate, and initial temperature of the compression process is essential. The isentropic power is often given by [81]:

$$Power\ isentropic\ [kW] = N_{stages} \cdot \left(\frac{k}{k-1}\right) \cdot Z \cdot T_1 \cdot Q_{compr} \cdot R \cdot \left[\left(\frac{p_2}{p_1}\right)^{\left(\frac{k-1}{N_{stages} \cdot k}\right)} - 1 \right]$$

This equation³ takes into consideration that the compressors utilized are multi-stage compressors which are characterized to use single isentropic compressor stages.

An isentropic efficiency has to be defined to calculate the real power. The isentropic efficiency is dependent on the type of compressor and respective capacity flow rates [82]. Reciprocating compressors have been often chosen for hydrogen applications because they can reach very high pressures [56]. Centrifugal compressors are better for applications that require higher mass flow rates and have been used for gas transmission pipelines [83]. Since reciprocating compressors are still the only commercialized compressor technology for hydrogen applications, the cost assessment of different compressors is a difficult task [81].

4.3.2 Liquefaction

Hydrogen liquefaction is characterized as the thermodynamic process of hydrogen phase changing, from gaseous form to liquid form which means lowering the hydrogen temperature to below its boiling point, -253°C. A hydrogen liquefaction plant is a process plant that transforms gaseous hydrogen into liquid hydrogen through a complex multi-stage process. The plant can be divided into three stages: compression, cooling, and expansion [84]. The compression stage is where the hydrogen elevates its pressure before entering the cooling stage which is divided in two substages: a pre-cooling stage and an extra cooling stage. In the first substage the hydrogen reduces its temperature by exchanging heat in a heat exchanger with liquid nitrogen, afterwards the hydrogen goes through other heat exchanger that guarantees that the temperature of hydrogen gets below -73°C, hydrogen's inversion temperature, to finally enter in the throttling valve [84]. This type of plants is particularly energy intensive because of the very low boiling point of hydrogen. Alekseev [84] reviews state-of-the-art liquefaction plants operating until 2016, and indicates a specific energy consumption of 10 to 13 kWh/kg. Corresponding to a efficiencies in the range of 30% to 40%. Ohlig and Decker [85] stated, back in 2013, a specific energy consumption of 11.9 kWh/kg, and affirms that this value can be lower down to levels in between 7.5 and 9 kWh/kg without

³ Refer to Section 5.6.1.4 for a detailed description of every variable present in this formula.

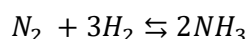
drastic changes in the liquefaction plant's technology. Also, Cardella *et al.* [86] confirm a decrease of the plant's energy consumption without great issues. Measurable mass losses of hydrogen are registered during the hydrogen liquefaction process, happening at different stages of the plant [87].

4.3.3 Regasification

The regasification process is characterized by the hydrogen phase change from liquid to gas. In a hydrogen supply chain that considers gaseous hydrogen at the end point, a regasification stage always follows a liquefaction stage. In this stage there is an evaporator that raises the temperature of the liquid hydrogen over its boiling point, -183°C , and evaporates it. Large liquid hydrogen regasification plants can benefit from the experience acquired by large LNG regasification plants that have been a structural part of the LNG supply chain. The LNG regasification plants located at import terminals mainly use a certain type of heat exchanger, which circulates sea water to heat up the LNG [88]. A similar concept could be used in a future hydrogen supply chain. In comparison to the hydrogen liquefaction stage, the regasification stage consumes much lower energy since the temperature of hydrogen evaporation at atmospheric pressure is very low. The supply chain costs model developed by Argonne National Laboratory [89] reports different evaporator costs with respect to different capacity throughputs.

4.3.4 Ammonia conversion

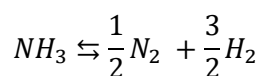
Ammonia conversion, also known as ammonia synthesis, is an exothermic reaction where hydrogen reacts with nitrogen to produce ammonia, as shown by the chemical reaction below. The enthalpy change characteristic of this reaction is -92 kJ/mol [90].



The ammonia production plant follows the Haber-Bosch (H-B) process which is the most used process nowadays for ammonia production. This process is characterized by requiring very high pressures and temperatures, so the hydrogen and nitrogen can react to originate ammonia. Ammonia production plants are complex chemical plants that input gaseous hydrogen and nitrogen, and output ammonia in the liquid form [91]. In order to achieve the required temperatures and pressures, a high level of energy is needed. Comparatively to hydrogen liquefaction, it is much less energy intensive [3]. Although, it has to be taken into account that ammonia production has a very high technical development level since it has been used for fertilizers production for many years now [3], [91].

4.3.5 Ammonia reversion

Ammonia reversion is an endothermic reaction where ammonia is cracked into hydrogen and nitrogen. The enthalpy change characteristic of this reaction is $+46\text{ kJ/mol}$ [90].



Ammonia reversion plants are constituted by a reactor which operates at very high temperatures to dissociate the ammonia into hydrogen and nitrogen molecules. As the stream out of the reactor is a mixture of nitrogen and hydrogen, an additional stage is needed to separate the mixture and produce a high purity hydrogen stream so it can meet the transportation sector requirements [90]. This technique is called pressure swing adsorption (PSA) [3]. Large-scale ammonia cracking plants with hydrogen purification techniques are not currently available [92]. In the same way, as ammonia synthesis plants, ammonia cracking plants also require high energy levels to reach sufficient temperatures in the reactor. Plus, they need extra energy for hydrogen purification.

4.4 Transmission and distribution

Clean hydrogen production and end-use applications are receiving great interest from the different stakeholders, from academia to investors to policymakers. However, the physical location of these two ends does not always correspond: a favorable supply from renewable sources is often located in remote

areas, while the demand will mainly grow in highly industrialized and populated regions. For this reason, the transportation of hydrogen is a crucial stage of its supply chain [93]. As for other energy vectors, hydrogen delivery can be divided into its transmission and distribution segments. Different options have been investigated, such as pipelines, ships, and trucks. As seen in Section 4.2, the low density of gaseous hydrogen makes its handling more difficult and expensive, thus other hydrogen carriers (i.e., LH₂, NH₃, and LOHC) are also studied.

4.4.1 Pipeline

Compressed gaseous hydrogen can be transported via pipeline with three different options: new hydrogen pipelines, retrofitting of the existing gas network, and blending with natural gas. This last mode is considered beyond the scope of this work, so it is not discussed. Hydrogen pipelines are usually made of carbon and stainless steel [94]. Before its injection, hydrogen is compressed to the operating pressure of the pipeline, that typically depends on the size, flowrate, and materials of the pipeline. Compression stations are also needed along the whole route, to maintain the pressure differential that drives the flow.

Two physical phenomena are particularly concerning for a hydrogen pipeline: steel embrittlement and pipeline erosion. The former is due to the interaction of hydrogen with metals, unlike natural gas. The adsorption and consequent absorption into the pipe wall cause a dangerous decrease in the material ductility and tensile strength. This limits the material choice to lower strength steels, which are operated at lower pressures and/or require thicker walls. Stricter safety standards are also required, determining higher costs [94], [95]. The second phenomenon is the wall erosion at high velocities. To avoid the pipe deterioration in the longer period, the flow velocity needs to be kept below a limit, the erosional velocity, that depends on gas properties, such as compressibility factor and density. At typical operating pressures, this value is 2.9 times higher for hydrogen than for natural gas, meaning that it can flow almost three times faster, with the related economic advantages [93], [94].

The current hydrogen pipeline network is limited to 5000 km globally, an infinitesimal portion of the 3-million-km natural gas infrastructure [3]. Nevertheless, they have a proven record of successful operations compared to other hydrogen transportation methods. Moreover, as the experience with natural gas confirms, this option has very low operational costs and long lifetimes. The main issues related with new infrastructure are the high capital expenses, the long construction times, and the complex bureaucracy, especially with cross-border pipelines [93]. The possibility to repurpose natural gas pipelines to hydrogen transportation is receiving attention given its potential to mitigate some of its disadvantages. The suitability to be retrofit depends on the pipeline steel and the hydrogen purity, given that the purer the hydrogen, the more aggressive [3].

4.4.2 Shipping vessel

With longer distances, pipelines might not be the most favorable option, especially if an intercontinental hydrogen trade will be established. Similarly to the natural gas market, shipping the liquefied product becomes a valid alternative in these cases. Moreover, hydrogen can also be transported as a different substance, such as ammonia and liquid organic hydrogen carriers (LOHCs). Besides the economic considerations, hydrogen shipping also strengthens the energy security of importing countries: compared to pipelines, it enables wider diversification and faster reaction times to change provider, particularly important with sudden geopolitical developments [3].

Transportation of LH₂ via shipping vessel has many similarities with the liquefied natural gas (LNG) process and infrastructure. The choice to liquefy the gas is mainly due to the higher density: LH₂ has a density 1.8 times higher than compressed gH₂ at 700 bar and 20°C. Hydrogen is liquefied at the export terminal and stored in insulated, double-hulled tanks, that limit the heat transfer from the environment. However, the liquid partially evaporates, with the boil-off gas that needs to be vented. This can be either used directly as a cooling fluid or as fuel. If LH₂ carriers are fueled with their load, either via direct combustion or fuel cells, the boil-off losses are restrained, making this option more competitive. At the import terminal, LH₂ can then either be regasified and compressed or further transported in the liquid

form. Despite the affinities with the LNG delivery, its storage is more difficult (LNG storage at -163°C ; LH_2 storage at -253°C , below air liquefaction temperature). This requires more complex components and large amounts of energy, which translates to high costs [3], [19], [93]. Currently, only one prototype exists, the Suiso Frontier, developed by the HySTRA joint venture [96], which includes several companies, such as Shell Japan and Kawasaki Heavy Industries. The ship can carry up to 75 tons of LH_2 in a single storage vessel with a volume of 1250 m^3 . This is relatively small if compared to large LNG carriers ($20000\text{--}40000\text{ m}^3$) [19]. The ship completed its first voyage in 2022, covering 9000 km between Southern Australia and Kobe, Japan [97]. Given the expertise gathered to build the Suiso Frontier, Kawasaki Heavy Industries already announced the project to develop a large LH_2 vessel with a volume of $160'000\text{ m}^3$ [98].

Among the hydrogen vectors, ammonia has the most mature shipping technology. Existing trade routes deliver ammonia from the Arabian Gulf to Europe, and ships rely on liquefied petroleum gas (LPG) tankers. Ammonia is transported in semi-refrigerated tanks at -33°C and ambient pressure [99]. If hydrogen is the desired final product, ammonia is reconverted at the import terminal, releasing the nitrogen into the atmosphere. Despite the technology readiness, the transmission of ammonia needs to observe very strict safety standards against toxicity and explosion risks [93]. Instead, LOHCs have the easiest handling, given their liquid properties at ambient pressure and temperature, similarly to diesel. Hydrogen is hydrogenated at the export hub, then dehydrogenated back at arrival. This second process occurs at high temperatures, increasing energy consumption and costs. Typical substances studied for shipping transportation are toluene, dibenzyltoluene, and benzyltoluene. Besides their simple handling, they also do not experience any fluid loss, which makes them ideal for longer transportation and storage times. The LOHC liquid can be reutilized, hence the dehydrogenated substance is shipped back. This adds complexity to the supply chain, and it might have a large impact on the supply chain CO_2 emissions, depending on the number of liquid life cycles. LOHC transportation is still in its R&D stages therefore its suitability still needs to be proven [93].

4.4.3 Truck

Hydrogen distribution with trucks is a well-established operation. For shorter distances ($<300\text{ km}$) compressed gH_2 trailers dominate the market, while LH_2 trucks are preferred when the distance offsets the liquefaction costs. Ammonia and LOHC can be also delivered via truck [3]. In general, this pathway starts at a distribution hub where hydrogen is converted to the desired form and substance. Once loaded on the trailer, it is transported to the end-use destination, where it can be reconverted. In both liquid and compressed gas cases, the payload is contained in cylinders that are packed with an arrangement dictated by the International Organization of Standards (ISO). Compressed gH_2 trucks must also follow local regulations that regulate the tanker size and pressure. For type I pressure vessels, up to 250 kg of gH_2 can be transported at 200 bar. These values increase for type III and IV to 1000 kg at 500 bar [100].

For longer distances, LH_2 becomes a viable solution. The payload is transported in super-insulated, cryogenic tanker trucks below 20 K [101]. This option has similar advantages and disadvantages to LH_2 delivery via shipping: despite the higher density, issues related to boil-off losses and high costs undermine the large-scale viability of this option. Moreover, the maximum distance possible is limited by the liquid heating and rise in pressure [3]. Ammonia trailers are also a mature technology. Ammonia is transported as a liquid in pressurized steel cylinders, with a capacity below 36 tons. Research suggests that they are not a viable option for large quantities of ammonia over long distances [70], [102].

4.5 Hydrogen economy and policy framework

The hydrogen trade is currently a local phenomenon, with 85% of it produced and consumed in the same location [103]. However, thanks to technological advancement and lower costs, wider institutional and private support, and a larger demand, a hydrogen economy is likely to develop in the following years. However, the extent of this market is still uncertain, evolving either on a global or on a regional scale. IRENA [103] forecasts that two-thirds of the green hydrogen production in 2050 will be consumed locally. Similarly, BloombergNEF [41] claims that large-scale local supply chains will provide the lowest-cost

hydrogen. Instead, IEA [3] suggests a case-by-case evaluation: the predominance of either imports or domestic use will depend on a series of market and location factors.

Despite the size unpredictability, the international trade is expected to grow exponentially. This is proven by the fact that more than 30 countries have included import and export plans in their hydrogen strategies [103]. These trends will shape the geopolitical balances globally. From one side, current fossil-fuel exporters look at hydrogen as a key commodity to diversify their economies. They have some competitive advantages in the first stages of a global hydrogen economy: for instance, expertise and workforce easily transferable to the new activity, and existing bilateral energy relations. On the other side, countries that were typically net energy importers might invert their position following the development of green hydrogen production. This is particularly beneficial for countries that have abundant renewable energy resources. In addition, with the declining cost of renewable and hydrogen technologies, local green hydrogen production might become competitive also with more modest conditions. This would strengthen energy security and decrease the price volatility of the commodity [103].

In the first phases, the hydrogen economy faces the risks of new markets. Large-scale energy-intense applications, such as clusters of industrial facilities, might be ideal to develop regional markets. In these settings, companies with different roles in the supply chain might create partnerships and joint ventures to mitigate the initial risks. Following the example of the early phases of the LNG market, bilateral contracts would also lower the price and volume uncertainty respectively for suppliers and customers. Together with these trends, policymakers and institutions will be essential to set standards, regulations and subsidies to spark the creation of a global hydrogen economy [103], [104]. In the following sections, the hydrogen strategies and initiatives of different countries are presented. The first focus is on the European Union, then limited to the three countries of study (Germany, France, and Spain). Last, a presentation of the hydrogen-producing countries within the scope of this work is carried out.

4.5.1 European Union

The European Union is currently undergoing a process of deep decarbonisation of its energy systems, that aims at tackling the climate crisis while also addressing the economic and geopolitical consequences due to the pandemic and the war in Ukraine. Hydrogen is regarded as a crucial element that complements other decarbonization solutions and strengthens the European energy security. Due to its low level of maturity, the EU acknowledges the necessity to back the early stages of its deployment with a solid framework. In this direction the European Commission published its hydrogen strategy in July 2020 [105]. This document inserts itself in the wider context of the European Green Deal [106], and it has been further elaborated in the 2022 REPowerEU Plan [107]. In addition to the initial support and legislation, the EU emphasizes the need for an open market where hydrogen is traded as any other commodity. A market-based pricing would encourage competition and decrease the entry barriers, with the advantage of providing clear signals to investors and other stakeholders [105].

The EU considers hydrogen from RES as the long-term solution. Two intermediate targets prove this will: the deployment of 6 GW and 40 GW in electrolysis capacity respectively in 2024 and in 2030. This would translate into 1 and 10 Mtpa of hydrogen produced from clean sources [105], [107]. However, low-carbon hydrogen from different sources and methods is included as a short-term option to phase out the conventional production. The EU Emission Trading System (EU-ETS) can play a substantial role in this gradual transition. Currently, fossil-based hydrogen production is already included in the EU-ETS. Nevertheless, due to the risk of carbon leakage associated with this industry, it receives complete free allocation. Either the inclusion of low-carbon hydrogen, the elimination of the free allocation, or the implementation of a Carbon Border Adjustment Mechanism have the potential to drive the diffusion of cleaner production methods and the retrofitting of existing plants with CCS technologies [105].

In the first phase, the EU reckons that the production and consumption locations will coincide, diminishing an immediate need for infrastructure [105]. However, given the high EU ambitions, domestic production will have to be integrated with imports. Three areas are cited as strategic import corridors: the Southern and Eastern Mediterranean, the North Sea, and Eastern Europe, in particular Ukraine. Thus, a

40-GW electrolysis capacity is also set for EU neighboring partners, together with the creation of a hydrogen diplomacy that can redesign the regional balances [105], [107]. A larger domestic and foreign production will require the planning of a pan-European network, that connects hydrogen valleys and import hubs. A European Hydrogen Backbone, as envisioned by a partnership of several European gas TSOs would cover 11600 km in pipeline by 2030, and then almost quadruplicate its length by 2040 [108].

A competitive supply side requires a stable and well-established demand. In addition to the current use of hydrogen, the EU also aims at supporting the diffusion of new applications. As already introduced, the decarbonization of HDVs will include hydrogen for applications and regions where this energy carrier and its infrastructure are economically competitive versus other low-carbon fuels like electricity or bio-LNG. In order to boost the deployment of FCEVs, the EU is currently defining targets and standards for hydrogen refueling stations (HRS). Despite the absence of a univocal document, the different proposals on alternative fuels infrastructure [109]–[111] share some points: focus on hydrogen as fuel for HDV with HRS at 700 bar every 200 km on the core highways. The setting of precise standards and the roll-out of HRS will be an essential signal for HDV manufacturers to proceed with the development of FCEVs.

4.5.2 Germany

Germany sees hydrogen as an important decarbonization pathway. The central document is the National Hydrogen Strategy [112], published in June 2020. Despite having many common points with the EU equivalent, it has some key differences and further considerations that are worth discussing. A first divergence is the role of blue and turquoise hydrogen. Both strategies include it as a short-term solution. Nonetheless, the German government has recently ruled out the possibility of subsidizing these production methods, fully favoring hydrogen from electrolysis [113]. This is reflected by the electrolysis capacity target of 5 GW by 2030.

However, this installed capacity can satisfy only a small fraction of the expected demand. For this reason, the German strategy gives more relevance to imports, amounting to around 85% of the total supply. This is largely different from the EU strategy, that forecasts only half of the supply coming from outside the European borders [105]. Germany has therefore signed bilateral partnerships, MoU and joint statements with several countries from every continent, much beyond the three areas mentioned in EU strategy. Giving some relevant examples, the list of countries include Norway [114], Algeria [115], Saudi Arabia [116], Australia [117], and Chile [118]. Within these documents and partnerships, Germany ensures financial and technological support to develop hydrogen-related projects, while strengthening future energy relations to prepare and plan a future global trade.

To sustain a forecasted hydrogen demand of 90-110 TWh by 2030 [112], the establishment of a reliable infrastructure is needed. Ports will be an essential hub, with the port of Hamburg and the neighboring port of Rotterdam preparing the path towards intercontinental trade [119], [120]. This will be coupled with the development of a hydrogen backbone, that initially feeds the industrial clusters in Western Germany and is connected to the Dutch network [108].

4.5.3 France

Hydrogen has been part of the French energy plans since 2015. Law No 2015-992 [121] sets the foundations towards a national hydrogen strategy, focusing on three fields: energy storage, mobility fuel, and power-to-gas business. The law does not state any targets or further details but formalizes the development of a national hydrogen strategy, then published in 2018 [122] and expanded in 2020 [123]. In addition to the three just-cited areas, the documents add its industrial deployment as a priority. With regards to its use in the transportation sector, the 2018 plan illustrates hydrogen's complementary role to BEVs, without however specifying the respective applications. The 2020 strategy corrects this, clarifying its primary importance for heavy land transportation.

France regards electrolysis as the key production method to develop, omitting any reference to blue hydrogen or other alternatives. Moreover, hydrogen imports do not appear as part of the strategy, that

instead hinges on national green hydrogen production. In particular, the hydrogen-nuclear duo is seen as the main way rather than imports, as also explained by the French president in the context of the France 2030 investment plan [124]. These factors justify the target of 6.5-GW electrolyzer capacity by the end of the decade [123], an amount even more ambitious than the German one. Another peculiarity of the French hydrogen plan is the explicit reference to the SOEC technology and its development. This can be explicated again with the heavy interest of the nuclear industry in the future French hydrogen economy: the Atomic Energy Commission (CEA) owns the largest portfolio of SOEC patents worldwide [122]. France aims therefore at becoming a global leader in the advancement and manufacturing of this high-temperature technology, also given its potential to be coupled with nuclear plants.

4.5.4 Spain

In line with the European Union strategies, also Spain gives a central role to hydrogen in its decarbonization strategies. The Spanish National Energy and Climate Plan emphasizes its large availability of solar and wind resources, that can and must be exploited with a variety of technology. Hydrogen production at low costs falls within the mentioned possibilities [125]. To support the hydrogen rollout, the Spanish government published its National Hydrogen Strategy in 2020 [126]. The document identifies three main end-use sectors: industry, for hydrogen-intensive and high-temperature processes; long-distance transportations; and as energy vector to enable a higher penetration of RES. To ensure the initial deployment, hydrogen valleys or clusters will be prioritized. Such projects gather demand and supply projects in a specific area, limiting the risks associated with the first phases.

Given the abundance of RES, the Spanish strategy only contemplates green hydrogen, without citing other production methods. Moreover, hydrogen is also seen as a vector to increase national energy security. For this reason, hydrogen imports are not included. On the contrary, Spain sees RES and green hydrogen as key resources to become an energy exporter. In this direction, the National Hydrogen Strategy sets a target of 4 GW in electrolysis installed capacity by 2030 [126]. This encouraged the creation of several green hydrogen projects, that are now being defined and raising investments [127].

4.5.5 Norway

Norway is currently the second largest gas exporter to the EU, satisfying one fifth of the European demand [38]. Hydrogen has the potential to ensure Norway's energy exports and simultaneously reach its climate targets. For this reason, the Norwegian National Hydrogen Strategy [128] considers both electrolysis and steam methane reforming as viable production methods, differently from most European plans. It is worth mentioning that Norway not only plans to use its own gas but also have production facilities that can employ gas imports. The development of CCS technologies is fundamental to guarantee the success of blue hydrogen, with projects such as the Northern Lights initiative [129]. Similarly, the deployment of an export infrastructure is vital to allow the creation of a hydrogen market. Small-scale hydrogen exports can be delivered by shipping, while a larger-scale supply can only be transported via pipelines. In this direction, Norway and Germany have recently signed a joint statement to commit to strengthened cooperation for the hydrogen rollout. In this framework, the realization of a pipeline network connecting the two countries is seen as paramount [114].

4.5.6 Algeria

Algeria's economy currently relies on gas and oil exports, which reach 20% of its GDP and 85% of its exports [130]. Algeria is the third largest supplier of natural gas to Europe, meeting 8% of the total demand, with Italy and Spain as the main destinations [38]. To diversify its imports and meet its environmental goals, Algeria looks with great interest at hydrogen as a molecule to gradually phase out its natural gas dependency. Due to its gas reserves and its large solar availability, both blue and green hydrogen are contemplated as future solutions. The Energy and Mining Minister announced in May 2022 the beginning of the process to develop a national hydrogen strategy [131]. Additionally, several exploration studies and memorandum of understanding (MoU) have already been signed. For instance, Germany and Algeria established an energy partnership in 2015, that has been lately very active to promote studies on hydrogen.

The German Corporation for International Cooperation (GIZ) [132] published a detailed, exploratory study to assess the hydrogen production and export potential. Private initiatives are also starting to take place, with Eni and the Algerian state-owned Sonatrach that signed several MoU to collaborate on green hydrogen production [133], [134].

The focus has been put in on Algeria in this research. However, the EU Hydrogen Strategy and the REPowerEU plan place strong emphasis on the whole North African region [105], [107]. Similar strategies and partnerships are also happening in the neighboring countries, such as Morocco and Egypt, and therefore considerations for Algeria can be extended to them [135].

4.5.7 Qatar

Qatar is one of the largest LNG exporters globally, facilitated by its technological advancement and large liquid-to-gas facilities. Despite the country is projected to become the largest LNG producer by 2030, it has recently started to show interest in hydrogen, in order to adapt to the shift in market preferences [136]. However, a national hydrogen strategy has not yet been published [137] and the existing initiatives comes mainly from private actors. A first official step has been done in May 2022, with the German-Qatari agreement to strengthen their energy partnership, with specific reference to LNG and hydrogen [138].

4.5.8 Saudi Arabia

Saudi Arabia is the largest crude-oil exported globally but recently started a process of income diversification to ensure future economic security, as described in the Saudi Vision 2030 [139], [140]. Given its expertise in the fossil fuel supply chain and its large availability of solar and wind resources, the country aspires to become the largest supplier of hydrogen globally [141]. A national hydrogen strategy is currently under development [137] but the country has already publicly set a production target equal to 3-4 mtpa by 2030 [140], [141]. A key project is the one to be realized close to the future city of Neom, where 4 GW of renewable capacity is expected to be built by 2026, translating to 1.2 mtpa of green hydrogen [142]. Germany has already signed agreements with Saudi Arabia to support the development of hydrogen projects, with Neom explicitly mentioned, towards a future trade between the two countries [116].

4.5.9 Australia

Given its large availability of natural resources, both renewable and fossil, Australia wants to position itself as a global leader in the nascent hydrogen economy. For this reason, the country released in 2019 its National Hydrogen Strategy [143] to set the path. The document includes both green and blue hydrogen production: in addition to the solar and wind optimal conditions, the country also has gas and coal reserves, and potential to efficiently store CO₂ underground. Nine gigawatt-scale projects are under development, with many others being announced [103], [144], [145]. Australia sees hydrogen both as a domestic and an export commodity. Subsequently, it recognizes the necessity to develop an infrastructure that supports both ends. With reference to the potential export, Australia can count on a strong expertise in LNG shipping, as the country is the largest exporter globally [146], that can give it a competitive advantage, especially in the first phases of the hydrogen global trade. Given its proximity, Australia looks at Asia as the main destination of its exports, aiming to be a top three supplier there [143]. However, Europe aims to be an important commercial partner, as demonstrated by several institutional MoU and private partnerships signed in recent years. For instance, the German and Australian government signed a common declaration of intent [117] where Germany commits to support the infrastructure development in Australia and prepare for future intercontinental supply chains. The port of Rotterdam has also been very active to sign MoU with different Australian states to secure its position as a key arrival hub in Europe [147]–[149], while E.On and Fortescue Future Industries entered a partnership to deliver 5 Mtpa to Europe by 2030 [150].

4.5.10 Chile

Chile is traditionally an energy net importer, due to its lack of fossil fuel resources [5]. However, the country has a unique position in terms of abundance of renewable energy sources. Its desert of Atacama,

in the North of the country, has one of the highest solar irradiance levels globally, while the southern regions of Patagonia have constant and intense winds. This opportunity, together with its remote position, drove the country to develop an ambitious hydrogen strategy. In a first phase, until 2025, Chile aims at setting up its local production and consumption while preparing the field for exports. In a second phase, from 2025 to 2030, the country expects to install 25 GW of electrolysers, building an export market equal to \$2.5 bn per year [151]. Different large-scale projects are under development: for instance, the Chilean Production Development Corporation (CORFO) shortlisted six hydrogen production projects to support and co-finance. Most of these projects are backed by European companies (e.g., Engie, Enel Green Power, Linde) with some entirely reserved for exports [152].

5. Methodology

The future hydrogen supply chain can be studied with different approaches and models. The choice of a methodology depends firstly on the desired result: an economic assessment might either produce a supply chain cost indication or a final hydrogen price value. The supply chain costs can be found with pathway models, that study multiple options and display feasible supply channels, based on economic, technical, and geographical factors. On the other hand, a hydrogen final price can be the result of simulation and optimization models, through different mathematical approaches. The most common approaches are linear modeling and mixed-integer linear programming [153]. Optimization models require a forecast of the hydrogen demand; however, given its incertitude, the final price value might also include a large uncertainty. Moreover, the large-scale deployment of hydrogen is still in its early stages. Despite the simple nature of pathway models, they can provide useful insights about the cheapest options and pathways. For these reasons, a similar approach has been chosen for this study.

5.1 Definition of Levelized Cost of Hydrogen

The objective of this research is to determine the production, transmission and distribution (T&D), and storage costs of hydrogen considering different low-carbon technologies. The different stages, and their costs, are then aggregated with different combinations, accounting for technical considerations and constraints. As a result, the hydrogen costs for the whole supply chain are calculated, with reference to different pathways (combinations of different technologies for hydrogen production, transportation, and storage). In particular, such costs are often levelized, i.e., they account for the time value of money. The main result of the tool is therefore the levelized cost of hydrogen, the LCOH. This concept originates from the levelized cost of energy and levelized cost of electricity (LCOE), that describe the average cost per unit produced by the system over the considered period, that is equivalent to the total lifecycle costs [154]. Adapting the LCOE formula [155] to the hydrogen case:

$$LCOH = \frac{NPV_{cost}}{NPV_{H_2}} = \frac{\sum_{n=0}^N \frac{C_n}{(1+d)^n}}{\sum_{n=0}^N \frac{Q_{H_2,n}}{(1+d)^n}} \quad (1)$$

where NPV is the net present value; C_n is the sum of the system costs in the year n ; $Q_{H_2,n}$ is the annual amount of hydrogen handled; N is the system economic lifetime; and d is the discount rate. If it is assumed that the system starts to operate one year from its construction (i.e., the sheer, initial investment occurs in year 0), and that costs and quantities of hydrogen handled are constant throughout the years of operation, equation (1) can be rewritten as:

$$\begin{aligned} LCOH &= \frac{C_0 + \sum_{n=1}^N \frac{C_n}{(1+d)^n}}{\sum_{n=1}^N \frac{Q_{H_2,n}}{(1+d)^n}} = \frac{CAPEX + \sum_{n=1}^N \frac{OPEX_{\%} \cdot CAPEX}{(1+d)^n}}{\sum_{n=1}^N \frac{Q_{H_2}}{(1+d)^n}} = \\ &= \frac{CAPEX + OPEX_{\%} \cdot CAPEX \cdot \sum_{n=1}^N \frac{1}{(1+d)^n}}{Q_{H_2} \cdot \sum_{n=1}^N \frac{1}{(1+d)^n}} = \\ &= \frac{CAPEX}{Q_{H_2}} \cdot \left(\frac{1}{\sum_{n=1}^N \frac{1}{(1+d)^n}} + OPEX_{\%} \right) \end{aligned} \quad (2)$$

Therefore, a simplified formula for the LCOH is:

$$LCOH = \frac{(a_{\%} + OPEX_{\%}) \cdot CAPEX}{Q_{H_2}} \quad (3)$$

where $OPEX_{\%}$ are the operating expenditures, expressed as a percentage of the $CAPEX$; and $a_{\%}$ is the amortization factor, function of the discount rate d and of the economic lifetime N :

$$a_{\%} = \frac{1}{\sum_{n=1}^N \frac{1}{(1+d)^n}} = \frac{d}{1 - (d+1)^{-N}} \quad (4)$$

The LCOH is calculated for each stage of the hydrogen supply chain:

- $LCOH_p$: levelized cost of hydrogen production
- $LCOH_s$: levelized cost of hydrogen storage
- $LCOH_{t\&d}$: levelized cost of hydrogen transportation, sum of the transmission ($LCOH_t$) and distribution ($LCOH_d$) components

The overall LCOH for the whole hydrogen supply chain is calculated as the sum of these components. It is worth mentioning that in the results the conversion components (compression, liquefaction, regassification, conversion to and reconversion from ammonia) are treated separately for consistency reasons.

$$\begin{aligned} LCOH &= LCOH_p + LCOH_s + LCOH_{t\&d} = LCOH_p + LCOH_s + LCOH_t + LCOH_d = \\ &= LCOH_p + LCOH_{s,w/o\ conv} + LCOH_{t\&d,w/o\ conv} + LCOH_{conv} \end{aligned} \quad (5)$$

Equation (3) is only used in the stages where its assumptions are valid, i.e., the operational expenses are constant throughout the years, and the hydrogen handled is constant. In the stages where instead those assumptions are not fulfilled, Equation (1) is preferred, using it in combination with a cash and hydrogen flow analysis year-per-year. In Section 5.4 to 5.7, each stage and its methodology are discussed. The LCOH formula used is also specified for each stage.

5.2 The Excel tool

The LCOH calculations for the different stages of the supply chain are gathered in a single Excel file, where the selection of a supply channel and the input values for each stage determine the final cost for the whole supply chain. The Excel tool is a general model, valid for any location, option, and year. The model has been applied to specific case studies in a precise timeframe, as described earlier in Section 3.1. Specific options for each stage and each country are selected, based on natural resource availability, existing infrastructure availability, national strategies, and commercial plans. The tool is set up to be accessible by external users, that can use it and input their values with increasing levels of detail and complexity. To describe the tool flexibility, three different degrees of freedom are identified and described in the subsequent paragraphs.

The *Home* sheet presents the first degree of freedom: here the user can input the general information of the hydrogen supply chain. Based on the choice of the year of interest, and the locations for production and final consumption, the tool displays the feasible options for each stage. The user can model a specific supply pathway by selecting different options for each stage. Few other input values can be edited in the *Home* sheet, such as the hydrogen carrier and the distance for T&D. In the same page, also the partial and

final results are displayed. Figure 13 shows a screenshot of the top part of the *Home* sheet, while Appendix II presents a graphical description of the *Home* sheet and the possible, alternative selections for each stage.

General input		PRODUCTION	
Select YEAR	Select DESTINATION COUNTRY	Select PRODUCTION LOCATION	Select PRODUCTION METHOD
2022	Germany	Algeria	Electrolysis
CoolProp can be used in the tool to have a better approximation of the different fluid properties and can be downloaded at the link		Plant capacity: [kW]	100000
Use CoolProp? No		Override: [kW]	
OBS: To design a new supply pathway, check and select every option (in red) in this table -> Excel does not update the toggle lists!		Select ELECTRICITY SOURCE:	Solar
		Select ELECTROLYZER TYPE:	PEM
Click here to change default values			
LCOH:	8 €/kg	4.03 €/kg	
	OVERALL	PRODUCTION	
TRANSMISSION		DISTRIBUTION	
Select TR. MODE by SEA	Select TR. MODE by LAND	Select DISTR. MODE	
Ship	Pipeline	Pipeline	
Select CARRIER	New or repurposed?	New or repurposed?	
LH2	New	New	
H2 carrier selection: AUTOMATIC or MANUAL?		Default distance: 200 km	
Default distance: 3174 km	Default distance: 0 km	Override below [km]	
Override below [km]	Override below [km]	Automatic	
Change default values	Change default values	Change default values	
2.85 €/kg			
TRANSMISSION AND DISTRIBUTION (without int. storage)			
STORAGE			
STORAGE at IMPORT TERMINAL?	STORAGE at EXPORT TERMINAL?	FINAL STORAGE?	Select H2 FINAL STATE
Yes	Yes	Yes	gH2
Default capacity: 11000 t_LH2	Default capacity: 11000 t_LH2	Default capacity:	Default final pressure: 300 bar
Change default capacity	Change default capacity	Change default capacity	Override below [bar]
		Select STORAGE TYPE	
		Geological - Depleted NG or Oil Reservoir	
		Obs: final storage only as gH2	
Change default values	Change default values	Change default values	
0.11 €/kg	0.86 €/kg	0.14 €/kg	
INTERMEDIATE STORAGE	FINAL STORAGE	FINAL CONVERSION	

Figure 13: Snapshot of the top part of the *Home* sheet in the Excel tool.

To provide further levels of flexibility, the *Home* page presents different messages (e.g., “*Change default values?*”) that redirect the user to more detailed sheets. The relevant parameters and their values for the selected year and locations are listed in these sheets. The tool gives the possibility to override one or multiple values, adding a second level of freedom to the user. The same sheets also include the partial calculations and the LCOH for the specific stage.

A third and last degree of freedom is given in the *Fuel data* sheet, where the prices for grid electricity, fuels, and emissions are summarized for each country and year. Here, the user can input his own projections for one or multiple prices, overriding the tool values. These three degrees of freedom are also correlated to the level of knowledge of the user. Any user, also with little knowledge on the topic, can select options and design a supply pathway in the *Home* sheet (first degree of freedom). A more expert user can instead edit the data and the assumptions behind the calculations, outputting a result that reflects more personalized supply chains (second and third degree of freedom). A more detailed description of the tool functionalities is presented in the next sections.

5.3 Other key concepts

This section introduces and describes some general concepts that are implemented in the different stages of the tool.

5.3.1 Inflation, exchange, and discount rates

Given that the input economic values used throughout the work come from a wide array of sources, it is necessary to harmonize them for inflation, currency, and unit of measurement. All costs in this study are

expressed in €₂₀₂₁, therefore values from prior years are adjusted using the EU Harmonized Index of Consumer Prices (HICP) [156]. Costs in different currencies are converted to € considering the average exchange rate in 2021 from the *Euro foreign exchange reference rates* tool of the European Central Bank [157]. Table 7 reports the rates for the currencies encountered in literature. The eventual harmonization for inflation, currency, and unit of measurement is usually stated explicitly when an economic parameter from literature is cited and used.

Table 7: Exchange rate for currencies found in literature, 2021 average, quoted against the euro [157].

<i>(quote against the euro)</i>	Exchange rate (2021)
US Dollar (\$, USD)	1.1827
Pound sterling (£, GBP)	0.89267
Canadian dollar (C\$, CAD)	1.4826
Japanese yen (¥, JPY)	129.88

For coherency and consistency, future values are also expressed in constant euros, i.e., in €₂₀₂₁. This means that the interest rate used is a real discount rate and the inflation is excluded [154].

$$d_r = \frac{1 + d_n}{1 + e} - 1 \quad (6)$$

where d_r and d_n are respectively the real and nominal discount rates, and e is the inflation rate. The latter parameter is approximated to be constant in the future and equal to the average rate in the European Union for the last 25 years⁴. This value corresponds to 1.78% [158]. In the following sections, the discount rates are usually reported in nominal terms, due to their larger frequency in literature, but then they are converted to real discount rates in the tool.

5.3.2 Economy of scale: learning and scaling effects

To investigate the capital expenses of a generic system, it is fundamental to introduce the concept of economy of scale, that has a double effect on the system costs. First, it affects the manufacturing process, being part of the technological learning, where its potential to cut down costs is described with learning curves [159]. Second, an economy of scale reduces the specific unitary investment costs, thanks to the upscaling of its capacity. In this case, scaling factors are used to describe this effect [160].

Learning effects

The reduction in capital costs of a technology throughout the years is usually described with the learning curve concept, that correlates the historical increase of manufactured units, or installed capacity, to a fall in cost. This principle has been often applied to the costs of renewable energy technologies in order to explain their downward trend, to predict their future curves in energy models, and to back investments [159]. This analysis is not exempted from similar considerations: the learning curves are adopted to project the trends of the examined technologies. They assume that the cost of a technology decreases by a constant factor, the learning rate (LR), with every doubling of the installed capacity [161]. The general expression of learning curves for the cost of a technology at time t is:

$$c(t) = c_0 \cdot \left(\frac{X(t)}{X_0} \right)^{-b} \quad (7)$$

⁴ The 1996-2021 timespan is considered since previous data are not available in the HICP database [158].

Where c_0 is the cost of the technology at the reference time t_0 ; $X(t)$ is the installed capacity at time t ; X_0 is the installed capacity at the reference time t_0 ; b is the slope of the function on a log-log plot and it is related to the LR by:

$$LR = 1 - 2^{-b} \quad (8)$$

The principle of the learning curve usually takes the perspective of the manufacturer since it relates the cost with the global, cumulative production or installed capacity. However, the developed tool aims at showing the dependence of technology costs to the considered year. Therefore, it is preferred to shift the independent value from the installed capacity to the year. It is assumed that the installed capacity of every technology will increase at a constant annual growth rate (AGR):

$$X(t) = (1 + AGR)^{t-t_0} \cdot X_0 \quad (9)$$

Equation (7) can be hence expressed as:

$$c(t) = c_0 \cdot (1 + AGR)^{-b(t-t_0)} \quad (10)$$

The learning curves, as expressed in Equation (10), depend only on the time t (in years), assuming a constant AGR , learning index b , and base year, t_0 .

Scaling effects

An economy of scale has also the potential to decrease the specific costs of an individual system, through the upscaling of its size. A common method to estimate the scaling effect is the “scaling factor” method [160], which relates the costs for a system with capacity (size) S to the reference one:

$$C = C_{ref} \cdot \left(\frac{S}{S_{ref}} \right)^{sf} \quad (11)$$

5.3.3 Levelized Cost of Electricity

The concept of levelized cost of electricity (LCOE) has been introduced previously to describe the LCOH. However, a more detailed explanation is needed since the LCOE is explicitly used and calculated in the tool. Similarly to what demonstrated in Equations (2) and (3), the LCOE can be expressed as:

$$LCOE = \frac{(a_{\%} + OPEX_{\%}) \cdot CAPEX_t}{E_t} \quad (12)$$

where E_t is the annual energy generated, assumed to be constant throughout the lifetime of the system [155]. If $CAPEX_t$ and E_t refer to a single unit of capacity, Equation (12) can be rewritten as:

$$LCOE = \frac{(a_{\%} + OPEX_{\%}) \cdot CAPEX}{CF \cdot 8760h} \quad (13)$$

where CF is the capacity factor.

5.4 Production

As presented in Section 3.1, three production methods are considered: natural gas SMR, natural gas pyrolysis, and electrolysis. The tool, based on the choice of a production location in the *Home* sheet, presents the different options available for that location. The user can then browse through the different production methods' sheets, where the input data can be overridden. In the same sheets, for each production method, different processes and sets of equations needs to be considered. However, the $LCOH_p$ is calculated in the same way for any method, using Equation (1), given the annual variability of some costs (e.g., electricity and gas prices) and produced quantities.

$$LCOH_p = \frac{\sum_{n=0}^N \frac{c_n}{(1+d)^n}}{\sum_{n=0}^N \frac{q_{H2,n}}{(1+d)^n}} \quad (14)$$

Both annual costs c_n and hydrogen production $q_{H2,n}$ are normalized per unit of capacity, in kW. For any production method, it is assumed that the nominal discount rate d_n is equal to 8%, which is the average of some values used in literature [3], [9], [43]. This translates into a real discount rate d of 6.1%. It is important to mention that in literature and industrial contexts the unit of capacity for electrolysis refers to the power consumption (kW_{el}), while for SMR and pyrolysis it refers to the production capacity ($kW_{H2,LHV}$). The same convention is used in this work. Since both costs and production might differ from year to year (e.g., components replacement, system degradation), an annual cash-flow analysis is carried out, presenting the unitary costs in €/kW/a. The following subsections present a more detailed explanation of the methodology applied for each production pathway.

5.4.1 Electrolysis

The tool models the electrolysis process considering three different technologies: alkaline, PEM and solid-oxide electrolyzers. Several technical and economic parameters vary depending on the electrolyzer type, as shown in this section. However, the methodology and equations used are general, meaning that they describe electrolysis regardless of the adopted technology. A generic electrolysis process produces annually:

$$Q_{H2,n} = \frac{P_{H2} \cdot CF^* \cdot 8760h}{LHV} \quad (15)$$

where CF^* is the electrolyzer capacity factor and P_{H2} is the nominal production capacity, in $kW_{H2,LHV}$. However, as explained previously, the electrolyzer capacity is more commonly expressed in terms of electrical demand, P_{el} (in kW_{el}):

$$Q_{H2,n} = \frac{(P_{el} \cdot \eta_{LHV,n}) \cdot CF^* \cdot 8760h}{LHV} \quad (16)$$

Equation (16) is then normalized per unit of capacity:

$$q_{H2,n} \left[\frac{kg_{H2}/a}{kW_{el}} \right] = \frac{Q_{H2,n}}{P_{el}} = \frac{\eta_{LHV,n} \cdot CF^* \cdot 8760h}{LHV} \quad (17)$$

When the electrolyzer is coupled with a dedicated RE plant, the electrolyzer capacity factor CF^* is linked to the RE plant capacity factor CF . If the power and hydrogen production facilities were sized with the

same capacity, the capacity factors would coincide. However, an optimal oversizing of the RE plant ensures a better utilization of the electrolyzer system. The optimization problem is beyond the scope of this work, therefore a global value from Brändle *et al.* [37] is used to assess the ratio between the power production and the electrolysis capacities, S_{RE}/S_{el} . This value is equal to 1.6 for solar PV, and 1.8 for onshore and offshore wind. The simplified equation relating the capacity factors is as follows:

$$CF^* = CF \cdot \frac{S_{RE}}{S_{el}} \quad (18)$$

where S_{RE} and S_{el} are respectively the RE plant and the electrolyzer capacity sizes. The capacity factors for RE plants in different locations are summarized in Appendix I.

The electrolyzer stack is subject to degradation, therefore this effect needs to be considered as a time-relevant decrease in efficiency. The end-of-life of an electrolyzer stack is usually determined when its efficiency has degraded by 10% [162]. As such, assuming that the efficiency degrades linearly during its lifetime, the average efficiency in a year n is equal to:

$$\eta_{el,n} = \eta_{el,0} - D_\eta \cdot \frac{\bar{h}_n}{LT} = \eta_{el,0} - D_\eta \cdot \frac{(h_n + h_{n-1})/2}{LT} \quad (19)$$

where $\eta_{el,0}$ is the nominal stack electrical efficiency; D_η is the lifetime efficiency degradation; \bar{h}_n is the cumulative average hours of use in year n ; LT is the stack lifetime. The nominal efficiencies are reported in Table 8. The annual hydrogen production thus decreases with an increasing number of hours of use of the stack.

Table 8: Electrical efficiency for different electrolyzer technologies [47]. Similar values can be found in [3], [162].

	Alkaline	PEM	SOEC
Electrical efficiency, LHV, 2020 ($\eta_{el,0}$)	52%	50%	67%
Electrical efficiency, LHV, 2050 ($\eta_{el,0}$)	74%	74%	83%

The system efficiency of a SOEC is actually lower than the electrical efficiency since the steam needs to be generated. It is assumed that the steam is injected at 800°C [46] and is heated with an electric heater of 97% efficiency [163]. The SOEC overall efficiency is calculated as follows:

$$\eta_{SOEC} = \frac{LHV_{H_2}}{E_{el} + E_{heating}} = \frac{LHV_{H_2}}{\eta_{el,n} + \frac{\Delta h \cdot m_{H_2O}/m_{H_2} \cdot (1 + \%_{unused\ steam})}{\eta_{heater}}} \quad (20)$$

where Δh is the water enthalpy for a temperature difference from 20°C to 800°C and m_{H_2O}/m_{H_2} is the theoretical mass of water needed per unit of hydrogen. However, part of the steam might come from an industrial or nuclear plant, as excess heat that can be considered “free”. To implement this possible advantage in the tool, the user can input the percentage χ of “free” excess steam. This lowers the overall electricity need and it is modelled simplifying it as an increase of the electrolyzer system efficiency.

$$\eta_{SOEC} = \frac{LHV_{H_2}}{E_{el} + E_{heating}} = \frac{LHV_{H_2}}{\eta_{el,n} + \frac{\Delta h \cdot m_{H_2O}/m_{H_2} \cdot (1 + \%_{unused\ steam})}{\eta_{heater}}} \cdot (1 - \chi) \quad (21)$$

Turning the attention to the cost of hydrogen production via electrolysis, it is composed by different parameters:

- Electrolyzer (whole system) capital expenses
- Operational expenses
- Stack replacement costs
- Electricity costs, either from the grid or from specific RE plant
- Water cost
- Revenues from oxygen sale

Electrolyzer capital expenses

It is assumed that the base year for the electrolyzer is 2021, and the reference electrolyzer capacity is equal to 1 MW. In Table 9, the costs for different electrolyzer technologies are summarized, referring to base year and reference capacity. The costs can be broken down in stack and other costs. The other costs, from now referred as auxiliary costs, include power electronics, gas conditioning, and balance of plant.

Table 9: Electrolyzer costs in 2021, 1 MW capacity [164]. Similar values can be found in [3], [47], [165].

	Alkaline	PEM	SOEC
Total system cost [€/kW]	900	1450	2300
Stack cost [€/kW]	450	870	690
Stack-to-total cost ratio, %_{st2tot,0}	50%	60%	30%

Learning and scaling effects are considered and, to add some levels of detail, they are determined at a component level, dividing the electrolyzer system in stack and auxiliary components. As reported in Table 10, Böhm *et al.* [164] estimate steep learning rates for the stack, compared to milder trends for the auxiliary components.

Table 10: Learning rates and indexes for different electrolyzer technologies [164].

	Alkaline		PEM		SOEC	
	Stack	Aux	Stack	Aux	Stack	Aux
Learning rate, LR	15.2%	10.9%	14.6%	11.1%	14.6%	12.1%
Learning index, b	0.29	0.07	0.29	0.12	0.29	0.12

Accounting for stack and other components independently, Equation (10) can be rewritten as:

$$c(t) = c_0 \cdot [\%_{st2tot,0} \cdot (1 + AGR)^{-b_{st}(t-t_0)} + (1 - \%_{st2tot,0}) \cdot (1 + AGR)^{-b_{aux}(t-t_0)}] \quad (22)$$

where $\%_{st2tot,0}$ is the ratio between the stack and the total electrolyzer system cost in 2021. Looking at the *AGR*, Guidehouse Insights [166] estimates that the global electrolyzer capacity will grow at an annual growth rate of 62.6% through 2031, from the 0.5 GW installed in 2022. This trend is slightly lower than the IRENA [47] and IEA [167] expectations in the next years, but then it meets the projections at the end of the decade, as shown in Figure 14. Therefore, the *AGR* provided by Guidehouse has been considered reasonable to use in this analysis.

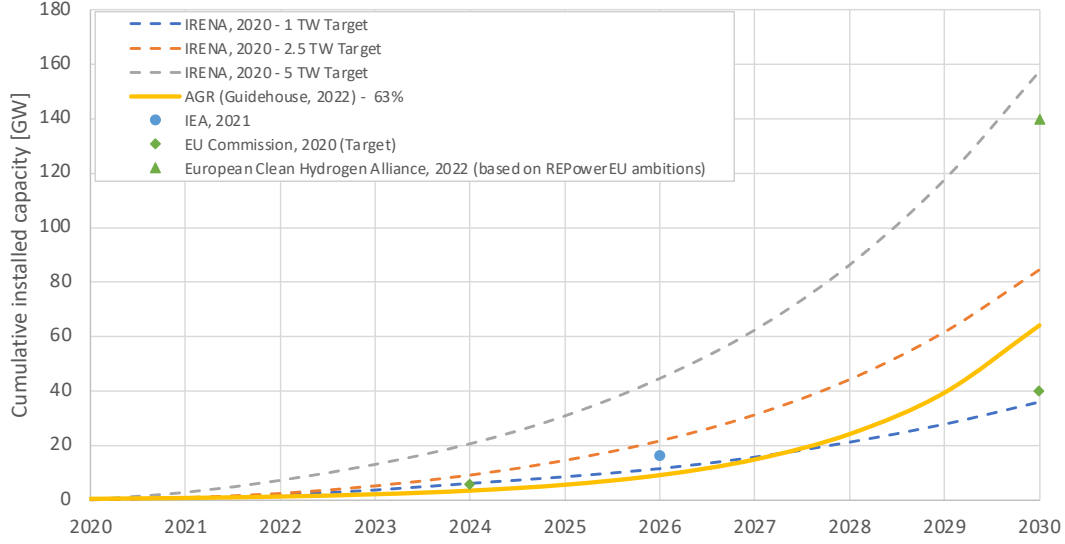


Figure 14: Electrolyzer global capacity projections. Own elaboration based on [47], [105], [166]–[168].

The learning curves are also used to evaluate the improvements for some key parameters, such as electrolyzer efficiency, system and stack lifetimes. In these cases, it is assumed that the AGR remains equal to 62.6%, while the learning index is characteristic for each parameter. If a parameter is known for two different years between 2020 and 2031, the learning index can be calculated with Equation (10):

$$b = - \frac{\log_{1+AGR} \left(\frac{X_{T_2}}{X_{T_1}} \right)}{T_2 - T_1} \quad (23)$$

where X_{T_1} and X_{T_2} are the parameter's value in year T_1 and T_2 . Combining Equation (10) and (23):

$$X(t) = X_{T_1} \cdot (1 + AGR)^{-\log_{1+AGR} \left(\frac{X_{T_2}}{X_{T_1}} \right) \cdot \frac{t-T_1}{T_2-T_1}} \quad (24)$$

The scaling effects are also taken into account, meaning that a larger electrolyzer system has a lower CAPEX per unit of capacity [160]. The system size reference, S_{ref} , is set equal to 1 MW_{el}. This analysis usually refers to specific costs (€/kW_{el}), therefore from Equation (11):

$$c = \frac{C}{S} = \frac{1}{S} \cdot \left[C_{ref} \cdot \left(\frac{S}{S_{ref}} \right)^{sf} \right] = \frac{1}{S} \cdot \left[(S_{ref} \cdot c_{ref}) \cdot \left(\frac{S}{S_{ref}} \right)^{sf} \right] = c_{ref} \cdot \left(\frac{S}{S_{ref}} \right)^{sf-1} \quad (25)$$

The scaling factor sf is specific to each component since the impact of the upscaling on the costs depends on the design and the structure of each component. Following the same approach used for the learning curves, where the electrolyzer is divided in two parts, stack and auxiliary components, Equation (25) can be rewritten as:

$$c_{el} = c_{ref} \cdot \left[\%_{st2sys} \cdot \left(\frac{S}{S_{ref}} \right)^{sf_{st}-1} + (1 - \%_{st2sys}) \cdot \left(\frac{S}{S_{ref}} \right)^{sf_{aux}-1} \right] \quad (26)$$

The electrolyzer stack has a modular design that prevents a large cost reduction due to its upscaling. In fact, the single cell is limited in size for different reasons (e.g., issues with leakage), with the maximum cell stack size expected to slightly increase thanks to learning effects [160]. Zauner *et al.* [160] use a dynamic scaling factor for the cell stack, that depends on the system size, and thus minimizes the scaling effects for large-scale applications:

$$sf_{st} = 1 - (1 - sf_{st,0}) \cdot e^{-\frac{S}{S_{max}}} \quad (27)$$

where $sf_{st,0}$ is the basic scaling factor and S_{max} is the average maximum stack size. The main values to evaluate the scaling effects are reported in Table 11. The future increase in S_{max} due to learning effects is assessed using the stack learning rates that have been previously introduced.

Table 11: Main parameters to assess economy-of-scale effects on electrolyzer CAPEX [160].

	Alkaline	PEM	SOEC
Stack basic scaling factor, $sf_{st,0}$	0.88	0.89	0.87
Aux. scaling factor, sf_{aux}	0.68	0.71	0.73
Maximum stack size, 2020 ($S_{max,2020}$) [kW _{el}]	3000	1200	500
Maximum stack size, 2030 ($S_{max,2030}$) [kW _{el}]	4000	2000	1000

The combination of learning and scaling effects is considered in the tool, where the system CAPEX can be obtained for a determined year and size, knowing the CAPEX for a 1 MW_{el} system in 2021. However, as explained in Section 5.2, the user has the possibility to overwrite the system CAPEX for any specific year and size, disregarding the suggested projections. The general formula used in the tool is here reported for the sake of completeness. It describes both learning and scaling effects, combining Equations (22), (26), and (27).

$$c_{el} = c_{ref} \cdot \left[\%_{st2sys} \cdot (1 + AGR)^{-(t-t_0) \cdot \log_2(1-LR_{st})} \cdot \left(\frac{S}{S_{ref}} \right)^{(1-sf_{st,0}) \cdot e^{-S/S_{max}}} + (1 - \%_{st2sys}) \cdot (1 + AGR)^{-(t-t_0) \cdot \log_2(1-LR_{aux})} \cdot \left(\frac{S}{S_{ref}} \right)^{sf_{aux}-1} \right] \quad (28)$$

Operational expenses and stack replacement costs

The operational expenses are a fixed annual value, calculated as a percentage of the initial investment. In particular, the value considered in this study is 1.5% of the electrolyzer initial investment, regardless of the electrolyzer technology [3]. The OPEX does not include neither the stack replacement nor the electricity costs. The stack is assumed to be replaced after a certain time, usually suggested by the producer or by the literature. In Table 12, the average stack lifetimes for different electrolyzer technologies are reported, with reference to both year 2020 and 2030. The technological advancement effect is projected with the relation presented in Equation (24).

Table 12: Stack lifetime for different electrolyzer technologies [3], [162].

	Alkaline	PEM	SOEC
Stack lifetime, 2020 [hours]	95000	74000	20000
Stack lifetime, 2030 [hours]	95000	78000	50000

Electricity cost

The cost of the electricity input is considered with two different methodologies, whether the necessary power comes from the grid or from a dedicated renewable energy plant. The cost for grid electricity is added to the annual costs in the cash-flow chart and is calculated in a year t as:

$$C_{electricity,t} = P_{electricity,t} \cdot CF^* \cdot 8760 \quad (29)$$

where $P_{electricity,t}$ is the grid electricity price in €/kWh_{electricity} and CF^* is the electrolyser capacity factor. When the electrolyzer is directly connected to the grid, it is assumed to work constantly. Considering the annual maintenance, CF^* is equal to 95% [169]. The grid electricity price is extrapolated from Alvarado and Buitrago [170] for each year and country considered, and reported in Appendix III.

If the electricity comes directly from a coupled RE plant, the electricity cost is not considered in the cash-flow analysis, but only added later in Equation (14)⁵, that becomes:

$$LCOH_p = \frac{\sum_{n=0}^N \frac{c_n}{(1+d)^n}}{\sum_{n=0}^N \frac{q_{H2,n}}{(1+d)^n}} + LCOE \cdot \frac{LHV_{H2}}{\eta_{el}} \quad (30)$$

The LCOE is calculated as explained in Section 5.3.3. In particular, the RE sources considered are solar PV, onshore and offshore wind. The capital expenses of such systems are also subject to learning effects, hence Equation (10) is adopted, assuming that the learning curve is valid for the entire system. Table 13 and Table 14 summarize the main input for the LCOE calculations.

Table 13: Renewable electricity sources, general data [171]. Similar values can be found in [172].

	Solar PV	Onshore wind	Offshore wind
System CAPEX, 2017⁶ [€/kW]	750	1218	3126
System CAPEX, 2030 [€/kW]	435	924	2314
OPEX [% of CAPEX]	1.5%	2.5%	3.5%
Nominal discount rate, d_n	7%	7%	7%
Lifetime, LT [years]	30	25	25

Table 14: Renewable electricity sources, learning effect data concerning capital costs. Own elaboration from [173]–[175].

	Solar PV	Onshore wind	Offshore wind
Learning rate, LR	18%	10%	15%
Learning index, b	0.29	0.15	0.23
Annual growth rate, AGR	16%	15%	11%

Water cost

The tool includes the calculations of the cost of water needed for electrolysis. Based on the stoichiometry of the reaction, 9 kg of water are fed for every kilogram of hydrogen produced [176]. Consequently, the annual cost of water per kW of hydrogen is equal to:

$$c_{H2O} \left[\frac{\text{€}}{\text{kWh}_{H2,LHV} \cdot a} \right] = c_{H2O} \left[\frac{\text{€}}{L_{H2O}} \right] \cdot \frac{m_{H2O}}{m_{H2}} \cdot q_{H2}$$

⁵ This is done to avoid accounting twice for the time value of money.

⁶ CAPEX values extrapolated from lower projection of Ram *et al.* [171] for EU and adjusted for inflation, reporting them to €₂₀₂₁.

Despite the water cost calculations are present in the tool, it is assumed that the water cost is negligible in this study. In fact, it has been demonstrated that the feedwater, both from fresh water supply and desalination plants, has a low impact on the overall costs [176]–[178].

Revenues from oxygen sale

Hydrogen is not the only product of water electrolysis but also oxygen is produced. Oxygen has several applications, especially in medical fields, with an already existing market. For this reason, additional revenues can come from the sale of oxygen from electrolysis, with the advantage of having a cleaner, more pure and decentralized supply compared to the current state [179]. The additional revenues, accounted as a negative cost in the electrolysis cashflow, are calculated as:

$$r_{O_2} \left[\frac{\text{€}}{kW_{H_2, LHV} \cdot a} \right] = -p_{O_2} \left[\frac{\text{€}}{kg_{O_2}} \right] \cdot \frac{m_{O_2}}{m_{H_2}} \cdot q_{H_2}$$

Based on the reaction stoichiometry, 8 kg of oxygen are produced per kilogram of hydrogen [179]. However, if the hydrogen market reaches the forecasted size, the simultaneously produced oxygen would exceed by far its demand, waning the advantages of the additional revenue. Therefore, these revenues are assumed to be negligible in this analysis.

5.4.2 Steam methane reforming

The SMR process can produce hydrogen with different levels of carbon emissions. The tool models three different modes of operation, originating from the combination of two factors: the presence or not of a carbon capture plant; and the choice of the process fuel, between natural gas and recirculated hydrogen. It should also be noted that the choice of the process fuel affects the position and the efficacy of the capture devices: in the former case, CO₂ is separated from the SMR flue gas; in the latter, from the shifted stream. The plant configuration follows the examples of Collodi *et al.* [9], as also summarized in Section 4.1.1. Figure 15 shows the possible combinations, with the related CO₂ emissions and natural gas need.

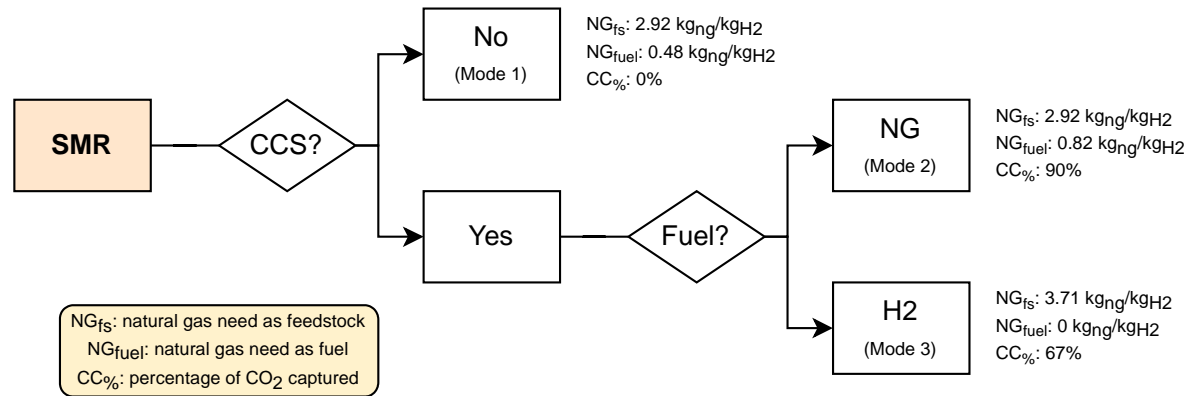


Figure 15: SMR modes, with related CO₂ emissions and natural gas need. Own elaboration, data from [9]. Similar data and configurations in [180], [181].

The hydrogen production does not depend on the chosen mode, since all the values refer to the plant output capacity parameter. The annual hydrogen production is equal to:

$$Q_{H_2} = \frac{P_{H_2} \cdot CF \cdot 8760h}{LHV_{H_2}}$$

where P_{H2} is the nominal production capacity, usually expressed in $\text{kW}_{H2,LHV}$ as discussed earlier. Hence, the annual hydrogen production per unit of capacity is:

$$q_{H2} \left[\frac{\text{kg}_{H2}/a}{\text{kW}_{H2,LHV}} \right] = \frac{Q_{H2}}{P_{H2}} = \frac{CF \cdot 8760h}{LHV_{H2}} \quad (34)$$

The capacity factor is independent of the SMR mode and corresponds to 95% [3], [9]. Instead, the costs are directly and indirectly influenced by the choice of the mode and need further elaboration. The break down of the SMR costs is as follows:

- Capital and operational expenses
- Natural gas cost
- CO₂ price, either from emission trading system or carbon tax
- CO₂ transportation-and-storage costs
- Revenues from combined steam turbine electricity

Capital and operational expenses

The CAPEX of a SMR plant can be divided between conventional plant components and the carbon capture plant. As for electrolysis, the notion of economy of scale influences the plant CAPEX, both due to learning and scaling effects. The learning effects include only the capture part, since it is assumed that the conventional plant components are well-established technologies and a decrease in their cost is not forecastable ($LR_{conv} = 0$). On the other hand, the scaling effect concerns the plant as a whole. The reference case is a 300 $\text{MW}_{H2,LHV}$ SMR plant in 2021. The combination of learning and scaling effects is described with the following equation:

$$c_{SMR} = \left[c_{conv,t_0,S_{ref}} \cdot (1 + AGR)^{-(t-t_0) \cdot \log_2(1-LR_{conv})} + c_{cc,t_0,S_{ref}} \cdot (1 + AGR)^{-(t-t_0) \cdot \log_2(1-LR_{cc})} \right] \cdot \left(\frac{S}{S_{ref}} \right)^{sf-1} \quad (35)$$

where the abbreviations *conv* and *cc* refer respectively to conventional and carbon capture components. The capital expenses are summarized in Table 15, while the learning and scaling factors are reported in Table 16.

Table 15: Capital expenses for a SMR reference plant (300 $\text{MW}_{H2,LHV}$ in 2021) [9]⁷. Similar values in [3], [180], [181].

		Mode 1	Mode 2	Mode 3
		NG-fueled	NG-fueled	H2-fueled
		No CCS	90% CCS	67% CCS
c_{conv} (2021, 300 MW plant)	[€/kW _{H2,LHV}]	612.7	612.7	668.2
c_{cc} (2021, 300 MW plant)		0	481.6	150.7

Table 16: Learning and scaling factors for different components of a SMR plant.

	Conventional components	CO ₂ capture plant	Source
Learning rate, LR	0%	11%	[161]
Annual growth rate, AGR	0%	38%	Own calculations, from [3], [161]
Scaling factor, sf		0.68	[180]

⁷ CAPEX values extrapolated from Collodi *et al.* [9], normalized to unitary plant capacity ($\text{kW}_{H2,LHV}$), and adjusted for inflation, reporting them to €₂₀₂₁.

The operational expenses, excluding gas and carbon costs, are calculated as percentage of the overall plant CAPEX and are equal to 3.9% [9].

Natural gas cost

Natural gas is the main energy input of a SMR facility, therefore its cost has a large impact on the plant economics. The annual natural gas consumption per unit of capacity is equal to:

$$q_{ng} \left[\frac{kWh_{ng,HHV}/a}{kW_{H2,LHV}} \right] = \left(q_{ng,fs} \left[\frac{kg_{ng}}{kg_{H2}} \right] + q_{ng,fuel} \left[\frac{kg_{ng}}{kg_{H2}} \right] \right) \cdot CF \cdot 8760h \cdot \frac{HHV_{ng}}{LHV_{H2}} \quad (36)$$

where $q_{ng,fs}$ and $q_{ng,fuel}$ are respectively the gas need as feedstock and as fuel per unit of output. These values are reported in Figure 15. It is worth mentioning that the energy units for natural gas refer to its higher heating value (HHV). The cost associated to the natural gas consumption are easily calculated:

$$c_{ng} = P_{ng} \cdot q_{ng} \quad (37)$$

where P_{ng} is the natural gas price, in €/kWh_{ng,HHV}. The natural gas price is interpolated from calculations of A. Kies⁸ (see methodology and summary in Appendix IV) and is reported for different countries in Appendix III.

CO₂ price and CO₂ transportation-and-storage costs

Together with hydrogen, CO₂ is a considerable by-product of the SMR process. A typical plant usually generates a yearly amount of emissions that is equal to:

$$q_{C,tot} = EF_{ng} \cdot q_{ng} \quad (38)$$

where EF_{ng} is the natural gas emission factor (50.5 t_{CO2}/TJ_{ng,HHV} = 2.6 kg_{CO2}/kg_{ng} [182]). A part of these emissions always gets released into the atmosphere, even in the least carbon intensive SMR case. For this reason, an emission surcharge needs to be added to the overall costs. The CO₂ emitted to the atmosphere in a year is equal to:

$$q_{C,em} = q_{C,tot} \cdot (1 - CC_{\%}) \quad (39)$$

where $CC_{\%}$ is the percentage of CO₂ captured, as reported in Figure 15. The emission tax or price P_C on the total costs is calculated in the following way:

$$c_{C,em} = P_C \cdot q_{C,em} \quad (40)$$

The captured fraction also has an associated cost, due to its transportation and storage:

$$c_{C,T\&S} \left[\frac{\text{€}}{kW_{H2,LHV}} \right] = c_{C,T\&S} \left[\frac{\text{€}}{t_{CO2}} \right] \cdot q_{C,T\&S} = c_{C,T\&S} \left[\frac{\text{€}}{t_{CO2}} \right] \cdot q_{C,tot} \cdot CC_{\%}$$

⁸ Industrial partner (Scania AB)

Table 17 shows the CO₂ transportation-and-storage costs for different locations.

Table 17: CO₂ transportation-and-storage costs for different locations [183]⁹. Similar values in [184], [185].

Reference denomination	Corresponding countries in this analysis	CO ₂ T&S cost [€/t _{CO2}]
Tier 1	Qatar	9.5
Tier 2	Australia	13.5
Tier 3	Algeria	21.9
Tier 4	EU, Norway	30.3

Revenues from combined steam turbine electricity

The SMR process produces excess steam, that can be converted to electricity in a steam turbine island. The electricity revenues are accounted as a negative cost:

$$c_{el} = p_{el,feed-in} \cdot el_{cons} \cdot q_{H2}$$

(42)

where $p_{el,feed-in}$ is the electricity feed-in tariff and el_{cons} is the electricity consumption. Since the SMR plant is a net electricity producer, this value is negative. Table 18 reports the electricity consumption values for the different modes.

Table 18: Electricity consumption of a SMR plant, for the three different modes considered [9].

	Mode 1	Mode 2	Mode 3
	NG-fueled No CCS	NG-fueled 90% CCS	H2-fueled 67% CCS
el_{cons} [kWh _{el} /kg _{H2}]	-1.10	-0.17	-0.05

To simplify the analysis, given the moderate impact of electricity revenues on the overall SMR costs, it has been assumed that the plant does not sell electricity to the grid, setting all the feed-in electricity tariffs to zero.

5.4.3 Pyrolysis

The pyrolysis process can present different configurations, as described in Section 4.1.2. It has been preferred to limit the modelling to the molten metal process, given the simplicity of the system and the availability of detailed information in the literature. With the objective of studying a completely CO₂-free process, a hydrogen-fired layout is selected, since other fuel supply options (electricity, natural gas) have indirect emissions. An electric arc configuration coupled with renewables would also have zero emissions, but it has been considered beyond the scope of this work given the higher degree of complexity. The annual hydrogen production is calculated similarly to the SMR one, keeping in mind that this value is normalized to the nominal production capacity, in kW_{H2,LHV}:

$$q_{H2} \left[\frac{kg_{H2}/a}{kW_{H2,LHV}} \right] = \frac{CF \cdot 8760h}{LHV_{H2}}$$

(43)

⁹ CO₂ T&S cost extrapolated from the Base Case in Smith *et al.* [183] and converted from \$ to €.

The plant capacity factor is assumed to be 95% [37]. The pyrolysis costs considered in the analysis can be divided into:

- Capital and operational expenses
- Natural gas cost
- Solid carbon cost (revenues from its sale v disposal costs)

The electricity consumption, and subsequently its costs, have been neglected given the small impact on the total cash flow for this pyrolysis configuration [43].

Capital and operational expenses

The capital cost for a 200-ktpa, molten-metal pyrolysis plant in 2022, fueled with hydrogen, is 538 M€, equivalent to 708 €/kW_{H₂,LHV} [43]. Comparable CAPEX values can be also found in Timmerberg *et al.* [45]. In this case, learning curves are not used, given the early development stage of the pyrolysis process. Instead, following the analysis of Parkinson *et al.* [43], the concept of Lang factor is introduced: the total cost of equipment is multiplied by a Lang factor that depends on the technology readiness level, resulting in the plant CAPEX. The total cost of equipment is approximated to correspond to the total CAPEX, with a similar assumption as in Parkinson *et al.* [43]. The CAPEX in 2022 corresponds to a Lang factor of 10 (first-of-a-kind). It is assumed that the Lang factor decreases linearly to 6 (nth-of-a-kind) in 2030, translating to an investment cost of 425 €/kW_{H₂,LHV}. The operational expenses are expressed as a percentage of the CAPEX and are equal to 5% [43].

Natural gas cost

Natural gas is the only input of the process, therefore its price is an important driver of the overall LCOH. The natural gas annual consumption is equal to:

$$q_{ng} \left[\frac{kWh_{ng,HHV}/a}{kW_{H_2,LHV}} \right] = q_{ng} \left[\frac{kg_{ng}}{kg_{H_2}} \right] \cdot q_{H_2} \left[\frac{kg_{H_2}/a}{kW_{H_2,LHV}} \right] \cdot HHV_{ng} \quad (44)$$

and its annual related cost as it follows:

$$c_{ng} = P_{ng} \cdot q_{ng} \quad (45)$$

where q_{ng} is the quantity of natural gas per mass of hydrogen produced, equal to 4.86 kg_{ng}/kg_{H₂} [43], [45]; and P_{ng} is the natural gas price, with its values for different countries summarized in Appendix III.

Solid carbon cost

Hydrogen and solid carbon are the only products of the pyrolysis reaction. For every kg of hydrogen, 3 kg of solid carbon are produced [37], [45]. This means that the solid carbon generated is as follows:

$$q_c \left[\frac{kg_c}{kW_{H_2,LHV}} \right] = y_c \cdot q_{H_2} \left[\frac{kg_{H_2}}{kW_{H_2,LHV} \cdot a} \right] \quad (46)$$

The solid carbon can then be either disposed, with associated costs, or sold, with associated revenues.

$$c_c \left[\frac{\text{€}}{kW_{H_2,LHV}} \right] = q_c \cdot c_c \left[\frac{\text{€}}{kg_c} \right] \quad (47)$$

The carbon cost can hence have a negative (sale) or positive (disposal) value. In this analysis, the presence of a solid carbon market can be selected or not by the user. If a solid carbon market exists, its price is assumed to be 0.95 €/kg [186]. Otherwise, a price equal to 0 €/kg is used.

5.5 Storage

The tool differentiates between a hydrogen final storage in its gaseous form, and an intermediate one, in the form of liquid hydrogen or ammonia.

5.5.1 Final storage

The final storage stage in the model represents a general storage terminal that serves as a buffer related to hydrogen supply chain security issues, as explained in Section 4.2.

5.5.1.1 System overview

In the final storage stage, only gaseous hydrogen storage is considered, compressed either into a storage tank or a geological reservoir. The stationary storage tanks considered in the tool are divided into high-pressure steel tanks (type I) [63] and high-pressure composite tanks (type II, III, and IV) [63]. Although composite tanks are mostly used for mobile applications, they are considered for stationary purposes in this model because they are foreseen to handle the problem of the space management [33] [27]. Unconventional hydrogen storage tanks (type II, III, and IV) can cover reduced areas when compared to conventional hydrogen storage tanks (type I). The reason behind this is the high operating pressures of such tanks that in turn leads to a more compact design [63] [58]. The stationary geological reservoirs are instead divided into porous media (depleted NG or oil reservoirs and aquifers) and caverns (salt caverns and rock caverns) [187, p. 1].

5.5.1.2 Storage sizing

The storage sizing for storage tanks and geological reservoirs follows the same reasoning. However, the biggest difference is the consideration of cushion gas in geological reservoirs. This factor adds on an increased volume to the overall storage capacity. Storage is sized based on the amount of hydrogen produced by the generating plant and the time duration that the hydrogen is expected to stay in the tank or reservoir. Figure 16 represents the possible choices in the Excel tool. Each choice represents one storage size which is linked to a certain storage time duration. For example, the case of daily storage is classified based on the small-scale and short-term hydrogen storage. Whereas, for the case of seasonal storage (1), the classification is based on large-scale and long-term hydrogen storage.

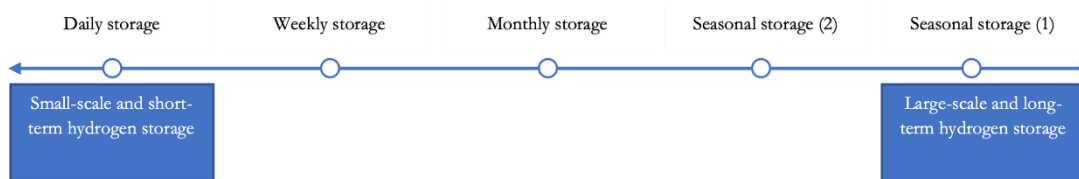


Figure 16: Classification of the different cases with respect to their capacity and time duration of each cycle.

Looking closely to Table 19, it is possible to note that for each of the considered cases there is an associated number of cycles, a time duration for the stored hydrogen in the tank or reservoir and a loading time. Considering the monthly storage case, there are 12 cycles per year and the time duration of storage is equal to the duration of complete full cycle, which is one month, or more precisely 730 hours in this case. Finally, the loading time required is about 365 hours. The loading time¹⁰ is assumed to be fifty percent of the storage time duration of the gas in the tank or reservoir [188]. This relation between loading time and full

¹⁰ is the time needed to charge all the amount of hydrogen in the tank or reservoir

cycle time duration is represented in Figure 17. The high charging and discharging time assumed in the model take into consideration the competing advantage of energy storage in the form of hydrogen which benefits from longer discharge rates as opposed to energy storage in batteries which are characterized by having fast discharge rates [188]. This assumption can meet the specific purpose of seasonal storage by discharging the stored hydrogen for an extensive period of time [188].

Table 19: Hydrogen storage for different time durations.

	N° of cycles per year	$t_{duration}/t_{cycle}$ [h]	Loading time [h]
Seasonal storage (1)	1	12 months \Leftrightarrow 365 days \Leftrightarrow 8760 hours	4380
Seasonal storage (2)	2	6 months \Leftrightarrow 182 days \Leftrightarrow 4380 hours	2190
Monthly storage	12	1 month \Leftrightarrow 30 days \Leftrightarrow 730 hours	365
Weekly storage	52	1 week \Leftrightarrow 7 days \Leftrightarrow 168 hours	84
Daily storage	365	1 day \Leftrightarrow 24 hours	12

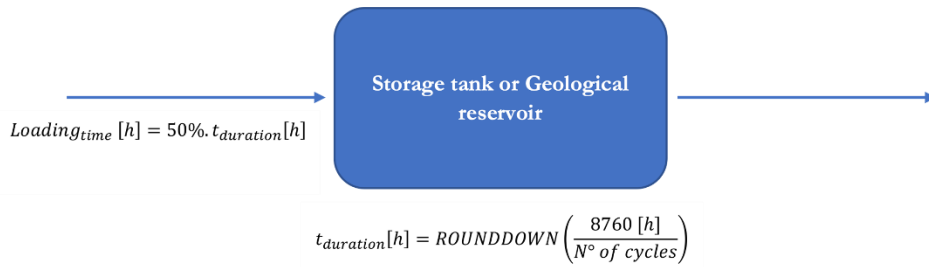


Figure 17: General diagram representing the relation between loading time and the storage time duration in the tank/reservoir.

Before starting to list the formulas used for the sizing calculations in the model, a constant hourly hydrogen production rate throughout the year is assumed since it is only possible to obtain the total amount of hydrogen produced in a year from the production stage. Furthermore, equation (48) gives the amount of hydrogen to be stored.

$$(C_{storage})_j [t_{H_2}] = \frac{Q_{H_2} [t_{H_2}/a]}{8760 [h]} \cdot Loading_{time} [h] \quad (48)$$

where:

- $j \in \left[\begin{array}{l} \text{Seasonal storage (1); Seasonal storage (2); Monthly storage;} \\ \text{Weekly storage; Daily storage} \end{array} \right]$
- Q_{H_2} is the net annual production of hydrogen.

The total volume of the desired tank is then calculated with help of the density formula, as described in equation (49).

$$Volume_{storage\ tank\ desired} [m^3] = \frac{(C_{storage})_j [t_{H_2}] \cdot 1000}{\rho_{H_2} \left[\frac{kg}{m^3} \right]} \quad (49)$$

where ρ_{H_2} is the hydrogen's density. This will depend on the temperature and pressure of the storage tank. For both storage tanks and geological storage, the considered pressure is the average pressure between the maximum and minimum values for each storage technology. The hydrogen density is obtained by using *CoolProp*, which is an open source thermophysical property library [189], [190].

Table 20: Hydrogen gas density per type of storage tank.

Type of storage tank	Temperature [°C]	Ref.	Pressure [bar]	Ref.	$\rho_{H_2} \left[\frac{kg}{m^3} \right]$	Ref.
Type I	25		200-300; (Avg. 250)	[62]	17.60	
Type II	25	[188]	250	Same as Type I	17.60	<i>CoolProp</i> [189], [190]
Type III	25		200-450; 700 (w/ some issues); (Avg. 325)	[62]	21.95	
Type IV	25		200-1000; (Avg. 600)		35.21	

In the case of geological storage, the total volume of the desired reservoir is, once again, obtained with the help of the density formula. However, there is an added cushion gas volume to the working gas volume, as shown in Equation (50).

$$\begin{aligned}
 & \text{Volume geological storage reservoir desired [m}^3\text{]} = \\
 & = \text{Working gas volume [m}^3\text{]} + \text{Cushion gas volume [m}^3\text{]} = \\
 & = \left(\frac{(C_{storage})_j [t_{H_2}] \cdot 1000}{\rho_{H_2} \left[\frac{kg}{m^3} \right]} \right) / (1 - \text{cushion gas}_{\%})
 \end{aligned}
 \tag{50}$$

where *cushion gas*_% is the cushion gas ratio, which varies with the type of geological storage selected in the tool. The values presented in Table 21 are applied for each of the three studied countries. However, the tool gives the possibility to edit them country by country, allowing a direct dependence on the storage location.

Table 21: Hydrogen gas density per type of geological reservoir.

Type of geological storage	Temperature [°C]	Ref.	Pressure [bar]	Ref.	$\rho_{H_2} \left[\frac{kg}{m^3} \right]$	Ref.
Depleted NG or Oil Reservoir	30-40; (Avg. 35)		15-285; (Avg. 150)		10.84	
Salt Cavern	30-40; (Avg. 35)	[191]	35-210; (Avg. 122.5)	[73]	8.99	<i>CoolProp</i> [189], [190]
Lined Rock Cavern (LRC)	30-40; (Avg. 35)		20-200; (Avg. 110)		8.13	
Aquifer	30-40; (Avg. 35)		30-315; (Avg. 172.5)		12.31	

5.5.1.3 CAPEX

Following Reuß *et al.* [49] and Wade A. Amos [192], the investment costs are obtained by the scaling functions following the scaling effect method, as defined in Section 5.3.2. The formula for assessing the capital expenditures varies for tank storage and geological storage. In the case of storing hydrogen in high-pressure tanks, the cost is adjusted both for different sizes and different pressures [192]. On the contrary, the cost of high-pressure geological reservoirs is associated with the change in volume sizes, independently of the operating pressure in the reservoir [192]. This is due to the fact that the operating pressure of the geological reservoirs is dependent on the specific conditions of each site and can differ a lot from one location to another [32, p. 3].

Tank storage

The scaling effect behavior of the capital expenditures formula is limited to the maximum design volume of each type of storage tank. This means that if the total volume of the desired tank, calculated in subdivision 5.5.1.2, is lower or equal to the maximum design volume of the selected tank, only one storage tank is required to store the amount of hydrogen produced (eq. (51)). If the total volume of the desired tank is bigger than the maximum design volume of the selected tank, then more than one tank are required to store the amount of hydrogen produced, with one or more tanks that have the maximum design volume and one extra smaller tank to store the remaining hydrogen produced (eq. (52)).

Table 22: Maximum design volume per type of storage tank [193].

	Tank – Type I	Tank – Type II	Tank – Type III	Tank – Type IV
Max. design volume [m³]	4500	4500	4500	4500

If Volume storage tank desired \leq Max. design volume:

$$CAPEX [\text{€}] = \text{Cost base storage tank} \cdot \left(\frac{\text{Volume storage tank desired}}{\text{Volume base storage tank}} \right)^{s.f.} \cdot \left(\frac{\text{pressure desired}}{\text{pressure base storage tank}} \right)^{s.f.'} \quad (51)$$

If Volume storage tank desired $>$ Max. design volume:

$$CAPEX [\text{€}] = n'_{tanks} \cdot \left(\text{Cost base storage tank} \cdot \left(\frac{\text{Max. design volume}}{\text{Volume base storage tank}} \right)^{s.f.} \cdot \left(\frac{\text{pressure desired}}{\text{pressure base storage tank}} \right)^{s.f.'} \right) + \left(\text{Cost base storage tank} \cdot \left(\frac{(n_{tanks} - n'_{tanks}) \times \text{Max. design volume}}{\text{Volume base storage tank}} \right)^{s.f.} \cdot \left(\frac{\text{pressure desired}}{\text{pressure base storage tank}} \right)^{s.f.'} \right) \quad (52)$$

Where:

- *Volume storage tank desired* is the total size of the tank desired to final storage
- *s.f.* is the storage tank cost scaling factor
- *s.f.'* is the storage tank pressure factor
- n_{tanks} is the number of tanks with maximum design volume:

$$n_{tanks} = \frac{\text{Volume storage tank desired}}{\text{Max. design volume}} \quad (53)$$

- n'_{tanks} is the number of tanks with maximum design volume (rounded to the unit number):

$$n'_{tanks} = \text{ROUNDDOWN} \left(\frac{\text{Volume storage tank desired}}{\text{Max. design volume}} \right)$$

(54)

Table 23: Economic parameters for each type of storage tank.

	Type of storage tank							
	Tank – Type I	Ref.	Tank – Type II	Ref.	Tank – Type III	Ref.	Tank – Type IV	Ref.
Cost base [M€] *	0.02 ¹¹	[194]	0.02 ¹¹	[194]	0.04	[195]	0.04	[195]
Size base [m ³]	2.11 ¹²	[194]	2.11 ¹²	[194]	2.11 ¹²	[194]	2.11 ¹²	[194]
Pressure base storage tank [bar]	160	[194]	160	[194]	160	[194]	160	[194]
s.f.	0.9 ; 0.95	[188], [196]	0.9 ; 0.95	[188], [196]	0.9 ; 0.95	[188], [196]	0.9 ; 0.95	[188], [196]
s.f. ²	0.44	[192]	0.44	[192]	0.44	[192]	0.44	[192]

Note: The values in bold are the selected values introduced in the model.

Large-scale and long-term hydrogen storage in pressure vessels have not been widely considered in hydrogen supply chain studies. To meet this purpose, more effort is put on the evaluation of geological reservoirs [49]. The few existing studies consider metal tanks for stationary storage of hydrogen. In other words, most of the costs in literature for hydrogen storage tanks are relevant to type I and type II tanks, while type III and IV tanks are disregarded because of the high price of carbon/glass fiber composites [195]. However, Elberry et al. [195] stated that the cost of type III tanks can be estimated to be double the price of type II tanks. At the same time, Hassan *et al.* [63] and Barthélémy [58] rank the cost performance of the four different types of compression vessels in Table 24.

Table 24: Cost performance of tank storage.

	Tank – Type I	Tank – Type II	Tank – Type III	Tank – Type IV
Cost performance	++	+	–	–

Note: (–) being a bad rating, still room for improvement; (+) being a good rating, costly appealing.

Geological storage

Two design constraints addressed in the model are the minimum [197] and maximum geological reservoir size [73]. These constraints are dependent on the type of geological storage and its location [73] [198]. Mainly due to lack of available data and to ease the calculations, it was assumed the same minimum and maximum geological reservoir size for all the four different technologies. It is never enough to stretch that the model is built for future usage, so that further adjustments to these parameters can and should be done when more data is available. The size capacities of the reservoirs in between the maximum and minimum geological reservoir sizes are considered to gather the necessary structural integrity and stability properties for the normal operation of the underground storage facility [73]. Defining a minimum geological reservoir size in the model can also be interpreted as a guarantee that building an underground hydrogen storage facility only makes sense for large-scale applications [199]. The values presented in Table 25 are valid for each of the three studied countries. However, the tool gives the possibility to edit them country by country, allowing a direct dependence on the storage location.

¹¹ Values converted from \$ to € and adjusted for inflation, reporting them to €₂₀₂₁.

¹² $\rho_{H_2}(T = 25^\circ C, p = 160bar) [kg/m^3] = \frac{m [kg]}{V [m^3]} \Leftrightarrow V = \frac{25}{11.854}$

Table 25: Minimum and maximum design volume per type of geological reservoir.

Type of geological storage	Min. geo. reservoir size [m ³]	Ref.	Max. geo. reservoir size [m ³]	Ref.
Depleted NG or Oil Reservoir				
Salt Cavern	7000	[200]	1000000	[33], [77]
Lined Rock Cavern				
Aquifer				

Similar to the calculations of the capital expenditures for pressure tanks, the cost of geological reservoirs is dependent on a set of conditional statements that relate the total volume of the desired reservoir (calculated in the previous subdivision) to the minimum and maximum geological reservoir size. If the total volume of the desired reservoir is lower than the minimum geological reservoir size, it is defined one and only one reservoir with the minimum geological reservoir size even though the total amount of hydrogen to be stored is less than the minimum capacity. For this conditional statement, the reservoir is clearly being oversized (eq. (55)). If the total volume of the desired reservoir is in between the minimum and the maximum geological reservoir size, it is only required one reservoir to store the amount of hydrogen produced (eq. (56)). If the total volume of the desired reservoir is bigger than the maximum geological reservoir size, it is required more than one reservoir to store the amount of hydrogen produced which one or more reservoirs have the maximum geological reservoir size and one extra small reservoir (but not smaller than the minimum geological reservoir size) to store the remaining hydrogen produced that could not fit in the reservoir(s) with maximum design capacity (eq. (57)).

If Volume geo. storage reservoir desired < Min. geo. reservoir size:

$$CAPEX [\text{€}] = \text{Cost base geological storage reservoir} \cdot \left(\frac{\text{Min. geo. reservoir size}}{\text{Volume base geo. storage reservoir}} \right)^{s.f.} \quad (55)$$

If Min. geo. reservoir size ≤ Volume geo. storage reservoir desired ≤ Max. geo. reservoir size:

$$CAPEX [\text{€}] = \text{Cost base geological storage reservoir} \cdot \left(\frac{\text{Volume geo. storage reservoir desired}}{\text{Volume base geo. storage reservoir}} \right)^{s.f.} \quad (56)$$

If Volume geo. storage reservoir desired > Max. geo. reservoir size:

$$CAPEX [\text{€}] = n'_{reservoirs} \cdot \left(\text{Cost base geological storage reservoir} \cdot \left(\frac{\text{Max. geo. reservoir size}}{\text{Volume base geo. storage reservoir}} \right)^{s.f.} \right) + \left(\text{Cost base geological storage reservoir} \cdot \left(\frac{(n_{reservoirs} - n'_{reservoirs}) \cdot \text{Max. geo. reservoir size}}{\text{Volume base geo. storage reservoir}} \right)^{s.f.} \right) \quad (57)$$

where:

- *Volume geological storage reservoir desired* is the total size of the geo. storage reservoir desired to final storage.
- *s.f.* is the geological storage reservoir cost scaling factor.
- $n_{reservoirs}$ is the number of tanks with maximum design volume:

$$n_{reservoirs} = \frac{\text{Volume geo. storage reservoir desired}}{\text{Max. geo. reservoir size}} \quad (58)$$

- $n'_{reservoirs}$ is the number of tanks with maximum design volume (rounded to the unit number):

$$n'_{reservoirs} = \text{ROUNDDOWN} \left(\frac{\text{Volume geo. storage reservoir desired}}{\text{Max. geo. reservoir size}} \right) \quad (59)$$

Table 62 in Appendix V reports and discusses the economic values for each type of geological reservoir.

5.5.1.4 OPEX

The cost of compressing hydrogen with regard to operating pressure of the selected storage tank or geological reservoir is not considered in the specific cost of hydrogen storage ($LCOH_s$) but it is included, instead, in the specific cost of hydrogen conversion ($LCOH_c$), the total operating costs of hydrogen storage are assumed to be only fixed OPEX. Being a percentage of the total CAPEX of the reservoir ($OPEX\%$), as it is represented in equation (60). The percentage varies with the type of hydrogen storage selected, as indicated in Table 26 and Table 27.

$$OPEX [\text{€}] = OPEX\% \cdot CAPEX[\text{€}] \quad (60)$$

Table 26: Fixed operating costs per type of storage tank.

Type of storage tank	OPEX% [%]	Ref.
Type I	0.5-2.5; (Avg. 1.5)	[199]
Type II		
Type III		
Type IV		

Table 27: Fixed operating costs per type of geological reservoir.

Type of geological storage	OPEX% [%]	Ref.
Depleted NG or Oil Reservoir	4	[79]
Salt Cavern	2; 5; (Avg. 3.5)	[30], [78]
Lined Rock Cavern	4	[79]
Aquifer	5	[78]

5.5.1.5 Levelized cost of storage

The levelized cost of hydrogen storage is obtained by Equation (61) and it follows the same logic explained in Section 5.1.

$$LCOH_s \left[\frac{\text{€}}{\text{kg}_{H_2}} \right] = \frac{\sum_{n=1}^N \frac{CAPEX[\text{€}] + OPEX[\text{€}]}{(1+i)^n}}{\sum_{n=1}^N \frac{Q_{H_2}[\text{kg}_{H_2}]}{(1+i)^n}} \quad (61)$$

Since the operation and maintenance costs are fixed throughout the economic lifetime of the storage facility, the levelized cost of hydrogen with respect to storage can be simplified as:

$$LCOH_s \left[\frac{\text{€}}{\text{kg}_{H_2}} \right] = \frac{(a_0 + OPEX\%) \cdot CAPEX[\text{€}]}{Q_{H_2}[\text{kg}_{H_2}]} \quad (62)$$

The annual amount of hydrogen handled Q_{H_2} is:

$$Q_{H_2}[\text{kg}_{H_2}] = (n_{cycles})_j \cdot Q'_{H_2}[\text{kg}_{H_2}] \quad (63)$$

Where:

- n_{cycles} is the number of cycles per year varying with the time duration of storage
- $j \in \left[\begin{array}{l} \text{Seasonal storage (1); Seasonal storage (2); Monthly storage;} \\ \text{Weekly storage; Daily storage} \end{array} \right]$
- Q'_{H_2} is the hydrogen dispensed by the storage tank/reservoir per cycle, equal to:

$$Q'_{H_2} = (C_{storage})_j [t_{H_2}] \cdot 1000 \times (1 - m_{losses})$$

where $(C_{storage})_i$ is the amount of available hydrogen stored in the tank/ reservoir.

Table 28 reports the financial parameters for storage tanks.

Table 28: Financial parameters for each type of storage tank.

	Type I	Ref.	Type II	Ref.	Type III	Ref.	Type IV	Ref.
Economic lifetime [years]	20;30; (Avg. 25)	[194], [199]						
Discount rate [%]	8	Own assumption						
Mass losses [%]	0	[28]	0	Same as Type I	0	Same as Type I	0	Same as Type I

The levelized cost of storage for geological reservoirs slightly differs from the formula used for storage tanks, because it considers the additional cost of the cushion gas. The added cost of the cushion gas to the levelized cost of hydrogen storage formula was based on the work developed by Lord *et al.* [51].

$$LCOH_S \left[\frac{\text{€}}{\text{kg}_{H_2}} \right] = \frac{(a_{\%} + OPEX_{\%}) \cdot CAPEX[\text{€}] + a_{\%} \cdot C_{gas}[\text{€}]}{Q_{H_2} [\text{kg}_{H_2}]} \quad (64)$$

where C_{gas} is the cost of the cushion gas kept in the reservoir:

$$C_{gas}[\text{€}] = \left(\left(\frac{(C_{storage})_j [t_{H_2}]}{(1 - cushion\ gas_{\%})} \right) \cdot 1000 \cdot cushion\ gas_{\%} \right) \cdot Price_{H_2} [\text{€/kg}_{H_2}] \quad (65)$$

with the price of hydrogen $Price_{H_2}$ assumed to be the sum of the levelized cost of production and transmission. This sum will be dependent on the selected pathway by the user, in such manner the price of hydrogen gas will vary accordingly. Table 29 summarizes the financial parameters for each reservoir type for geological storage. As for other parameters, the values are assumed to be constant for each of the three studied countries, but the tool gives the possibility to override them for each of the studied countries: Germany, France, and Spain.

Table 29: Financial parameters for each type of geological reservoir.

Type of geological storage	Economic lifetime [years]	Ref.	Discount rate [%]	Ref.	Mass losses [%]	Ref.
Depleted NG or Oil Reservoir	40		8		1.5	[78]
Salt Cavern	40	[199]	8	[30]	0	[157]
Lined Rock Cavern	40		8		0	[157]
Aquifer	40		8		1.5	[78]

According to Bourgeois *et al.* [78], the mass losses for cyclic hydrogen storage in salt caverns are considered to be zero. Stating that there are no notable losses. At the same time van Leeuwen *et al.* [199] mentions that experience tells that for yearly hydrogen losses below 0.1% in salt caverns, the losses can be neglected.

5.5.2 Intermediate storage

The intermediate storage stage in the model represents a buffer storage in the export and import terminal for the specific type of hydrogen transmission overseas by ships.

5.5.2.1 System overview

Figure 18 illustrates an overview of the intermediate storage system. These terminals store either liquid hydrogen or liquid ammonia [27], which require large cryogenic tanks [66]. This type of tanks is particularly made to store very low temperature liquids. For this reason, these tanks usually have thick double wall with a vacuum gap between them [62], which makes it difficult for the low temperature liquid to exchange heat with the outside environment [62]. Finally, the specific cost of intermediate storage is the sum of the cost of storing liquid hydrogen or ammonia in the export and import terminals.

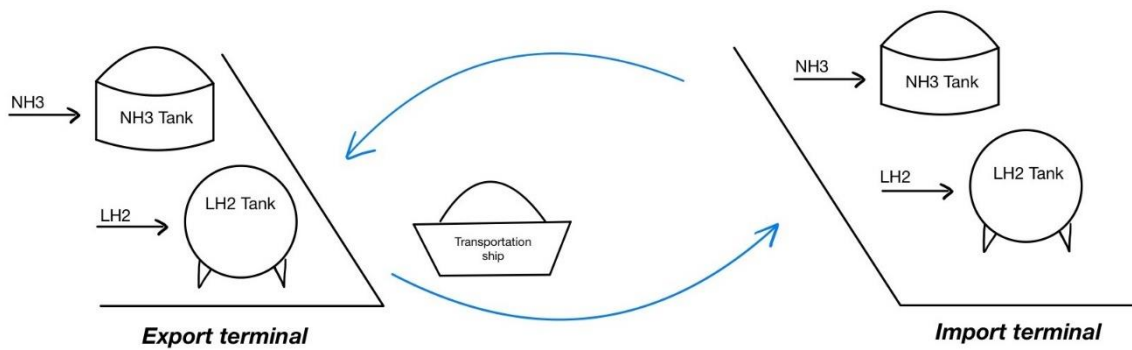


Figure 18: General diagram of intermediate storage in the hydrogen supply chain.

5.5.2.2 Storage sizing

Sizing the intermediate storage is not only dependent on the type of energy carrier, either liquid hydrogen or liquid ammonia, but also influenced by the location of the tanks (at the export or import terminal). The sizing of the cryogenic tanks for liquid hydrogen and liquid ammonia is necessarily different because, for the case of transporting liquid ammonia, in between the production site and the intermediate storage terminal, there is an ammonia synthesis plant where the net amount of hydrogen produced is converted into ammonia. In this process, hydrogen reacts with nitrogen to originate ammonia. In other words, the amount of ammonia outputted from this plant is necessarily different from the amount of hydrogen inputted in the considered plant. For a more detailed explanation, refer to subsection 5.6.4.

In order to build all the necessary infrastructure for hydrogen transportation by ship, it is important to guarantee that there is a developed market for the consumption of the imported hydrogen with multiple end use applications. In other words, due to the very high cost of export and import terminals, including conversion and reconversion plants, it is important to assure that multiple stakeholders are interested in taking advantage of the imported hydrogen [3]. For example, using the hydrogen for fueling road vehicles but also airplanes and ships, as well as utilizing the hydrogen for domestic and industrial purposes by injecting the hydrogen directly into the gas grid. With increased demand, the relative cost of infrastructure will immediately decrease and guarantee that the storage time duration at the harbor is short [3]. Having said that, the cryogenic tanks at the export and import terminals are sized to hold the liquid hydrogen or liquid ammonia for a short period of time.

As a means to arrive to Equations (66) and (67), it is important to define a set of assumptions taken in the model. As it was assumed for final storage, a constant hourly production rate is also considered throughout the year. It is also assumed that charging and discharging the cryogenic tanks occurs instantaneously. In addition, whenever the ship arrives at the port, it is immediately charged or discharged. Furthermore, there is no constraint on the number of ships available for liquid hydrogen or ammonia transportation. Finally, it is assumed that the amount of hydrogen produced is converted to liquified hydrogen without losses. This is done to lower the response time of the model and offer a smoother experience to the user. At the same time these losses are already accounted for in the conversion process of liquefaction.

Export terminal

The storage capacity at the export terminal is assessed by equation (66). It is dependent on the type of energy carrier, either liquid hydrogen or liquid ammonia, the net amount of hydrogen produced from the selected generation site, and the time duration of storage. The mathematical notation in equation (66) means that the capacity of the export terminal is either equal to the amount of hydrogen produced for a time period equal to the average time spent by the ship at the harbor ($t_{storage}$) or to the capacity transported by one ship. The equation always chooses the biggest value out of these two.

$$\begin{aligned} & \text{Storage tank capacity desired } [t_{LH_2} \text{ or } t_{NH_3}] \\ & = \max \left(\frac{Q_{H_2} [tpa] \text{ or } Q_{NH_3} [tpa]}{8760 [\text{hours}]} \cdot (t_{storage} [h]); (Q_{ship})_k [t_{LH_2} \text{ or } t_{NH_3}] \right) \end{aligned} \quad (66)$$

Where:

- $Q_{H_2} [tpa]$, net annual production of hydrogen
- $Q_{NH_3} [tpa] = m_{NH_3} [kg/a]/1000$, mass of NH3 converted from the net amount of hydrogen produced annually (this value comes from the NH3 conversion sheet in the model)
- $t_{storage} [h]$, average time spent by the ship in the harbor. The average time in the harbor is considered to be 48 hours [3], the same harbor time considered in the transmission stage by ship in the model (Section 5.7.2)
- $Q_{ship} [t]$, capacity of a single ship for liquid hydrogen/liquid ammonia
- $k \in [LH_2; NH_3]$.

Import terminal

The import terminal is sized to host the entire capacity of a single ship. This is done by assuming a well-established hydrogen market ruled by constant demand, meaning there is a constant discharge flow from the import terminal to the final consumer.

$$\text{Storage tank capacity desired } [t_{LH_2} \text{ or } t_{NH_3}] = (Q_{ship})_k [t_{LH_2} \text{ or } t_{NH_3}] \quad (67)$$

5.5.2.3 CAPEX

To be consistent with the capital expenditures assessment methodology used for the other stages of the supply chain, the investment cost of the export and import terminal follows the “scaling factor” methodology, as previously explained in Section 5.3.2.

The CAPEX formula is the same for both export and import terminals and, as explained in Section 5.5.1.3 regarding the cost of final storage, the initial investment equation for intermediate storage will vary depending on the relation between the total capacity of the desired tank, calculated in Section 5.5.2.2, and the maximum design capacity of the cryogenic tank. Table 30 shows the upper limit size capacity for cryogenic tanks storing liquid hydrogen and liquid ammonia. It is notable how high is the maximum tank capacity allowable for liquid ammonia storage compared to liquid hydrogen storage. Also verifiable in [71], work developed by DNV GL.

Table 30: Maximum design capacity per type of cryogenic tank.

	Type of hydrogen carrier			
	LH2	Ref.	NH3	Ref.
Max. tank design capacity [t]	3800; 4732; (Avg. 4300)	[201], [202]	50000	[203]

If the total capacity of the desired tank is lower or equal to the maximum design volume of the cryogenic tank, then only one storage tank is required to store the liquid hydrogen or liquid ammonia:

If $\text{Storage tank capacity desired} \leq \text{Max. tank design capacity}$:

$$\text{CAPEX } [€] = \text{Cost base storage tank} \cdot \left(\frac{\text{Storage tank capacity desired}}{\text{Storage tank base capacity}} \right)^{s.f.} \quad (68)$$

where:

- *Storage tank capacity desired* [t_{LH_2} or t_{NH_3}], total capacity needed to store in the export terminal storage tanks or in the import terminal storage tanks.
- *s.f.*, storage tank cost scaling factor.

If the total capacity of the desired tank is bigger than the maximum design volume of the cryogenic tank, then more than one tank are required to store the capacity of liquid hydrogen or ammonia required. One or more tanks have the maximum design capacity and one extra small tank is needed to store the remaining liquid hydrogen or ammonia:

If *Storage tank capacity desired* > *Max. tank design capacity*:

$$\begin{aligned}
 CAPEX \text{ [€]} = & n'_{tanks} \cdot \left(\text{Cost base storage tank} \cdot \left(\frac{\text{Max. tank design capacity}}{\text{Storage tank base capacity}} \right)^{s.f.} \right) \\
 & + \left(\text{Cost base storage tank} \right. \\
 & \cdot \left. \left(\frac{(n_{tanks} - n'_{tanks}) \cdot \text{Max. tank design capacity}}{\text{Storage tank base capacity}} \right)^{s.f.} \right)
 \end{aligned} \tag{69}$$

where:

- n_{tanks} , number of tanks with maximum design capacity:

$$n_{tanks} = \frac{\text{Storage tank capacity desired}}{\text{Max. tank design capacity}} \tag{70}$$

- n'_{tanks} , number of tanks with maximum design capacity (rounded to the unit number):

$$n'_{tanks} = \text{ROUNDDOWN} \left(\frac{\text{Storage tank capacity desired}}{\text{Max. tank design capacity}} \right) \tag{71}$$

Table 31 and Table 32 report the economic parameters, respectively for export and import terminals.

Table 31: Economic parameters for each type of cryogenic tank located in the export terminal.

	Type of hydrogen carrier			
	LH2	Ref.	NH3	Ref.
Cost base [M€]	290		68	
Size base [t]	3190	[3]	34100	[3]
s.f.	1	[192]	1	[192]

Table 32: Economic parameters for each type of cryogenic tank located in the import terminal.

	Type of hydrogen carrier			
	LH2	Ref.	NH3	Ref.
Cost base [M€]	320		97	
Size base [t]	3550	[3]	56700	[3]
s.f.	1	[192]	1	[192]

5.5.2.4 OPEX

Given that the conversion and reconversion plants are not considered in the specific cost of intermediate storage but in the specific cost of hydrogen conversion, the operation and maintenance costs only account for the fixed costs. The fixed OPEX is a percentage of the total CAPEX of the terminal ($OPEX_{\%}$), as it is represented in equation (72). The percentage varies with the type of cryogenic tank (Table 33 and Table 34). Also, it is important to mention that an additional variable operating cost could be considered in the analysis. This variable cost is related to the energy consumed to operate a pump located at the terminals, which purpose is to charge and discharge the tanks [66].

$$OPEX [\text{€}] = OPEX_{\%} \cdot CAPEX[\text{€}] \quad (72)$$

Table 33 and Table 34 report the OPEX values, respectively for export and import terminals, respectively.

Table 33: Fixed operating costs per type of cryogenic tank located in the export terminal.

	Type of hydrogen carrier			
	LH2	Ref.	NH3	Ref.
OPEX _% [%]	4; 2	[3], [71]	4; 2	[3], [71]

Table 34: Fixed operating costs per type of cryogenic tank located in the import terminal.

	Type of hydrogen carrier			
	LH2	Ref.	NH3	Ref.
OPEX _% [%]	4; 2	[3], [71]	4; 2	[3], [71]

5.5.2.5 Levelized cost of storage

The levelized cost of intermediate storage is assessed by Equation (73) and it follows the same reasoning explained in Section 5.1.

$$LCOH_s \left[\frac{\text{€}}{\text{kg}_{H_2}} \right] = \frac{\sum_{n=1}^N \frac{CAPEX[\text{€}] + OPEX[\text{€}]}{(1+i)^n}}{\sum_{n=1}^N \frac{Q_{H_2} [\text{kg}_{H_2}]}{(1+i)^n}} \quad (73)$$

Since the operation and maintenance costs are fixed throughout the economic lifetime of the storage facility, the levelized cost of hydrogen with respect to storage can be simplified as:

$$LCOH_s \left[\frac{\text{€}}{\text{kg}_{H_2}} \right] = \frac{(a_{\%} + OPEX_{\%}) \cdot CAPEX[\text{€}]}{Q_{H_2} [\text{kg}_{H_2}]} \quad (74)$$

The annual amount of hydrogen handled Q_{H_2} is equal to:

$$Q_{H_2} [\text{kg}_{H_2}] = (n_{cycles})_j \cdot Q'_{H_2} [\text{kg}_{H_2}] \quad (75)$$

where:

- n_{cycles} , number of cycles per year varying with the time duration of storage.
- $j \in [Export\ terminal; Import\ terminal]$.
- $Q'_{H_2} [kg_{H_2}]$, equivalent hydrogen dispensed by the storage tank per cycle $[kg_{H_2}]$.

Table 35 shows the formula to calculate the number of cycles endured by the tank per year based on the time duration of storing liquid hydrogen or ammonia at the port.

Table 35: Relation between the number of cycles per year in the tank and the storage time duration at the harbor.

	Time duration	N° of cycles per year
Export terminal or Import terminal	$t_{storage} [h]$	$ROUNDDOWN \left(\frac{1}{\frac{t_{storage} [h]}{8760 [h]}} \right)$

For liquid hydrogen, the equivalent hydrogen dispensed by the storage tank per cycle Q'_{H_2} is equal to:

$$Q'_{H_2} [kg_{H_2}] = (C_{storage\ desired} [t_{LH_2}])_n \cdot 1000 \cdot (1 - m_{losses}) \quad (76)$$

where:

- $C_{storage\ desired} [t_{H_2}]$ is the storage tank capacity desired
- $n \in [export\ terminal; import\ terminal]$
- m_{losses} are the mass losses related to the liquid hydrogen boil-off:

$$m_{losses} [\%] = \frac{(boil - off_{\%})_{LH_2} [\%/day]}{24 [h]} \cdot t_{storage} [h] \quad (77)$$

where $t_{storage} [h]$ is the average time spent by the ship in the harbor which is considered to be 48 hours [3], the same harbor time considered in the transmission stage by ship in the model in Section 5.7.2.

For liquid ammonia, the equivalent hydrogen dispensed by the storage tank per cycle Q'_{H_2} is equal to:

$$Q'_{H_2} [kg_{H_2}] = ((C_{storage\ desired} [t_{NH_3}])_n \cdot 0.1765) \cdot 1000 \cdot (1 - m_{losses}) \quad (78)$$

where:

- $n \in [export\ terminal; import\ terminal]$.
- 17.65%, percentage of hydrogen present in ammonia [90].
- m_{losses} , mass losses related to the liquid ammonia boil-off:

$$m_{losses} [\%] = \frac{(boil - off_{\%})_{NH_3} [\%/day]}{24 [h]} \cdot t_{storage} [h]$$

- $t_{storage} [h]$, average time spent by the ship in the harbor. The average time in the harbor is considered to be 48 hours [3], the same harbor time considered in the transmission stage by ship in the model in Section 5.7.2.

Table 36: Financial parameters for each type of cryogenic tank for the export and import terminal.

	Type of hydrogen carrier			
	LH2	Ref.	NH3	Ref.
Economic lifetime [years]	30	[3]	30	[3]
Discount rate [%]	8		8	
boil-off [%/day]	0.1	[3], [71]	0.04	[66]

As previously mentioned in subsection 4.2.1.2, there is a linear relation between hydrogen boil-off in the stationary storage tanks and their respective storage capacity suggesting a future adaptation of the model to consider the mentioned relation.

5.6 Conversion

This section describes the methodology adopted in the study for the stages of compression, liquefaction, regasification, conversion from and to ammonia.

5.6.1 Compression

The following sections present the methodology for the compression process.

5.6.1.1 System overview

To select the appropriated compressor, a handful of parameters have to be evaluated in first place. Some of these parameters are mass flow rate of the hydrogen gas, inlet pressure and temperature, as well as outlet pressure and temperature [83]. Depending on the end use application of the compressor, the set of parameters will change. Figure 19 shows an outline for every type of application that uses a compressor station provided in the Excel tool.

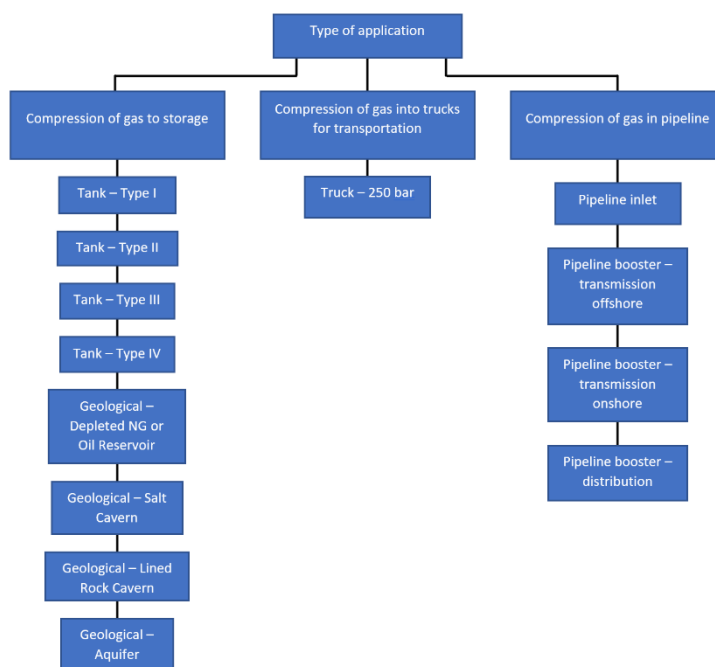


Figure 19: Considered end use applications that integrate a compressor station.

From Figure 20, it can be concluded that the technology type of the compressor is directly dependent on the capacity flow rate and compression ratio required. The cost assessment tool considers two types of compressors: multi-stage centrifugal compressor and multi-stage reciprocating compressor. The multi-

stage reciprocating compressors are used for gas compression into truck for transportation and gas storage [83] Increased operating pressures required by stationary storage technologies, led to the choose multi-stage reciprocating compressors for this end-use. Moreover, they tend to respond better to "wide-capacity swings"¹³ [204]. The multi-stage centrifugal compressors are used for gas compression in pipelines since this application has a steady workflow. At the same time, multi-stage centrifugal compressors are more suitable for higher volume flow rates.

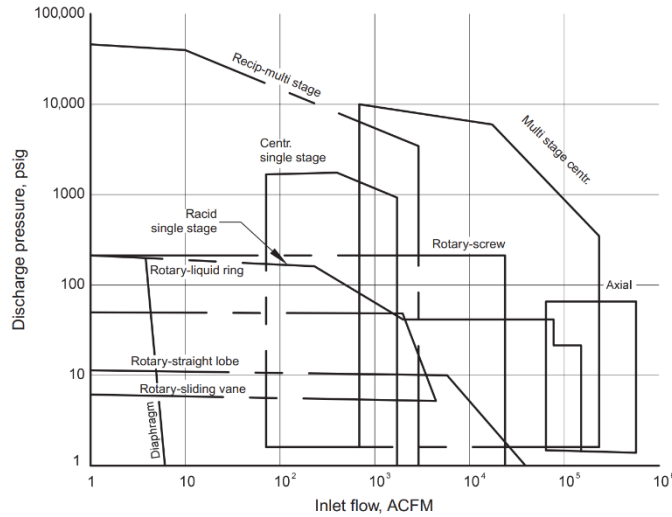


Figure 20: Type of compressor selection based on mass flow rate and discharge pressure [205].

5.6.1.2 Compressor station sizing

For a correct assessment of the compressor station size and its energy requirements, choosing the final application for the compressor is essential. Table 63 in Appendix VI indicates all the necessary pressures and temperatures with respect to the type of application for the compressor station, while Table 37 shows the formulas to calculate the capacity flow rate for each type of application.

Table 37: Capacity flow rate of the compression station per type of application.

Type of application		$Q_{compr} \left[\frac{kg}{h} \right]$
Storage	Pressure tank	$(C_{storage})_j [t_{H_2}] \cdot 1000$
	Geological storage	$\frac{Loading_{time} [h]}{Loading_{time} [h]}$
Trucks	Truck – 250 bar	$\frac{Q_{H_2, truck} \left[\frac{kg_{H_2}}{truck} \right] \cdot Routes \text{ per year (round trip)}}{8760 [h] \cdot 1 [trucks]}$
	Pipeline inlet - transmission	$\frac{Q_{H_2} [t_{H_2}/a] \cdot 1000}{8760 [hours]}$
Pipeline	Pipeline inlet - distribution	$\frac{Q_{H_2} [t_{H_2}/a] \cdot 1000 / 4}{8760 [hours]} \text{ Or } \frac{Q_{pipeline H_2} [GW] \cdot 10^6}{LHV_{H_2} \left[\frac{kWh}{kg} \right]}$

¹³ In other words, these compressors are fitted for situations where different capacity flow rates are required, instead of steady operating flow rates. These capacity swings can happen specially when producing green hydrogen due to intermittent electricity production.

¹⁴ If in transmission by sea, the selected distance is 0 km; if in transmission by land, it is 0 km; if the user selects no final storage.

Pipeline booster	$\frac{Q_{\text{pipeline } H_2} [\text{GW}] \cdot 10^6}{LHV_{H_2} \left[\frac{\text{kWh}}{\text{kg}} \right]}$
------------------	---

In Table 37, it is noticeable that the formula to calculate the capacity flow rate of the compressor for the compression of gas to storage is common to every type of storage technology. This formula is dependent on the amount of working (available) hydrogen to be stored in the tank or reservoir, $(C_{\text{storage}})_j$, where $j \in \left[\begin{array}{l} \text{Seasonal storage (1); Seasonal storage (2); Monthly storage;} \\ \text{Weekly storage; Daily storage} \end{array} \right]$, and the time needed to charge all the amount of hydrogen in the tank or reservoir, $Loading_{\text{time}}$. For the case of hydrogen compression into a transportation truck, the capacity flow rate of the compressor is dependent on the truck hydrogen storage capacity, $Q_{H_2, \text{truck}}$, and the number of routes per year.

Finally, the capacity flow rate of the compressor used in pipelines varies with the type of pipeline (transmission onshore, transmission offshore, or distribution pipeline) and with the location of the compressor station (beginning of the pipeline or along the pipeline). The capacity flow rate of the compressor at the inlet of the transmission pipeline is dependent on the net annual production of hydrogen, Q_{H_2} , because it is assumed that the compressor station is in between the production site and the transmission pipeline.

The capacity flow rate of the compressor at the inlet of the distribution pipeline is dependent on the net annual production of hydrogen, Q_{H_2} , if the transmission before distribution is zero kilometers and no final storage has been selected. Otherwise, it is dependent on the distribution pipeline design capacity referring to LHV_{H_2} , $Q_{\text{pipeline } H_2}$. The capacity flow rate of the booster compressor for transmission offshore and onshore pipeline, and distribution pipeline is calculated based on the respective pipeline design capacity with reference to LHV_{H_2} , $Q_{\text{pipeline } H_2}$.

5.6.1.3 CAPEX

Without exception, the formula to calculate the capital expenditures for hydrogen compressors obey the "scaling factor" methodology, explained in Section 5.3.2. Based on the work developed by Amin Lahnaoui *et al.* [206] and Wade A. Amos [192], the initial capital investment cost of the compressor is calculated using a scaling factor $s.f.$ to adjust from the baseline size, *Size base compressor*, and baseline cost, *Cost base compressor*. At the same time, the initial capital investment cost of the compressor uses a sizing exponent for pressure $s.f.'$ to adjust the baseline pressure, *pressure base compressor*, of the compressor selected from literature.

Considering both technical briefs of Khan *et al.* [83], [94], the CAPEX formula is dependent on a set of conditional statements that relate the rated power desired, determined in Section 5.6.1.2 to the maximum design electrical rated power, which is assumed to be 16000 kW [83]. If the calculated rated power desired of the compressor is lower or equal to the maximum design electrical rated power, then only required one compressor is required at the compressor station and the CAPEX formula is dictated by equation (79).

If Power rated desired ≤ Max. design power (16000 kW):

$$CAPEX [\text{€}] = \text{Cost base compressor} \cdot \left(\frac{\text{Power rated desired}}{\text{Size base compressor}} \right)^{s.f.} \cdot \left(\frac{\text{pressure desired}}{\text{pressure base compressor}} \right)^{s.f.'}$$

(79)

Where:

- *Power rated desired* [kW], rated power of the compressor station.
- *s.f.*, compressor cost scaling factor.
- *s.f.'*, compressor pressure factor.

If the calculated rated power desired of the compressor is bigger than the maximum design electrical rated power, then more than one compressor at the compressor station to be able to compress all the required capacity flow rate of hydrogen. In this case, there will be one or more compressors that have the maximum design electrical rated power and one extra compressor with lower power:

If Power rated desired > Max. design power (16000 kW):

$$\begin{aligned}
 CAPEX [\text{€}] = N_{max} & \cdot \left(\text{Cost base compressor} \cdot \left(\frac{\text{Power rated desired}}{\text{Size base compressor}} \right)^{s.f.} \right. \\
 & \cdot \left. \left(\frac{\text{pressure desired}}{\text{pressure base compressor}} \right)^{s.f.'} \right) \\
 & + \left(\text{Cost base compressor} \cdot \left(\frac{(N_{max} - N_{max}') \cdot \text{Power rated desired}}{\text{Size base compressor}} \right)^{s.f.} \right. \\
 & \cdot \left. \left(\frac{\text{pressure desired}}{\text{pressure base compressor}} \right)^{s.f.'} \right)
 \end{aligned}
 \tag{80}$$

where:

- *N_{max}* is the number of compressors with maximum design power (16000 kW):

$$N_{max} = \frac{\text{Power rated desired}}{\text{Max. design power}}$$

- *N_{max'}* is the number of compressors with maximum design power (16000 kW) (rounded to the unit):

$$N_{max}' = \text{ROUNDDOWN} \left(\frac{\text{Power rated desired}}{\text{Max. design power}} \right)$$

Table 38 presents the relevant economic parameters.

Table 38: Economic parameters for a generalized multi-stage compressor.

	Multi-stage compressor (general multi-stage compressor technology)	Ref.
Cost base [€/kW]	1254.6 ¹⁵	
Size base [kW]	4000	
Pressure base compressor [bar]	200	[192], [206]
s.f.	0.8	
s.f.'	0.18	

¹⁵ Values converted from \$ to € and adjusted for inflation, reporting them to €₂₀₂₁.

5.6.1.4 OPEX

The cost of operation and maintenance for compression is dependent on variable and fixed costs as presented in equation (81).

$$OPEX [\text{€}] = \text{Variable OPEX} [\text{€}] + \text{Fixed OPEX} [\text{€}] \quad (81)$$

Variable operation and maintenance costs

The variable costs related to operation and maintenance of the compressor station reflect the energy consumption of the station throughout the year. It is assumed that the energy needed for compression is provided by an electrical source [83] and the variable OPEX due to the electricity consumption is equal to:

$$\begin{aligned} \text{Variable OPEX} [\text{€}] &= \text{Electricity} [\text{€}] \\ &= \text{Annual electricity consumption} [\text{kWh}] \cdot \text{Cost elect.} \left[\frac{\text{€}}{\text{kWh}} \right] \end{aligned} \quad (82)$$

The annual electricity consumption for hydrogen compression into truck and into pipeline is calculated as:

$$\begin{aligned} \text{Annual electricity consumption} [\text{kWh}] \\ &= \text{Power rated desired} [\text{kW}] \cdot \text{Availability} [\%] \cdot 8760 [\text{h}] \end{aligned} \quad (83)$$

and for compression into storage:

$$\begin{aligned} \text{Annual electricity consumption} [\text{kWh}] \\ &= \text{Power rated desired} [\text{kW}] \cdot \text{Loading time} [\text{h}] \cdot n_{\text{cycles}} \end{aligned} \quad (84)$$

The rated power desired is:

$$\text{Power rated desired} [\text{kW}] = \frac{\text{Power real} [\text{kW}]}{\eta_{\text{electric motor}}} = \left(\frac{\text{Power isentropic} [\text{kW}]}{\eta_{\text{isentropic}}} \right) \cdot \frac{1}{\eta_{\text{electric motor}}} \quad (85)$$

Where:

- *Power real* [kW], is the mechanical power required by the compression station
- $\eta_{\text{electric motor}}$, is the compressor's electric motor efficiency. This value is set to 95% following reference [83].
- $\eta_{\text{isentropic}}$, is the isentropic efficiency. The isentropic efficiency will vary depending on the compressor technology. Taking an efficiency of 80% for multi-stage centrifugal compressors [83] and 85% for multi-stage reciprocating compressors [188].
- *Power isentropic* [kW], is the isentropic power required by the compression station, described with Equation (86) [60], [83], [207], [208].

$$\text{Power isentropic} [\text{kW}] = N_{\text{stages}} \cdot \left(\frac{k}{k-1} \right) \cdot Z \cdot T_1 \cdot Q_{\text{compr}} \cdot R \cdot \left[\left(\frac{p_2}{p_1} \right)^{\frac{k-1}{N_{\text{stages}} \cdot k}} - 1 \right] \quad (86)$$

where:

- N_{stages} is the number of compressor stages
- k , heat capacity ratio or isentropic expansion factor is set 1.41 [83].
- Z , gas compressibility factor.
- T_1 [K], temperature of the feed gas flow.
- Q_{compr} $\left[\frac{kg}{h}\right]$, mass flow rate of the gas flowing through the compressor.
- R $\left[\frac{J}{\frac{kg}{K}}\right]$, universal gas constant
- p_2 [bar], pressure of the gas exiting the compressor.
- p_1 [bar], pressure of the gas entering the compressor.

The compressibility factor is calculated with the help of *CoolProp* [189], [190], based on the average pressure between inlet and outlet pressures (p_{avg}) and on the average temperature between inlet and outlet temperatures (T_{avg}):

$$p_{avg} = \frac{2}{3} \cdot \left(\frac{p_2^3 - p_1^3}{p_2^2 - p_1^2} \right) \quad (87)$$

$$T_{avg} = \frac{T_1 + T_2}{2} \quad (88)$$

where the temperature of the discharge gas flow T_2 [K] is calculated as follows:

$$T_2 = T_1 \cdot \left[1 + \frac{\left(\frac{p_2}{p_1} \right)^{\left(\frac{k-1}{N_{stages} \cdot k} \right)} - 1}{\eta_{isentropic}} \right] \quad (89)$$

The number of compressor stages is equal to:

$$N_{stages} = \text{ROUNDUP} \left(\frac{\log \left(\frac{p_2}{p_1} \right)}{\log(x)} \right) \quad (90)$$

where x is the compression ratio for each stage which is set to 2.1 in the model [83]. For the universal gas constant, it can be calculated as follows:

$$R = \frac{8314 \left[\frac{J}{\frac{kmol}{K}} \right]}{M_{H_2} \left[\frac{kg}{kmol} \right]} \quad (91)$$

where $M_{H_2} \left[\frac{kg}{kmol} \right]$ is the hydrogen molar mass, which is $2.016 \left[\frac{kg}{kmol} \right]$ [54].

Fixed operation and maintenance costs

The fixed OPEX is a percentage of the total CAPEX of the compressor station ($OPEX_{\%}$) as it is represented in equation (92). The percentage is set for a generalized multi-stage compressor, which amounts to 6% [194].

$$Fixed\ OPEX\ [€] = OPEX_{\%} \cdot CAPEX \quad (92)$$

5.6.1.5 Levelized cost of compression

The levelized cost of hydrogen compression is assessed by Equation (93) and it follows the same reasoning explained in Section 5.1.

$$LCOH \left[\frac{€}{kg_{H_2}} \right] = \frac{\sum_{n=1}^N \frac{CAPEX[€] + OPEX_{variable}[€] + OPEX_{fixed}[€]}{(1+i)^n}}{\sum_{n=1}^N \frac{Q_{H_2}[kg_{H_2}]}{(1+i)^n}} \quad (93)$$

Table 39 summarizes the economic parameters for a generalized multi-stage compressor.

Table 39: Financial parameters for a generalized multi-stage compressor.

	Multi-stage compressor	Ref.
Economic lifetime [years]	15	
Discount rate [%]	8	[83]
Availability [%]	90	
Mass losses [%]	0.5	[209]

For hydrogen compression into truck and into pipeline, the compressed hydrogen per year Q_{H_2} is:

$$Q_{H_2}[kg_{H_2}] = Availability\ [%] \cdot 8760\ [h] \cdot Q_{compr} \left[\frac{kg}{h} \right] \cdot (1 - mass_{losses}) \quad (94)$$

while for hydrogen compression to storage is:

$$Q_{H_2}[kg_{H_2}] = \left(Loading_{time}\ [h] \cdot Q_{compr} \left[\frac{kg}{h} \right] \cdot (1 - mass_{losses}) \right) \cdot n_{cycles} \quad (95)$$

Where n_{cycles} is the number of cycles per year varying with the duration of storage.

5.6.2 Liquefaction

The following sections describe the methodology adopted for the hydrogen liquefaction process.

5.6.2.1 System overview

The hydrogen liquefaction stage in the model constitutes the conversion stage characterized by the change of gaseous hydrogen to liquid hydrogen. Such process takes place in a hydrogen liquefaction plant where various technologies can be considered to liquefy hydrogen: Linde Process, Claude Process, Collins Process, and Brayton Process [210]. However, the most common process that have been used in industry

over the years is the Claude Process [211]–[213]. The cost assessment tool allows the user to select two of the following technologies: Conventional Liquefaction Plant or Proposed Liquefaction Plant. Below there is a detailed explanation of each one of the liquefaction plants.

Conventional Liquefaction Plant

In this model, a conventional liquefaction plant is defined to follow the Claude Process. Figure 21 shows a general diagram of a conventional liquefaction plant.

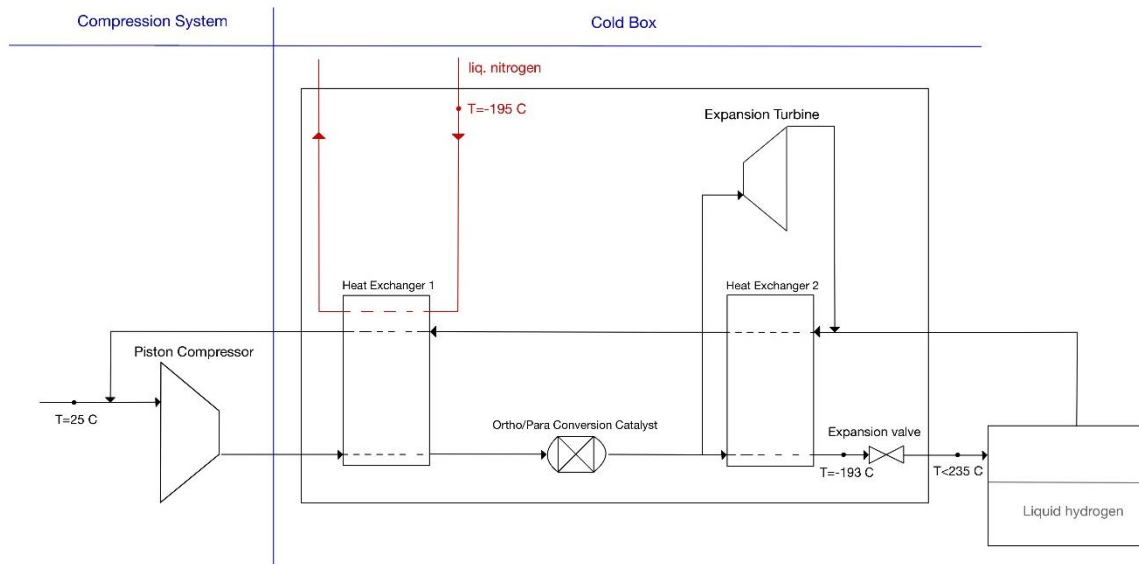


Figure 21: General diagram of a conventional liquefaction plant [210].

As can be seen in Figure 21, the work flow of the conventional liquefaction plant is divided in two main stages: the compression system and the liquefier cold box. The compression system consists of a piston compressor where the hydrogen enters at around 25°C [214]. The liquefier cold box begins with a pre-cooling stage where the heat is transferred from hydrogen with help of circulating liquefied nitrogen at -195°C (Heat Exchanger 1) [215]. A partial mass of the cooled hydrogen coming out of Heat Exchanger 1 goes through an expansion turbine, which lowers its temperature significantly. This partial mass of hydrogen at a lower temperature helps with further cooling of the other remaining mass of gaseous hydrogen, as shown in Heat Exchanger 2. This recycling cooling process taking place in Heat Exchanger 2 helps lowering the hydrogen temperature to way below hydrogen’s inversion temperature, -73°C [210]. This is important as hydrogen has to enter the expansion valve below this inversion temperature, otherwise the Joule-Thomson expansion process would raise the hydrogen temperature when passing through the expansion valve instead of lowering it [210]. It is important to mention that inside the Heat Exchanger 2 there is an ortho/para conversion catalyst that help accelerate this conversion process, leading to a reduction of boil-off. Finally, the hydrogen coming out of the expansion valve is at a temperature below -253°C in which hydrogen is at liquid form. Some of the hydrogen that had not been liquefied is injected back to the compressor [210].

Proposed Liquefaction Plant

Undoubtedly, the very high energy consumption of hydrogen liquefaction plants is the main issue around this technology. Yang *et al.* [214], Faramarzi *et al.* [216], and Cho *et al.* [217] reflect on the techno-economic performance of base hydrogen liquefaction plants and suggest a new design focused on optimizing the energy consumption in these plants. The main idea around this technology improvement is the reduction of energy consumption by utilizing an additional cooling stream of liquified natural gas (LNG) coming from an LNG regasification plant. As it can be seen in Figure 22, the green line represents the LNG coming out of the LNG regasification plant and entering the hydrogen liquefaction plant in the pre-cooling stage, more precisely in Heat Exchanger 1. The cooling energy from LNG is used to help decreasing the

hydrogen temperature. The heat exchange between fluids leads up to the increase of the LNG temperature, making it change from its liquid form to gaseous form. Afterwards, the gaseous natural gas exits the hydrogen liquefaction plant to enter a steam methane reforming (SMR) plant to be converted into hydrogen.

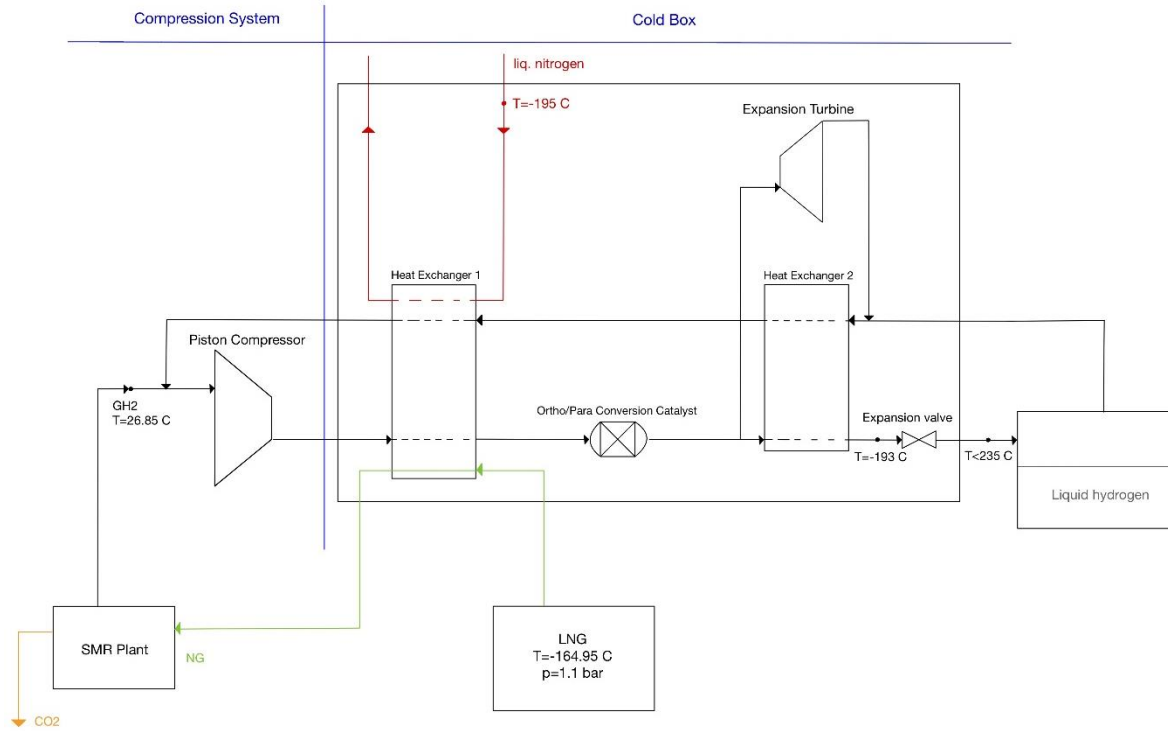


Figure 22: General diagram of the proposed liquefaction plant [210], [214].

With this proposed hydrogen liquefaction plant, a more efficient process is achieved by lowering the energy required for the pre-cooling stage. This slight change in the technology allows the hydrogen liquefaction plant to use a lower mass flow rate of nitrogen, leading to a decrease of the compressors' operating power used in the Air Separation Unit (ASU) that produces the nitrogen [214], [216], [217].

5.6.2.2 Liquefaction plant sizing

The capacity of the hydrogen liquefaction plant is defined based on the amount of hydrogen generated from the hydrogen production plant:

$$C_{H_2 \text{ liquefaction plant}} [tpd_{H_2}] = \frac{Q_{H_2} [t_{H_2}/a]}{365 [days]} \quad (96)$$

where Q_{H_2} is the net annual production of hydrogen in $[t_{H_2}/a]$.

5.6.2.3 CAPEX

The cost of initial capital expenditures scales with the change of the liquefaction plant capacity, as represented by Equation (97) where the liquefaction plant capacity desired is equal to the hydrogen liquefaction plant capacity obtained in the previous chapter.

$$CAPEX [€] = \text{Cost base liq. plant} \cdot \left(\frac{\text{Liq. plant capacity desired}}{\text{Size base liq. plant}} \right)^{s.f.} \quad (97)$$

Table 40: Economic parameters for each type of liquefaction plant.

	Conventional Liquefaction Plant	Ref.	Proposed Liquefaction Plant	Ref.
Cost base [M€] ¹⁶	1253.5	[3]	843.6	[216]
Size base [tpdH ₂]	722.2	[3]	722.2	[3]
Scaling factor (s.f.)	0.7 ; 0.65	[192], [218]	0.7 ; 0.65	[192], [218]

Note: The values in bold are the values introduced in the model.

Faramarzi *et al.* [216] show in their results that the total capital expenditures for the Proposed Liquefaction Plant is 32.7% less than that of the Conventional Liquefaction Plant. Based on this cost relation between the two technologies, the cost base of the proposed liquefaction plant is defined as:

$$\begin{aligned}
 (\text{Cost base liq. plant})_{\text{Proposed Liq.Plant}} & \\
 &= (100\% - 32.7\%) \cdot (\text{Cost base liq. plant})_{\text{Conventional Liq.Plant}}
 \end{aligned}
 \tag{98}$$

5.6.2.4 OPEX

Since one of the biggest distinctive factors between hydrogen conversion and reconversion technologies is the energy consumption. The equation used for the calculation of the cost of operation and maintenance for hydrogen liquefaction considers both fixed and variable operation and maintenance costs.

$$\text{OPEX [€]} = \text{Variable OPEX [€]} + \text{Fixed OPEX [€]}
 \tag{99}$$

Variable operation and maintenance costs

The variable OPEX is due to the energy consumption in the liquefaction process:

$$\begin{aligned}
 \text{Variable OPEX [€]} &= \text{Electricity [€]} \\
 &= \text{Annual electricity consumption [kWh]} \cdot \text{Cost elect.} \left[\frac{\text{€}}{\text{kWh}} \right]
 \end{aligned}
 \tag{100}$$

The annual electricity consumption is equal to:

$$\begin{aligned}
 \text{Annual electricity consumption [kWh]} & \\
 &= \text{Specific Energy Consumption} \left[\frac{\text{kWh}_{\text{electricity}}}{\text{kg}} \right] \\
 &\cdot \left(Q_{\text{H}_2 \text{ liquefaction plant}} [\text{tpd}_{\text{H}_2}] \cdot \frac{1000}{24} \right) \cdot \text{Availability [\%]} \cdot 8760 [\text{h}]
 \end{aligned}
 \tag{101}$$

From all literature reviewed and data collected, the repetitive variation of the specific energy consumption (SEC) with respect to the liquefaction plant's capacity has been verified, showing a decrease in the energy required by the plant with an increase of the plant's capacity. For this reason, Table 41 shows the SEC

¹⁶ Values converted from \$ to € and adjusted for inflation, reporting them to €₂₀₂₁.

values collected from literature for different plant's capacities. In Figure 23, the values from Table 41 are plotted and the power function is obtained.

Table 41: Collected data for hydrogen liquefaction plant's specific energy consumption (SEC) for different plant sizes.

Liquefaction Plant Capacity [tpd]	SEC [kWh/kg _{H2}]	Ref.
5	11.40	[89]
15	10.20	[89]
35	9.40	[89]
40	6.41	[87]
50	9.00	[89]
50	6.41	[87]
100	6.00	[219]

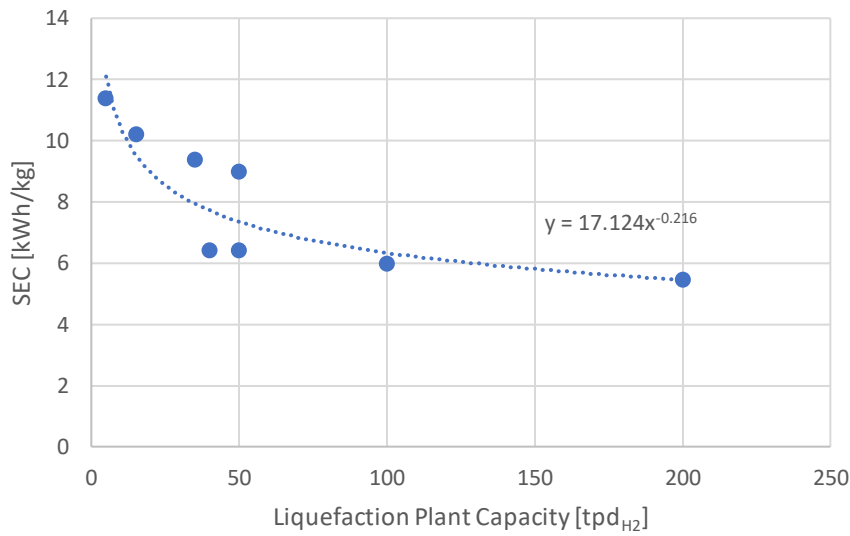


Figure 23: Liquefaction plant performance: SEC as a function of the liquefaction plant capacity.

The power function obtained from the collected data has to be limited to a maximum liquefaction plant capacity of 200 tonnes per day [89]. Otherwise, the SEC of bigger plants would assume unrealistic energy consumptions.

If Liquefaction Plant Capacity ≤ 200 :

$$SEC \left[\frac{kWh}{kg} \right] = 17.124 \times (\text{Liquefaction Plant Capacity} [tpd])^{-0.216} \quad (102)$$

If Liquefaction Plant Capacity > 200 :

$$SEC \left[\frac{kWh}{kg} \right] = 17.124 \times (200 [tpd])^{-0.216} = 5.45 \quad (103)$$

The tool also outputs the hydrogen liquefaction plant exergy efficiency¹⁷, defined by Equation (104).

$$\eta_{exergy} = \frac{\text{Ideal energy consumption (IEC)} \left[\frac{kWh}{kg} \right]}{\text{Real specific energy consumption (SEC)} \left[\frac{kWh}{kg} \right]} \quad (104)$$

where the real SEC is obtained by either Equation (102) and (103), whereas the ideal energy consumption (IEC) is obtained by Equation (105).

$$IEC \left[\frac{kWh}{kg} \right] = T_0(s_1 - s_3) - (h_1 - h_3) \quad (105)$$

where:

- T_0 is the temperature at the beginning of the liquefaction process.
- s_1 is the entropy at the beginning of the liquefaction process.
- s_3 is the entropy at the end of the liquefaction process.
- h_1 is the enthalpy at the beginning of the liquefaction process.
- h_3 is the enthalpy at the end of the liquefaction process.

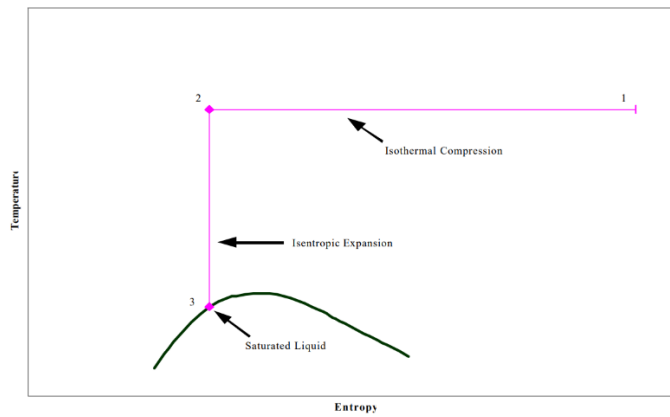


Figure 24: Ideal liquefaction temperature-entropy diagram [192].

The temperatures and pressures considered at the beginning and at the end of the liquefaction process are presented in Table 42.

Table 42: Thermophysical properties of hydrogen at the beginning and end of the hydrogen liquefaction plant [214].

	Temperature [K]	Pressure [bar]	Enthalpy [kJ/kg]	Entropy [kJ/kg.K]
Beginning of liquefaction process	300	21	3967.09	40.94
End of liquefaction process	20	1.3	-3.29	-0.18

¹⁷ The efficiency equation is obtained from [86], [192], [219].

The values for entropy and enthalpy at the beginning and end of the liquefaction process are calculated with the help of *CoolProp* [189], [190].

Fixed operation and maintenance costs

The fixed OPEX are calculated as a percentage of the CAPEX, $OPEX_{\%}$, equal to 4% for both conventional and proposed liquefaction plant [3].

$$Fixed\ OPEX\ [€] = OPEX_{\%} \cdot CAPEX\ [€] \quad (106)$$

5.6.2.5 Levelized cost of liquefaction

The levelized cost of hydrogen liquefaction is determined by Equation (107), which is the general formula used to calculate the specific cost of each of the supply chain stages, as explained in Section 5.1.

$$LCOH\ \left[\frac{€}{kg_{H_2}} \right] = \frac{\sum_{n=1}^N \frac{CAPEX[€] + OPEX_{variable}[€] + OPEX_{fixed}[€]}{(1+i)^n}}{\sum_{n=1}^N \frac{Q_{H_2}[kg_{H_2}]}{(1+i)^n}} \quad (107)$$

Table 43 summarizes the financial parameters for the hydrogen liquefaction plants.

Table 43: Financial parameters for each hydrogen liquefaction plant.

	Conventional Liquefaction Plant	Ref.	Proposed Liquefaction Plant	Ref.
Economic lifetime [years]	20	[219]	20	[219]
Discount rate [%]	8	[3]	8	[3]
Availability [%]	95	[219]	95	[219]
Mass losses [%]	2	[87]	2	[87]

The hydrogen liquefied per year is equal to:

$$Q_{H_2}[t_{H_2}] = Availability\ [%] \cdot 365\ [days] \cdot C_{H_2\ liquefaction\ plant}[tpd_{H_2}] \cdot (1 - mass_{losses}) \quad (108)$$

5.6.3 Regasification

Due to the lack of cost data on hydrogen regasification plants, the regasification stage is often disregarded in hydrogen supply chain cost assessment reports [3], [220]. However, it has been decided to include this stage in this study. The following sections describe the methodology for the regasification stage.

5.6.3.1 System overview

The liquid hydrogen regasification process is represented by Figure 25. This stage of the supply chain portrays the physical conversion process of liquid hydrogen to gaseous hydrogen with the help of the thermal resistance. These types of plants can use very different types of evaporators. For example, there are some liquefied natural gas (LNG) regasification plants that currently operating using a heat exchanger, which relies on sea water to heat the circulating LNG. Another technology that is characterized to have very low operating costs is a regasification plant that heats up the liquid gas by using a heat exchanger that uses warm ambient air as the main source of energy [88].

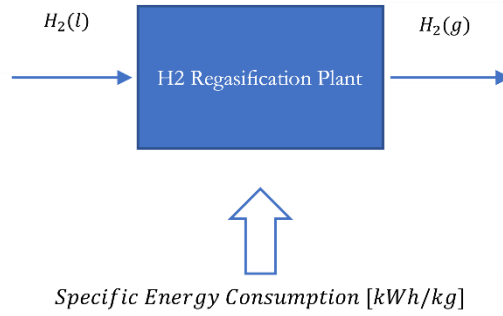


Figure 25: Block diagram of a general hydrogen regasification plant.

5.6.3.2 Regasification plant sizing

The capacity of the liquid hydrogen regasification plant is obtained from Equation (109) and it is sized based on the net liquid hydrogen dispensed from the liquefaction plant annually, Q_{LH_2} .

$$C_{regas.plant} [tpd] = \frac{Q_{LH_2} [t/a]}{365 [days]} \quad (109)$$

5.6.3.3 CAPEX

The CAPEX of the hydrogen regasification plant is based on the cost data provided in the *Hydrogen Delivery Scenario Analysis Model (HDSAM)* [89]. Figure 26 was obtained from the *HDSAM* model [89] and plots the uninstalled cost of the hydrogen regasification plant versus the plant capacity.

Table 44. Collected data on the uninstalled cost of the hydrogen regasification plant with varying plant capacities [89].

H2 Regasification Plant Capacity, tpd _{H2} ¹⁸	€ ₂₀₂₁
24	208428
48	328317
72	448206
96	568096
120	687985
144	807874
168	927763
192	1047653

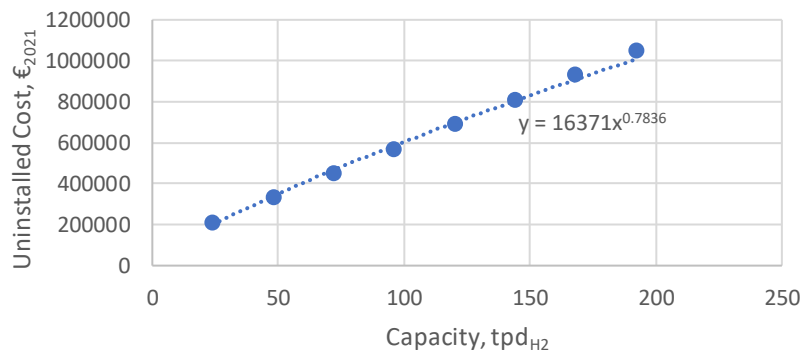


Figure 26: Hydrogen regasification plant uninstalled cost as a function of the respective plant capacity.

¹⁸ Values converted from \$ to € and adjusted for inflation, reporting them to €₂₀₂₁.

In the HDSAM, they use the linear trend between the regasification plant cost and the respective plant's capacity. However, the trendline used in this model is a power relation between the regasification plant's cost and the respective plant capacity so it respects the scaling functions utilized in every other hydrogen supply chain stage. Equation (110) represents the power trendline for the given data:

$$H2 \text{ Regas. Plant Uninstalled Cost [€]} = 16371 \cdot (\text{Capacity [tpd}_{H_2}\text{]})^{0.7836} \quad (110)$$

The final CAPEX formula takes in consideration an installation factor (IF) of 1.3 [89]:

$$CAPEX \text{ [€]} = 1.3 \cdot \left(\text{Cost base regas. plant} \cdot \left(\frac{\text{Regas. plant capacity desired [tpd]}}{\text{Size base regas. plant [tpd]}} \right)^{s.f.} \right) \quad (111)$$

Table 45: Economic parameters for the hydrogen regasification plant.

	H2 Regasification Plant	Ref.
Cost base [€]	16371	
Size base [tpdH2]	1	[89]
Scaling factor (s.f.)	0.7836	

5.6.3.4 OPEX

In the same way as every other conversion and reconversion process, the cost of operation and maintenance is set by a fixed and variable OPEX:

$$OPEX \text{ [€]} = \text{Variable OPEX [€]} + \text{Fixed OPEX [€]} \quad (112)$$

Variable operation and maintenance costs

The variable OPEX considers the energy consumption of the regasification plant and varies annually with the price of electricity.

$$\begin{aligned} \text{Variable OPEX [€]} &= \text{Electricity [€]} \\ &= \text{Annual electricity consumption [kWh]} \cdot \text{Cost elect.} \left[\frac{\text{€}}{\text{kWh}} \right] \end{aligned} \quad (113)$$

The annual electricity consumption is equal to:

$$\begin{aligned} \text{Annual electricity consumption [kWh]} \\ &= \text{Specific Energy Consumption} \left[\frac{\text{kWh}}{\text{kg}} \right] \cdot \left(C_{\text{regas.plant}} \text{ [tpd]} \cdot \left(\frac{1000}{24} \right) \right) \\ &\quad \cdot \text{Availability [\%]} \cdot 8760 \text{ [h]} \end{aligned} \quad (114)$$

Considering the work developed by Reuß *et al.* [49], [221], the specific energy consumption (SEC) is considered to be fixed for this type of plants with varying sizes, equal to 0.6 kWh_{el}/kg_{H2}.

Fixed operation and maintenance costs

The fixed OPEX are calculated as a percentage of the CAPEX, $OPEX_{\%}$, equal to 3% [49], [221].

$$\text{Fixed OPEX} [\text{€}] = \text{OPEX}_{\%} \cdot \text{CAPEX} [\text{€}]$$

(115)

5.6.3.5 Levelized cost of hydrogen regasification

The levelized cost of transforming liquid hydrogen back to gaseous hydrogen is given by Equation (116).

$$\text{LCOH} \left[\frac{\text{€}}{\text{kg}_{\text{H}_2}} \right] = \frac{\sum_{n=1}^N \frac{\text{CAPEX}[\text{€}] + \text{OPEX}_{\text{variable}}[\text{€}] + \text{OPEX}_{\text{fixed}}[\text{€}]}{(1+i)^n}}{\sum_{n=1}^N \frac{Q_{\text{H}_2}[\text{kg}_{\text{H}_2}]}{(1+i)^n}}$$

(116)

Table 46 summarizes the financial parameters for the hydrogen regasification plants.

Table 46: Financial parameters for a hydrogen regasification plant.

	H2 Regasification Plant	Ref.
Economic lifetime [years]	10	[49], [221]
Discount rate [%]	8	[49]
Availability [%]	95	<i>Same as liquefaction plant</i>
Mass losses [%]	0	[49], [221]

Note that the operation availability of the liquid hydrogen regasification plant is set to be the same as the hydrogen liquefaction plant. This guarantees that the number of operating hours is the same for both plants. The hydrogen regasified per year Q_{H_2} is equal to:

$$Q_{\text{H}_2} [t_{\text{H}_2}] = \text{Availability} [\%] \cdot 365 [\text{days}] \cdot C_{\text{regas.plant}} [tpd_{\text{H}_2}] \cdot (1 - \text{mass}_{\text{losses}})$$

(117)

5.6.4 Ammonia conversion

The following sections illustrate the methodology for the conversion of hydrogen into ammonia.

5.6.4.1 System overview

Ammonia production technologies have been widely known for a long time. With the discovery of the Haber-Bosch (H-B) process in the beginning of the 20th century, ammonia synthesis from hydrogen and nitrogen became economically feasible [222]. This in turn helped in increasing the production of fertilizers and consequently decreasing world hunger [223]. Conventional ammonia production generates hydrogen from Steam Methane Reforming and produces nitrogen with the help of an Air Separation Unit (ASU) [224]. The two streams then enter the reactor where high pressure and temperature conditions accelerate the conversion of hydrogen and nitrogen into ammonia. This process is highly energy intensive but over the years the increased energy efficiency have kept H-B process as the most desirable ammonia synthesis process [223], [224].

This stage of the supply chain is outlined in Figure 27, that shows a general diagram of the ammonia production plant.

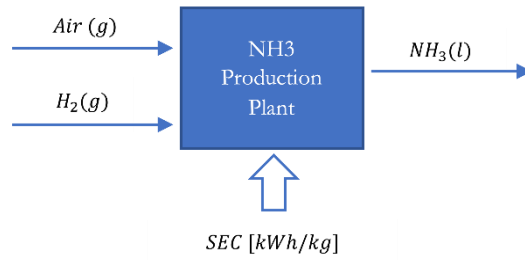


Figure 27: General diagram of the ammonia production plant.

In Figure 28, the general diagram of the ammonia production plant is split into the two most important stages: Air Separation Unit (ASU) and Haber-Bosch (H-B) Process [224]. In the ASU, the air is separated into its components, with nitrogen being the dominant one of them. The Haber-Bosch process is where the nitrogen reacts with hydrogen and produces ammonia.

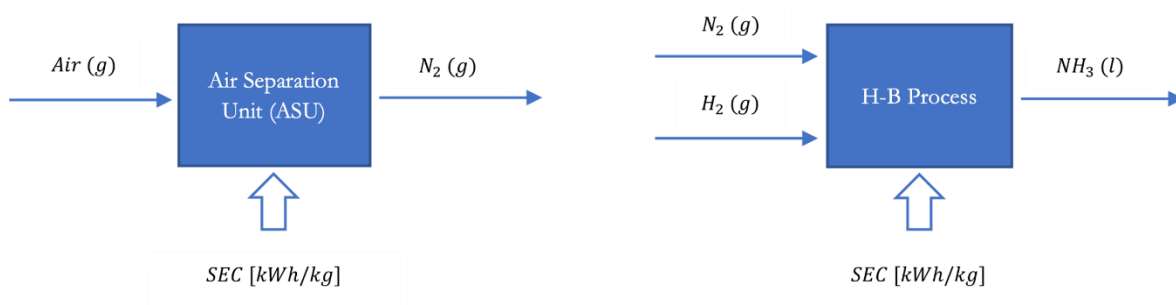


Figure 28: Detailed overview of the ammonia production plant.

The H-B process is then divided into two stages, as shown in Figure 29.

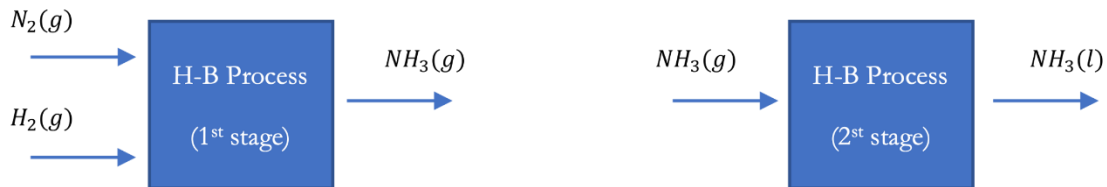
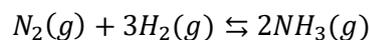


Figure 29: Detailed overview of the H-B process.

The first stage of the H-B process is represented by the following chemical reaction:



The chemical reaction presented above produces ammonia by reacting nitrogen and hydrogen at different pressure and temperature conditions.

H-B Process – 1st stage (no recycling in the converter)

Martin B. Hocking [225] outlined the different concentrations of ammonia at various temperature and pressure conditions of the mixing reactants, as reported in Table 47. It is important to note that the concentrations of ammonia obtained are based on a reacting gas mixture of 1 mole nitrogen to 3 mole hydrogen.

Table 47: Equilibrium percent concentrations of ammonia at various temperatures and pressures [225].

Temperature, °C	Absolute pressure (atm)						
	1	10	50	100	300	600	1000
200	15.3	50.7	74.4	81.5	89.9	95.4	98.3
300	2.2	14.7	39.4	52.0	71.0	84.2	92.6
400	0.4	3.9	15.3	25.1	47.0	65.2	79.8
500	–	1.2	5.6	10.6	26.4	42.2	57.5
600	–	0.5	2.3	4.5	13.8	23.1	31.4
700	–	–	1.1	2.2	7.3	11.5	12.9

To take advantage of the favorable equilibrium final concentrations of ammonia at pressures of 100 to 300 atm (101.33 to 303.98 bar) and at temperatures of 400 to 500 °C, an iron catalyst was added to the converter helped by alumina (Al_2O_3) and potassium oxide (K_2O) [225]. Making the ammonia synthesis process faster as well.

Considering the converter to be at 300 atm (303.98 bar) and 400 °C, it is possible to obtain an approximate estimate of the final mass of ammonia at the end of the reaction with reference to the total amount of hydrogen produced from the respective hydrogen production site:

$$m_{\text{NH}_3} [\text{kg}/\text{a}] = 0.470 \cdot (m_{\text{H}_2} [\text{kg}/\text{a}] + m_{\text{N}_2} [\text{kg}/\text{a}]) \quad (118)$$

where m_{H_2} and m_{N_2} are the mass of hydrogen and nitrogen, respectively at the beginning of chemical reaction. The mass of hydrogen is equal to:

$$m_{\text{H}_2} [\text{kg}/\text{a}] = Q_{\text{H}_2} [t_{\text{H}_2}/\text{a}] \cdot 1000 \quad (119)$$

where Q_{H_2} is the net annual production of hydrogen [t_{H_2}/a]. The equivalent number of hydrogen moles at the beginning of the reaction is obtained from the net amount of hydrogen produced.

$$n_{\text{H}_2} [\text{mol}/\text{a}] = \left(\frac{m_{\text{H}_2} [\text{kg}/\text{a}]}{M_{\text{H}_2} \left[\frac{\text{kg}}{\text{kmol}} \right]} \right) \cdot 10^3 \quad (120)$$

where $M_{\text{H}_2} \left[\frac{\text{kg}}{\text{kmol}} \right]$ is the hydrogen molar mass, which is $2.016 \left[\frac{\text{kg}}{\text{kmol}} \right]$ [54]. From the previous chemical reaction, nitrogen and hydrogen are fed in the H-B process in a ratio of 1 to 3, respectively.

$$n_{\text{N}_2} [\text{mol}/\text{a}] = \left(\frac{n_{\text{H}_2} [\text{mol}/\text{a}]}{3} \right) \quad (121)$$

Subsequently, the mass of nitrogen can be calculated as:

$$m_{N_2} [kg/a] = M_{N_2} \left[\frac{kg}{kmol} \right] \times (n_{N_2} \times 10^{-3}) [kmol/a] \quad (122)$$

Where $M_{N_2} \left[\frac{kg}{kmol} \right]$ is the nitrogen molar mass, which is 28.01 $\left[\frac{kg}{kmol} \right]$ [54].

H-B Process – 1st stage (recycling in the converter)

Wang *et al.* [91] referred to the fact that a 97% overall conversion can be achieved when having converters with continuous recycling.

$$m_{NH_3} [kg/a] = 97\% \cdot (m_{H_2} [kg/a] + m_{N_2} [kg/a]) \quad (123)$$

H-B Process – 2nd stage

The second stage of the H-B process is characterized by a change of ammonia gaseous phase to liquid phase. The electricity consumption for the H-B Process accounts for both stages of the process. However, for some cases, Martin B. Hocking [225] stated that for ammonia synthesis “processes operating at pressures of 400 atm or above, ordinary process cooling water at 10-20°C is sufficient to condense the ammonia”.

5.6.4.2 Ammonia conversion plant sizing

From the annual ammonia mass production calculated in the previous section, the approximate capacity of the ammonia conversion plant can be obtained as follows:

$$C_{NH_3 \text{ prod. plant}} [tpd_{NH_3}] = \frac{m_{NH_3} [kg/a] \times 10^{-3}}{365 [days]} \quad (124)$$

5.6.4.3 CAPEX

The cost of initial capital expenditures is given by Equation (125) and takes into consideration the scaling effect of chemical plants.

$$CAPEX [€] = (Cost \text{ base } H - B \text{ process} + Cost \text{ base } ASU) \cdot \left(\frac{NH_3 \text{ prod. plant capacity desired}}{Size \text{ base } NH_3 \text{ prod. plant}} \right)^{s.f.} \quad (125)$$

Table 48: Economic parameters for the ammonia production plant.

	NH ₃ Prod. Plant	Ref.
Cost base [M€] ¹⁹	428.9 ²⁰	[226]
Size base [tpd _{NH3}]	2200	
Scaling factor (s.f.)	0.7	[218]

¹⁹ Values converted from \$ to € and adjusted for inflation, reporting them in €₂₀₂₁.

²⁰ The cost of the ammonia conversion plant is assumed to be the sum of the cost of the reactor’s cost where the H-B process takes place plus the cost of the ASU. The base costs of H-B process reactor and ASU are 244.36 M€ and 184.52 M€, respectively [226].

5.6.4.4 OPEX

The cost of operation and maintenance is defined by Equation (126) and considers both variable and fixed costs.

$$OPEX [\text{€}] = \text{Variable OPEX} [\text{€}] + \text{Fixed OPEX} [\text{€}] \quad (126)$$

Variable operation and maintenance costs

The variable OPEX accounts for the energy consumption of the ammonia production plant which is dependent on a variable electricity cost:

$$\begin{aligned} \text{Variable OPEX} [\text{€}] &= \text{Electricity} [\text{€}] \\ &= \text{Annual electricity consumption} [kWh] \cdot \text{Cost elect.} \left[\frac{\text{€}}{kWh} \right] \end{aligned} \quad (127)$$

The annual electricity consumption is equal to:

$$\begin{aligned} \text{Annual electricity consumption} [kWh] &= \text{Specific Energy Consumption} \left[\frac{kWh_{\text{electricity}}}{kg_{NH_3}} \right] \\ &\cdot \left(C_{NH_3 \text{ prod. plant}} [tpd_{NH_3}] \cdot \frac{1000}{24} \right) \cdot \text{Availability} [\%] \cdot 8760 [h] \end{aligned} \quad (128)$$

The SEC of the ammonia production plant is assessed by the sum of the main building blocks of the chemical plant, the H-B process reactor, and the ASU:

$$\begin{aligned} \text{Specific Energy Consumption} \left[\frac{kWh_{\text{electricity}}}{kg_{NH_3}} \right] &= SEC_{HB \text{ Process}} \left[\frac{kWh_{\text{electricity}}}{kg_{NH_3}} \right] + SEC_{ASU} \left[\frac{kWh_{\text{electricity}}}{kg_{NH_3}} \right] \end{aligned} \quad (129)$$

Table 49: Specific energy consumption in the ammonia production plant.

	Haber-Bosch (H-B) Process	Ref.	Air Separation Unit (ASU)	Ref.
SEC [kWh _{el} /kg _{NH₃}]	0.78	[91]	0.39	[91]

Fixed operation and maintenance costs

The remaining operation and maintenance costs, the fixed OPEX, are calculated as a percentage of the CAPEX as follows:

$$\text{Fixed OPEX} [\text{€}] = OPEX_{\%} \cdot CAPEX [\text{€}] \quad (130)$$

Table 50: Fixed operating costs of the ammonia production plant.

	NH ₃ Prod. Plant	Ref.
OPEX% [%]	2.5; 4; (Avg. 3.25)	[71]

5.6.4.5 Levelized cost of converting hydrogen to ammonia

The levelized cost of converting hydrogen to ammonia is then given by Equation (131).

$$LCOH \left[\frac{\text{€}}{\text{kg}_{H_2}} \right] = \frac{\sum_{n=1}^N \frac{CAPEX[\text{€}] + OPEX_{variable}[\text{€}] + OPEX_{fixed}[\text{€}]}{(1+i)^n}}{\sum_{n=1}^N \frac{Q_{H_2}[\text{kg}_{H_2}]}{(1+i)^n}} \quad (131)$$

Table 51 reports the financial parameters for the ammonia production plant.

Table 51: Financial parameters for the ammonia production plant.

	NH ₃ Prod. Plant	Ref.
Economic lifetime [years]	25; 30; (Avg. 28)	[3], [227]
Discount rate [%]	8	[3], [227]
Availability [%]	90	[3]
Mass losses [%]	0	Assumption

The hydrogen present in the annual amount of converted ammonia is:

$$Q'_{H_2}[t_{H_2}] = 17.65 [\%] \cdot Q_{NH_3}[t_{NH_3}] \quad (132)$$

Thomas *et al.* [90], endorsed ammonia over the other energy carriers because of its large weight fraction, which amounts to about 17.65% of the mass of ammonia, which is the percentage value considered all over this study. A different publication stated that hydrogen constitutes 17% of the mass of ammonia [228]. The ammonia converted annually can be calculated as follows:

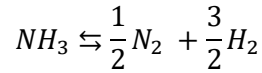
$$Q_{NH_3}[t_{NH_3}] = Availability [\%] \cdot 365 [days] \cdot C_{NH_3 \text{ prod. plant}} [tpd_{NH_3}] \cdot (1 - mass_{losses}) \quad (133)$$

5.6.5 Ammonia reconversion

The following sections describe the methodology for the reconversion of ammonia into hydrogen.

5.6.5.1 System overview

The reconversion of ammonia into hydrogen and nitrogen follows the ammonia conversion chemical reaction, presented in Section 5.6.4.1. The following chemical reaction is endothermic, in other words, it requires energy to decompose the ammonia into hydrogen and nitrogen, having a system enthalpy change of +46kJ/mol [90].



Contrary to the ammonia conversion processes, the process of ammonia reconversion has not had that much of technological improvements in the past years [92], mainly due to the lack of interest in using ammonia as a hydrogen carrier. However, a lot of interest in developing better ammonia splitting technologies has risen with the increased importance of hydrogen in various industries [229].

There are two significant technical problems with ammonia reconversion. The first one is the high-temperature requirement to split the bigger molecule of ammonia into smaller molecules of hydrogen and nitrogen. For this reason, complex catalysts must be used to lower ammonia cracking temperature. The second issues arises from the high level of hydrogen purity (<99.99%) required by some end-use

applications such as fuel cells used in FCEVs [224]. Figure 30 shows the general ammonia reversion plant with the consideration of the high hydrogen purity requirements (>99.99%).

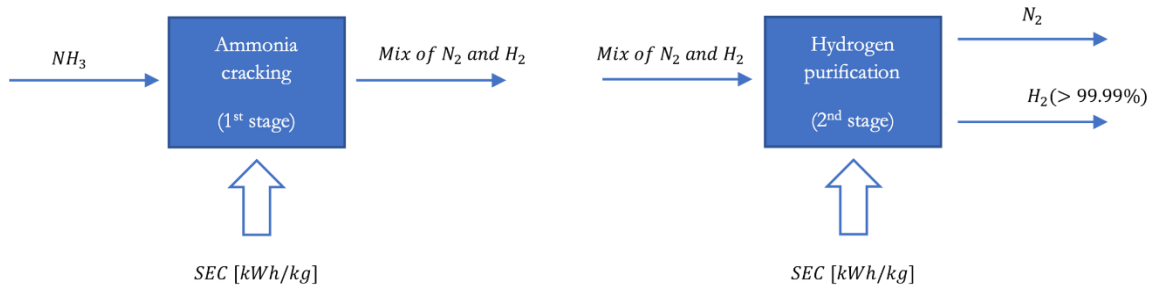


Figure 30: General diagram of the ammonia reversion plant.

The first stage of the ammonia reversion plant is characterized by the splitting process of ammonia in the reactor with the help of a catalyst. State-of-the-art ammonia reversion plants use alkaline-based catalysts such as sodium and lithium, which lead to ammonia cracking temperatures ranging from 400 °C to 500 °C. The exhaust stream coming out of the ammonia cracking phase is a mixture of hydrogen molecules and nitrogen molecules [224][224]. The second stage of the ammonia reversion plant is defined to be where the mix stream of hydrogen and nitrogen is separated into two streams by using a pressure swing adsorption (PSA) process, that allows the creation of the two output streams of nitrogen and hydrogen, where hydrogen has purity level is above 99.99% [224], [230].

5.6.5.2 Ammonia reversion plant sizing

The capacity of the ammonia reversion plant is sized based on the annual ammonia production from the NH₃ production plant, Q_{NH_3} .

$$C_{NH_3 \text{ reconv. plant}} [tpd_{NH_3}] = \frac{Q_{NH_3} [t_{NH_3}/a]}{365 [days]} \quad (134)$$

5.6.5.3 CAPEX

The cost of the initial capital investment is given by Equation (135), with the relevant economic parameters summarized in Table 52.

$$CAPEX [€] = (\text{Cost base } NH_3 \text{ reversion plant}) \cdot \left(\frac{NH_3 \text{ reversion plant capacity desired}}{\text{Size base } NH_3 \text{ reversion plant}} \right)^{s.f.} \quad (135)$$

Table 52: Economic parameters for the ammonia reversion plant.

	NH ₃ Reversion Plant	Ref.
Cost base [M€] ²¹	411.9	[3]
Size base [tpd _{NH₃}]	4109.6 ²²	
Scaling factor (s.f.)	0.7	[218]

²¹ Values converted from \$ to € and adjusted for inflation, reporting them to €₂₀₂₁.

²² $\frac{1500 [kt_{NH_3}/a] \cdot 1000}{365 [days]}$

5.6.5.4 OPEX

In congruence with the other conversion and reconversion technologies, the cost of operation and maintenance is defined by the sum of the fixed and variable costs of operation and maintenance.

$$OPEX [\text{€}] = \text{Variable OPEX} [\text{€}] + \text{Fixed OPEX} [\text{€}] \quad (136)$$

Variable operation and maintenance costs

The variable OPEX is determined by the energy consumption of the ammonia reconversion plant and calculated as follows:

$$\begin{aligned} \text{Variable OPEX} [\text{€}] &= \text{Electricity} [\text{€}] \\ &= \text{Annual electricity consumption} [\text{kWh}] \cdot \text{Cost elect.} \left[\frac{\text{€}}{\text{kWh}} \right] \end{aligned} \quad (137)$$

The annual electricity consumption is calculated as follows:

$$\begin{aligned} \text{Annual electricity consumption} [\text{kWh}] &= \text{Specific Energy Consumption} \left[\frac{\text{kWh}_{\text{electricity}}}{\text{kg}_{\text{H}_2}} \right] \\ &\cdot \left(17.65 [\%] \cdot C_{\text{NH}_3 \text{ reconversion plant}} [\text{tpd}_{\text{NH}_3}] \cdot \frac{1000}{24} \right) \cdot \text{Availability} [\%] \cdot 8760 [\text{h}] \end{aligned} \quad (138)$$

As explained in Section 5.6.4.5, the 17.65% is with respect to the weight fraction of hydrogen present in ammonia [90]. This means that the amount of hydrogen coming out of the reconversion plant is 17.65% of the total amount of ammonia inputted in the plant without losses. The total SEC of the plant is assumed to be the sum of the energy required for ammonia cracking and the energy required for PSA process:

$$\begin{aligned} \text{Specific Energy Consumption} \left[\frac{\text{kWh}_{\text{electricity}}}{\text{kg}_{\text{H}_2}} \right] &= SEC_{\text{heat req. for NH}_3 \text{ cracking}} \left[\frac{\text{kWh}_{\text{electricity}}}{\text{kg}_{\text{H}_2}} \right] \\ &+ SEC_{\text{H}_2 \text{ purification (PSA)}} \left[\frac{\text{kWh}_{\text{electricity}}}{\text{kg}_{\text{H}_2}} \right] \end{aligned} \quad (139)$$

Table 53: Specific energy consumption in each stage of the ammonia reconversion plant.

	Heat required for NH ₃ cracking	Ref.	H ₂ purification (PSA)	Ref.
SEC [kWh _{elect.} /kg _{H2}]	9.7	[3]	1.5	[3]

5.6.5.4.1 Fixed operation and maintenance costs

The fixed operating cost is given by a percentage of the total CAPEX, $OPEX_{\%}$, equal to 4% [3].

$$\text{Fixed OPEX} [\text{€}] = OPEX_{\%} \cdot \text{CAPEX} [\text{€}] \quad (140)$$

5.6.5.5 Levelized cost of reconverting hydrogen from ammonia

The levelized cost of reconverting hydrogen from ammonia follows the same LCOH formula defined in the other conversion and reversion processes' sections.

$$LCOH \left[\frac{\text{€}}{\text{kg}_{H_2}} \right] = \frac{\sum_{n=1}^N \frac{CAPEX[\text{€}] + OPEX_{variable}[\text{€}] + OPEX_{fixed}[\text{€}]}{(1+i)^n}}{\sum_{n=1}^N \frac{Q_{H_2}[\text{kg}_{H_2}]}{(1+i)^n}} \quad (141)$$

Table 54 summarizes the financial parameters for the ammonia reversion plant.

Table 54: Technical and financial parameters for the ammonia reversion plant.

	NH3 Reconversion Plant	Ref.
Economic lifetime [years]	30	
Discount rate [%]	8	
Availability [%]	90	[3]
Mass losses, H ₂ recov. rate [%]	1 (100%-99%)	
Mass losses, PSA H ₂ recov. rate [%]	15 (100%-85%)	

The quantity of hydrogen reconverted from ammonia per year is equal to:

$$Q_{H_2} [t_{H_2}] = Availability [\%] \cdot 365 [days] \cdot (17.65 [\%] \cdot C_{NH_3 \text{ reconv.plant}} [tpd_{NH_3}]) \cdot (1 - (m_{losses})_{H_2 \text{ recov.rate}}) \cdot (1 - (m_{losses})_{PSA H_2 \text{ recov.rate}}) \quad (142)$$

where $(m_{losses})_{H_2 \text{ recov.rate}}$ is defined as the hydrogen mass loss due to the rate of reconverting ammonia into hydrogen in the first stage of the ammonia reversion plant process, and $(m_{losses})_{PSA H_2 \text{ recov.rate}}$ is the hydrogen mass loss due to the rate of purifying hydrogen in the second stage of the ammonia reversion plant process.

5.7 Transmission and distribution

The hydrogen delivery is conceptually divided into transmission and distribution. Based on the production and destination locations, the tool shows the possible transportation options. Once an option is selected, the related distances get displayed, with the possibility to override them if needed. The transmission distances for the studied supply pathways are estimated from different sources: for pipelines, the main source is the existing gas infrastructure map from ENTSOG [231], gauged with the measure tool of Google Earth [232]; for shipping routes, the *CERDI-Seadistance* database [233] is combined with the *SeaRoutes* online tool [234]. It is generally assumed that the production site is close to the coast and the arrival point is at the border of the destination country. However, the user can select a hypothetical hub in the middle of the country as arrival point or directly override the transportation distance. The considered distances are summarized in Appendix VII. For distribution, an average distance equal to 200 km is assumed in every case. Different methodologies and equations are used to calculate the $LCOH_{T\&D}$ for each mode, as presented in detail in the following sections.

5.7.1 Pipelines

Pipelines can be used for both transmission and distribution, onshore and offshore. Either new pipelines are built, or the existing gas network is retrofitted. This choice is included in the tool, affecting several parameters such as the initial investment. A second choice available in the tool is the pipeline size, selecting an option between *Small*, *Medium*, and *Large*, which is based on the classification of Jens *et al.* [108]. Equation (143) describes the $LCOH_i$:

$$LCOH_t \left[\frac{\text{€}}{\text{kg}_{H_2}} \right] = (a_{\%} + OPEX_{\%}) \cdot CAPEX \cdot l \cdot \frac{LHV_{H_2}}{Q_{H_2} \cdot CF \cdot 8760h} + LCOH_{t,compr} \quad (143)$$

where the $CAPEX$ is expressed in €/km; l is the pipeline length in km; Q_{H_2} is the pipeline design capacity in kW of hydrogen (LHV); CF is the average load factor of the pipeline, $LCOH_{t,compr}$ is the compression cost component. Table 55 shows the values used for these parameters in the onshore case. It is assumed that offshore pipeline costs are 25% higher than the onshore pipeline ones [235].

Table 55: New and repurposed (rep.) onshore pipeline parameters. Data from [94], [108] and own calculations.

		Small		Medium		Large	
		new	rep.	new	rep.	new	rep.
Diameter, D	[mm]	500		900		1200	
	[', inches]	20		36		48	
Operating pressure, p_{op}	[bar]	50		40		80	
Segment length, l_{segment}²³	[km]	300		500		700	
Design capacity, Q_{H2}	[GW]	1.2		3.6		13	
	[t/h]	36		108		390	
CAPEX	[M€/km]	1.5	0.3	2.2	0.4	2.8	0.5

Given the high uncertainty about future projections, it is assumed that the capital costs for pipelines are constant throughout the whole period of investigation. Some values are independent of the pipeline size and location and are reported in Table 56.

Table 56: General parameters for pipelines.

Parameter	Value	Ref.
OPEX (as % of CAPEX)	2%	[235]
Economic lifetime [years]	40	[3]
Utilization rate, CF	75%	[3]
Nominal discount rate, d_n	6%	[108]

The compression cost component, $LCOH_{t,compr}$, is composed of the costs needed for the inlet compressor and the booster compressors distributed along the pipeline:

$$LCOH_{t,compr} = LCOH_{t,compr,inlet} + n_{compr} \cdot LCOH_{t,compr,booster} \quad (144)$$

where n_{compr} is the number of compressors necessary for the hydrogen flow:

$$n_{compr} = \text{rounddown} \left(\frac{l}{l_{segment}} \right) \quad (145)$$

The detailed discussion about the $LCOH_{t,compr}$ components is presented in Section 5.6.1. However, some considerations can be carried out here, especially concerning the segment length ($l_{segment}$, distance between two consecutive pipeline compressors), and the flow pressures and velocities. The segment length is reported in Table 56, and it has been assumed through an iterative process that is based on Khan *et al.*

²³ Distance between two consecutive compressor stations

[94]. The calculations also provide the pressure value at the end of the pipeline segment, p_{out} , that corresponds to the input pressure for the next booster compressor.

$$p_{out} = \left[p_{op}^2 - G \cdot T_f \cdot l_{segment} \cdot Z \cdot f \cdot \left(\frac{Q_{H2}}{K \cdot D^{2.5}} \cdot \frac{P_b}{T_b} \right)^2 \right]^{0.5} \quad (146)$$

where G is the hydrogen specific gravity (0.0696); T_f is the average flow temperature, assumed to be 15°C; Z is the compressibility factor, approximated to be equivalent to the one at base pressure and temperature (1.031); K is an equation constant (0.0011494); P_b and T_b are the base pressure (101.352 kPa) and temperature (288.706 K); f is the friction factor, calculated from the Haaland equation that is shown hereby:

$$\frac{1}{\sqrt{f}} = -1.8 \cdot \log_{10} \left(\left(\frac{\varepsilon}{3.7 \cdot D} \right)^{1.11} + \frac{6.9}{Re} \right) \quad (147)$$

where ε is the pipeline roughness (0.0178 mm) and Re is the flow average Reynolds number. The Reynolds number also depends on the velocity, that can be calculated as follows:

$$v = 14.734 \cdot \frac{P_b}{T_b} \cdot \frac{Z \cdot T}{p} \cdot \frac{Q}{D^2} \quad (148)$$

Equation (148)(148) is dependent on the pressure, and therefore also the friction factor (Equation (147)), explaining the iterative nature of Equation (146). To avoid pipe erosion, as explained in Section 4.4.1, the velocity needs to be maintained below a limit erosional velocity:

$$v_{max} = 100 \cdot \sqrt{0.05131 \cdot \frac{Z \cdot R \cdot T_f}{G \cdot p_{op}}} \quad (149)$$

The Excel tool ensures that the velocity is always below this limit value by controlling the segment outlet pressure p_{out} (minimum pressure in the pipe segment) to be always higher than the minimum value p_{min} , from Equation (148):

$$p_{min} = 14.734 \cdot \frac{P_b}{T_b} \cdot \frac{Z \cdot T}{v_{max}} \cdot \frac{Q}{D^2} \quad (150)$$

5.7.2 Shipping

Shipping vessels are the other transmission option available in the tool. They can either transport liquid hydrogen or ammonia. Using the same assumptions as IEA [3], NH₃ carriers are fueled with HFO, while LH₂ ones with boil-off gas. In the first case, the LCOH_t is given by the sum of four components, respectively related to the vessel, fuel, terminal, and conversion/reconversion costs:

$$LCOH_{t,NH3} = LCOH_{t,vessel} + LCOH_{t,fuel} + LCOH_{t,terminal} + LCOH_{t,(re)conv} \quad (151)$$

Costs for liquid hydrogen carriers are instead given by the sum of vessel, terminal, and liquefaction costs, along with the maximum between fuel costs and boil-off losses since the boil-off gas is either used as a propellant or wasted.

$$LCOH_{t,LH_2} = LCOH_{t,vessel} + \max(LCOH_{t,fuel} + LCOH_{t,boiloff}) + LCOH_{t,terminal} + LCOH_{t,(re)conv} \quad (152)$$

The terminal and conversion/reconversion costs are discussed respectively in Section 5.5.2 and 5.6. The vessel component is calculated as follows:

$$LCOH_{t,vessel} = \frac{(a_{\%} + OPEX_{\%}) \cdot \frac{CAPEX_{ship}}{Q_{ship}}}{rpa} \quad (153)$$

where the $CAPEX_{ship}$ is expressed in € per vessel and the hydrogen shipping capacity Q_{ship} in kg of hydrogen per vessel. This means that in case the vector is ammonia, the shipping capacity needs to be adjusted to its corresponding hydrogen mass content (17.6 wt%, [236]). The rpa denominator stands for routes per year, since the $LCOH_t$ refers to a single round-trip.

$$rpa = \frac{8760h}{2 \cdot \left(\frac{l}{v} + t_{harbor}\right)} \quad (154)$$

where l is the route distance, v is the average velocity, and t_{harbor} is the time spent in the harbor for loading and unloading operations.

The fuel cost depends on the propellant used, but follows in any case the same equation:

$$LCOH_{t,fuel} = \frac{P_{fuel} \cdot E_{fuel} \cdot 2l}{Q_{H_2}} \quad (155)$$

where P_{fuel} is the fuel price and E_{fuel} is the fuel consumption per km. For LH₂ carriers, the fuel used is hydrogen and its cost corresponds to its production cost. For NH₃ carriers, heavy fuel oil (HFO) is used as fuel. The values for HFO price are reported in Appendix III.

For liquid hydrogen, the boil-off losses need also to be considered and are calculated as a percentual loss of the production LCOH:

$$LCOH_{t,boiloff} = \frac{b_{\%}}{24h} \cdot \left(\frac{l}{v} + t_{harbor}\right) \cdot LCOH_p \quad (156)$$

Where $b_{\%}$ is the liquid hydrogen boiloff rate, equal to 0.2% per day [3]. Instead, the ammonia boil-off losses are not considered, given their negligible value. The main parameters used are reported in Table 57.

Table 57: General shipping parameters.

Parameter	Unit	LH ₂ NH ₃		Source
		Value		
CAPEX ²⁴	[M€/ship]	369	76	[3], [209]
OPEX (as % of CAPEX)	[-]	4%		[3]
Economic lifetime, LT	[years]	30		[164]
Nominal discount rate, d _n	[-]	8%		[3]
Capacity, Q	[kton _{vector} /ship]	11	53	[3]
	[kton _{H2} /ship]	11	9.3	[3], [236]
Velocity, v	[km/h]	30		[3]
Harbor time, t _h	[h]	48		[164]

A 10% linear decrease in CAPEX is considered from 2020 to 2030, as assumed by Brändle *et al.* [37].

5.7.3 Truck

The second distribution option besides pipelines is hydrogen-carrying trucks. Hydrogen can be transported via truck in different forms: gH₂ at 250 bar, LH₂, or NH₃. Several factors define the truck-related costs that are represented as follows:

$$LCOH_t = LCOH_{t,truck} + LCOH_{t,fuel} + LCOH_{t,driver} + LCOH_{t,boiloff} + LCOH_{t,(re)conv} \quad (157)$$

The vehicle costs are the sum of the three truck components: tractor, tank, and trailer chassis. Since they have different lifetimes, their amortization factors differ, therefore the formula to assess the vehicle LCOH is equal to:

$$LCOH_{t,truck} = \frac{CAPEX_{tractor} \cdot a_{\%,tractor} + CAPEX_{tank} \cdot a_{\%,tank} + CAPEX_{tr.chassis} \cdot a_{\%,tr.chassis} + OPEX \cdot l_n}{Q_{H2} \cdot rpa} \quad (158)$$

where the *OPEX* is expressed in € per km, and l_n is the annual distance covered by a truck. As for shipping, the transported capacity Q_{H2} refers to the specific carrier and is hence converted to gaseous hydrogen equivalent mass for the calculations. The routes per year, *rpa*, are expressed as the ratio between the annual mileage and the average distance per round trip. The annual mileage is defined based on the truck range: the user can either select distribution (50'000 km/a) or haulage mode (110'000 km/a). The choice also has a direct or indirect impact on other input values, such as fuel consumption and tractor lifetime.

The fuel cost follows a similar equation to the shipping counterpart, Equation (155):

$$LCOH_{t,fuel} = \frac{P_{fuel} \cdot E_{fuel} \cdot 2l}{Q_{H2}} \quad (159)$$

For simplicity, it is assumed that the fuel used in every case is diesel. The reason behind this assumption is that, despite a switch to cleaner modes of transportation is desired, a switch from diesel to cleaner fuels (e.g., electricity) will occur only when the two options have similar TCOs. Therefore, it is considered reasonable to have a similar assumption, without large impacts on the result.

²⁴ CAPEX values extrapolated from IEA's *The future of Hydrogen*, converted from \$ to € and adjusted for inflation, reporting them to €₂₀₂₁.

In the truck case, driver costs are explicitly calculated given their impact on the TCO and dependence on the truck range.

$$LCOH_{t,driver} = \frac{c_{driver} \cdot t_{op}}{Q_{H_2} \cdot rpa} \quad (160)$$

where c_{driver} is the driver salary per hour and t_{op} are the annual hours of operation.

The boil-off costs, only occurring with the transportation of LH₂, are evaluated in a similar manner to Equation (156):

$$LCOH_{t,boiloff} = \frac{b_{\%}}{24h} \cdot \left(t_{op} \cdot \frac{l}{d_n} \right) \cdot LCOH_p \quad (161)$$

Conversion and reconversion costs are better described in Section 5.6. Table 58 and Table 59 report the main input data for hydrogen distribution via truck.

Table 58: General truck parameters. Internal assumptions and [100], [237], [238].

Parameter	Value		
	gH ₂	LH ₂	NH ₃
Capacity, Q [kg _{vector} /truck]	690	4300	16000
CAPEX _{tractor} [€/truck]	100000		
CAPEX _{tank} [€/truck]	571000	544000	20000
CAPEX _{trailer chassis} [€/truck]	16000		
LT _{tank} [10 ⁶ km]	1		
LT _{trailer chassis} [10 ⁶ km]	1.44		
LT _{tank}	5000 cycles	20 years	20 years
OPEX [€/km]	0.04		
Nominal discount rate, d _n	7%		

Table 59: Truck parameters dependent on the annual mileage. Internal assumptions.

Parameter	Value	
	Distribution	Haulage
Annual mileage, single shift [km]	50000	110000
Annual hours of operation, top [h]	1700	2300
Driver cost [€/h]	17.5	20
Diesel consumption [L/km]	0.3	0.27

The user has the option to select the number of shifts of operation, from 1 to 3. The actual annual mileage is thus given by:

$$mileage_{a,n\ shifts} = mileage_{a,1\ shift} \cdot n_{shifts} \quad (162)$$

In this analysis, it is assumed that the preferred option is the three shifts.

5.8 Scenarios

Due to the high volume of results that the tool can generate, it is essential to define some scenarios, or supply pathways, to simplify the analysis and focus it on relevant topics. For each stage (production, T&D, storage), different options are identified, which in turn create supply pathways, that are then discussed and compared. It is important to mention that the comparison is carried out among different hydrogen options, and not among alternative energy carriers. For this reason, the term *competitive* refers in this work to the cheapest hydrogen supply chains, thus *competitive* and *not competitive* are freely used to rank them, assuming that a low-carbon hydrogen rollout occurs in any case. Further work could focus on the analysis of different energy carriers. However, a mere comparison of the specific costs by energy unit would not be enough: for many hydrogen applications, fuel costs are not the only driver, but also other expenses depend on the type of energy carrier, such as the initial investment and different operational costs. Therefore, other indicators would be more appropriate than a fuel cost comparison. For heavy-duty vehicles for instance, as for other work equipment, the total cost of ownership (TCO) is used to assess and compare different options. This usually indicates a break-even point for a fuel cost to become competitive over another. Due to time and scope limitations, this typology of analysis is not carried out in this work but the resulting LCOHs can be used as an input in similar work.

Hydrogen production can either occur within or outside of Europe. For each of the three studied European countries, a slightly different perspective is taken, based on their natural resource availability, their hydrogen strategies, and the current state of their energy systems. For Germany, a wider number of scenarios is studied, given its strong will to develop a diversified hydrogen economy that include several methods and suppliers. The scenario definition aims at analyzing different hydrogen supply chains with two different points of view: first, comparing the hydrogen costs from a domestic production with its imports; second, comparing different production methods. The assessment from the two perspectives is parallel and simultaneous. For local green hydrogen production, five variations are assessed: AEL and SOEC fed with grid electricity, PEM fed with electricity from either reserved solar PV, onshore wind, or offshore wind plants. Only PEM modules are associated with renewable sources, due to their higher adaptability to variable loads, while alkaline and solid-oxide electrolyzers are more commonly connected to stable feeding sources. For both domestic and foreign green hydrogen production, a large scale (100 MW_e) system is taken into consideration. It is also worth mentioning that the gas prices in Europe refer to the retail price for big customers, while in the gas-producing countries it refers to the upstream costs (i.e., full cycle breakeven price, costs including search, drilling, extraction). This is done to show the possible lowest value for the LCOH_p from SMR and pyrolysis. Additionally, for every supply chain considered a seasonal buffer storage for hydrogen is added. This is done not only to allow for intermittent hydrogen production due to intermittent renewable energy generation but also to account for any emergency disruption at any stage of the supply chain, as well as to manage demand variations. For the case of Germany, both seasonal and monthly storage in geological reservoirs is evaluated. Monthly storage is only considered for the cases of non-green hydrogen production and assuming a hydrogen market with constant flux of demand. Due to the high availability of geological storage in Germany, all types of available technologies are considered: salt caverns, depleted NG and oil reservoirs, and lined rock caverns.

Figure 31 depicts a flowchart for all the scenarios studied for Germany. To provide a clear presentation of the results, not all the scenarios are explicitly presented but only the ones represented by white blocks. For distribution, this means that initially both methods are assessed and a delta between their LCOH is calculated. Later, only the truck option is considered, given its easier operational deployment in the first phases of a hydrogen market. Supply chains with pipelines can be easily estimated applying the delta calculated before²⁵. Similarly for storage, only the cases with depleted NG or oil reservoir with monthly duration are initially evaluated. In the last part, the cheapest domestic and foreign supply pathways are

²⁵ This is done assuming that the distribution costs are independent of the upstream stages, and it can be demonstrated that this assumption is valid in most cases. However, to produce more accurate results for the omitted scenarios, it is suggested to directly use the Excel tool.

selected, and their LCOH is calculated varying the storage type and duration. Results for other supply chains can be calculated applying a delta to the base case (depleted NG or oil reservoir, monthly storage) with a methodology equivalent to the distribution case.

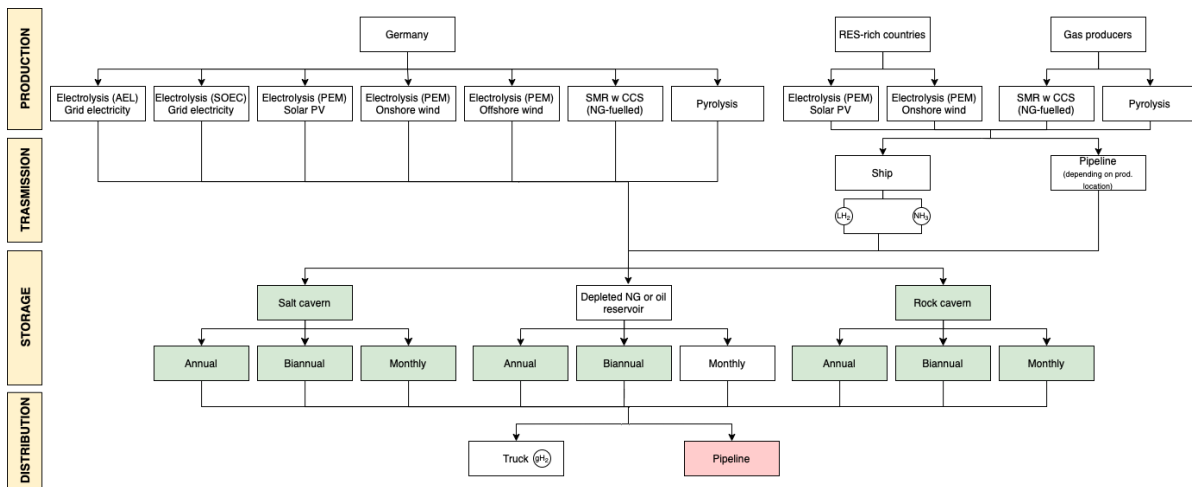


Figure 31: Scenario flowchart for Germany.

A similar investigation can be easily carried out for France and Spain with the aid of the tool. To avoid repeating similar conclusions, the scenarios for these two countries refer to specific cases of special interest, which are based on resource availability and national plans. For Spain, two business models are compared: local and centralized green hydrogen production. A local production, for example closer to the HRS, corresponds also to a small-scale plant (1 MW_{el}); a centralized to large scale (100 MW_{el}). Given Spain's high solar availability, the production scenarios only refer to electricity from PV being fed into a PEM electrolyzer. For central large scale PV production in Spain, a large scale and long-term hydrogen storage facility is considered. More specifically, the scenarios include a depleted NG or oil reservoir, with either a seasonal and monthly duration, and a distribution distance of 200 km, either by truck or pipeline. For decentralized small-scale production, the storage requirements are split in two scenarios: weekly and daily storage. For both weekly and daily storage, the impact of storage in the final cost of hydrogen is assessed with considering the installation of high-pressure steel tanks. In these cases, the delivery of hydrogen is neglected given the proximity to the end-use location.

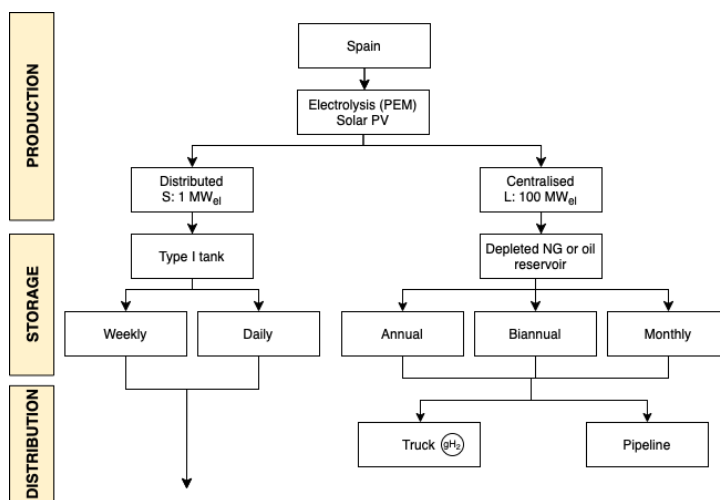


Figure 32: Scenario flowchart for Spain.

For France, the focus is shifted towards nuclear, which dominates its electricity mix. Nuclear electricity is coupled both with a large-scale alkaline and solid oxide electrolyzer system. The electrolyzer modules are

combined with a European pressurized reactor (EPR, LCOE 120 €/MWh [239]). The costs associated with nuclear electricity to fuel the electrolysis process are compared both with grid and domestic renewable electricity. The hydrogen is stored in salt caverns, with its cost evaluated for seasonal and monthly storage. Salt caverns are available in France and have shown interest by French gas companies such as Storengy and Teréga. In fact, these companies are developing pilot projects to evaluate the feasibility of hydrogen storage in salt caverns, some of these projects are the HyPSTER project [240] and STOPIL-H2 [241].

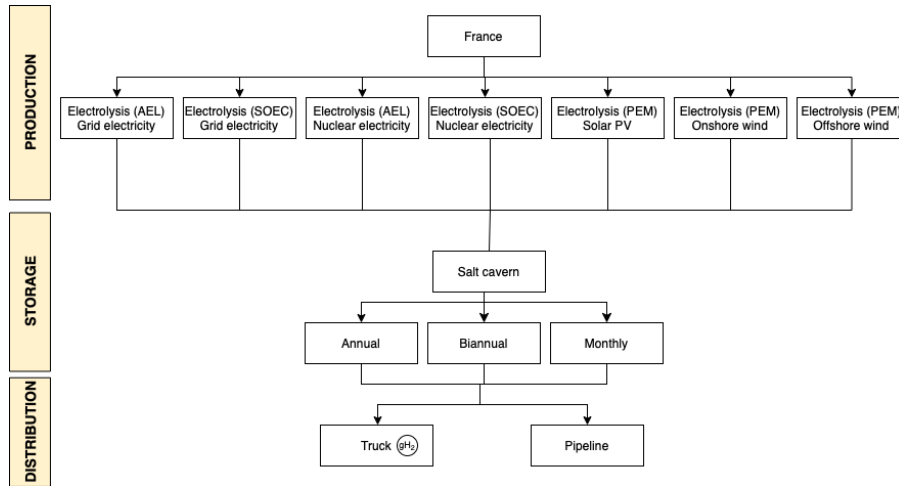


Figure 33: Scenario flowchart for France.

6. Results and discussion

This section presents and discusses the results for the single stages (production, transmission and distribution, storage) and the overall supply chain.

6.1 Production

In this section, the cost of different hydrogen production methods and their main drivers are analyzed. The levelized cost of hydrogen production ($LCOH_p$) results of the scenarios identified in Section 5.8 are then presented. A comparison with literature is also performed, to validate the partial results and strengthen the plausibility of the overall LCOH.

6.1.1 Levelized Cost of Electricity

The LCOE is directly calculated in the tool despite not being a central element of the analysis, since it is an important element to assess the hydrogen production costs when the electrolyzer is connected with a dedicated renewable energy plant. For these reasons, an analysis of its results is presented. Figure 34, Figure 35 and Figure 36 show the LCOE for different RES. The first point that can be noticed is the competitive advantage of solar PV and onshore wind from remote locations outside of Europe. Among the studied cases, the cheapest electricity in 2022 comes from the Chilean wind in the Magallanes region with a LCOH of 19 €/MWh. The steeper decrease in the cost of solar PVs makes the Chilean solar the most competitive source of electricity in 2030: it falls below 16 €/MWh, with onshore wind slightly above it. This confirms Chile as the most advantageous location to install renewable energy plants. In addition, it is worth mentioning the change in trend in Germany: around 2027, solar PV becomes on average the cheapest RES, overcoming onshore wind.

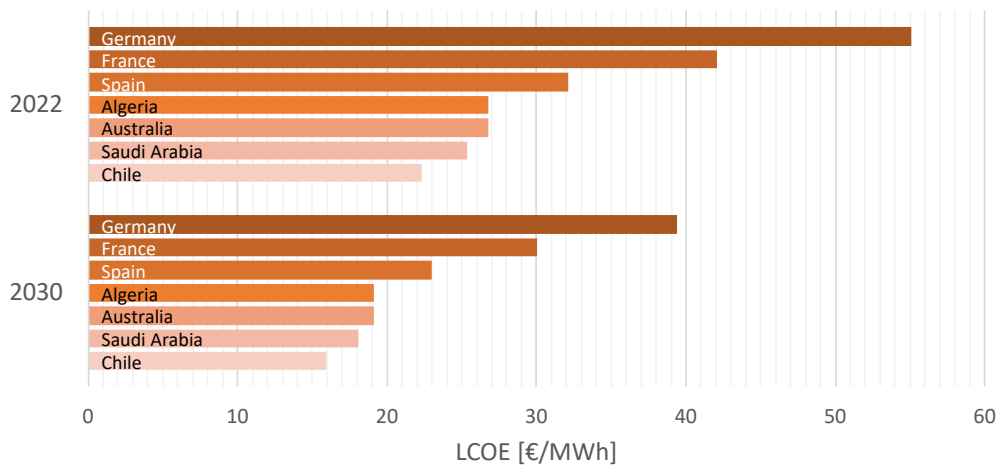


Figure 34: Levelized cost of electricity from solar PV in 2022 and 2030, for selected locations.

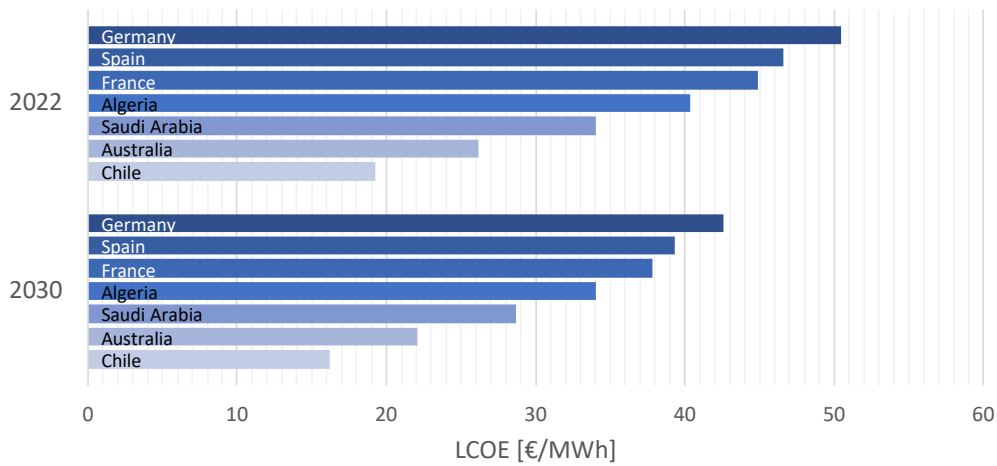


Figure 35: Levelized cost of electricity from onshore wind in 2022 and 2030, for selected locations.

The higher CAPEX of an offshore wind plant makes this resource uncompetitive with its alternatives in Europe. However, technological improvement and further expertise allow a more rapid reduction in offshore costs than onshore wind: in Germany, the difference between the two options goes from 30.6 €/MWh in 2022 to 21.6 €/MWh in 2030.

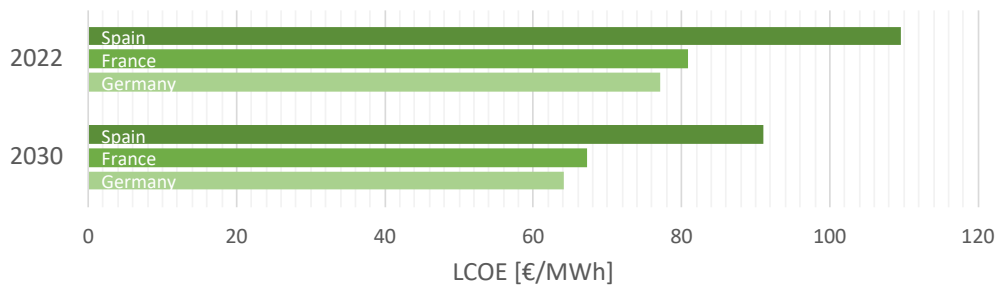


Figure 36: Levelized cost of electricity from offshore wind in 2022 and 2030, for selected locations.

Figure 37 juxtaposes the results for Germany with different trends from literature, extending the analysis to 2017. Despite some differences, the results from this study are within similar ranges, hence these charts verify the plausibility of the LCOE results.

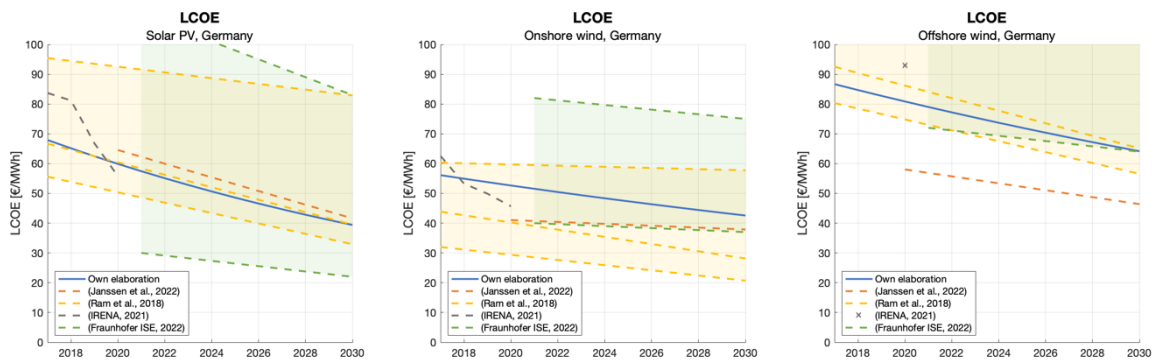


Figure 37: Comparison between the calculated LCOE in Germany and values from the literature, for different RES [15], [171], [172], [242].

Similar charts for France and Spain are also presented in Appendix VIII.

6.1.2 Electrolyzer CAPEX

Together with the LCOE, the other main driver of the cost of green hydrogen from dedicated renewable energy sources is the electrolyzer CAPEX. As illustrated in Section 5.4.1, the electrolyzer system is divided in stack and auxiliary components. Two effects determine a decrease in the cost of these elements: scaling and learning effects. Figure 38 assesses the impact of scaling up the electrolyzer size on its costs per unit of capacity. In general, the electrolyzer stack cost initially decreases but then stabilizes at a certain value. This occurs around the maximum cell size, that is in the order of magnitude of 1 MW_{el}: if larger capacities are desired, the stack design becomes modular, and scaling effects are minimized. Instead, the specific expenses for auxiliary components keep declining, even for large-scale applications. This is because no size limitations are linked with this equipment (gas conditioning, power electronics, balance of plant), therefore an economy of scale is particularly advantageous. It can also be noted that the solid oxide stack has a much lower share of the overall costs. The reason is the need for more complex auxiliary parts: for instance, the outlet gas is a mixture of steam and hydrogen, which needs further separation and purification steps [13]. This has two interesting implications: first, the current cost for a SOEC stack is lower than for a PEM, and second, scaling up an SOE system is more advantageous than for alkaline and PEM, that instead have a similar, flatter trend.

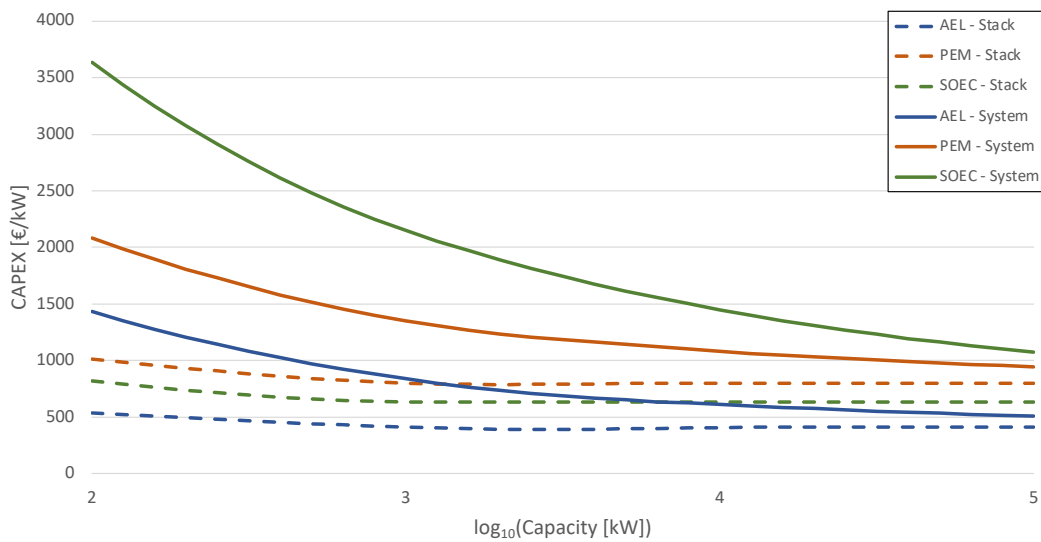


Figure 38: Impact of scaling effects on the CAPEX of an electrolyzer system (stack + auxiliary components) in 2022.

Economy of scale also influences the specific electrolyzer cost due to the technological improvement. In Figure 39, the trend of the CAPEX throughout the years is studied. Alkaline electrolysers maintain their competitiveness: with reference to a 1-MW_{el} system, their cost goes from 840 €/kW_{el} in 2022 to 390 €/kW_{el} in 2030. However, PEM and SOEC reduce the gap, respectively falling from 1350 and 2150 €/kW_{el} in 2022 to 610 and 1000 €/kW_{el} in 2030. Contrary to the scaling effect case, the main driver of the overall cost decline due to learning effects is the electrolyzer stack.

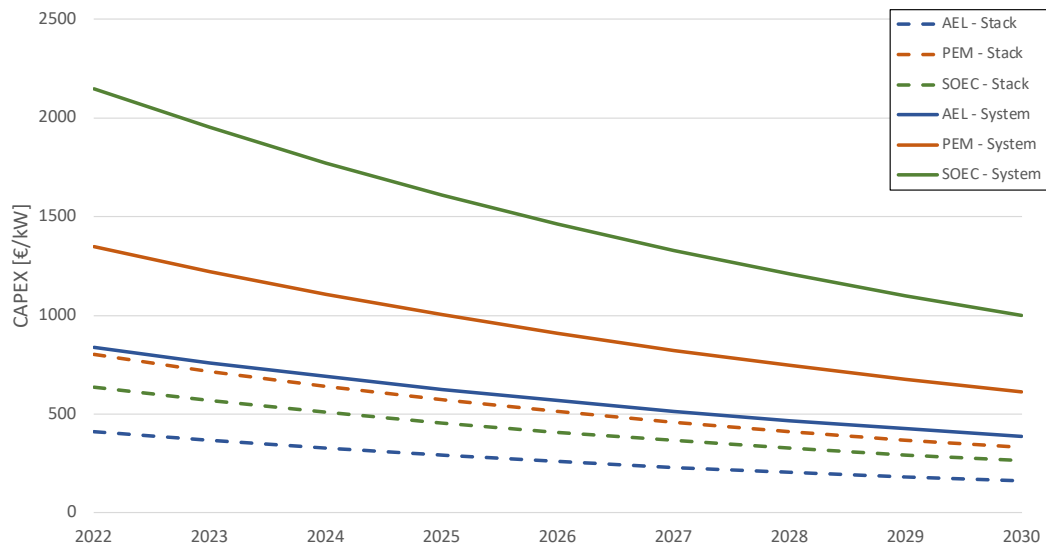


Figure 39: Impact of learning effects on the CAPEX of a 1 MW electrolyzer system (stack + auxiliary components).

Two limitations concerning the electrolyzer CAPEX calculations can be mentioned. First, the high uncertainty of both economy-of-scale effects, given the low level of maturity and absence of mass production. Results for SOEC need to be considered even more carefully due to the early stages of its development. The second limitation of this analysis is the deployment rate until 2030, that has been considered identical for every electrolyzer technology. However, it is likely that in the next few years alkaline will experience a faster growth, but then PEM, and later SOEC, will become the dominant technologies. This would translate to a steeper drop in costs at the beginning for alkaline systems, then flattening when PEM and SOEC catch up. Instead, these two technologies would have a slower improvement initially, then plummet towards the end of the decade [164]. Due to these limitations and uncertainties, the results are compared to literature projections in Appendix VIII, to check for their plausibility.

6.1.3 Levelized Cost of Hydrogen production, general cases

This section illustrates the LCOH results for general production cases with varying electricity, gas, and carbon prices, hence independently from any specific country. The aim is to compare the different technologies and configurations, to help the later country- and case-specific analysis. For this reason, the main interest in this section is not the precise value of the LCOH, but rather its trend for different options and commodity prices.

A first assessment covers the three electrolyzer types, directly connected to the power grid: their $LCOH_p$ is studied as a function of the electricity price and year. Figure 40 shows the impact of an electricity price ranging between 0 and 15 c€/kWh on the $LCOH_p$, assuming a 1-MW_{el} system and a 95% utilization rate. Currently, alkaline is the most competitive technology, and it remains in 2030, even though the gap shrinks. Given the linear relationship between the two values, a step increase of 1 c€/kWh translates to a 0.68 €/kg higher $LCOH_p$ for alkaline in 2022, diminishing to 0.61 €/kg in 2030 due to technological learning and higher efficiencies. PEM and SOEC present similar results but slightly different trends: the former is more sensitive to a rise in electricity prices due to its lower efficiency, approaching the $LCOH_p$ of the latter with higher values. This strengthens the competitive advantage of alkaline and solid-oxide options when directly connected to the power grid. Instead, a PEM electrolyzer fits better with lower electricity costs. This is the case with dedicated renewable energy plants, where PEM has also the great advantage of higher flexibility to follow a variable load. For this reason, the analysis of PEM will gain importance in the later study of low-cost solar and wind cases.

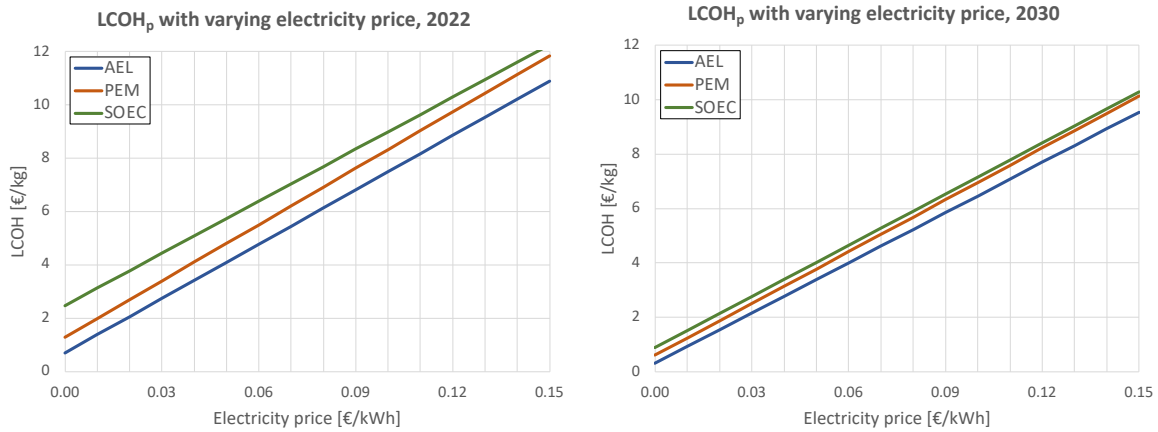


Figure 40: $LCOH_p$ via electrolysis (1-MW_{el} system) with varying electricity price in 2022 and 2030.

Setting the electricity price at an average value of 8 c€/kWh, the annual $LCOH_p$ trend is examined between 2022 and 2030. Figure 41 depicts the $LCOH_p$ both with and without the electricity component (dashed line, sum of capital and fixed operational costs). It is evident that electricity at this price is the main cost factor. As mentioned earlier, the cost difference between the cheaper alkaline and the other two technologies narrows down, with SOEC approaching PEM at the end of the decade.

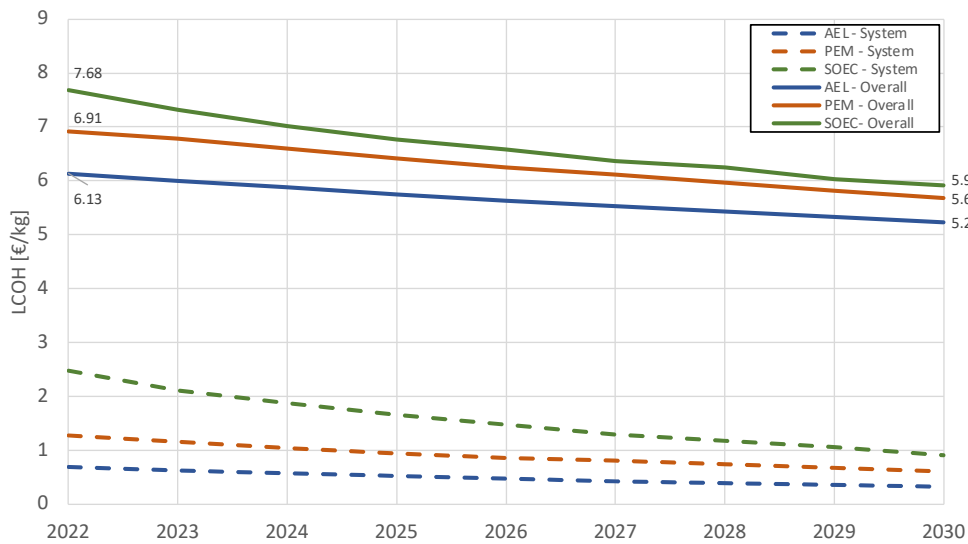


Figure 41: $LCOH_p$ via electrolysis with fixed electricity price at 8 c€/kWh_{el}.

For now, the result analysis mainly covered hydrogen from electrolysis. However, natural gas might still play an important role in the following years as feedstock for hydrogen production, either via SMR or pyrolysis. The possibility to couple SMR with CCS technologies reduces the carbon footprint of hydrogen but also increases the production costs. For this reason, it is important in the first place to assess the competitiveness of blue hydrogen with conventional grey hydrogen (mode 1). As mentioned before, two configurations are considered for SMR with CCS: natural gas-fueled plant with 90% capture rate (mode 2) and hydrogen-fueled plant with 65% capture rate (mode 3). Two external prices have large influence on the SMR production cost: the natural gas one (feedstock and fuel), and the by-product CO₂ one. Figure 42 studies the cheapest option for a wide range of gas and carbon prices. Even though grey hydrogen is beyond the scope of this work, its cost gives an important benchmark for alternative production methods, and it is therefore included in this section. In the left chart, the most competitive option in 2022 is presented, complemented by the corresponding $LCOH_p$ isolines on the right. At low carbon prices, grey hydrogen is the best option in economic terms, and the carbon price threshold that makes it disadvantageous increases with higher gas prices. Mode 3 is very competitive with low-medium gas prices

(below 5 c€/kWh_{ng,HHV}) and average carbon prices. This can be explained by its lower CAPEX for the carbon capture components, and slightly better efficiency compared to mode 2. However, its lower carbon capture rate makes it less advantageous with rising carbon prices, where instead mode 2 becomes the most suitable option.

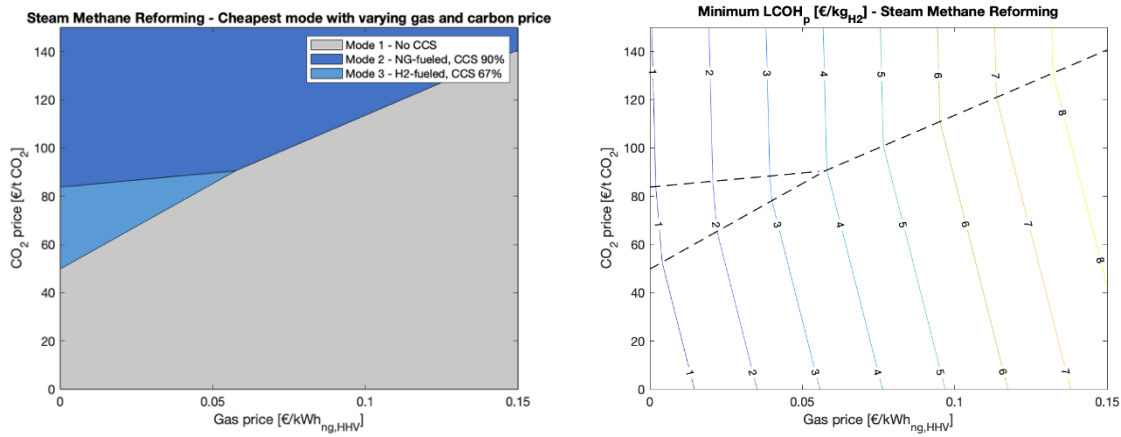


Figure 42: SMR configuration comparison in 2022 with varying gas and carbon prices. Cheapest configuration (left) and its LCOH isolines (right).

Figure 43 presents the same analysis but for 2030. The expectations for a decline in carbon capture CAPEX makes mode 2 even more appealing. The learning effects and the forecasted higher carbon prices advise mode 2 as the most suitable solution in the long term. Mode 3 is however an appealing solution in the short-medium term, given its lower capital expenses and the simpler nature of the carbon capture components.

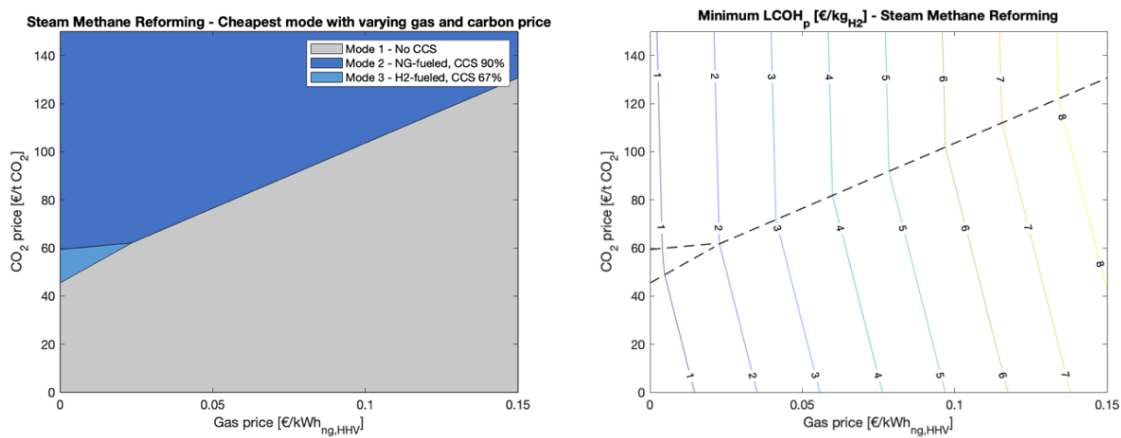


Figure 43: SMR configuration comparison in 2030 with varying gas and carbon prices. Cheapest configuration (left) and its LCOH isolines (right).

The third production method, pyrolysis, can be added to the analysis and compared for now to SMR, given their common dependence on the gas price. As shown in Figure 44, pyrolysis is in a similar cost range to SMR, explaining the interest in this emission-free technology. With a carbon price fixed at 100 €/tCO₂ and gas prices below 4 c€/kWh_{ng,HHV}, pyrolysis is the most competitive option already in 2022. Similar conclusions can be drawn for 2030. Due to its higher need for natural gas per mass unit of hydrogen, pyrolysis costs increase steeply: for every additional c€/kWh_{ng,HHV}, its LCOH_p grows by 0.7 €/kg, compared to values around 0.5 €/kg for the different SMR modes.

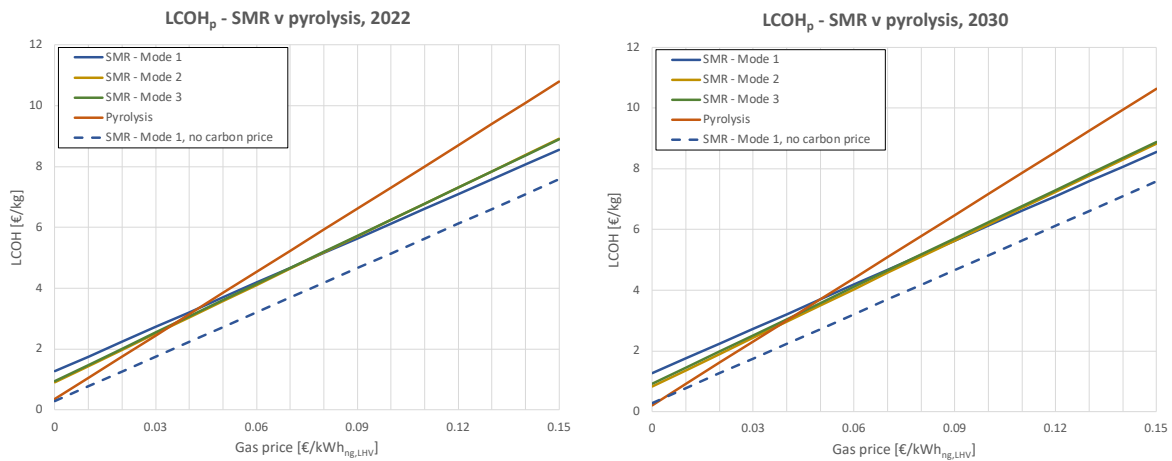


Figure 44: Levelized cost of hydrogen production for different SMR configurations and pyrolysis in 2022 and in 2030. If not indicated otherwise, carbon price fixed at 100 €/t_{CO2}.

This section gives an important, general starting point for the following analysis of the specific production cases. The consideration and results here discussed should be kept in mind for a deeper evaluation of the hydrogen cost prognosis and its conclusions. In the next sections the production costs of the different scenarios are discussed. This is done to facilitate the later assessment of the whole supply chains, carried out in Section 6.5.

6.1.4 Germany

Figure 45 compares the cost of several low-carbon production methods in Germany. In general, the processes based on natural gas present the lowest costs: SMR²⁶ and pyrolysis are currently around 2.8 €/kg, then approaching 2.2 €/kg by 2030, with pyrolysis becoming the cheapest production option. The wide difference between green and blue/turquoise hydrogen costs shrinks by the end of the decade. Considering PEM electrolysis powered by a dedicated onshore wind facility, the gap goes from 2.6 €/kg in 2022 to 1.2 €/kg in 2030. The solar solution experiences the fastest decline, approaching onshore wind in 2030, with LCOH_p respectively equal to 4.0 and 3.4 €/kg. The high electricity price suggests the uncompetitive nature of models with the power grid and electrolyzers directly connected: despite the higher capacity factors and the lower CAPEX in the case of AEL, their LCOH_p is around 6.8-7.2 €/kg in 2030. The possible use of curtailed electricity might bring the LCOH down for systems connected to the grid. This is not studied in this research, but can be an interesting case for future work.

²⁶ From this section on SMR refers to steam methane reforming in mode 2 (with carbon capture and storage, fueled with natural gas).

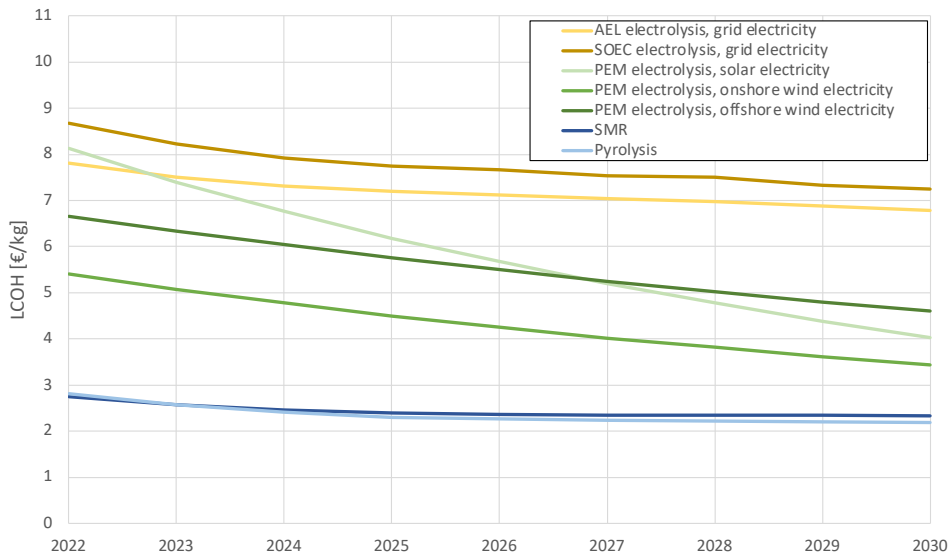


Figure 45: Levelized cost of hydrogen production in Germany, from 2022 to 2030.

6.1.5 Spain

The great availability of solar resource in Spain makes hydrogen production a very attractive alternative. Two possible business models are compared in Figure 46: a small-scale (1 MW_{el}), local system and a large-scale (100 MW_{el}), centralized system. Due to economy of scale, centralized large-scale production is currently 1 €/kg cheaper than local small-scale systems, with respectively an LCOH of 4.8 and 5.9 €/kg. In 2030, the gap halves, with large- and small-scale respectively at 2.8 and 2.4 €/kg.



Figure 46: Levelized cost of hydrogen production via electrolysis from solar PV electricity in Spain. Comparison between a small-scale (1 MW_{el}) and a large-scale (100 MW_{el}) plant.

6.1.6 France

In France, the discussion covers production methods that employ electrolysis and different sources of electricity. Figure 47 gathers their LCOH_p trends in the following years. As pointed out for Germany, also in France green hydrogen options present lower costs compared to grid-powered electrolyzers. The PEM technology with reserved solar and onshore wind has a current LCOH_p respectively of 6.2 and 4.8 €/kg, then overlapping at 3.1 €/kg in 2030. This is about half of the cost for AEL and SOEC directly powered by the national grid, respectively at 6 and 6.5 €/kg in the same year. It is also interesting to highlight the very expensive pink hydrogen: the high LCOE of an EPR undermines the possibility to produce hydrogen directly at the nuclear facility with this type of reactors. The study is limited to this nuclear plant type and these hydrogen production configurations. However, different configurations might achieve a lower LCOH.

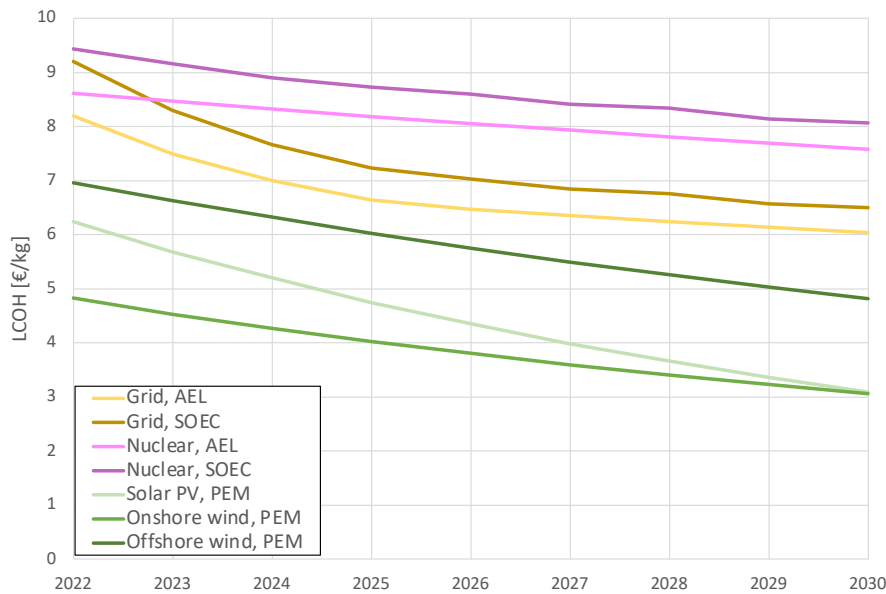


Figure 47: Levelized cost of hydrogen production via electrolysis in France, from 2022 to 2030.

6.1.7 Green hydrogen from non-European countries

The cost of hydrogen production via electrolysis varies globally, mainly depending on the electricity source and its availability. The main results for the exporting countries within the scope are presented in Figure 48. The two charts also show the European values as a term of comparison. Chilean onshore wind corresponds to the lowest LCOH_p among the studied cases, with a value of 2.3 €/kg in 2022 and 1.5 €/kg in 2030. Chile also delivers the cheapest hydrogen from solar electricity: due to the steep learning curves for PVs, this LCOH_p falls below 1.8 €/kg in 2030. Solar-powered electrolysers have a similar LCOH_p in Australia, Saudi Arabia, and Algeria: the cost around 4 €/kg in 2022 get halved in 2030 for all three cases.

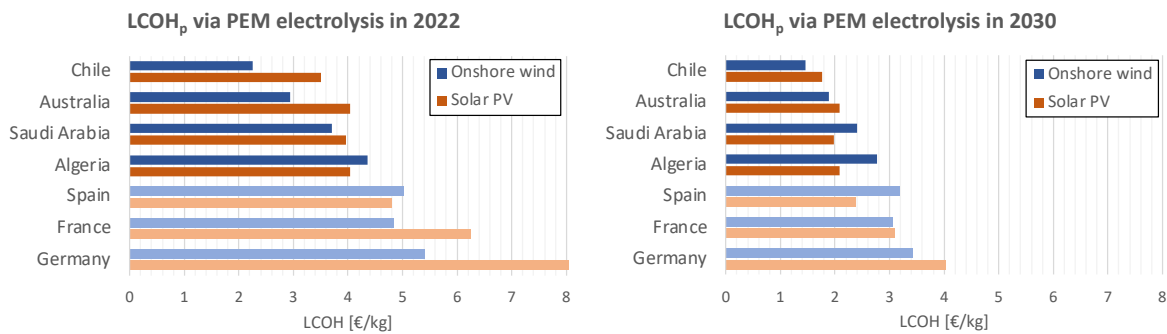


Figure 48: LCOH_p for green hydrogen production in different countries, with reference to a 100-MW PEM electrolyzer in 2022 and in 2030.

6.1.8 Blue and turquoise hydrogen in Europe and gas-producing countries

Blue hydrogen production in Europe could be an important alternative to electrolysis, especially in the short-medium term. Following the results of Section 6.1.3 and the range of input costs (ETS, natural gas), only mode 2 (natural gas fueled, carbon capture rate at 90%) is considered. The LCOH_p of SMR is influenced by both the gas and the carbon price, with the former going back to average levels in the following years, and the latter instead rapidly increasing. Figure 49 shows that despite the ETS cost slightly increase, this component does not have a relevant impact on the LCOH_p, also since most of the emissions are captured. Instead, the gas price is the main driver, responsible for about two-thirds of the costs. Its

price decline, together with the technological learning linked with carbon capture, determines a $LCOH_p$ that goes from 2.8 €/kg in 2022 to 2.4 €/kg in 2030.

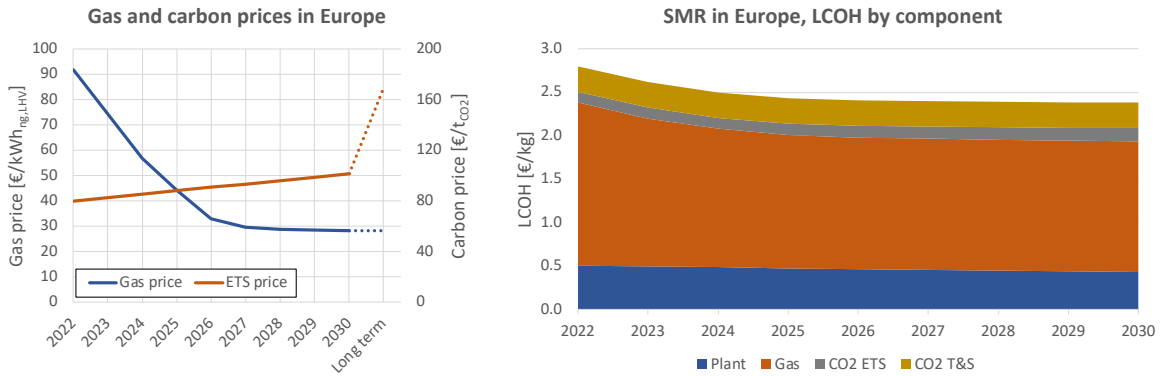


Figure 49: Gas and carbon prices (left) and $LCOH_p$ for SMR by component in Europe.

Steam methane reforming coupled with CCS is an attractive solution especially for economies largely relying on natural gas extractions and exports, enabling a smoother transition. Qatar and Algeria can produce hydrogen at costs as low as 0.74 and 0.80 €/kg in 2030. Both countries currently do not have a carbon pricing mechanism, and it is presumed that this will not be implemented before 2030. However, even if a carbon border adjustment at the same price level of the EU-ETS is implemented, their $LCOH_p$ is below 1 €/kg. Norwegian blue hydrogen is slightly more expensive, about 1.3 €/kg.

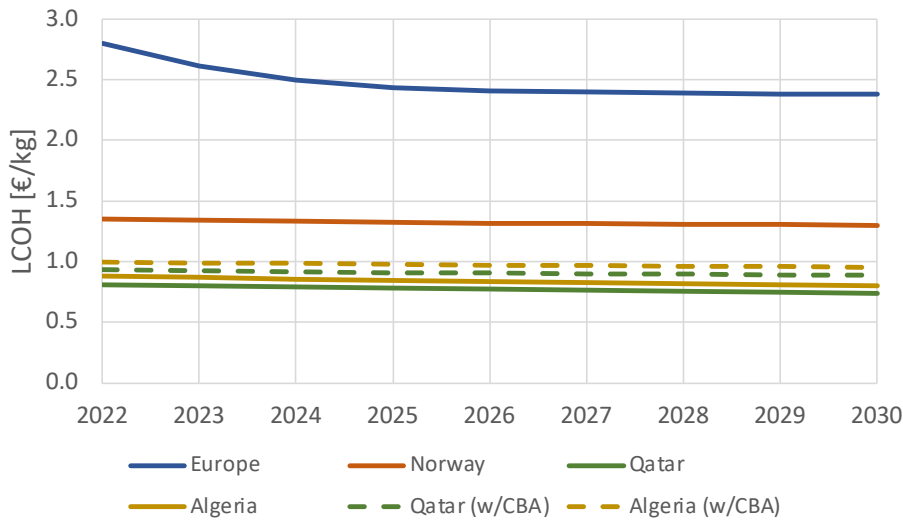


Figure 50: $LCOH_p$ for SMR in Europe and gas-producing countries.

Pyrolysis has values in the same range as SMR, as presented in Figure 51. Algeria becomes the cheapest location to produce hydrogen, with a $LCOH_p$ in 2030 of 0.43 €/kg, inverting the order seen for SMR. This can be explained by its more expensive cost to store CO_2 compared to Qatar, that instead does not influence the pyrolysis expenses. Norway is also able to produce hydrogen at a cost below 1 €/kg.

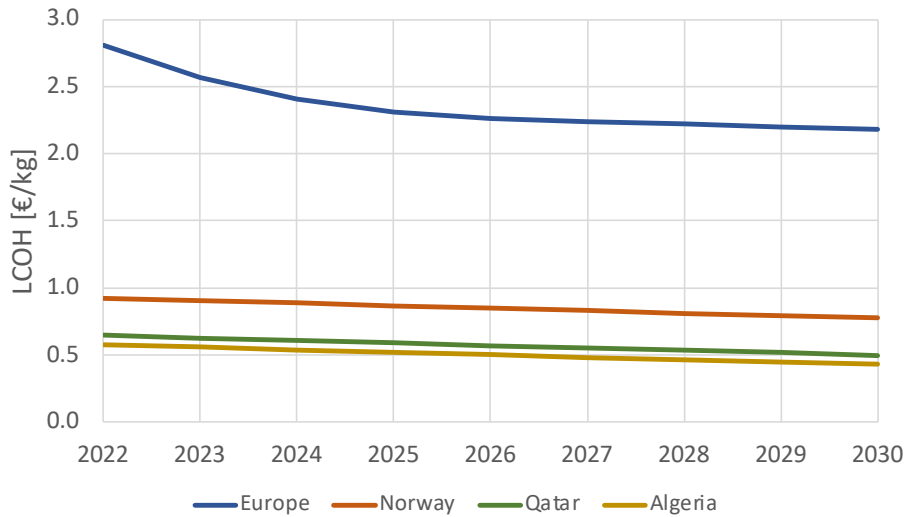


Figure 51: LCOH_p for pyrolysis in Europe and gas-producing countries.

To have a closer look at the comparison between SMR with CCS and pyrolysis, Figure 52 reports the results only for Europe and one gas-producing country, in this case Qatar. Currently, blue and turquoise hydrogen have the same cost in Europe, at 2.8 €/kg. In Qatar instead, pyrolysis is already more competitive at 0.6 €/kg, 20 eurocents below SMR. Both gaps widen towards the end of the decade: in Europe, the LCOH_p for pyrolysis and SMR respectively decrease by 22% and 15%, corresponding to 2.2 and 2.4 €/kg. In Qatar, the SMR trend is flatter with a 9% decrease, while pyrolysis also declines quickly by 23%.

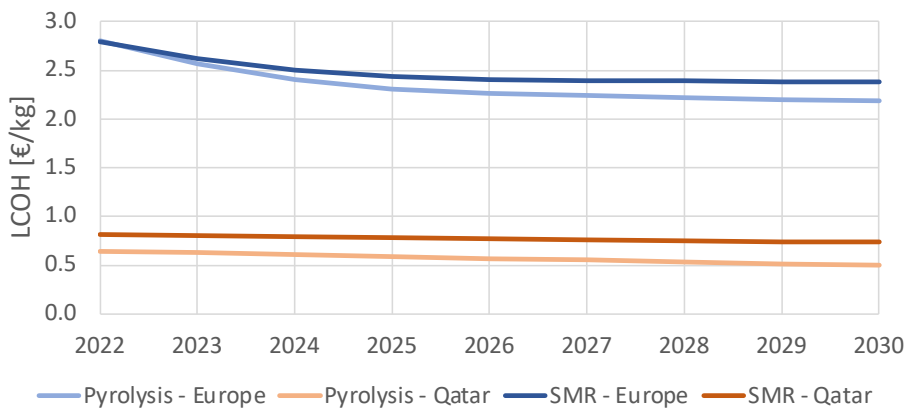


Figure 52: Comparison between LCOH_p for SMR and for pyrolysis in Europe and in Qatar.

6.2 Transmission and distribution

This section aims at illustrating the results of the transmission and distribution stages. To do so, the different options are compared with varying route distances. Despite the usefulness of this first assessment, it is worth mentioning that it might not give a complete comparison between the different options from one location to another one. In fact, an option might have a shorter route distance compared to the others, with a direct implication on the final LCOH_t. Giving an example, the transmission by ship from Saudi Arabia to Germany is almost twice as long as the one done by pipeline.

Figure 53 analyses the different transmission options for the transmission segment: hydrogen shipping as LH₂ and NH₃, and gH₂ pipelines. The LCOH_t includes the conversion, delivery, intermediate storage, and reconversion stages. For pipelines, both new and repurposed options are considered. However, only the offshore infrastructure is shown: despite a CAPEX 25% higher, the LCOH_t only differs by around 1%. Therefore, the onshore values are not reported in the chart. Figure 53 also depicts the LCOH_t without the final conversion when the final form is not gaseous hydrogen. Despite the high initial investment for

shipping, it does not directly depend on the distance²⁷, determining a flatter trend. Pipelines have instead a closer dependence on the route distance, which results in a steeper variation: every 1000 km, the LCOH_t via new pipelines increases by about 0.18 €/kg; via repurposed pipelines by about 0.10 €/kg. Considering a hydrogen final use in its gaseous form, repurposed pipelines are always the cheapest option below 10000 km, while LH₂ becomes competitive with new pipeline infrastructure around 10000 km. NH₃ shipping is not economically feasible if gH₂ is eventually desired. In fact, the last reconversion has a large impact on ammonia shipping: it adds 2.1 €/kg, almost tripling its LCOH_t. However, if the final state is the same as the delivery one (i.e., no reconversion), NH₃ shipping has similar results to LH₂ shipping, with lower LCOH_t than the new network above 3000 km, and repurposed above 7500 km.

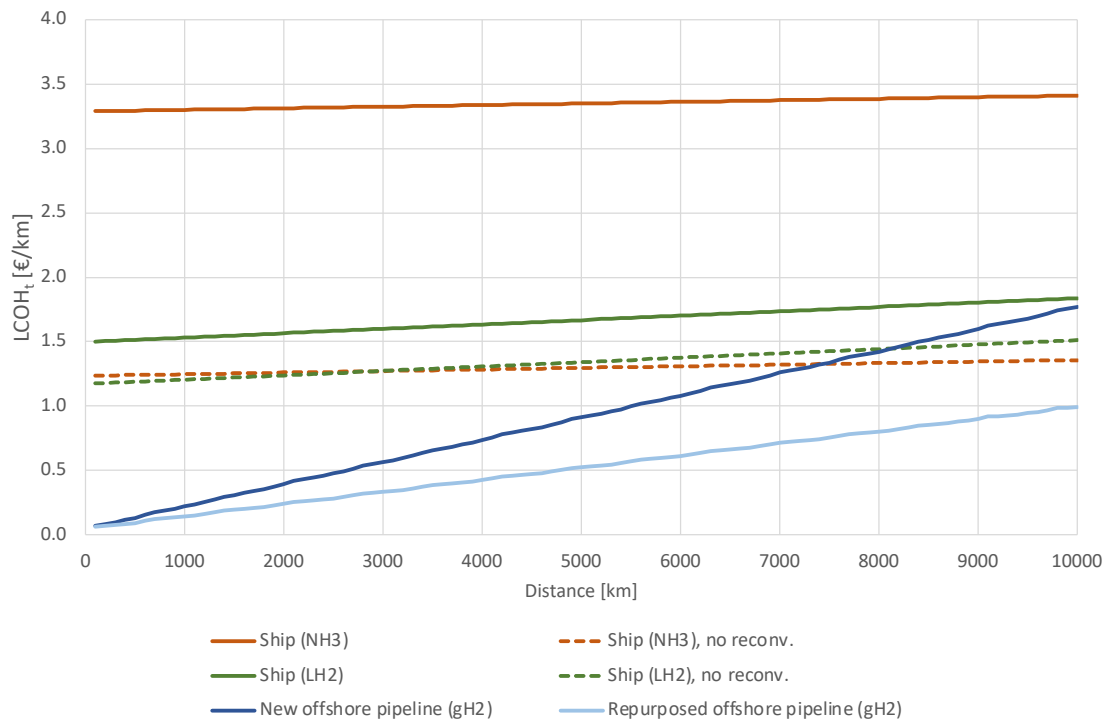


Figure 53: Comparison of transmission options with varying route distance.

Similarly to transmission, Figure 54 presents a similar assessment for the distribution segment. In this case, new and repurposed pipelines, in their small and medium size (respectively, 500 and 900 mm) are compared with truck delivery with three different carriers: gH₂ at 250 bar, LH₂, and NH₃. Small diameter pipelines are limited to a maximum distance of 200 km, following Jens *et al.* [108] assumptions. In the distance range considered, pipelines are always the cheapest distribution mode. The difference between small and medium pipelines is limited: the medium option has a cost 0.02-0.07 €/kg lower than the smaller one. Despite a steeper trend, gH₂ delivery is the cheapest truck option with a gaseous final use. In fact, LH₂ transportation has a generally higher cost, while ammonia requires a very expensive reconversion at the final point of use. Due to the large share of the reconversion stage, NH₃ distribution and direct use shows the lowest LCOH_d via truck above 700 km.

²⁷ However, the distance has a more limited impact on the CAPEX and its amortization time: shorter distances allow for more trips per year, and hence a larger hydrogen quantity. This translates into a shorter amortization time and a lower LCOH_t.

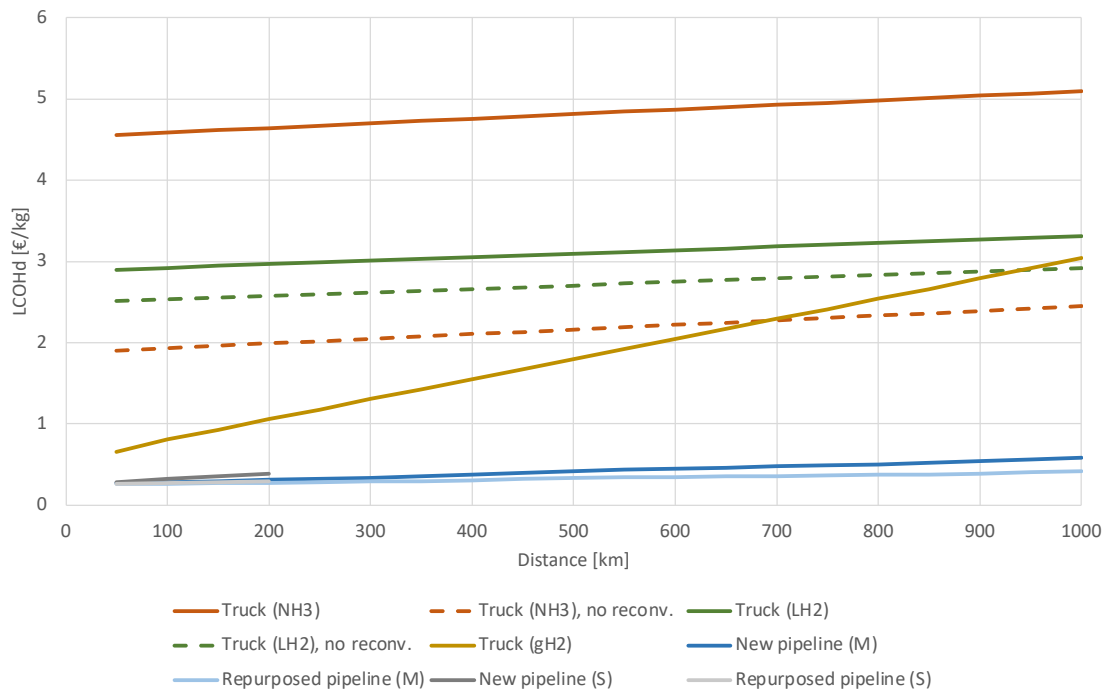


Figure 54: Comparison of distribution options with varying route distance.

6.3 Storage

The purpose of this chapter is to observe how the levelized cost of hydrogen final storage varies with respect to the most important factors. A comparison between the different storage technologies used in the model is performed as well. Also, there is a reflection on how the scaling effect is affecting the cost of initial capital expenditures and, consequently, the levelized cost of hydrogen at this stage. Finally, there is a reflection on the learning effect in hydrogen storage costs. It is important to mention that the compression stage associated with each type of gaseous hydrogen storage technology is not considered in this chapter because the specific cost of conversion technologies is considered separately in the tool and is discussed in subsection 6.4.1.

6.3.1 Geological storage

Figure 55 establishes a comparison of the levelized cost of final storage between depleted NG or oil reservoirs, salt caverns, and lined rock caverns. For the specific case of seasonal storage, considering only one charge and discharge cycle of the hydrogen produced from a site in Spain. The levelized cost of final storage varies with the hydrogen production plant capacity. As the hydrogen production plant capacity increases, the total storing volume of the underground facility increases as well.

In Figure 55, it is observed that the levelized cost of final storage in lined rock caverns is significantly higher than the levelized cost of final storage in both salt caverns, and depleted NG reservoirs for every hydrogen production plant capacity considered in the range of 100 MW to 1000 MW. This can be justified by the current CAPEX of lined rock caverns which is much higher than for salt caverns and depleted NG reservoirs (Figure 56). The levelized cost of final storage in salt caverns and depleted NG reservoirs are relatively similar. However, being the levelized cost of final storage in salt caverns slightly higher than depleted NG reservoirs for most of the hydrogen production plant capacities due to the slightly higher cost of initial capital expenditures of salt caverns.

At the same time, it is possible to see an uneven behavior of the levelized cost of final storage function for every type of geological reservoir technology. Multiple points of inflection are encountered. Depending on the geological reservoir technology, the points of inflection will occur at different hydrogen production plant capacities due to the different cushion gas requirements for each technology. On a side note, it must

be recalled that the total volume of geological reservoirs is a sum of the working gas volume and the cushion gas volume.

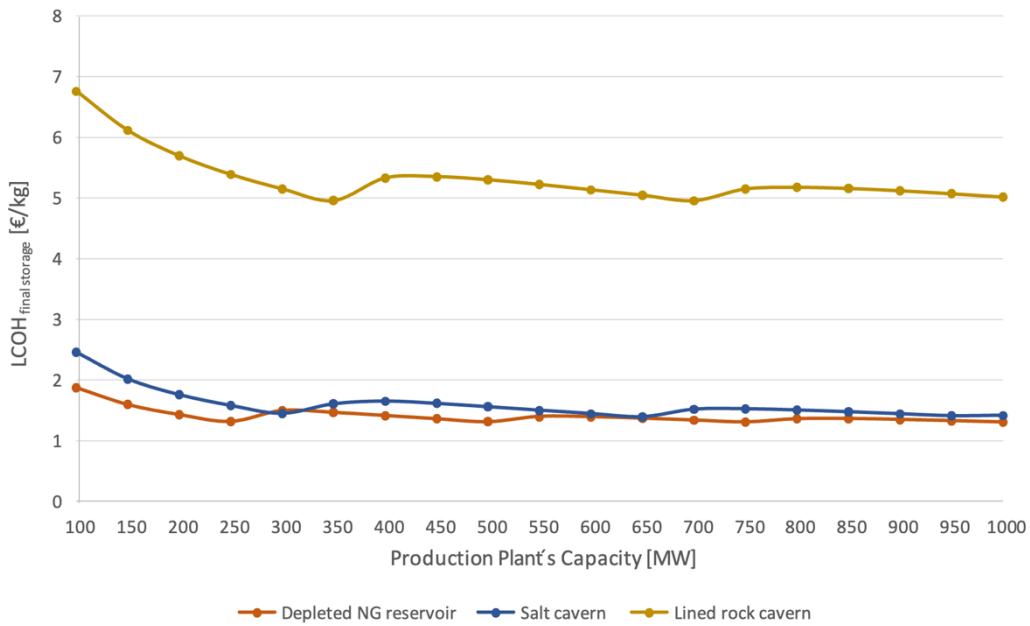


Figure 55. Variation of the levelized cost of hydrogen final storage with respect to the production plant's capacity.

A more detailed analysis on the points of inflection is done later in this section. In Figure 56, the cost of initial capital expenditures for different hydrogen production plant's capacities, considering different underground hydrogen storage technologies is plotted. The CAPEX results reflect the scaling effect in each type of technology. It is noticeable a faster increase in the CAPEX of lined rock caverns when compared to the CAPEX of salt caverns and depleted NG reservoirs. This slower increase in CAPEX means that salt caverns and depleted NG or oil reservoirs have a better scaling effect than lined rock caverns.

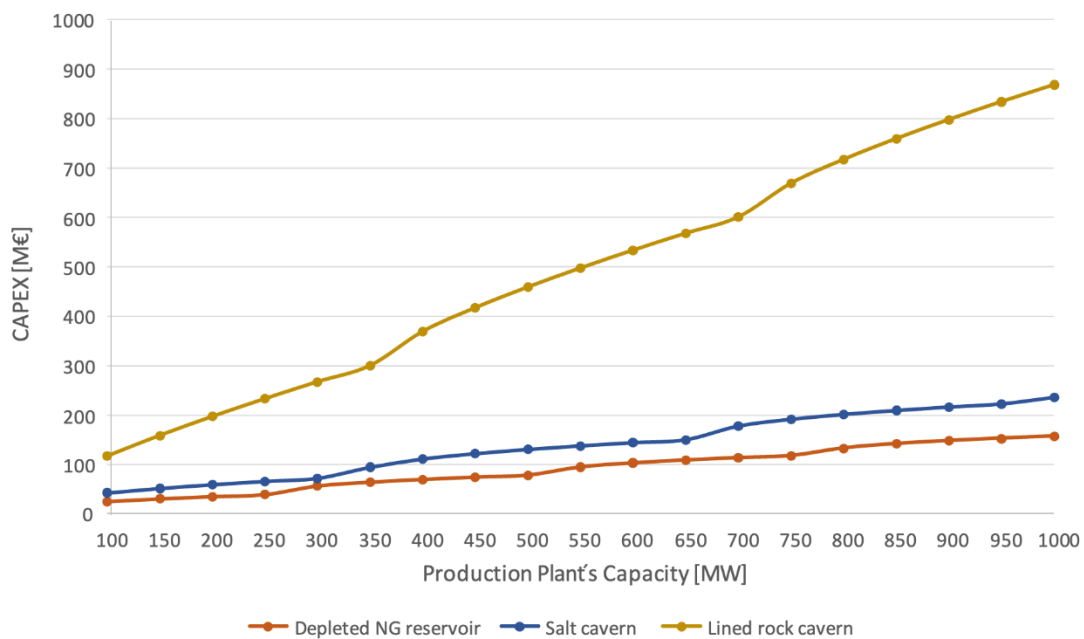


Figure 56. Variation of the CAPEX with respect to the production plant's capacity.

The points of inflection found in the results of the levelized cost of final storage per type of technology with varying volumes of hydrogen to be stored are explained in Figure 57, Figure 58, and Figure 59.

In the middle graph of Figure 57, representing the analysis for seasonal storage in salt caverns, it is possible to identify three different points of inflection: ($V_{\text{storage desired}} = 0.90 \text{ M m}^3$; $\text{LCOH}_{\text{final storage}} = 1.45 \text{ €/kg}$), ($V_{\text{storage desired}} = 1.96 \text{ M m}^3$; $\text{LCOH}_{\text{final storage}} = 1.40 \text{ €/kg}$), and ($V_{\text{storage desired}} = 2.86 \text{ M m}^3$; $\text{LCOH}_{\text{final storage}} = 1.41 \text{ €/kg}$). These points occur because they mark the transition phase characterized by an increase of the number of reservoirs required to store the amount of hydrogen produced, as it is represented in the bottom graph of Figure 57. The occurrence of inflection points for depleted NG or oil reservoirs and lined rock caverns can be explained in the same way in Figure 58 and Figure 59, respectively.

Looking at the values of $\text{LCOH}_{\text{final storage}}$ inside the red hollow rectangle in Figure 57, it is noticeable that there is a constant decrease in values with a constant increase in the reservoir size. The values inside the red hollow rectangles in the three graphs of Figure 57 represent the specific case when the total hydrogen storage volume is less than the maximum reservoir design volume, which is assumed to be 1 million m^3 as it is described in subsection 5.5.1.3. For this reason, only one reservoir is needed to store the hydrogen volumes comprehended in the red rectangle. The same interpretation can be made for the values limited by the green, blue, and yellow hollow rectangles. However, the values inside these rectangles represent the situation when the desired hydrogen reservoir volume is bigger than the maximum reservoir design volume. The underground hydrogen storage facility is constituted by one (green hollow rectangle), two (blue hollow rectangle), or three (yellow hollow rectangle) salt cavern(s) with the maximum reservoir design volume and one smaller salt cavern with a volume in between the minimum and maximum reservoir design volumes.

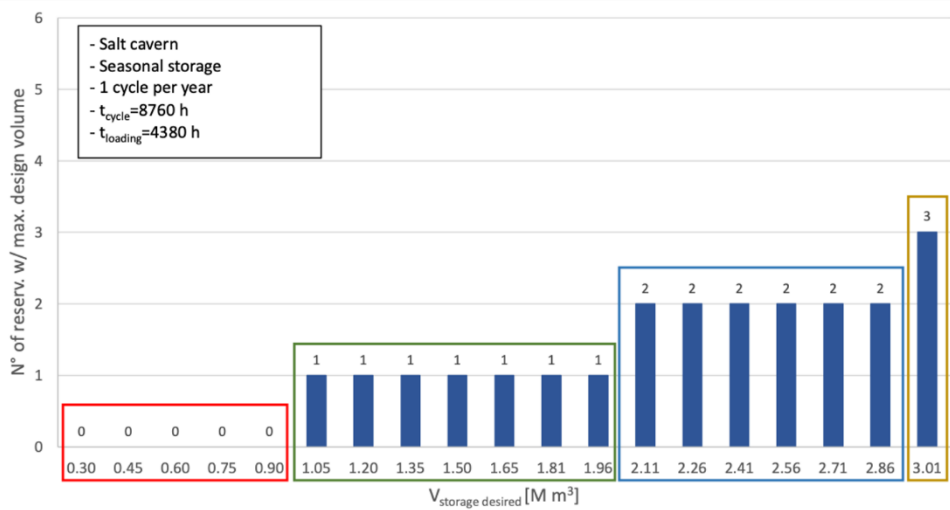
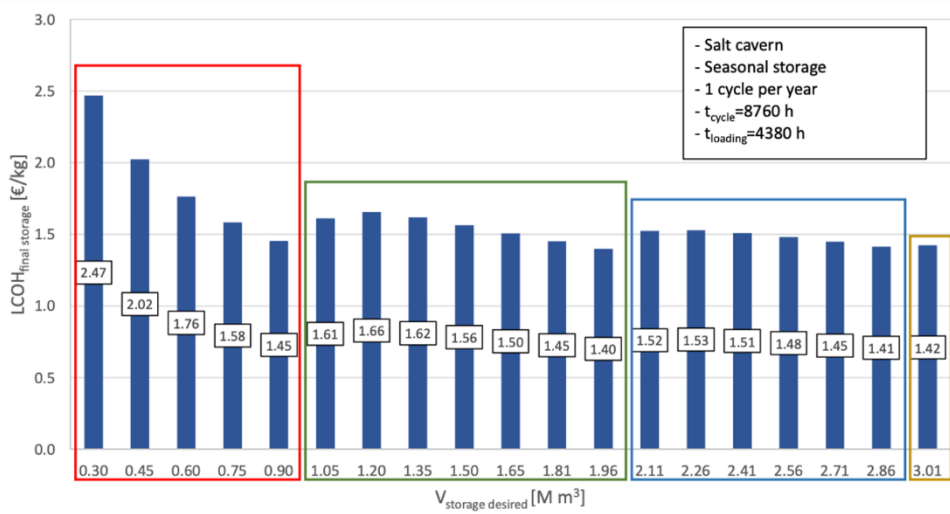
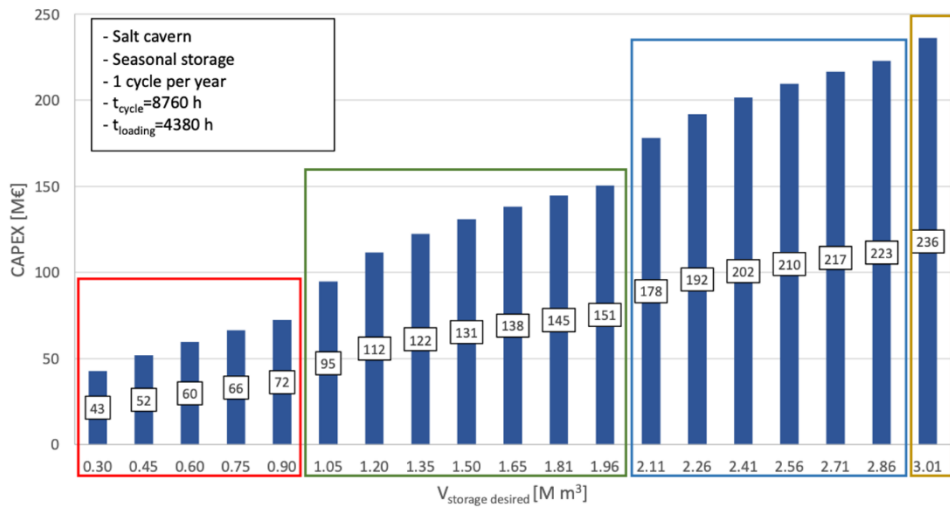


Figure 57: Compilation of three graphs representing the variation of the levelized cost of hydrogen final storage, CAPEX, and number of geological reservoirs in the considered underground storage facility with maximum design volume with respect to the desired volume of the reservoir, in other words the total volume of hydrogen to be stored. Case of seasonal storage in salt caverns.

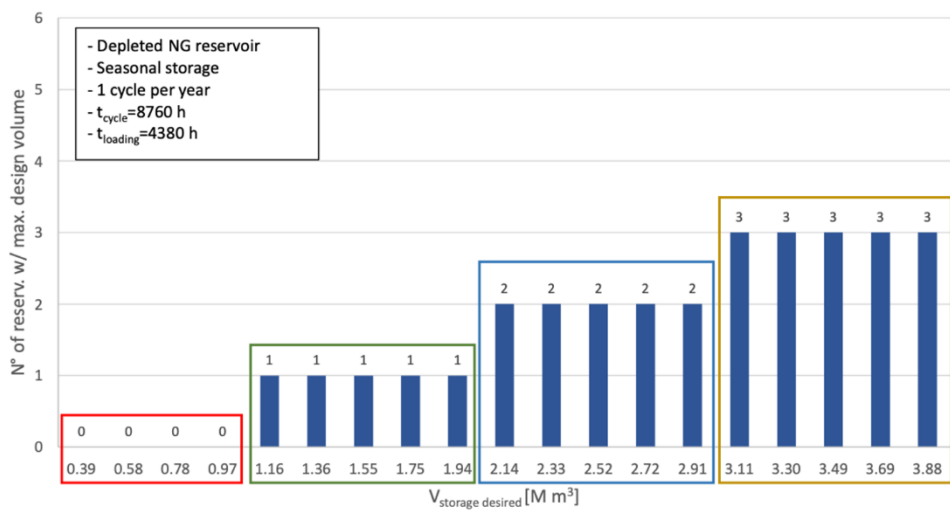
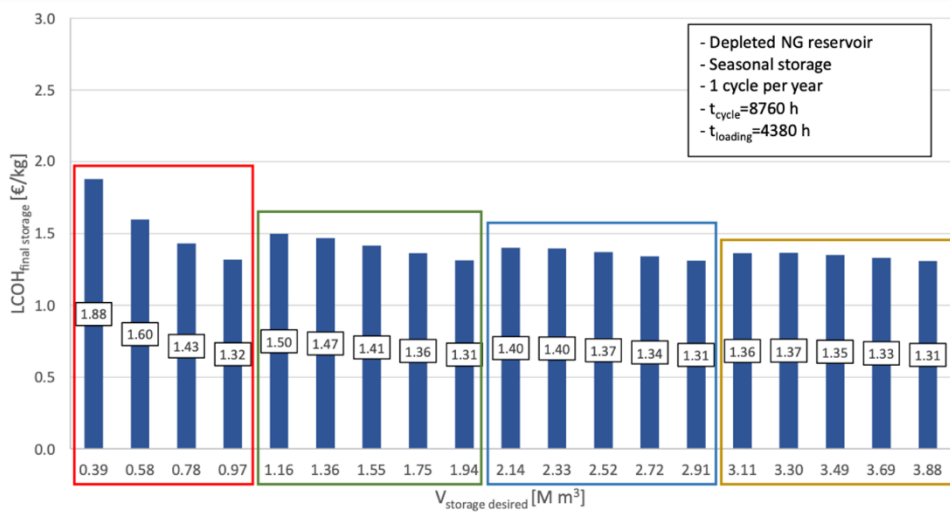
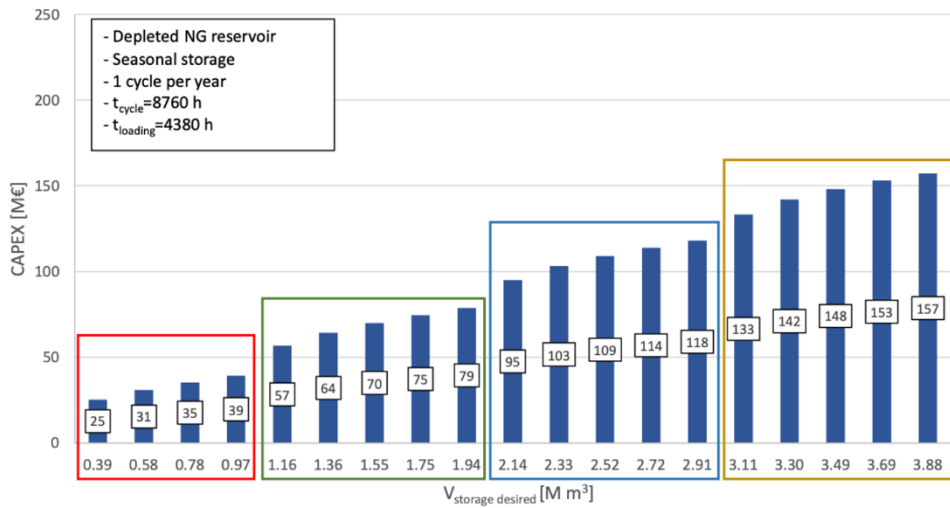


Figure 58: Compilation of three graphs representing the variation of the levelized cost of hydrogen final storage, CAPEX, and number of geological reservoirs in the considered underground storage facility with maximum design volume with respect to the desired volume of the reservoir, in other words the total volume of hydrogen to be stored. Case of seasonal storage in depleted NG or oil reservoirs.

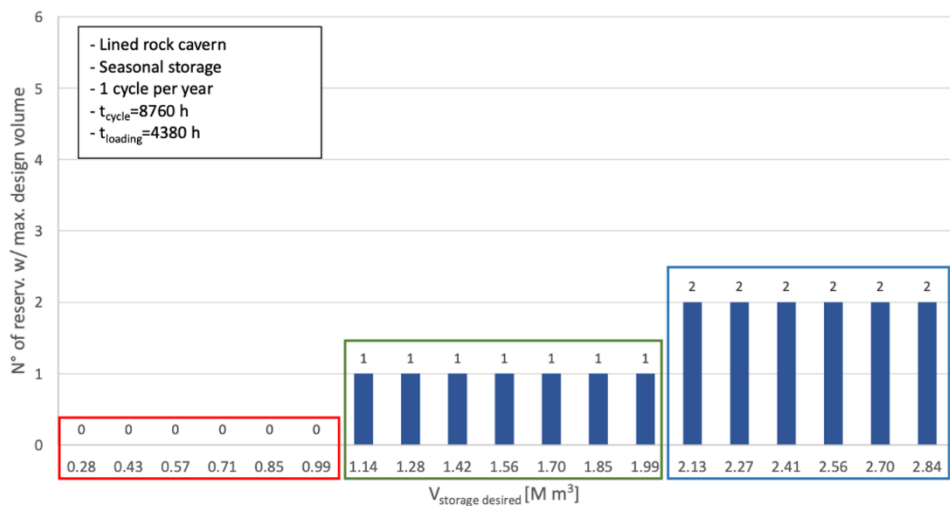
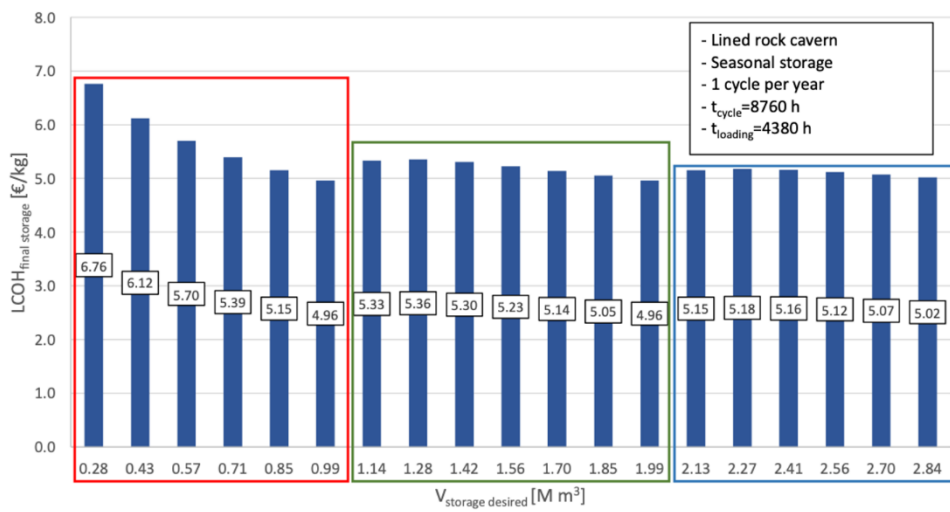
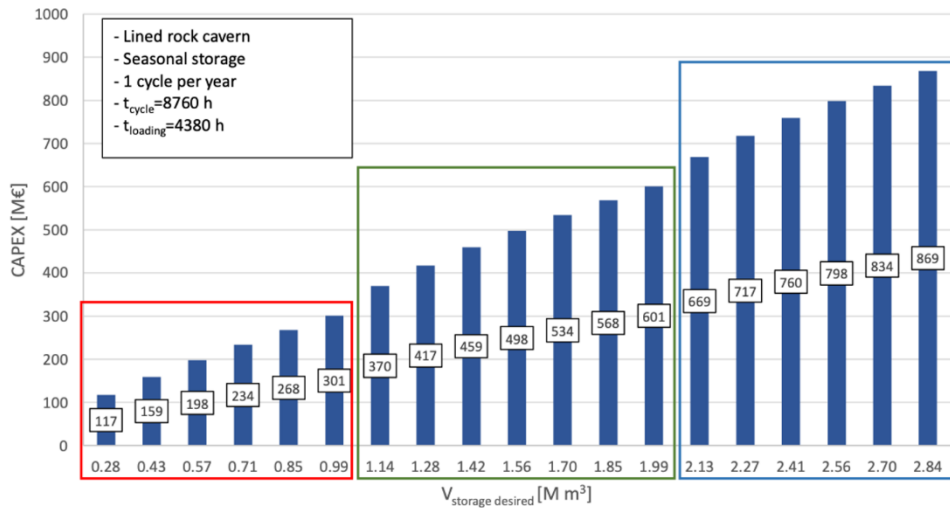


Figure 59: Compilation of three graphs representing the variation of the levelized cost of hydrogen final storage, CAPEX, and number of geological reservoirs in the considered underground storage facility with maximum design volume with respect to the desired volume of the reservoir, in other words the total volume of hydrogen to be stored. Case of seasonal storage in lined rock caverns.

To sum up, only small changes in the specific cost of final storage are identified by using a CAPEX formula that changes depending on the maximum and minimum reservoir design size (Equation (55), (56), and (57)). From the previous analysis, whenever it is required larger storage capacities and it is needed the addition of one smaller reservoir to the underground storage facility, the CAPEX registers a sudden steeper increase in magnitude, as shown in Figure 60. This is due to the normal behavior of scaling functions that tend to have a more rapid increase for small dependent variables, in this particular case for small hydrogen storage volumes. Additionally, it can be said that it is more beneficial to construct an underground hydrogen storage facility constituted by one or more geological reservoirs with volumes equal to or close to the maximum reservoir design volume, instead of having a facility constituted by one or more geological reservoirs with maximum reservoir design volume and an extra small geological reservoir. In this way, when developing a real hydrogen supply chain, the amount of hydrogen produced should be optimal, so it avoids a storage site with a small reservoir which increases the specific cost of storage.

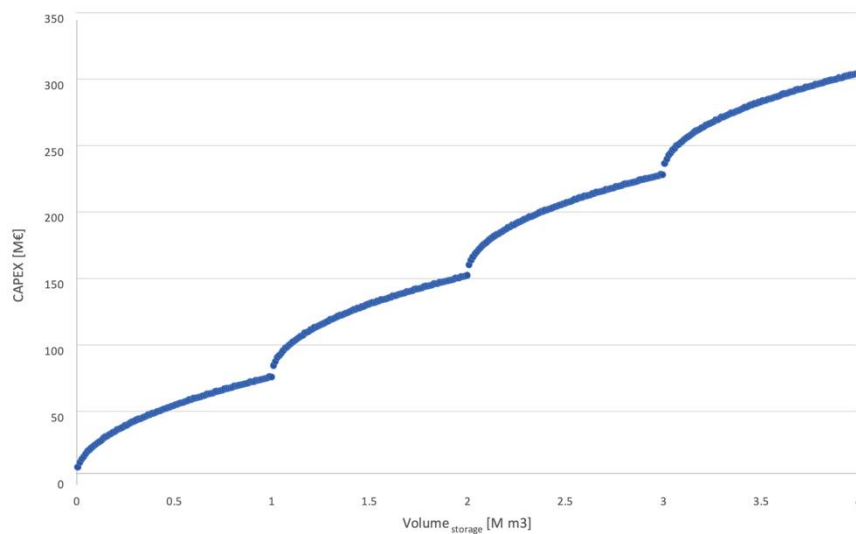


Figure 60. CAPEX versus volume storage in salt caverns.

A sensitivity analysis was conducted in order to assess how the change in the scaling factor of the initial cost of capital expenditures formula would affect the specific cost of underground hydrogen storage per type of technology. Figure 61 plots both CAPEX and levelized cost of final hydrogen storage in salt caverns with varying hydrogen production plant's capacity. Recalling again that as the hydrogen production plant capacity increases, the total storing volume of the underground facility increases as well. At the same time, the graphs in Figure 61 show the variation of the indicated parameters with an incremental and decremental change of 0.1 and 0.2 of the original scaling factor used for salt caverns which is assumed to be 0.48. From Figure 61, it is noticeable that small changes of the scaling factor for salt caverns do not significantly affect the CAPEX values with varying reservoir sizes. Therefore, the levelized cost of final storage in salt caverns does not register significant changes.

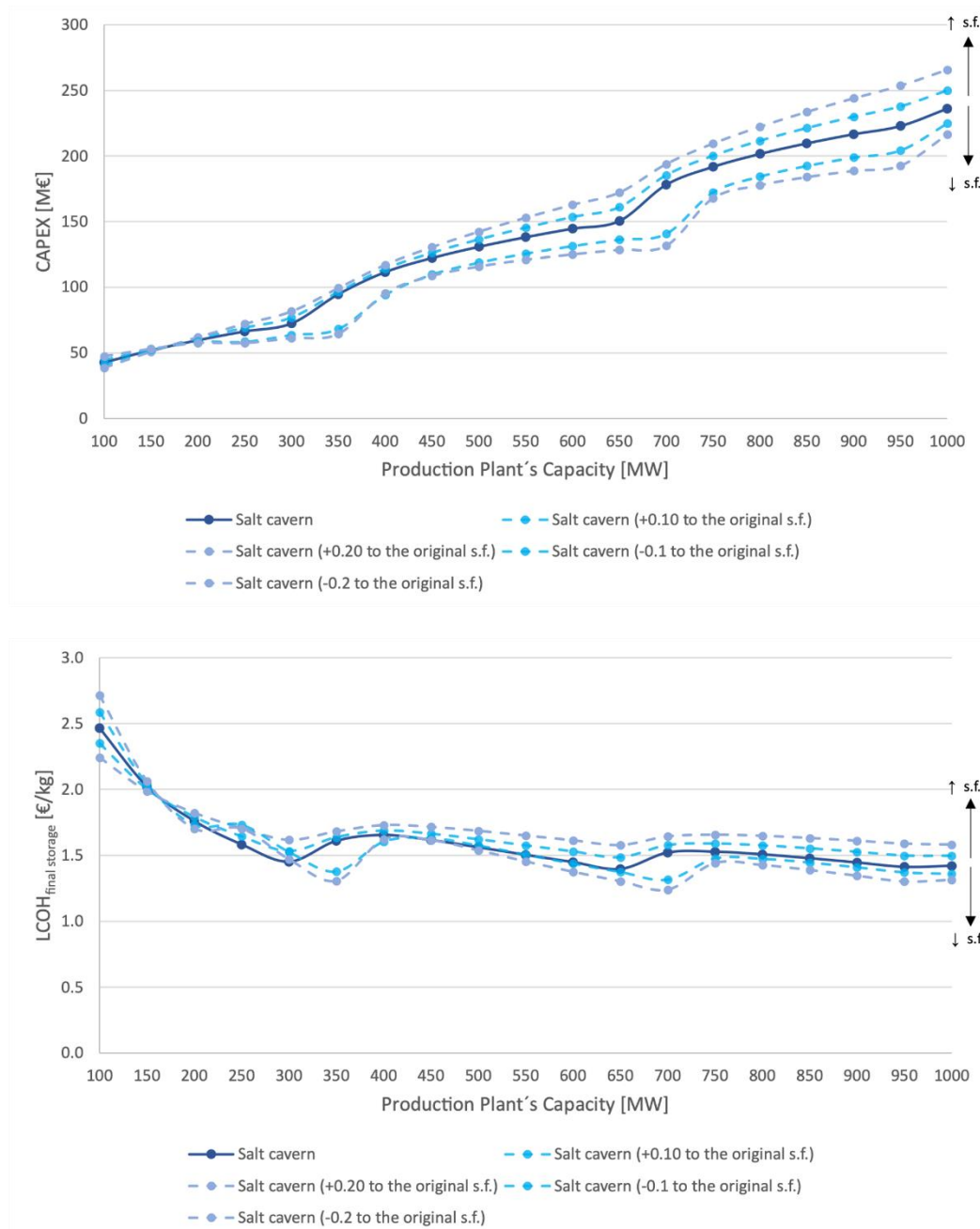


Figure 61: a) Top graph shows the CAPEX variation of hydrogen storage in salt caverns with the hydrogen production plant capacity. b) Bottom graph shows the variation of the levelized cost of final storage of hydrogen in salt caverns with the hydrogen production plant.

Similar analysis was conducted for lined rock caverns. The results are shown in Figure 62. For this technology, the incremental and decremental changes of the scaling factor, which is assumed to be 0.75, had more impact on its own CAPEX and, as a result, a noticeable variation of the specific cost of final storage. Considering that the scaling factor represents the scalability potential of a certain technology. For example, a smaller scaling factor indicates a better scaling effect of the technology which means that with an increase in the reservoir size, the initial cost of capital expenditures does not increase as much as for larger scaling factors. For this reason, the incremental and decremental variation of a larger scaling factor registers a larger variation in the CAPEX and LCOH_{final storage} values.

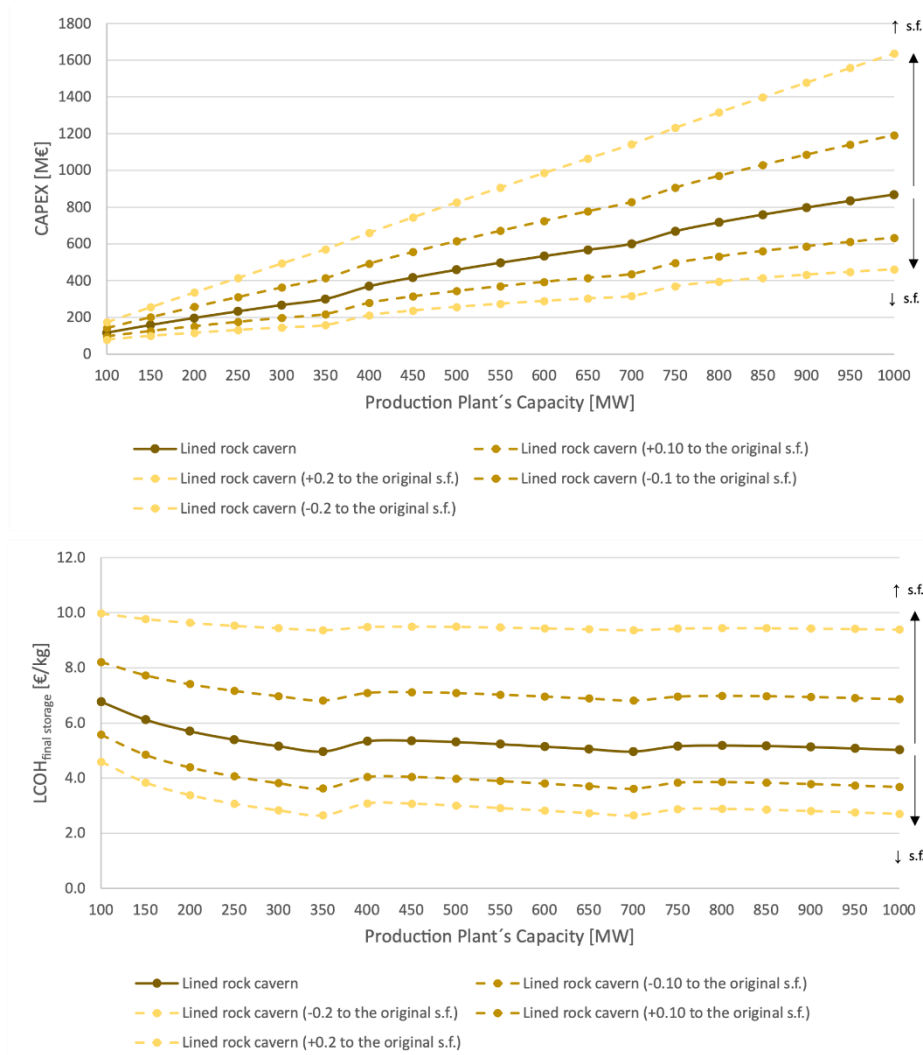


Figure 62: a) Top graph shows the CAPEX variation of hydrogen storage in lined rock caverns with the hydrogen production plant capacity. b) Bottom graph shows the variation of the levelized cost of final storage of hydrogen in lined rock caverns with the hydrogen production plant capacity.

6.3.2 Tank storage

Hydrogen storage in pressurized tanks for the specific case of daily, weekly, and monthly storage is evaluated in this section. In this section it is considered lower volumes of production with hydrogen production plant capacities ranging from 1MW to 100MW. To better visualize how the relation between the hydrogen plant capacity and the respective amount of hydrogen that is stored in each of the considered cases (see Figure 63).

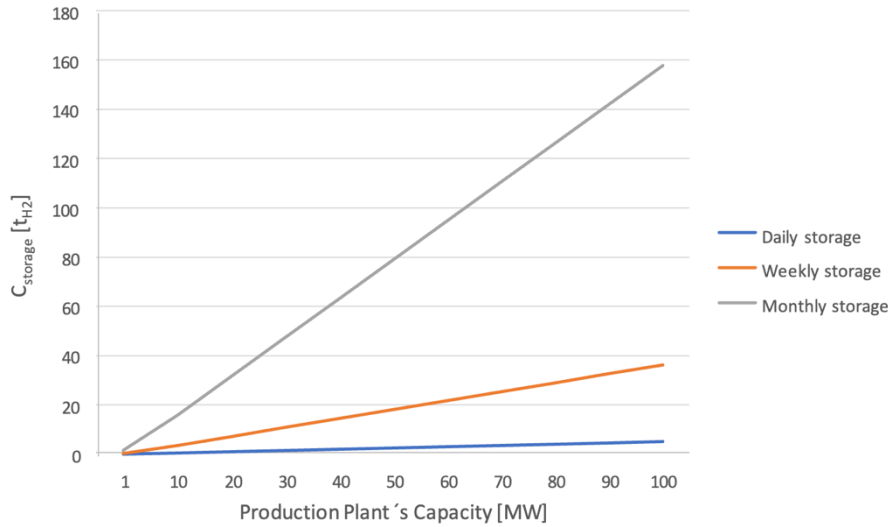


Figure 63: Amount of hydrogen that it is being stored in the pressurized tanks for the case of daily, weekly, and monthly storage for each of the hydrogen production plant's capacity considered.

Figure 64 shows how the hydrogen production plant capacity is related to the volume of hydrogen that is stored in the different pressurized tanks for different time durations. It is interesting to note that the type I storage tanks have to accommodate larger volumes than type III and even more when compared to type IV tanks. This is due to the lower operating pressure set for the steel tanks.

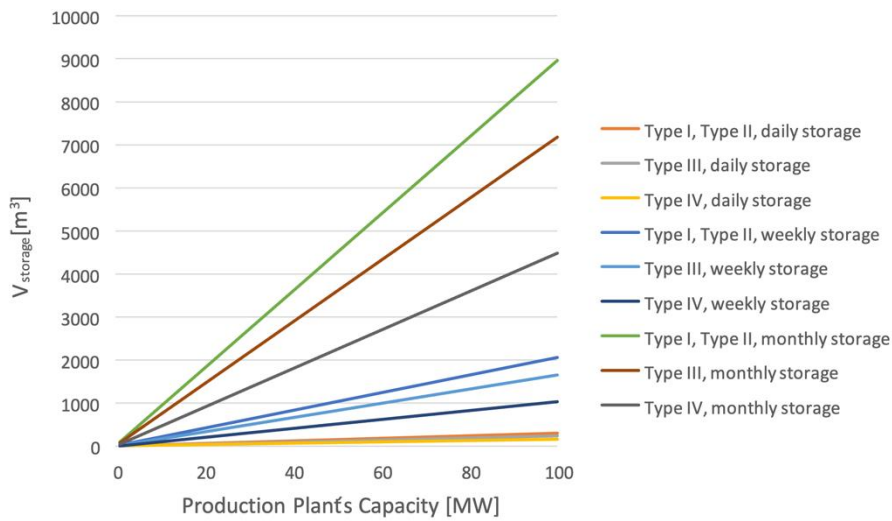


Figure 64: Volume of hydrogen that it is being stored in each type of pressurized tank for the case of daily, weekly, and monthly storage for each of the hydrogen production plant's capacities considered.

In Figure 65, a certain pattern is found in the evolution of the LCOH for the three different cases: daily, weekly, and monthly storage. Type I and type II tanks register always a lower levelized cost of hydrogen storage for every plant production capacity considered. This is due to the lower cost of these particular tanks. It is also observed that as the number of cycles per year in the storage tanks decreases the LCOH of hydrogen storage increases. This means that even though lower volumes of hydrogen storage are considered for the daily storage case, the fact that the tank is having higher charging and discharging cycles leads to a lower LCOH when compared to weekly or monthly storage. At the same time, it is noticeable that as the hydrogen production plant capacity increases, the LCOH tends to stabilize. Additionally, all different types of tanks register the same decreasing rate as the amount of hydrogen to be stored increases. This has to do with the fact that the scaling factors used for each technology are the same. One other interesting observation is that even though the base cost of type III and type IV tanks is the same, increased

operating pressure allowable in type IV leads to a higher energy density meaning that a lower volume tank can store the same amount of hydrogen.

It is interesting to observe that for the case of monthly hydrogen storage, the levelized cost of hydrogen storage in type I and type II tanks stops decreasing at a hydrogen production plant capacity of 50MW and registers a small increase afterwards followed by a constant decrease. This point is identified as an inflection point which indicates that the hydrogen storage facility no longer can have only one storage tank and needs an extra one to store the increased hydrogen production. The same thing happens for the type III tank but for an hydrogen production plant of 60MW. In the case of the type IV tank it is not needed any additional tanks to store the amount of hydrogen coming from the plant in the studied range of production capacities. This is interesting because it allows type IV tanks to register a slightly steeper decrease in the LCOH. To sum up, the levelized cost of hydrogen storage does not reflect a significant change for a point of transition in other words whenever it is required an extra hydrogen tank for the hydrogen storage facility.

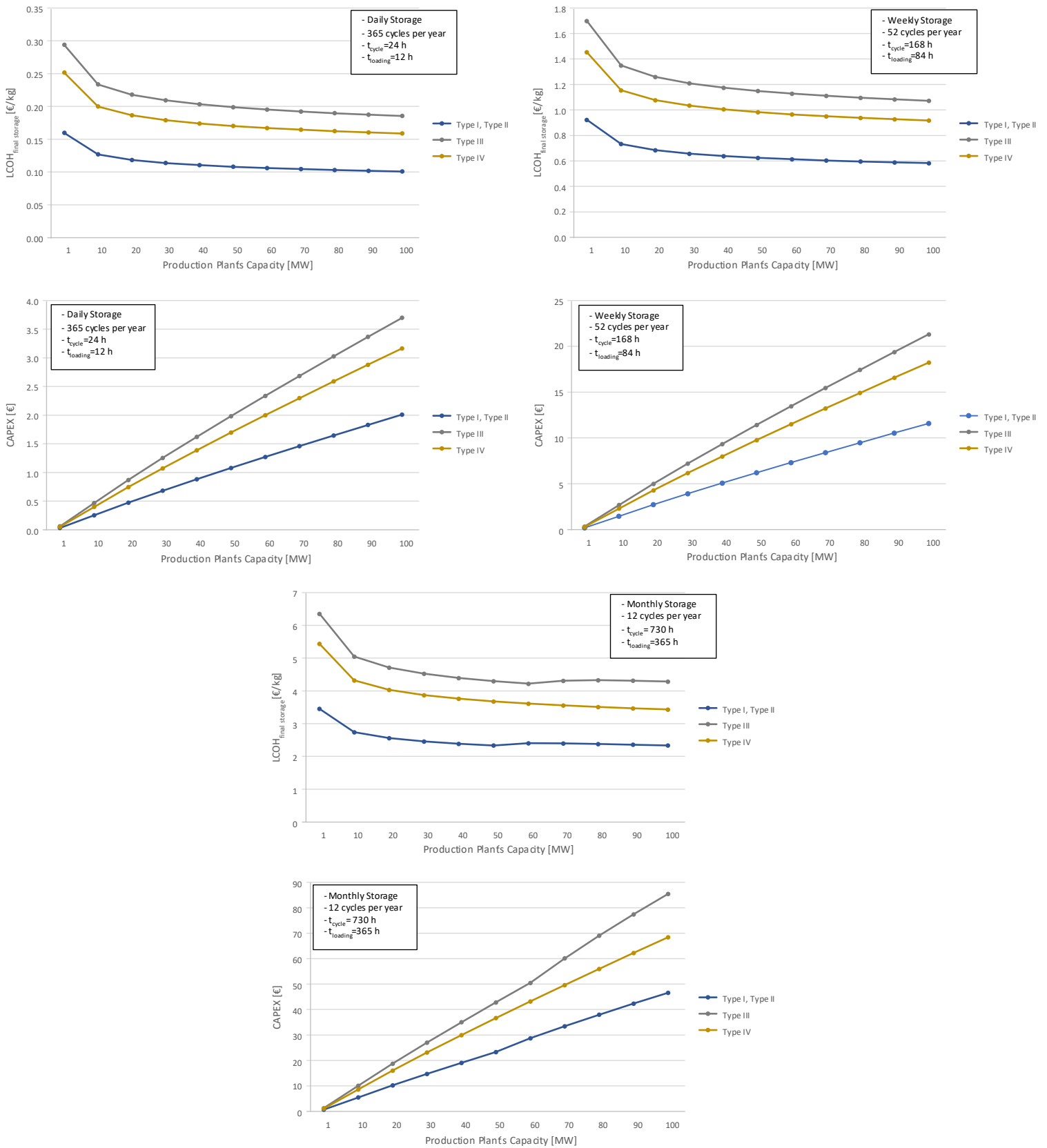


Figure 65: Impact of the amount of hydrogen to be stored on the levelized cost of hydrogen storage in each type of storage tank for the case of daily, weekly, and monthly storage.

With regards to the learning effect, there are several variables affecting learning curves, but the most important is the added experience in the entire manufacturing process. Future costs can be assessed by using learning curves which bring past cost reductions to production levels. Each learning curve has a particular learning rate. The learning rate can be interpreted as "a proportional reduction of the costs for each doubling of the cumulative capacity or production" [243]. New technologies, such as hydrogen storage technologies, lack historical data which results in additional difficulties in the assessment of the learning rates associated with each technology. For example, the recent StoreFAST model developed by the National Renewable Energy Laboratory does not consider any learning effect of salt caverns [244].

However, some predictions can be made regarding the cost reduction of hydrogen storage technologies. Hydrogen storage in composite tanks other than steel tanks have more potential to decrease its costs in the upcoming years when compared to hydrogen storage in geological reservoirs since the costs of building geological reservoirs will be always dependent on the specific properties encountered in each site. For instance, the construction time can vary from one location to another which indicates difficulties in the optimization of the construction processes. On the other hand, storage tanks, both composite high-pressure and cryogenic, are produced in a standardized way.

6.4 Conversion and reconversion

The objective of this section is to identify the main parameters affecting the levelized cost of hydrogen conversion and reconversion processes. A general comparison between hydrogen liquefaction, hydrogen regasification, ammonia synthesis and ammonia cracking processes is first reviewed. Afterwards, an individual assessment of the levelized cost of hydrogen compression is performed.

Figure 66 shows the behavior of the levelized cost of hydrogen for the (re)conversion processes with a variation of the respective plant's capacity. First, it is noticeable a very low specific cost of hydrogen regasification when compared to the other (re)conversion technologies. This is not only due to the very low initial capital investment cost of hydrogen regasification plants (Figure 67), but also due to the very low specific energy consumption in this reconversion process (Figure 68).

For the other three (re)conversion technologies, there is a quite steep decrease of the $LCOH_{re(conversion)}$ for lower capacities and then it stabilizes for bigger capacities, over 100 tonnes per day. It is interesting to observe in Figure 66 that the levelized cost of hydrogen liquefaction is bigger for a plant capacity of 2 tonnes per day than ammonia cracking and synthesis plants of the same size. However, it becomes smaller than the levelized cost of ammonia cracking for a plant capacity of over 7 tonnes per day but not smaller than the levelized cost of ammonia synthesis. This indicates the fast-decreasing behavior of the specific cost of hydrogen liquefaction. This behavior cannot be justified from Figure 67. In fact, the CAPEX of the liquefaction plant is the highest for every plant capacity when compared to the other (re)conversion technologies. However, by looking at Figure 68, it is noticeable that the hydrogen liquefaction plant is the only technology where the specific energy consumption reduces with an increase in the plant's capacity. As for the other conversion and reconversion technologies, it is considered a constant specific energy consumption with increased capacity. Figure 69, was plotted to show how the hydrogen liquefaction plant efficiency varies with different plant's capacities.

One last result that is interesting to look at is the higher levelized cost of ammonia cracking for increased plant capacities when compared to the levelized cost of ammonia synthesis, despite the fact that the CAPEX of an ammonia synthesis plant is higher than an ammonia cracking plant, as Figure 67 shows. This is due to the energy consumption for reconverting hydrogen from ammonia being much higher than the energy needed for converting hydrogen to ammonia (Figure 68).

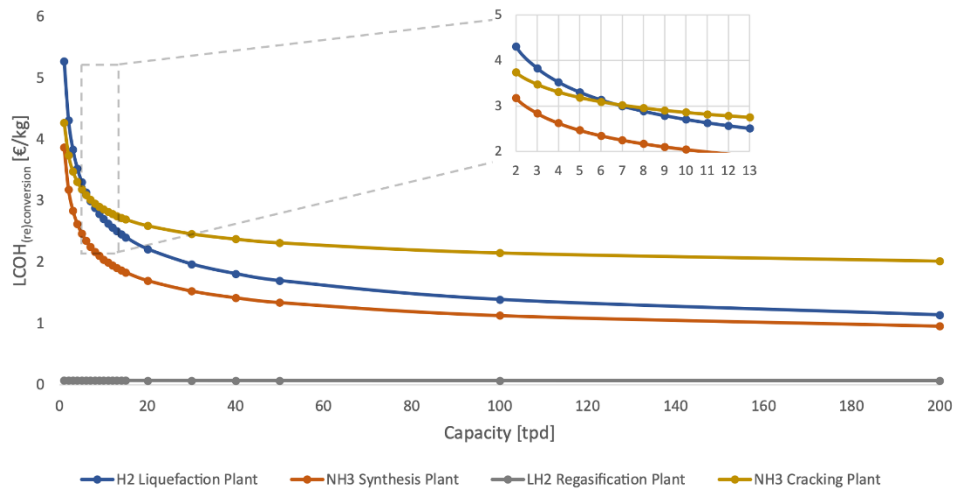


Figure 66: Variation of the levelized cost of (re)conversion processes with respect to different plant's size capacities.

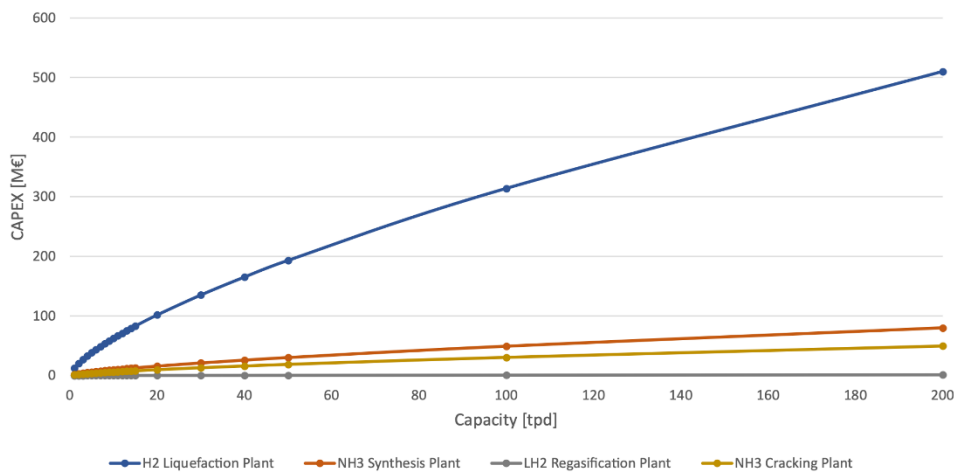


Figure 67: Variation of the cost of initial capital expenditures for each considered hydrogen conversion and reconversion process with respect to different plant's size capacities.

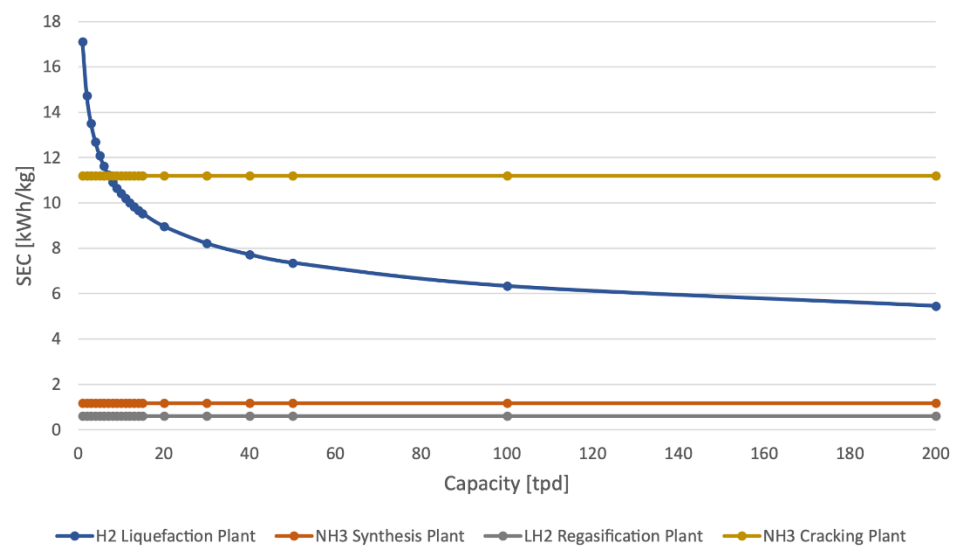


Figure 68: Variation of the specific energy consumption (SEC) of each (re)conversion process with respect to different plant's size capacities.

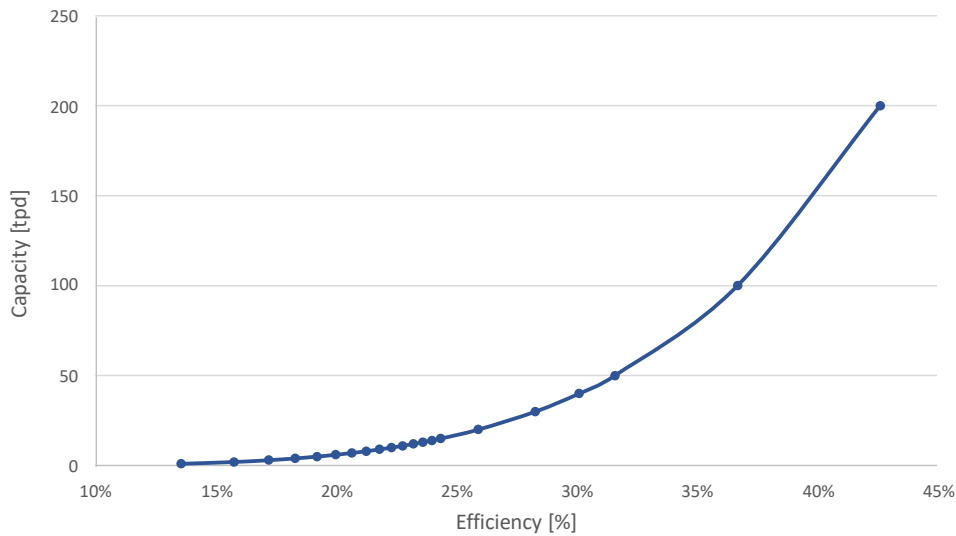


Figure 69: Relation between hydrogen liquefaction plant capacities and respective plant's efficiency.

6.4.1 Compression

To evaluate the main drivers affecting the LCOH of hydrogen compression, a green hydrogen production facility located in Germany is taken as example, for the case of seasonal storage (1 cycle) in a salt cavern. For this particular supply chain, the underground hydrogen storage facility is located right next to the production site. Since the compression station is located in between the hydrogen production plant and the storage facility, the inlet pressure of the compressor is 30 bar.

In Figure 70, graph a) represents the variation of the LCOH of the compression stage if the outlet pressure of the compressor would change between the minimum and the maximum operating pressure values in salt caverns (35 bar - 210 bar). As indicated in Appendix VI, this range of pressures was obtained from [73]. Graph b) shows the variation of the LCOH of compression with an increasing hydrogen flow rate passing through the compressor. From these results, it can be concluded that the levelized cost of hydrogen compression is more sensitive to the variation of the pressure ratio in the compressor than the actual capacity flow rate. For this reason, the pressure ratio between stages of the supply chain should be minimized.

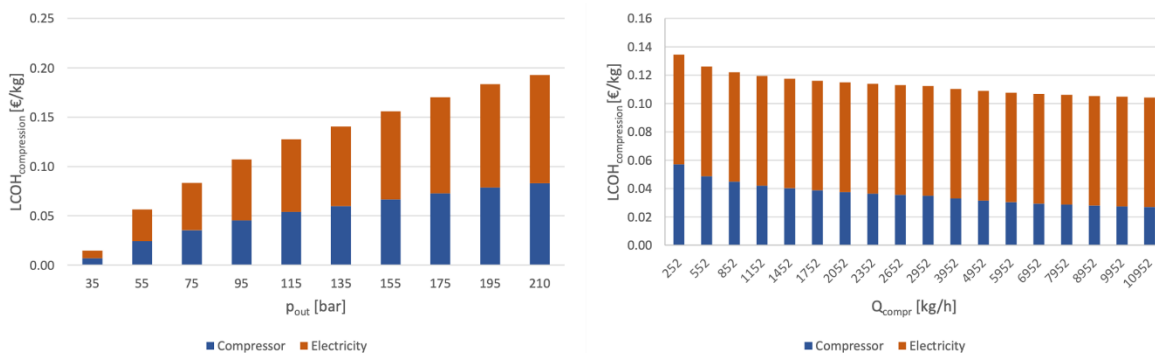


Figure 70: Levelized cost of hydrogen compression a) with varying compressor's discharge pressure (left graph) and b) with varying compressor's capacity flow rate (right graph).

6.5 Overall supply chain

In the next sections, the results for the entire supply chain are discussed. It is important to highlight that for consistency reasons the LCOH is subdivided into the following components: production, T&D, storage, and conversions (compression, liquefaction, regasification, conversion to and reconversion from

NH₃). This means that the T&D and storage components do not include their upstream and downstream conversions, which are instead all gathered in the conversion one.

6.5.1 Germany

For Germany, several scenarios need to be studied to provide a clear overview of current and future supply pathways. As also explained in Section 5.8, the results are before presented considering a fixed monthly geological storage, in particular a depleted natural gas or oil reservoir. Results for domestic supply chains, and then for green and blue imports are displayed. Then, the focus moves to the implications of storage on these supply chains. To do so, the most competitive solutions are used as exemplary cases.

Figure 71 and Figure 72 illustrate the LCOH for domestic supply chains in 2022 and 2030, with both pipeline and truck distribution. It can be highlighted that the difference between the two delivery modes is constant, independently from the upstream stages and year. In fact, pipeline is always 0.5 €/kg cheaper than truck delivery in the case of Germany. Due to the easier operational rollout, the following discussion exclusively centers on gH₂ truck delivery. However, this constant difference between the two cases can be kept in mind to easily calculate the LCOH for supply chains with distribution via pipeline. In Figure 71, it can be seen that the SMR and the pyrolysis scenarios have the lowest LCOH, respectively equal to 3.9 and 4.2 €/kg in 2022, confirming what was discussed in Section 6.1.4. Despite similar production costs, SMR is overall cheaper than pyrolysis. This can be explained by recalling the larger scale of an SMR facility (300 MW_{H₂,LHV} versus 10 MW_{H₂,LHV} for pyrolysis), which determines lower distribution and storage costs due to economy of scale. This suggests that competitive pyrolysis supply chains can be achieved not only with a production cost decline but also with an increase of their production facility scales. Instead, hydrogen production via electrolysis is not competitive, with an LCOH that ranges between 6.7 and 10.1 €/kg depending on the electricity source.

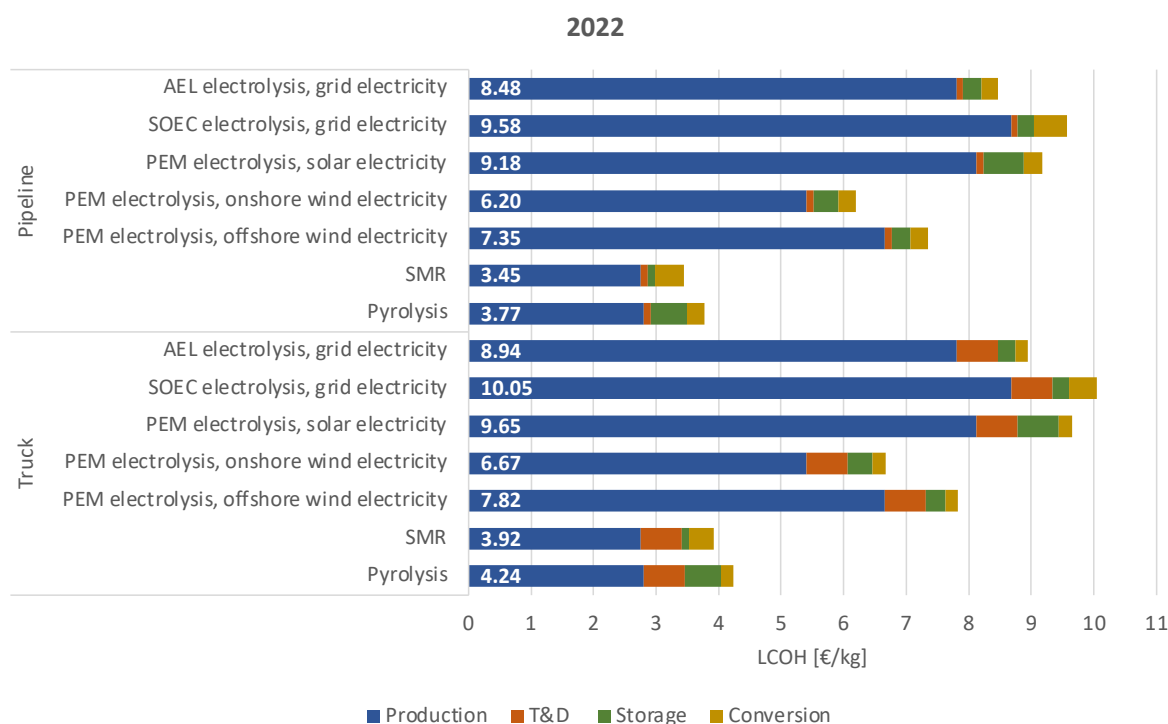


Figure 71: Levelized cost of hydrogen for domestic supply chains in Germany, in 2022.

In 2030, hydrogen from electrolysis experiences a steep decline in its costs: onshore wind plants can produce it at a LCOH of 4.7 €/kg, with solar PV and offshore wind at a cost 1 €/kg higher. However, the gap with gas-based hydrogen is still wide: hydrogen from SMR and pyrolysis can be respectively delivered at an LCOH of 3.5 and 3.6 €/kg.

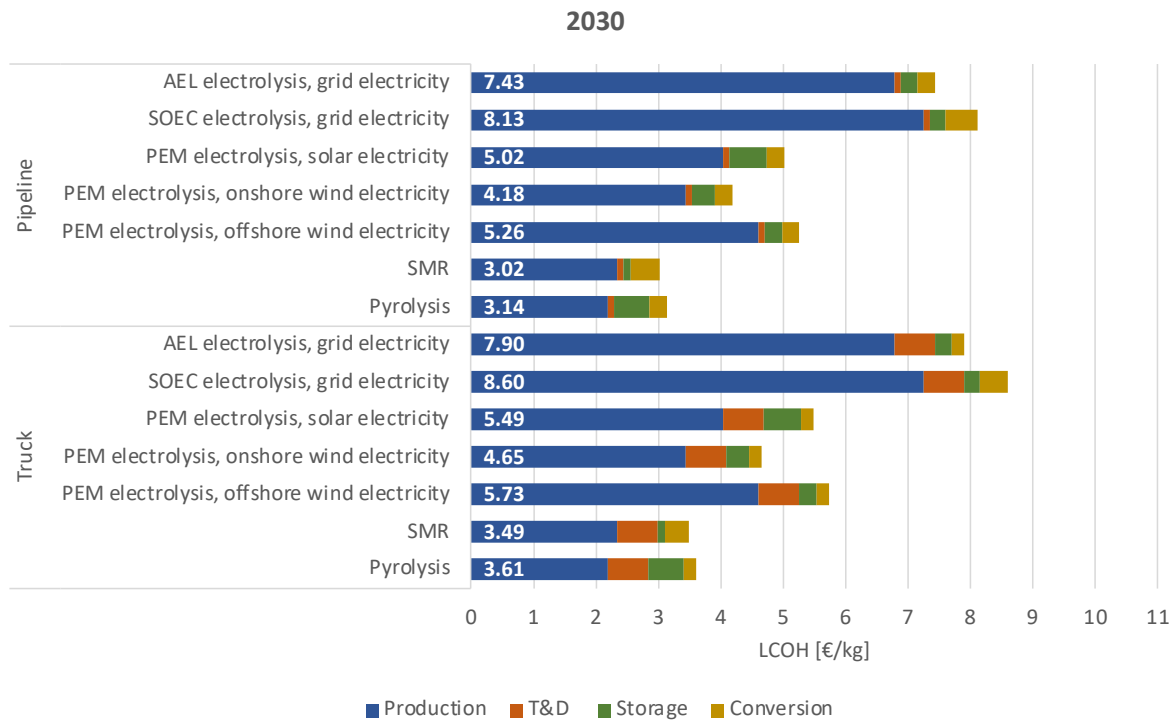


Figure 72: Levelized cost of hydrogen for domestic supply chains in Germany, in 2022.

The German mediocre RES conditions and the dependence on foreign gas determine the necessity to also explore import pathways. The first part of the following analysis is dedicated to green hydrogen imports, mentioning once more that storage refers to depleted natural gas or oil reservoir with a monthly duration, and distribution is carried out by gH₂ truck. Figure 73 shows that, where available, imports via pipeline are always the least costly solution. In 2022, hydrogen from dedicated renewable plants in Algeria and Saudi Arabia is in the same cost range, between 5.5 and 6 €/kg. The analysis here considers only the new hydrogen network. However, the retrofit and repurposing of natural gas pipelines would bring down costs even further, as presented in Section 6.2 Pathways with transmission via LH₂ are 2.3-3.1 €/kg more expensive than gH₂ pipelines. Costs related to ammonia are even higher, averaging a 3.0-3.8 €/kg increase compared to their pipeline equivalent routes. It can be noticed that for both LH₂ and NH₃ these gaps decrease with longer distances. Subsequently, LH₂ becomes a competitive alternative for remote locations with very low LCOE and the unfeasibility of a direct grid connection. For instance, Chilean hydrogen from an onshore wind facility can be delivered at 6 €/kg, in the same range as Algerian and Saudi pipeline imports. Due to its very expensive reconversion process, scenarios with ammonia are always above average costs when gaseous hydrogen is the final product. Despite being beyond the scope of this study, it can be suggested that ammonia imports from remote locations can be very competitive if the same transportation vector is also the desired final product.

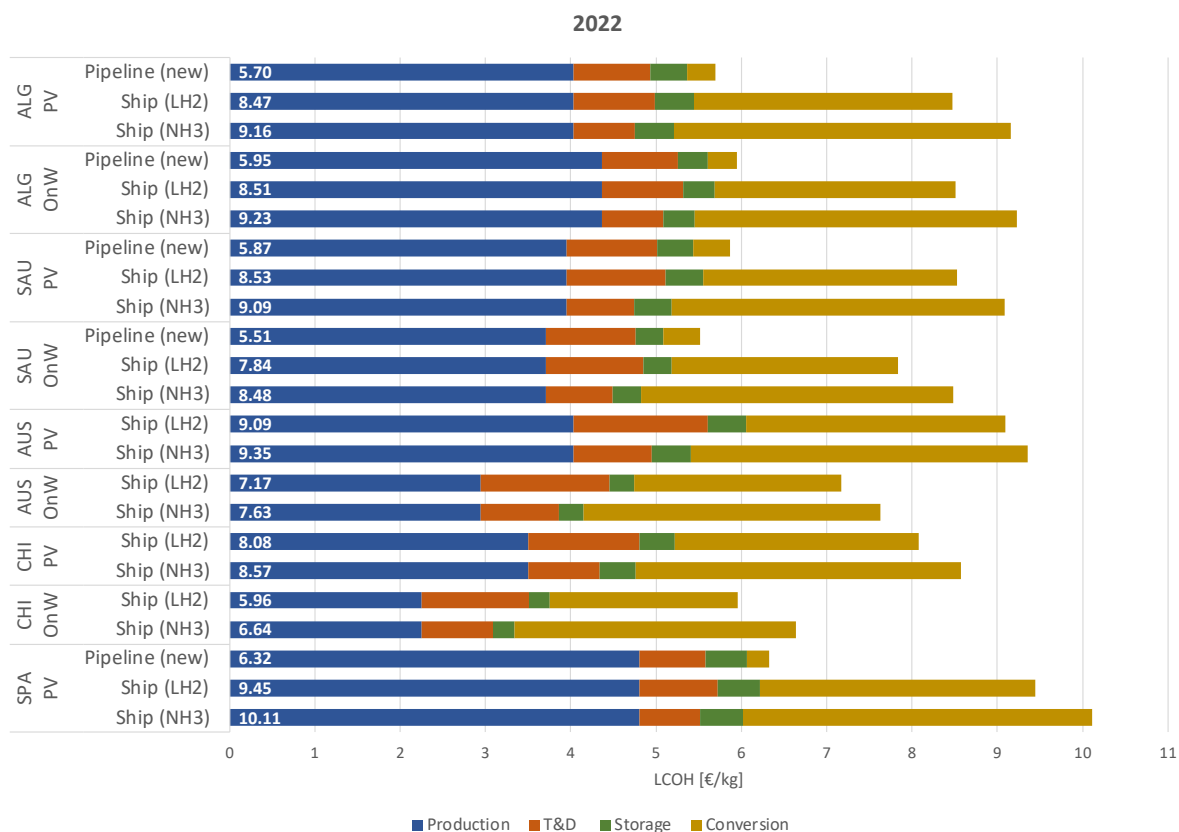


Figure 73: Levelized cost of hydrogen for green hydrogen imports to Germany, in 2022²⁸.

Figure 74 complements Figure 73 with the results for 2030. The general trends do not vary, with pipeline transmission that keeps its economic advantages, and production that remains the main driver of cost decrease. The steeper cost decline of the PV technology determines the Algerian hydrogen from solar electricity to be the cheapest import pathway in 2030 at 3.7 €/kg, with the Spanish equivalent joining the lowest-cost range around 3.9 €/kg, together with Saudi Arabia. Instead, imports from Chile lose competitiveness, with hydrogen from onshore wind, being 1.3 €/kg more expensive. This is mainly due to the flatter trend for onshore wind CAPEX than for PVs.

²⁸ OnW abbreviates Onshore wind. The same abbreviation is repeated in following charts.

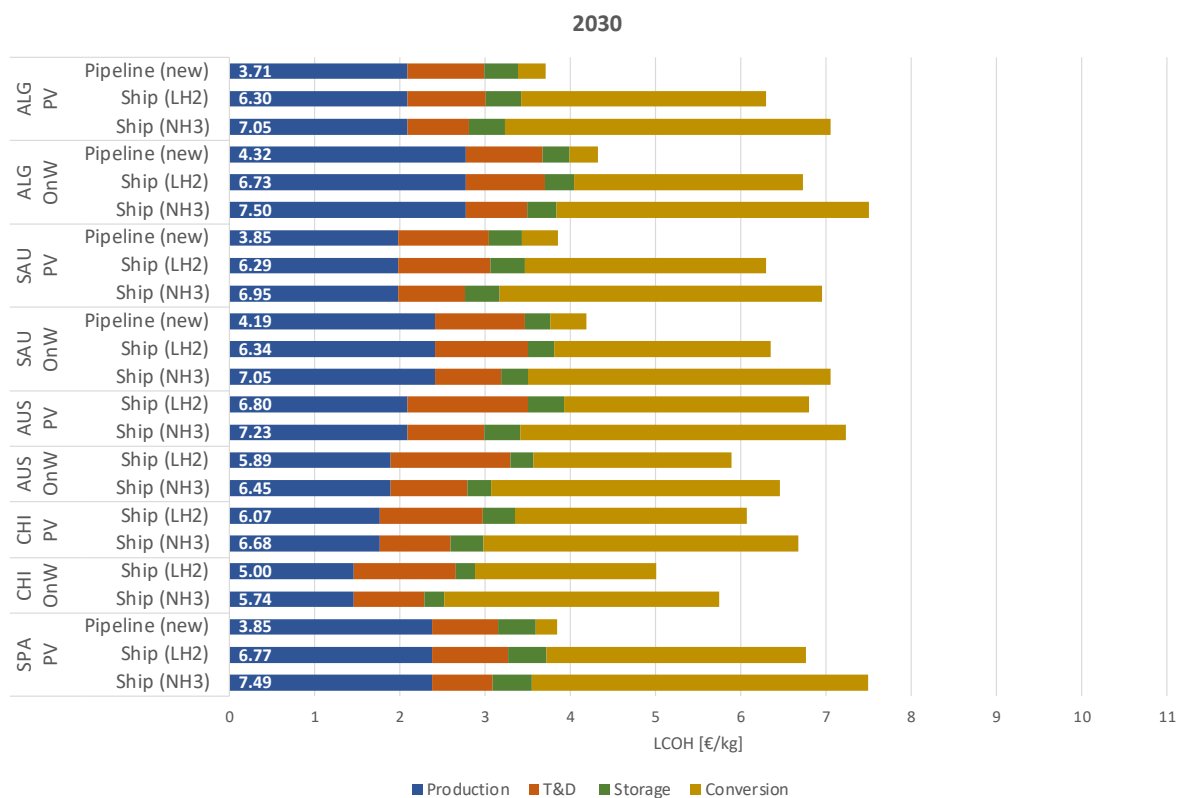


Figure 74: Levelized cost of hydrogen for green hydrogen imports to Germany, in 2030.

A second focus is given to blue and turquoise hydrogen imports. In fact, gas-exporting countries have the possibility to produce hydrogen at very low costs, given the inexpensive gas and carbon storage prices. This is demonstrated by Figure 75 and Figure 76. Similarly to green hydrogen imports, scenarios with pipeline transmission have the lowest LCOH. Due to its proximity and low gas price, Algeria is again the most competitive option, delivering hydrogen at 2.2 €/kg. The LCOH for Norway and Qatar is respectively equal to 2.4 and 2.7 €/kg. The difference with Algeria is due to the higher gas costs in Norway, and the farther location of Qatar. As discussed earlier for domestic production, supply chains of turquoise hydrogen generally have a higher LCOH given their smaller scale.

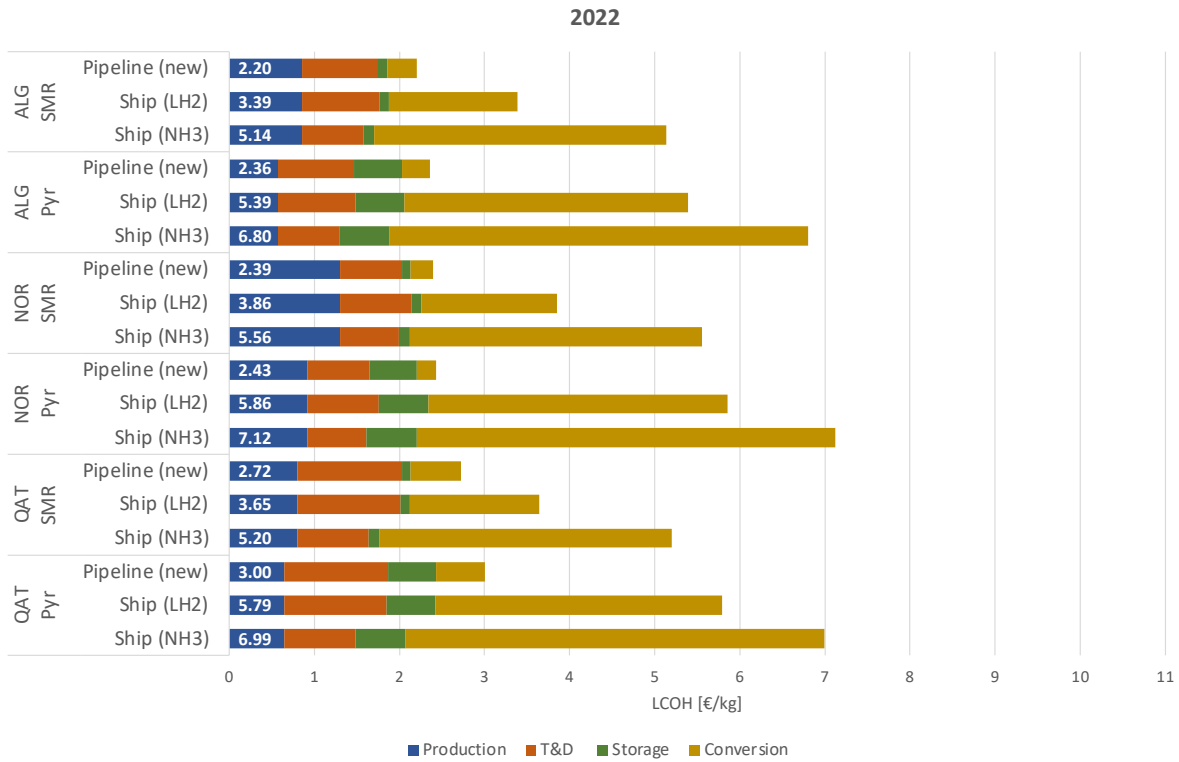


Figure 75: Levelized cost of hydrogen for blue hydrogen imports to Germany, in 2022.

The cost decrease for blue and turquoise hydrogen in 2030 is quite narrow, with results and considerations analogous to 2022. SMR and pipeline scenarios in Algeria, Norway, and Qatar experience the same reduction of 0.08 €/kg. They remain the three cheapest options, respectively at 2.1, 2.3, and 2.6 €/kg.

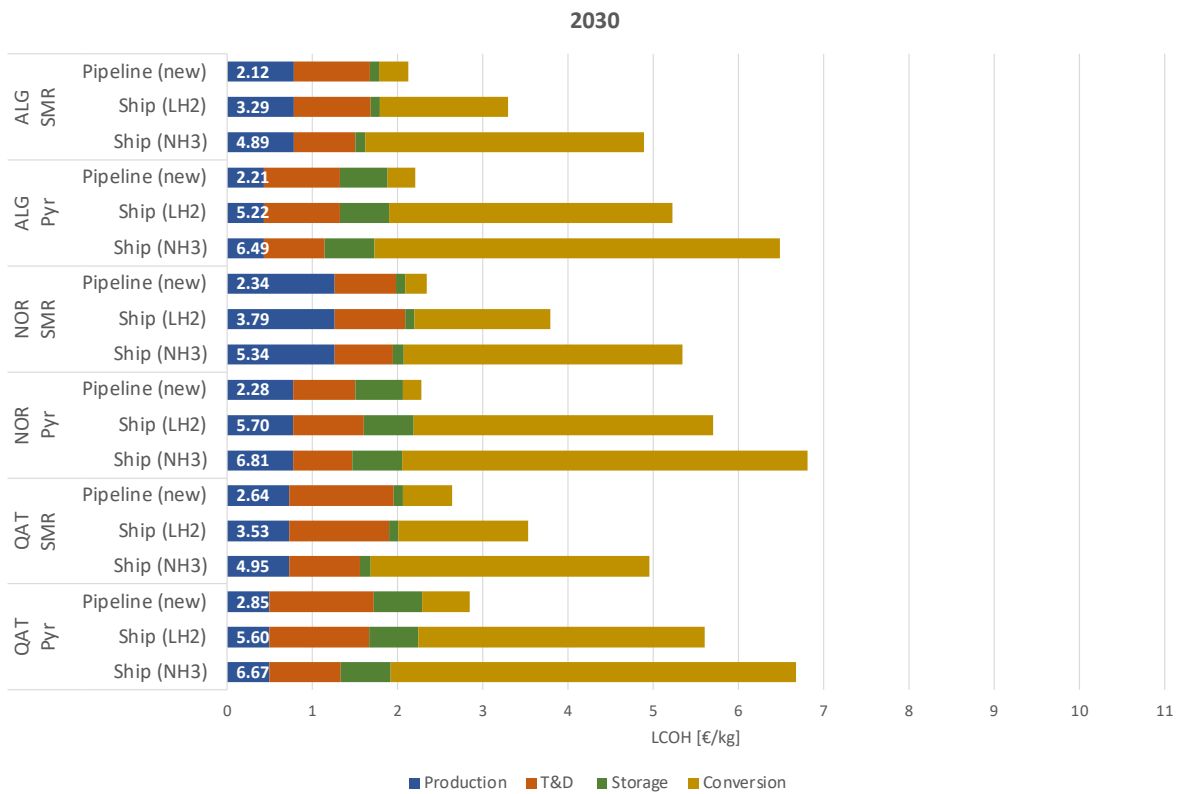


Figure 76: Levelized cost of hydrogen for blue hydrogen imports to Germany, in 2030.

So far, the scenarios for Germany have been investigated separately. Figure 77 aims at gathering some relevant supply pathways among the ones presented earlier in this section (from Figure 71 to Figure 76). In particular, it shows the cheapest green and blue hydrogen options, both domestic and imported, to which hydrogen from electrolysis and grid electricity is added. These values also approximate the lowest-cost range for each option, so that their comparison can be extended to more general considerations. The coupling of SMR and CCS technologies can produce hydrogen at very low costs, especially in gas-rich countries. In fact, the Algerian blue hydrogen arrives at its destination at a cost as low as 2.2 €/kg in 2022, 1.7 €/kg cheaper than the local production. The imports of green hydrogen from Algeria via pipeline are also more competitive than green hydrogen directly produced in Germany. However, the LCOH of this option is currently very distant from the blue alternative. Towards the end of the decade electrolysis in Algeria can produce hydrogen delivered in Germany at 3.7 €/kg, approaching the domestic blue hydrogen, that falls at 3.5 €/kg. Nevertheless, it does not come close to the cost of imported blue hydrogen, that is equal to 2.1 €/kg. This LCOH, the lowest for Germany as end-user, translates to 63.1 €/MWh_{LHV} in energy units.

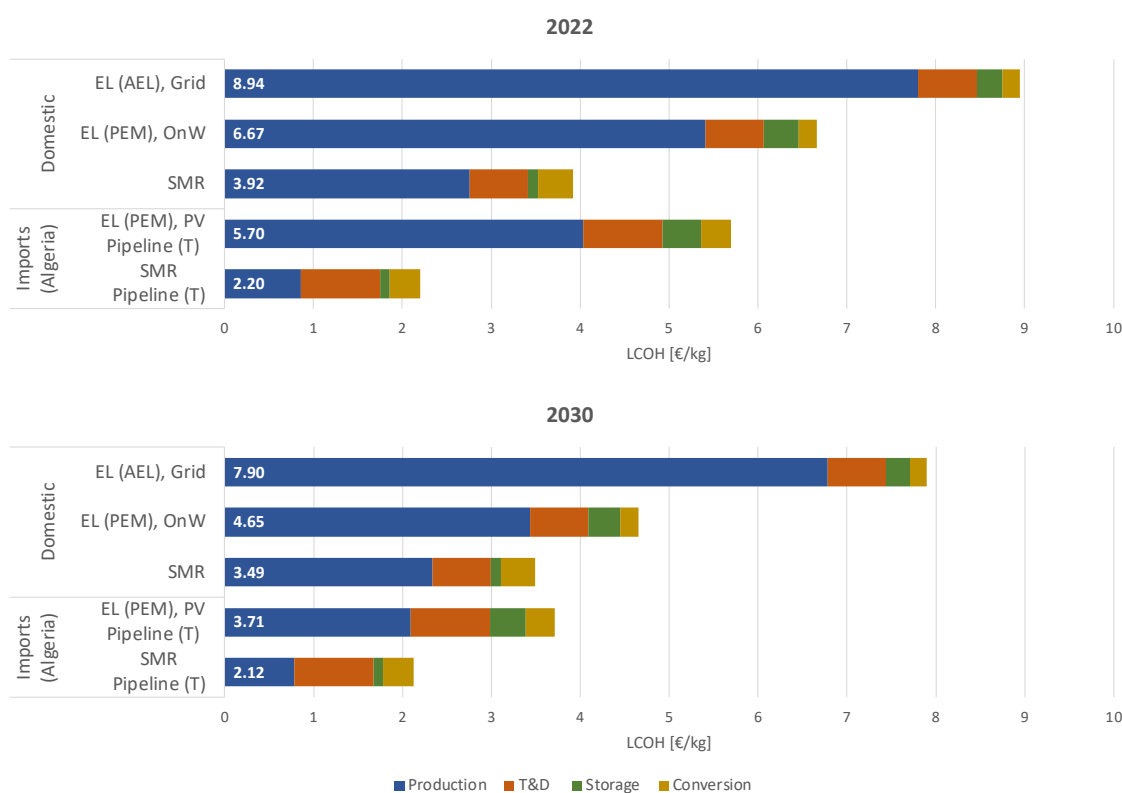


Figure 77: Levelized cost of hydrogen for relevant scenarios in Germany, in 2022 and in 2030.

Summing up, hydrogen imports from close regions where a pipeline connection is feasible are the most competitive options. Imports via ship present higher LCOHs, with only the exception of onshore wind in Chile, which has costs comparable to domestic supply pathways. This means that, if the presented values reflect the reality, the hydrogen economy might develop within regional boundaries. A global trade might not be economically sustainable: only cases with exceptional conditions might be able to overcome the surcharge due to the high costs of long-distance transportation. Given the very low LCOHs of blue hydrogen, gas-producing countries might have a competitive advantage compared to other sources. In fact, the diversification of their exports is a key process to safeguard their economies relying on fossil fuel trade. Therefore, it is in their interest to develop hydrogen supply chains. It is worth mentioning that hydrogen from some gas-producing countries and remote locations might have some sustainability implications that cannot be included in cost terms. For instance, the water need for electrolysis from areas where this resource is scarce can be very debatable, especially if nearby populations still do not have a clean access to it. For this reason, the hydrogen production in developing countries needs a proper

planning, considering not only the economic sustainability aspect, but also the social and environmental ones. Using again the water example, it has been presented in Section 5.4.1 that water does not have a large impact on the LCOH, even if it comes from expensive desalination plants. Thus, hydrogen production plants can help the diffusion of this technology, bringing the advantages also to local populations.

So far, the assessment considered only monthly storage in depleted NG or oil reservoirs. However, the analysis can be extended to other storage options. To reduce the number of output scenarios, only the cases in Figure 77 and the year 2030 are considered. It can also be mentioned that this part of the study considers monthly storage only for steam methane reforming, given the steadier output flow of hydrogen production, that facilitates the coordination between hydrogen supply and demand. From Figure 78, the cheapest leveled cost of blue hydrogen is the option considering monthly storage in depleted natural gas reservoirs (3.5 €/kg). This is an interesting result because however salt caverns having low permeability meaning low mass losses and, supposedly, giving better support to additional cycling throughout the year [51], the relatively lower CAPEX of depleted NG reservoirs weighs more in the final leveled cost of hydrogen, although currently there are already salt caverns storing hydrogen while there are not depleted NG reservoirs. The risk of the unknown resulting factors of storing hydrogen in the very new technology, can lead investors to opt for salt caverns instead. For the case of green hydrogen with onshore wind, the cheapest supply chain option considers depleted NG reservoirs for seasonal storage with two cycles per year (5.2 €/kg). In general, it can be concluded that a higher number of cycles can lower the specific cost of the final leveled cost of hydrogen. However, some other parameters should be looked at to better assess the influence of cycling in reservoirs. For example, mass flow rates entering and exiting the reservoir can have different requirements for each underground technology. This can directly influence the speed of charge and discharge of the reservoir. In the present analysis, a constant capacity flow rate for charge and discharge of the reservoir is assumed for every technology, as explained in the methodology chapter. Moreover, larger storage capacities and a lower number of cycles increase supply security. For this reason, the choice of the most appropriate storage can be considered a compromise between costs and system resiliency. Despite being beyond the scope of this work, an analysis accounting supply and demand would be paramount to enable an optimal selection of the storage size and duration.

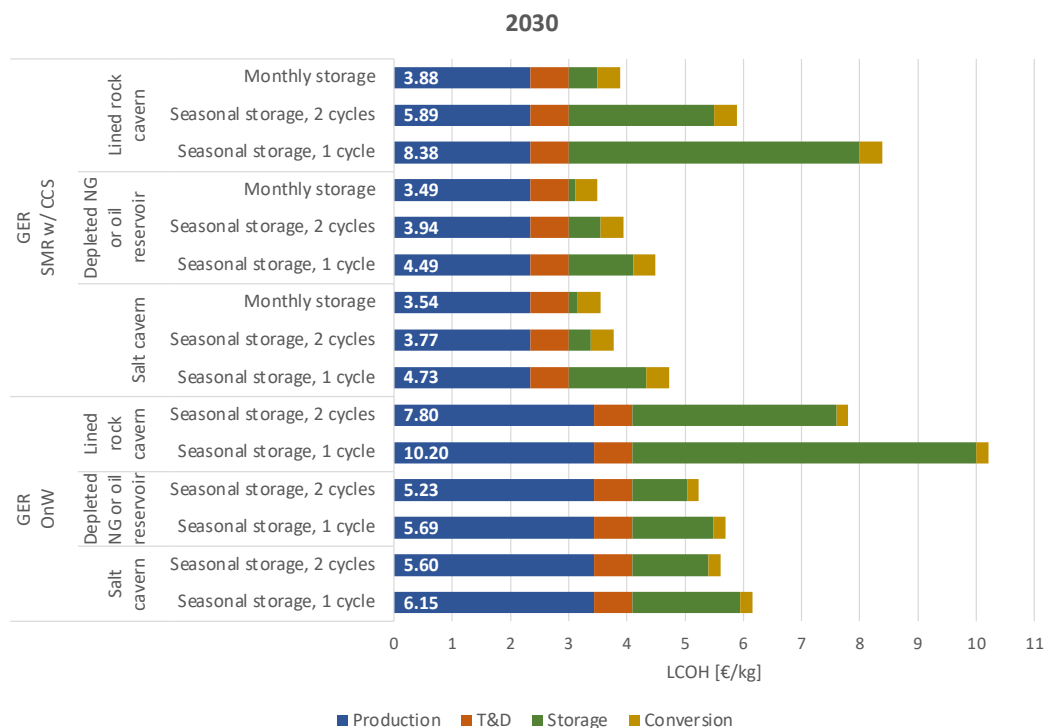


Figure 78. Levelized cost of hydrogen domestically produced in Germany and distribution by truck, in 2030.

For the hydrogen imports scenario, the results are equivalent to the domestic hydrogen production scenario when considering underground hydrogen storage options. The cheapest blue hydrogen supply chain is the one considering depleted NG reservoirs for monthly storage (2.1 €/kg). The cheapest green hydrogen supply chain is the one considering depleted NG reservoirs for seasonal storage, considering two cycles (4.3 €/kg). Finally, it is possible to conclude that the most costly technology for underground hydrogen storage evaluated in this analysis is lined rock caverns, followed by salt caverns, and then depleted natural gas or oil reservoirs which are the cheapest option.

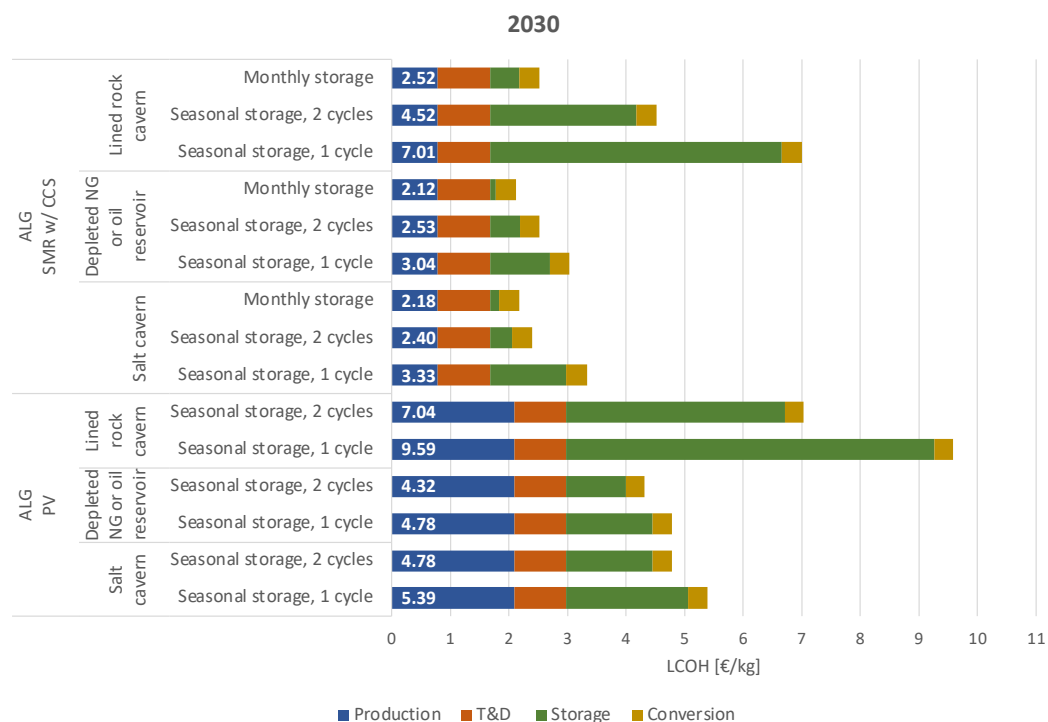


Figure 79. Levelized cost of hydrogen imported from Algeria, transmission by pipeline and distribution by truck, in 2030.

Although being out of the scope of this project, handling the storage stage of the supply chain as an optimization problem would be beneficial in order to achieve the optimal reservoir or tank size and give an even lower levelized cost of hydrogen by considering a real hydrogen production and demand profile. At the same time, the optimization work eliminates the hurdle of trying several scenarios for very different hydrogen production as well as consumption profiles in order to arrive to the lowest LCOH. Finally, the results could then be implemented in the tool, providing even more accurate results. This is an example of how the developed tool could be used in the future.

6.5.2 Spain

In Spain, two different business models are compared: local small-scale against centralized large-scale production from solar PV. In 2022, the small-scale case with a daily steel tank storage corresponds to an LCOH as low as 6.6 €/kg. If a longer storage duration is required, for instance weekly, this value increases by 0.8 €/kg. The centralized cases with seasonal storage have generally a comparable LCOH to the distributed ones. However, if the storage requirement diminishes to monthly, the centralized case becomes the most competitive scenario, regardless of the delivery mode. If available, the delivery by pipeline results in a 0.5 €/kg cheaper LCOH than its truck equivalent.

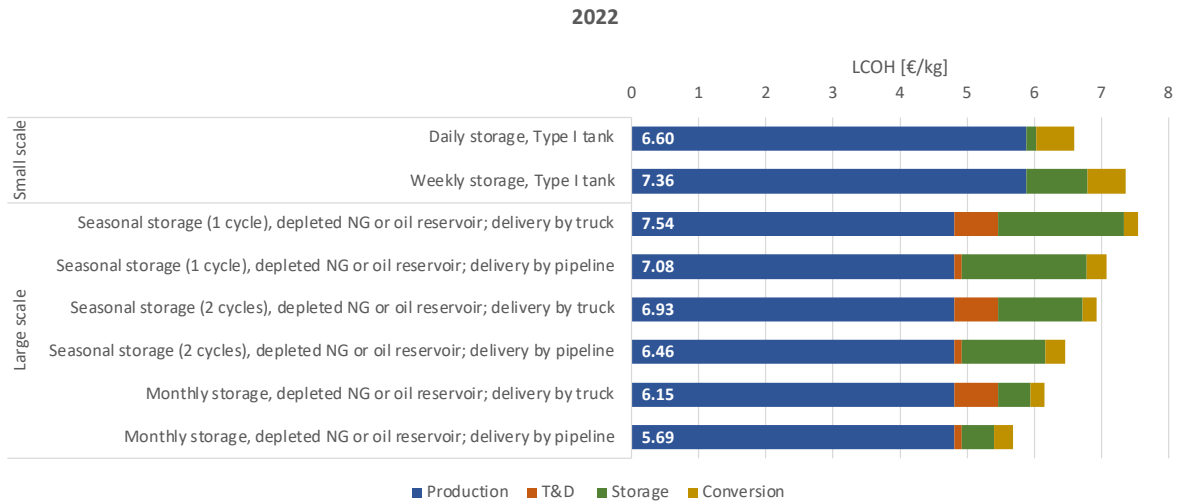


Figure 80: Levelized cost of hydrogen from electrolysis powered with solar electricity in Spain, in 2022.

In 2030, decentralized scenarios experience the largest decrease compared to 2022 levels, more than 3 €/kg, mainly due to the lower production component. However, due to both lower production and storage costs, also the centralized scenarios have much lower LCOH, with a reduction that goes from 2.7 €/kg for the annual storage to 2.5 €/kg for the monthly one. This slightly changes the overall ranking in 2030, when small-scale systems with daily storage and large-scale with monthly storage and truck delivery are in the same range. This corresponds to a LCOH of 3.6-3.7 €/kg, whether the hydrogen is produced locally and stored for one day or its production is centralized and its storage duration monthly.

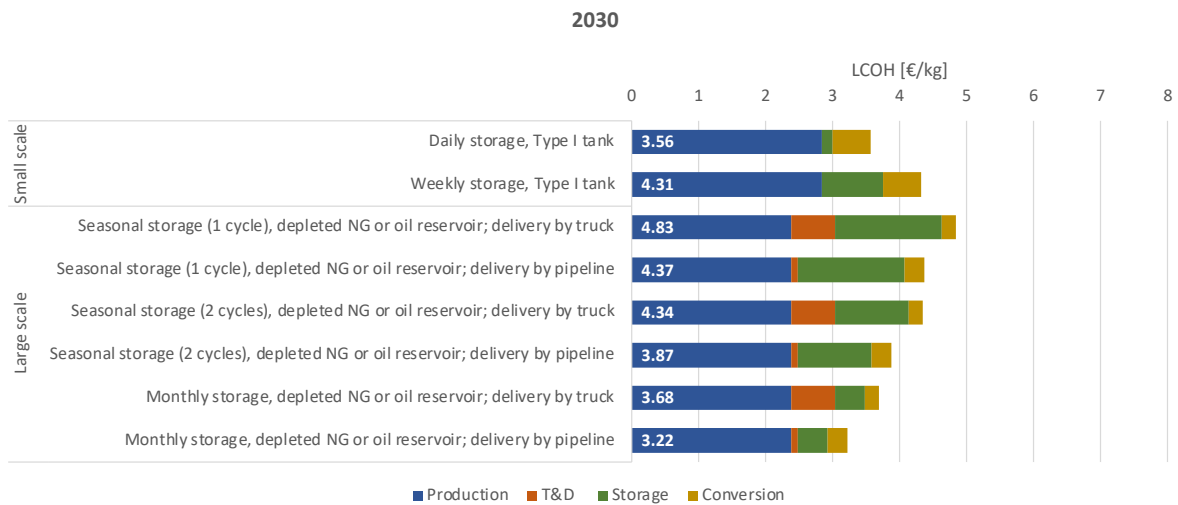


Figure 81: Levelized cost of hydrogen from electrolysis powered with solar electricity in Spain, in 2030.

6.5.3 France

The cases studied for France exclusively considers hydrogen produced domestically with electrolysis, powered by different electricity sources. The French scenarios entail a storage in lined rock cavern and a delivery by truck. In a parallel fashion to the considerations for Germany, the results for pipeline delivery can be easily calculated, keeping in mind that this distribution mode is 0.5 €/kg cheaper than the truck alternative. Figure 82 presents the LCOH for different electricity sources and varying storage duration. In general, hydrogen from dedicated RES plants has the lowest costs. This complements what was discussed in Section 6.1.6. If monthly storage is sufficient, an onshore wind facility coupled with PEM electrolyzers

can produce hydrogen with a final LCOH of 6.3 €/kg, the lowest option in 2022. If longer storage durations are necessary, the same LCOH increases by 10% for biannual, and by 20% for annual. Similar trends can also be observed for the other green hydrogen scenarios. Looking at yellow and pink hydrogen pathways, their higher capacity factor, and therefore their larger production of hydrogen, determine lower downstream costs due to economy of scale. Nonetheless, the production stage remains the main driver, translating to an overall higher LCOH for these scenarios. When directly connected to the grid or a nuclear plant, alkaline electrolysis currently has lower costs than SOE. The reason is twofold: a lower LCOH_p and the need for fewer compression stages, given the higher output pressure of this electrolyzer type.

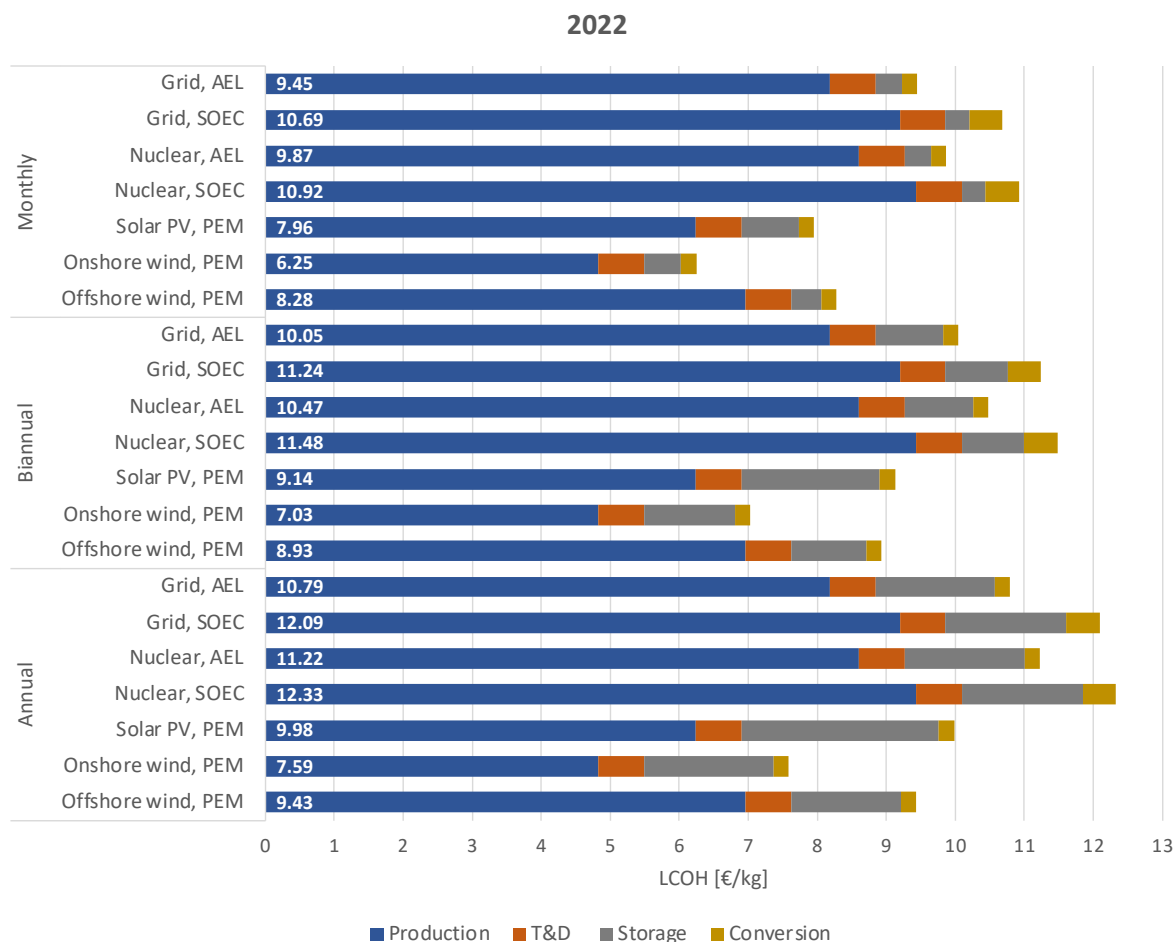


Figure 82: Levelized cost of hydrogen domestically produced via electrolysis in France and delivered by truck, in 2022.

Figure 83 presents the results for 2030. The combination of electrolysis and onshore wind remains the scenario with the lowest LCOH, around 4.4 €/kg if monthly storage is enough. The pathway with solar PV gets closer, presenting a cost of 4.7 €/kg. The gap between grid- and nuclear-powered electrolysis increase, given the fast decline in renewable costs and the quite stable trend for the wholesale electricity price. A last interesting aspect to observe is that solar PV becomes less and less competitive with larger duration needs. For instance, with annual storage its LCOH is slightly lower than offshore wind (6.6 v 7.1 €/kg), and quite distant from onshore wind (5.7 €/kg).

2030

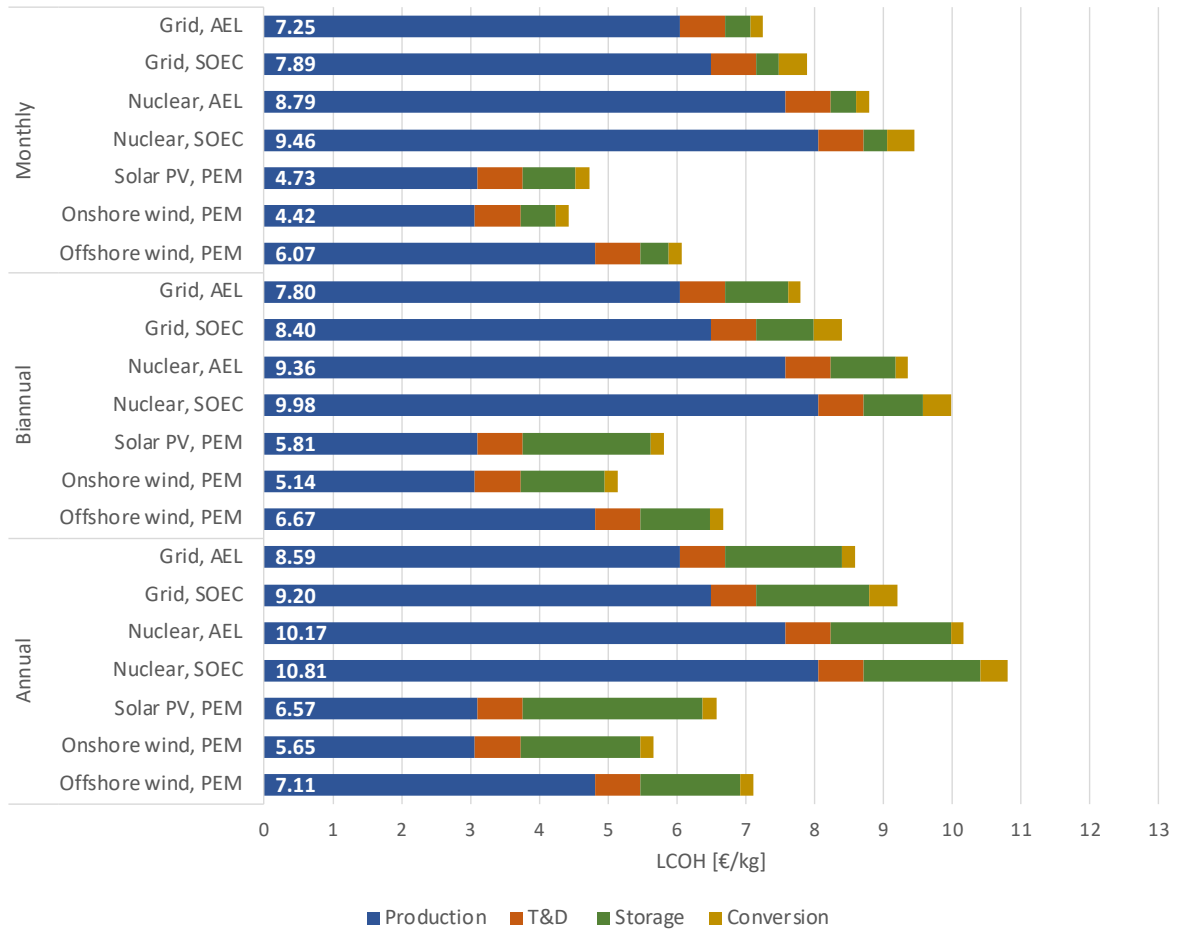


Figure 83: Levelized cost of hydrogen domestically produced via electrolysis in France and delivered by truck, in 2030.

7. Contribution to sustainability

The needed decarbonization of the energy systems relies on the development of alternative solutions to the conventional, carbon-intensive methods. Among others, hydrogen has the potential to replace fossil fuels in several hard-to-abate sectors. For instance, the transportation sector, and in particular its heavy-duty segment, might largely benefit from the establishment of a hydrogen infrastructure and economy. However, to ensure an efficient and sustainable transition, it is necessary to carry out precise assessments of its feasibility, also in comparison with other clean alternatives, e.g., electricity. This research contributes to gather and increase the knowledge about one of the sustainability dimensions, the economic one. In fact, the study compares different supply chains, showing the most competitive options until 2030.

Despite only covering the economic aspect of sustainability, this work provides an important perspective that could support informed and efficient decision-making. The main benefit would be an acceleration of the phase-out of fossil fuels, with a drastic and earlier reduction of the GHG emissions. This would contribute to the achievement of the Paris Agreement and other targets to limit global warming well-below the 1.5°C threshold compared to pre-industrial levels [1].

The creation of a simple Excel tool aims at increasing and facilitating access to knowledge about hydrogen. It is believed that it can support informed decision-making, with different levels of depth, depending on the stakeholder and the final objective of its use. Despite the tool being developed for, and in collaboration with a heavy-duty vehicle company, its scope goes well beyond the transportation sector. In fact, the end-use application does not influence its supply chain costs, only the hydrogen final state is determinant. For instance, this also means that the tool can be used to assess supply chains where ammonia is the final vector.

However, it is worth mentioning again that this study focuses on economic aspects, and the reference to the environmental and social spheres only regards the social cost of carbon, allocated to the low-carbon (and not zero-) production processes. Subsequently, the research neglects possible social implications and related emissions along the supply chain (e.g., emissions from hydrogen delivery with fossil-fueled vehicles). For the effective and sustainable establishment of a hydrogen economy, it is therefore necessary to complement these results with parallel research on the environmental and social aspects of the different hydrogen supply chains.

8. Conclusion

In the transition towards decarbonized energy systems, hydrogen has the potential to play a central role given its properties, which make it the main alternative to many conventional, hard-to-abate processes. Among others, the transportation sector and its heavy-duty subsegment could particularly benefit from the hydrogen rollout to replace the currently dominant diesel while keeping similar operational advantages. Therefore, the development of reliable and competitive supply chains is vital for a well-established hydrogen economy. Within this transformation, the European Union aims at positioning itself as a global hydrogen leader. In particular, three of its members are developing strong but dissimilar strategies: Germany, France, and Spain. To assess the competitiveness of hydrogen supply chains in these three countries, an Excel tool was developed to support this study, which uses the levelized cost of hydrogen as a central indicator.

Among the three countries, Germany has the highest hydrogen aspirations. To achieve its ambitious demand targets, Germany envisions both domestic and foreign hydrogen production, from both low- and zero-carbon processes. Subsequently, the supply chains are heavily characterized by the production location and method. Regarding the former, this study concludes that imports from locations with favorable hydrogen production and with the possibility of a pipeline connection can provide the cheapest final product. Above all, Algeria can deliver the most competitive gH_2 , mainly due to a couple of factors: its low-cost natural gas and electricity from renewable sources; and its proximity to Europe, which makes hydrogen pipelines a feasible option, also given the existing gas network connecting the two continents. Imports from remote locations are in most cases not competitive, especially if ammonia is the transmission vector. Onshore wind in Chile can be considered an exception: the extraordinary natural conditions provide a hydrogen with the lowest production costs overall, and a final LCOH comparable with domestic green hydrogen production, if its transmission is done with LH_2 ships.

With regards to the production method, steam methane reforming with carbon capture and storage is the lowest-cost supply chain, both domestically and among imports. The steep cost decline of renewables and electrolysers can reduce the gap between blue and green hydrogen. However, the low capacity factors, that result in lower production capacity and more expensive downstream stages, undermine the competitiveness of green hydrogen. A similar consideration can be carried out also for pyrolysis: despite production costs similar to blue hydrogen, turquoise hydrogen has a higher LCOH due to the limited size of its plants. The combination of the two conclusions about production location and method leads to the Algerian blue hydrogen transported via pipeline being the cheapest supply pathway considered in this study: its LCOH in 2030 can be as low as 2.1 €/kg.

Storage has also a wide impact on the supply chain costs. To guarantee supply security, the German scenarios assume a long-term storage, with monthly storage in depleted NG or oil reservoirs being the base case and the cheapest option. Salt caverns have lower permeability, which translates to higher hydrogen recovery rates per discharge. However, their LCOH is slightly higher, being CAPEX the main cost driver. Instead, lined rock caverns generally present the highest associated costs, despite the difference within monthly durations being quite small. Increasing the storage duration to seasonal configurations improves the resiliency of the supply chains. However, this also means lower cycling throughout the year, which determines a steep increase in the overall LCOH. For depleted NG or oil reservoirs and salt caverns, the Algerian blue hydrogen delivered to Germany increases by around 0.4 and 0.9 €/kg if seasonal storage with respectively two and one cycle per year are considered. Lined rock caverns are instead more sensitive to a duration increase: two cycles increase the LCOH by 2.0 €/kg, a single cycle by 4.5 €/kg. The choice of the most appropriate storage is therefore a compromise between supply security and economic considerations.

For different reasons, Spain and France only foresee domestic hydrogen production via electrolysis in their national plans. For Spain, this can be explained by the large availability of renewable resources, solar above all. With these conditions, different business models are possible. In particular, this study focused on two general cases: large-scale centralized and small-scale local (close to the end-use) production. The

lower production costs for the centralized case, due to economy of scale, also entail higher delivery costs and larger storage needs. Interestingly, the two cases have an equivalent LCOH in 2030, equal to 3.6-3.7 €/kg in their configurations with daily storage for the local one, monthly storage and truck delivery for the centralized one. Different storage needs and delivery modes may affect the comparison. For instance, pipeline distribution has a LCOH usually 0.5 €/kg lower than the truck alternative but might be operationally more complex to realize in the first stages of the hydrogen rollout. In any case, the Spanish case shows that different business models can have similar costs with good solar conditions, enhancing the competition and sparking the creation of a diversified hydrogen economy.

France prefers hydrogen from electrolysis due to the high levels of electrification and electricity sources in the country. Specifically, the nuclear predominance suggests this path and led France to specialize in the development of SOEC modules. Still, the high current costs of nuclear electricity and the projections for the CAPEX of SOEs do not indicate a simple diffusion of similar supply chains. In fact, RES connected with PEM electrolyzers can generate hydrogen at half the cost of SOEs with nuclear electricity. Even the cheaper alkaline electrolyzers connected to the grid results more expensive than domestic hydrogen from onshore wind electricity, which is the cheapest option at 4.4 €/kg in 2030. Comparing the French results with the ones of the other two countries, France might not be able to have low-cost hydrogen if the cases are limited to the ones in its national plans. However, if lower nuclear LCOEs are available and if the SOEC technology is coupled with novel high-temperature gas reactors, the LCOH might decrease to more competitive levels.

Some general conclusions can be presented, considering all the studied cases. First, if the hydrogen economy develops following market drivers, it might experience a regionalization of its trades. In fact, imports from favorable close location in the first place, followed by domestic production, are the most competitive options, excluding remote locations. This is closely connected to the second point, which is the economic advantage of pipelines for both transmission and distribution. Despite the difficulties to realize a capillary hydrogen networks, its realization would be determinant to cut down costs. A third point concerns the possible reliance of hydrogen production on natural gas, especially in the first stages. In fact, the very low LCOH and the comparatively high maturity level of blue hydrogen suggests its possible wide diffusion, also driven by gas producing countries to safeguard their exporting economies. A last point concerns the hydrogen storage, that has a large impact on the overall LCOH. Its extent is a compromise between lower costs and improved supply security. This strengthens the considerations about a regionalization of the hydrogen economy: especially at the beginning, hydrogen clusters would decrease the storage need, given a better optimization between supply demands, also translating into a lower LCOH.

This last point has a more speculative nature, and hints at some of the limitations of this study. In fact, the presented work is based on linear modeling, that disregards any kind of supply chain optimization. This is replaced by several assumptions. However, the developed Excel model can be a powerful tool if integrated with further work about the single stages and the overall supply chain. Citing some examples, one of the main limitations of this work is the dependence of each stage on the amount of produced hydrogen. For this reason, a system optimization might be able to provide more detailed results, and likely lower LCOHs. An optimization approach would also provide improved results for the single stages. For instance, the accuracy of the production stage would benefit from an investigation that includes factors such as seasonal/hourly electricity and weather data, connection of RES plants with the grid, and solar-wind hybrid facilities. Similarly, this would also help the study of the storage stage. In particular, the introduction of demand projections would determine an improved design of the supply chains, not only refining the cost results but also extending the research to the future price of hydrogen. This economic assessment provides only one perspective on this topic: complementing this research with detailed social and environmental notions would be essential to support a sustainable hydrogen rollout.

9. Bibliography

- [1] UNFCCC, “The Paris Agreement,” 2015. <https://unfccc.int/process-and-meetings/the-paris-agreement/the-paris-agreement> (accessed Feb. 03, 2022).
- [2] Hydrogen Council, “Path to Hydrogen Competitiveness: A Cost Perspective - Hydrogen Council,” <https://hydrogencouncil.com/en/>, 2020. <https://hydrogencouncil.com/en/path-to-hydrogen-competitiveness-a-cost-perspective/> (accessed Feb. 03, 2022).
- [3] International Energy Agency, “The Future of Hydrogen,” *IEA*, 2019. <https://www.iea.org/reports/the-future-of-hydrogen> (accessed Feb. 03, 2022).
- [4] M. Kayfeci, A. Keçebaş, and M. Bayat, “Chapter 3 - Hydrogen production,” in *Solar Hydrogen Production*, F. Calise, M. D. D’Accadia, M. Santarelli, A. Lanzini, and D. Ferrero, Eds. Academic Press, 2019, pp. 45–83. doi: 10.1016/B978-0-12-814853-2.00003-5.
- [5] International Energy Agency, “Data and Statistics,” *IEA*. <https://www.iea.org/data-and-statistics> (accessed Feb. 03, 2022).
- [6] A. E. Farrell, D. W. Keith, and J. J. Corbett, “A strategy for introducing hydrogen into transportation,” *Energy Policy*, vol. 31, no. 13, pp. 1357–1367, Oct. 2003, doi: 10.1016/S0301-4215(02)00195-7.
- [7] C. Cunanan, M.-K. Tran, Y. Lee, S. Kwok, V. Leung, and M. Fowler, “A Review of Heavy-Duty Vehicle Powertrain Technologies: Diesel Engine Vehicles, Battery Electric Vehicles, and Hydrogen Fuel Cell Electric Vehicles,” *Clean Technol.*, vol. 3, no. 2, Art. no. 2, Jun. 2021, doi: 10.3390/cleantechnol3020028.
- [8] M. A. Rosen and S. Koochi-Fayegh, “The prospects for hydrogen as an energy carrier: an overview of hydrogen energy and hydrogen energy systems,” *Energy Ecol. Environ.*, vol. 1, no. 1, pp. 10–29, Feb. 2016, doi: 10.1007/s40974-016-0005-z.
- [9] G. Collodi, G. Azzaro, N. Ferrari, and S. Santos, “Techno-economic Evaluation of Deploying CCS in SMR Based Merchant H₂ Production with NG as Feedstock and Fuel,” *Energy Procedia*, vol. 114, pp. 2690–2712, Jul. 2017, doi: 10.1016/j.egypro.2017.03.1533.
- [10] S. Roussanaly, R. Anantharaman, and C. Fu, “Low-Carbon Footprint Hydrogen Production from Natural Gas: A Techno-Economic Analysis of Carbon Capture and Storage from Steam-Methane Reforming,” *Chem. Eng. Trans.*, vol. 81, pp. 1015–1020, Aug. 2020, doi: 10.3303/CET2081170.
- [11] J. C., E. S. Hamborg, T. van Keulen, A. Ramírez, W. C. Turkenburg, and A. P. C. Faaij, “Techno-economic assessment of CO₂ capture at steam methane reforming facilities using commercially available technology,” *Int. J. Greenh. Gas Control*, vol. 9, pp. 160–171, Jul. 2012, doi: 10.1016/j.ijggc.2012.02.018.
- [12] Z. Navas-Anguita, D. García-Gusano, J. Dufour, and D. Iribarren, “Revisiting the role of steam methane reforming with CO₂ capture and storage for long-term hydrogen production,” *Sci. Total Environ.*, vol. 771, p. 145432, Jun. 2021, doi: 10.1016/j.scitotenv.2021.145432.
- [13] J. Chi and H. Yu, “Water electrolysis based on renewable energy for hydrogen production,” *Chin. J. Catal.*, vol. 39, no. 3, pp. 390–394, Mar. 2018, doi: 10.1016/S1872-2067(17)62949-8.
- [14] S. M. Saba, M. Müller, M. Robinius, and D. Stolten, “The investment costs of electrolysis – A comparison of cost studies from the past 30 years,” *Int. J. Hydrog. Energy*, vol. 43, no. 3, pp. 1209–1223, Jan. 2018, doi: 10.1016/j.ijhydene.2017.11.115.
- [15] J. L. L. C. C. Janssen, M. Weeda, R. J. Detz, and B. van der Zwaan, “Country-specific cost projections for renewable hydrogen production through off-grid electricity systems,” *Appl. Energy*, vol. 309, p. 118398, Mar. 2022, doi: 10.1016/j.apenergy.2021.118398.

- [16] Engineering Toolbox, “Gases - Densities,” 2003. https://www.engineeringtoolbox.com/gas-density-d_158.html#google_vignette (accessed Apr. 28, 2022).
- [17] Engineering Toolbox, “Fuels - Higher and Lower Calorific Values,” 2003. https://www.engineeringtoolbox.com/fuels-higher-calorific-values-d_169.html (accessed Apr. 28, 2022).
- [18] M. J. Chae, J. H. Kim, B. Moon, S. Park, and Y. S. Lee, “The present condition and outlook for hydrogen-natural gas blending technology,” *Korean J. Chem. Eng.*, vol. 39, no. 2, pp. 251–262, Feb. 2022, doi: 10.1007/s11814-021-0960-8.
- [19] R. R. Ratnakar *et al.*, “Hydrogen supply chain and challenges in large-scale LH2 storage and transportation,” *Int. J. Hydrog. Energy*, vol. 46, no. 47, pp. 24149–24168, Jul. 2021, doi: 10.1016/j.ijhydene.2021.05.025.
- [20] D. R. MacFarlane *et al.*, “A Roadmap to the Ammonia Economy,” *Joule*, vol. 4, no. 6, pp. 1186–1205, Jun. 2020, doi: 10.1016/j.joule.2020.04.004.
- [21] P. C. Rao and M. Yoon, “Potential Liquid-Organic Hydrogen Carrier (LOHC) Systems: A Review on Recent Progress,” *Energies*, vol. 13, p. 6040, Nov. 2020, doi: 10.3390/en13226040.
- [22] M. E. Demir and I. Dincer, “Cost assessment and evaluation of various hydrogen delivery scenarios,” *Int. J. Hydrog. Energy*, vol. 43, no. 22, pp. 10420–10430, May 2018, doi: 10.1016/j.ijhydene.2017.08.002.
- [23] D. DeSantis, B. D. James, C. Houchins, G. Saur, and M. Lyubovsky, “Cost of long-distance energy transmission by different carriers,” *iScience*, vol. 24, no. 12, p. 103495, Nov. 2021, doi: 10.1016/j.isci.2021.103495.
- [24] B. Miao, L. Giordano, and S. H. Chan, “Long-distance renewable hydrogen transmission via cables and pipelines,” *Int. J. Hydrog. Energy*, vol. 46, no. 36, pp. 18699–18718, May 2021, doi: 10.1016/j.ijhydene.2021.03.067.
- [25] F. H. Saadi, N. S. Lewis, and E. W. McFarland, “Relative costs of transporting electrical and chemical energy,” *Energy Environ. Sci.*, vol. 11, no. 3, pp. 469–475, Mar. 2018, doi: 10.1039/C7EE01987D.
- [26] DOE, Office of Energy Efficiency & Renewable Energy, “Hydrogen Storage,” *Energy.gov*. <https://www.energy.gov/eere/fuelcells/hydrogen-storage> (accessed Jul. 30, 2022).
- [27] Z. Abdin, C. Tang, Y. Liu, and K. Catchpole, “Large-scale stationary hydrogen storage via liquid organic hydrogen carriers,” *iScience*, vol. 24, no. 9, p. 102966, Sep. 2021, doi: 10.1016/j.isci.2021.102966.
- [28] V. Tietze and D. Stolten, “Chapter 25 - Thermodynamics of Pressurized Gas Storage,” in *Hydrogen Science and Engineering: Materials, Processes, Systems, and Technology, 2 Volume Set*, vol. 1, Wiley. Accessed: Jul. 30, 2022. [Online]. Available: <https://www.wiley.com/en-gb/Hydrogen+Science+and+Engineering%3A+Materials%2C+Processes%2C+Systems%2C+and+Technology%2C+2+Volume+Set-p-9783527332380>
- [29] HyUnder, “HyUnder - Project overview,” *HYUNDER*. <http://hyunder.eu/project-overview/> (accessed Jul. 30, 2022).
- [30] A. Le Duigou, A.-G. Bader, J.-C. Lanoix, and L. Nadau, “Relevance and costs of large scale underground hydrogen storage in France,” *Int. J. Hydrog. Energy*, vol. 42, no. 36, pp. 22987–23003, Sep. 2017, doi: 10.1016/j.ijhydene.2017.06.239.
- [31] R. Tarkowski, “Underground hydrogen storage: Characteristics and prospects,” *Renew. Sustain. Energy Rev.*, vol. 105, pp. 86–94, May 2019, doi: 10.1016/j.rser.2019.01.051.

- [32] Charlotte van Leeuwen and Andreas Zauner, “Deliverable 8.3 Report on the costs involved with PtG technologies and their potentials across the EU,” *STORE&GO*. <https://www.storeandgo.info/publications/deliverables/> (accessed Jul. 31, 2022).
- [33] Y. Zhu, “From Hydrogen Production to Storage: A Process for Sustainable Development of Underground Hydrogen Storage in Caverns,” in *2021 3rd International Academic Exchange Conference on Science and Technology Innovation (IAECST)*, Dec. 2021, pp. 1658–1663. doi: 10.1109/IAECST54258.2021.9695812.
- [34] Cate Holtz and Hannes Beushausen, “Navigating the maze of energy storage costs, PV Tech Power, May 2016.” Jun. 09, 2016. Accessed: Aug. 01, 2022. [Online]. Available: <https://apricum-group.com/pv-tech-power-navigating-maze-energy-storage-costs-june-2016/>
- [35] F. Stockl, W.-P. Schill, and A. Zerrahn, “Optimal supply chains and power sector benefits of green hydrogen,” *Sci. Rep.*, vol. 11, no. 1, p. 14191, Dec. 2021, doi: 10.1038/s41598-021-92511-6.
- [36] A. Almansoori and N. Shah, “Design and Operation of a Future Hydrogen Supply Chain: Snapshot Model,” *Chem. Eng. Res. Des.*, vol. 84, no. 6, pp. 423–438, Jun. 2006, doi: 10.1205/cherd.05193.
- [37] G. Brändle, M. Schönfisch, and S. Schulte, “Estimating long-term global supply costs for low-carbon hydrogen,” *Appl. Energy*, vol. 302, p. 117481, Nov. 2021, doi: 10.1016/j.apenergy.2021.117481.
- [38] European Commission, “Shedding light on energy in the EU: From where do we import energy?,” *Shedding light on energy in the EU*. <https://ec.europa.eu/eurostat/cache/infographs/energy/bloc-2c.html> (accessed May 21, 2022).
- [39] International Energy Agency, “Hydrogen – Analysis,” *IEA*, 2021. <https://www.iea.org/reports/hydrogen> (accessed May 30, 2022).
- [40] Fortune Business Insights, “Hydrogen Generation Market Size Worth USD 220.37 Billion, Globally, by 2028 at 5.6% CAGR: Fortune Business Insights™,” *GlobeNewswire News Room*, Apr. 08, 2022. <https://www.globenewswire.com/news-release/2022/04/08/2419052/0/en/Hydrogen-Generation-Market-Size-Worth-USD-220-37-Billion-Globally-by-2028-at-5-6-CAGR-Fortune-Business-Insights.html> (accessed Aug. 16, 2022).
- [41] BloombergNEF, “Hydrogen Economy Outlook - Key Messages,” 2020. <https://data.bloomberglp.com/professional/sites/24/BNEF-Hydrogen-Economy-Outlook-Key-Messages-30-Mar-2020.pdf> (accessed May 30, 2022).
- [42] M. Lambert *et al.*, “The role of hydrogen in the energy transition,” no. 127, p. 61, 2021.
- [43] B. Parkinson, J. W. Matthews, T. B. McConnaughey, D. C. Upham, and E. W. McFarland, “Techno-Economic Analysis of Methane Pyrolysis in Molten Metals: Decarbonizing Natural Gas,” *Chem. Eng. Technol.*, vol. 40, no. 6, pp. 1022–1030, 2017, doi: 10.1002/ceat.201600414.
- [44] N. Sánchez-Bastardo, R. Schlögl, and H. Ruland, “Methane Pyrolysis for Zero-Emission Hydrogen Production: A Potential Bridge Technology from Fossil Fuels to a Renewable and Sustainable Hydrogen Economy,” *Ind. Eng. Chem. Res.*, vol. 60, no. 32, pp. 11855–11881, Aug. 2021, doi: 10.1021/acs.iecr.1c01679.
- [45] S. Timmerberg, M. Kaltschmitt, and M. Finkbeiner, “Hydrogen and hydrogen-derived fuels through methane decomposition of natural gas – GHG emissions and costs,” *Energy Convers. Manag. X*, vol. 7, p. 100043, Sep. 2020, doi: 10.1016/j.ecmx.2020.100043.
- [46] A. Ursua, L. M. Gandia, and P. Sanchis, “Hydrogen Production From Water Electrolysis: Current Status and Future Trends,” *Proc. IEEE*, vol. 100, no. 2, pp. 410–426, Feb. 2012, doi: 10.1109/JPROC.2011.2156750.

- [47] IRENA, “Green hydrogen cost reduction,” *IRENA*, 2020. <https://www.irena.org/publications/2020/Dec/Green-hydrogen-cost-reduction> (accessed Mar. 30, 2022).
- [48] M. Carmo, D. L. Fritz, J. Mergel, and D. Stolten, “A comprehensive review on PEM water electrolysis,” *Int. J. Hydrog. Energy*, vol. 38, no. 12, pp. 4901–4934, Apr. 2013, doi: 10.1016/j.ijhydene.2013.01.151.
- [49] M. Reuß, T. Grube, M. Robinius, P. Preuster, P. Wasserscheid, and D. Stolten, “Seasonal storage and alternative carriers: A flexible hydrogen supply chain model,” *Appl. Energy*, vol. 200, pp. 290–302, Aug. 2017, doi: 10.1016/j.apenergy.2017.05.050.
- [50] Axel Liebscher, Jürgen Wackerl, and Martin Streibel, “Chapter 26 - Geological storage of hydrogen - fundamentals, processing, and projects,” in *Hydrogen Science and Engineering*, Accessed: Aug. 01, 2022. [Online]. Available: <https://www.wiley.com/en-gb/Hydrogen+Science+and+Engineering%3A+Materials%2C+Processes%2C+Systems%2C+and+Technology%2C+2+Volume+Set-p-9783527332380>
- [51] A. S. Lord, P. H. Kobos, and D. J. Borna, “Geologic storage of hydrogen: Scaling up to meet city transportation demands,” *Int. J. Hydrog. Energy*, vol. 39, no. 28, pp. 15570–15582, Sep. 2014, doi: 10.1016/j.ijhydene.2014.07.121.
- [52] L. Li, H. Manier, and M.-A. Manier, “Hydrogen supply chain network design: An optimization-oriented review,” *Renew. Sustain. Energy Rev.*, vol. 103, pp. 342–360, Apr. 2019, doi: 10.1016/j.rser.2018.12.060.
- [53] NIST Chemistry WebBook, SRD 69, “Thermophysical Properties of Fluid Systems.” <https://webbook.nist.gov/chemistry/fluid/> (accessed Aug. 01, 2022).
- [54] M. J. Moran, H. N. Shapiro, D. D. Boettner, and M. B. Bailey, *Fundamentals of Engineering Thermodynamics*, 8^o edizione. Hoboken, N.J: John Wiley & Sons Inc, 2014.
- [55] A. Valera-Medina, H. Xiao, M. Owen-Jones, W. I. F. David, and P. J. Bowen, “Ammonia for power,” *Prog. Energy Combust. Sci.*, vol. 69, pp. 63–102, Nov. 2018, doi: 10.1016/j.pecs.2018.07.001.
- [56] M. Hirscher, *Handbook of Hydrogen Storage: New Materials for Future Energy Storage | Wiley*. Wiley, 2010. Accessed: Aug. 01, 2022. [Online]. Available: <https://www.wiley.com/en-gb/Handbook+of+Hydrogen+Storage%3A+New+Materials+for+Future+Energy+Storage-p-9783527322732>
- [57] Z. Abidin and K. R. Khalilpour, “Chapter 4 - Single and Polystorage Technologies for Renewable-Based Hybrid Energy Systems,” in *Polygeneration with Polystorage for Chemical and Energy Hubs*, K. R. Khalilpour, Ed. Academic Press, 2019, pp. 77–131. doi: 10.1016/B978-0-12-813306-4.00004-5.
- [58] H. Barthelemy, M. Weber, and F. Barbier, “Hydrogen storage: Recent improvements and industrial perspectives,” *Int. J. Hydrog. Energy*, vol. 42, no. 11, pp. 7254–7262, Mar. 2017, doi: 10.1016/j.ijhydene.2016.03.178.
- [59] J. Zheng, X. Liu, P. Xu, P. Liu, Y. Zhao, and J. Yang, “Development of high pressure gaseous hydrogen storage technologies,” *Int. J. Hydrog. Energy*, vol. 37, no. 1, pp. 1048–1057, Jan. 2012, doi: 10.1016/j.ijhydene.2011.02.125.
- [60] C. Azzaro-Pantel, *Hydrogen Supply Chain - Design, Deployment, and Operation*, 1st Edition. Academic Press, 2018. Accessed: Jul. 15, 2022. [Online]. Available: <https://www.elsevier.com/books/hydrogen-supply-chain/azzaro-pantel/978-0-12-811197-0>
- [61] T.-P. Chen, “Hydrogen Delivery Infrastructure Option Analysis,” Nexant, Inc., 101 2nd St., San Francisco, CA 94105, GO15032F, May 2010. doi: 10.2172/982359.

- [62] H. W. Langmi, N. Engelbrecht, P. M. Modisha, and D. Bessarabov, "Chapter 13 - Hydrogen storage," in *Electrochemical Power Sources: Fundamentals, Systems, and Applications*, T. Smolinka and J. Garche, Eds. Elsevier, 2022, pp. 455–486. doi: 10.1016/B978-0-12-819424-9.00006-9.
- [63] I. A. Hassan, H. S. Ramadan, M. A. Saleh, and D. Hissel, "Hydrogen storage technologies for stationary and mobile applications: Review, analysis and perspectives," *Renew. Sustain. Energy Rev.*, vol. 149, p. 111311, Oct. 2021, doi: 10.1016/j.rser.2021.111311.
- [64] Vanessa Tietze, Sebastian Luhr, and Detlef Stolten, "Chapter 27 - Bulk Storage Vessels for Compressed and Liquid Hydrogen," in *Wiley.com*, Accessed: Aug. 01, 2022. [Online]. Available: <https://www.wiley.com/en-gb/Hydrogen+Science+and+Engineering%3A+Materials%2C+Processes%2C+Systems%2C+and+Technology%2C+2+Volume+Set-p-9783527332380>
- [65] D. D. Papadias and R. K. Ahluwalia, "Bulk storage of hydrogen," *Int. J. Hydrog. Energy*, vol. 46, no. 70, pp. 34527–34541, Oct. 2021, doi: 10.1016/j.ijhydene.2021.08.028.
- [66] M. Al-Breiki and Y. Bicer, "Technical assessment of liquefied natural gas, ammonia and methanol for overseas energy transport based on energy and exergy analyses," *Int. J. Hydrog. Energy*, vol. 45, no. 60, pp. 34927–34937, Dec. 2020, doi: 10.1016/j.ijhydene.2020.04.181.
- [67] The European Space Station (ESA), "Zero-Boil Off Propulsion System Feasibility Demonstration." https://www.esa.int/Enabling_Support/Space_Engineering_Technology/Shaping_the_Future/Zero-Boil_Off_Propulsion_System_Feasibility_Demonstration (accessed Aug. 01, 2022).
- [68] W. U. Notardonato, A. M. Swanger, J. E. Fesmire, K. M. Jumper, W. L. Johnson, and T. M. Tomsik, "Zero boil-off methods for large-scale liquid hydrogen tanks using integrated refrigeration and storage," *IOP Conf. Ser. Mater. Sci. Eng.*, vol. 278, p. 012012, Dec. 2017, doi: 10.1088/1757-899X/278/1/012012.
- [69] A. Swanger, W. Notardonato, W. Johnson, and T. Tomsik, "Integrated Refrigeration and Storage for Advanced Liquid Hydrogen Operations," Jan. 2017.
- [70] O. Elishav, B. Mosevitzky Lis, A. Valera-Medina, and G. S. Grader, "Chapter 5 - Storage and Distribution of Ammonia," in *Techno-Economic Challenges of Green Ammonia as an Energy Vector*, A. Valera-Medina and R. Banares-Alcantara, Eds. Academic Press, 2021, pp. 85–103. doi: 10.1016/B978-0-12-820560-0.00005-9.
- [71] DNV GL, "Study on the Import of Liquid Renewable Energy: Technology Cost Assessment," p. 32, 2020.
- [72] A. Patonia and R. Poudineh, "Ammonia as a storage solution for future decarbonized energy systems," *Oxford Institute for Energy Studies*, 2020. <https://www.oxfordenergy.org/publications/ammonia-as-a-storage-solution-for-future-decarbonized-energy-systems/> (accessed Aug. 05, 2022).
- [73] Gas Infrastructure Europe and Guidehouse, "Picturing the value of underground gas storage to the European hydrogen system," *Gas Infrastructure Europe*, Jun. 15, 2021. <https://www.gie.eu/gie-presents-new-study-picturing-the-value-of-underground-gas-storage-to-the-european-hydrogen-system/> (accessed Jul. 26, 2022).
- [74] Olaf Kruck, Fritz Crotogino, Ruth Prelicz, and Tobias Rudolph, "Deliverable 3.1 - Overview of all known underground storage technologies," *HYUNDER*. <http://hyunder.eu/publications/> (accessed Jul. 31, 2022).
- [75] L. Louis, "Four Ways to Store Large Quantities of Hydrogen," Dec. 2021. doi: 10.2118/208178-MS.

- [76] A. Mortazavi and H. Nasab, "Analysis of the behavior of large underground oil storage caverns in salt rock," *Int. J. Numer. Anal. Methods Geomech.*, vol. 41, no. 4, pp. 602–624, 2017, doi: 10.1002/nag.2576.
- [77] N. S. Muhammed, B. Haq, D. Al Shehri, A. Al-Ahmed, M. M. Rahman, and E. Zaman, "A review on underground hydrogen storage: Insight into geological sites, influencing factors and future outlook," *Energy Rep.*, vol. 8, pp. 461–499, Nov. 2022, doi: 10.1016/j.egy.2021.12.002.
- [78] B. Bourgeois, L. Duclercq, H. Jannel, and A. Reveillere, "Life Cycle Cost Assessment of an underground storage site," p. 74, 2022.
- [79] Directorate-General for Energy (European Commission) *et al.*, *Hydrogen generation in Europe: overview of costs and key benefits*. LU: Publications Office of the European Union, 2020. Accessed: Jul. 29, 2022. [Online]. Available: <https://data.europa.eu/doi/10.2833/122757>
- [80] Nichola Smith and Ceri Vincent, "Deliverable 1.2-0 - Geological database report," *Hystories*, 2022. <https://hystories.eu/publications-hystories/> (accessed Aug. 02, 2022).
- [81] P. Preuster, A. Alekseev, and P. Wasserscheid, "Hydrogen Storage Technologies for Future Energy Systems," *Annu. Rev. Chem. Biomol. Eng.*, vol. 8, no. 1, pp. 445–471, 2017, doi: 10.1146/annurev-chembioeng-060816-101334.
- [82] D. Grouset and C. Ridart, "Lowering Energy Spending Together With Compression, Storage, and Transportation Costs for Hydrogen Distribution in the Early Market," in *Hydrogen Supply Chains*, Elsevier, 2018, pp. 207–270. doi: 10.1016/B978-0-12-811197-0.00006-3.
- [83] M. A. Khan, C. Mackinnon, and D. Layzell, "Technical Brief: The Techno-Economics of Hydrogen Compression," The Transition Accelerator, Oct. 2021. Accessed: Jul. 27, 2022. [Online]. Available: <https://transitionaccelerator.ca/techbrief-techno-economics-hydrogen-compression/>
- [84] A. Alekseev, "Hydrogen Liquefaction," in *Hydrogen Science and Engineering: Materials, Processes, Systems and Technology*, John Wiley & Sons, Ltd, 2016, pp. 733–762. doi: 10.1002/9783527674268.ch30.
- [85] K. Ohlig and L. Decker, "The latest developments and outlook for hydrogen liquefaction technology," *AIP Conf. Proc.*, vol. 1573, no. 1, pp. 1311–1317, Jan. 2014, doi: 10.1063/1.4860858.
- [86] U. Cardella, L. Decker, and H. Klein, "Economically viable large-scale hydrogen liquefaction," *IOP Conf. Ser. Mater. Sci. Eng.*, vol. 171, p. 012013, Feb. 2017, doi: 10.1088/1757-899X/171/1/012013.
- [87] K. Stolzenburg and R. Mubbala, "Integrated Design for Demonstration of Efficient Liquefaction of Hydrogen (IDEALHY)," 2013. Accessed: Jul. 30, 2022. [Online]. Available: https://www.idealhy.eu/uploads/documents/IDEALHY_D3-16_Liquefaction_Report_web.pdf
- [88] V. Semaskaite and M. Bogdevicius, "Liquefied Natural Gas Regasification Technologies," 2022, pp. 270–280. doi: 10.1007/978-3-030-94774-3_27.
- [89] Argonne National Laboratory and U.S. Department of Energy, "Hydrogen Delivery Scenario Analysis Model." <https://hdsam.es.anl.gov/index.php?content=hdsam> (accessed Jul. 30, 2022).
- [90] G. Thomas and G. Parks, "Potential Roles of Ammonia in a Hydrogen Economy," U.S. Department of Energy, 2006. [Online]. Available: https://www.energy.gov/sites/prod/files/2015/01/f19/fcto_nh3_h2_storage_white_paper_2006.pdf
- [91] L. Wang *et al.*, "Greening Ammonia toward the Solar Ammonia Refinery," *Joule*, vol. 2, no. 6, pp. 1055–1074, Jun. 2018, doi: 10.1016/j.joule.2018.04.017.
- [92] Ecuity, Engie, STFC, and Siemens, "Ammonia to Green Hydrogen Project - Feasibility Study," 2019.

https://assets.publishing.service.gov.uk/government/uploads/system/uploads/attachment_data/file/880826/HS420_-_Ecuity_-_Ammonia_to_Green_Hydrogen.pdf (accessed Jul. 30, 2022).

[93] Roland Berger, “Transporting the fuel of the future,” 2021. Accessed: May 26, 2022. [Online]. Available: <https://www.rolandberger.com/en/Insights/Publications/Transporting-the-fuel-of-the-future.html>

[94] M. A. Khan, C. Young, and D. Layzell, “Technical Brief: The Techno-Economics of Hydrogen Pipelines,” The Transition Accelerator, Nov. 2021. Accessed: May 19, 2022. [Online]. Available: <https://transitionaccelerator.ca/techbrief-techno-economics-hydrogenpipelines/>

[95] J. R. Fekete, J. W. Sowards, and R. L. Amaro, “Economic impact of applying high strength steels in hydrogen gas pipelines,” *Int. J. Hydrog. Energy*, vol. 40, no. 33, pp. 10547–10558, Sep. 2015, doi: 10.1016/j.ijhydene.2015.06.090.

[96] HySTRA, “HySTRA,” *HySTRA - CO₂-free Hydrogen Energy Supply-chain Technology Research Association*. <http://www.hystra.or.jp/> (accessed May 27, 2022).

[97] HySTRA, “News & Gallery - HySTRA,” 2022. <https://www.hystra.or.jp/en/gallery/article.html#news05> (accessed May 27, 2022).

[98] Kawasaki Heavy Industries, “Kawasaki Obtains AIP for Large, 160,000m³ Liquefied Hydrogen Carrier,” 2022. https://global.kawasaki.com/en/corp/newsroom/news/detail/?f=20220422_3378 (accessed Aug. 16, 2022).

[99] M. Fasihi, R. Weiss, J. Savolainen, and C. Breyer, “Global potential of green ammonia based on hybrid PV-wind power plants,” *Appl. Energy*, vol. 294, p. 116170, Jul. 2021, doi: 10.1016/j.apenergy.2020.116170.

[100] K. Reddi, A. Elgowainy, N. Rustagi, and E. Gupta, “Techno-economic analysis of conventional and advanced high-pressure tube trailer configurations for compressed hydrogen gas transportation and refueling,” *Int. J. Hydrog. Energy*, vol. 43, no. 9, pp. 4428–4438, Mar. 2018, doi: 10.1016/j.ijhydene.2018.01.049.

[101] Hydrogen and Fuel Cell Technologies Office, “Liquid Hydrogen Delivery,” *Energy.gov*. <https://www.energy.gov/eere/fuelcells/liquid-hydrogen-delivery> (accessed May 27, 2022).

[102] R. M. Nayak-Luke, C. Forbes, Z. Cesaro, R. Bañares-Alcántara, and K. H. R. Rouwenhorst, “Chapter 8 - Techno-Economic Aspects of Production, Storage and Distribution of Ammonia,” in *Techno-Economic Challenges of Green Ammonia as an Energy Vector*, A. Valera-Medina and R. Banares-Alcantara, Eds. Academic Press, 2021, pp. 191–207. doi: 10.1016/B978-0-12-820560-0.00008-4.

[103] IRENA, “Geopolitics of the Energy Transformation: The Hydrogen Factor,” 2022. <https://www.irena.org/publications/2022/Jan/Geopolitics-of-the-Energy-Transformation-Hydrogen> (accessed Jun. 08, 2022).

[104] M. Ludwig *et al.*, “The Green Tech Opportunity in Hydrogen,” *BCG Global*, Apr. 06, 2021. <https://www.bcg.com/publications/2021/capturing-value-in-the-low-carbon-hydrogen-market> (accessed Jun. 08, 2022).

[105] European Commission, “A hydrogen strategy for a climate-neutral Europe.” 2020. Accessed: Mar. 30, 2022. [Online]. Available: https://ec.europa.eu/energy/sites/ener/files/hydrogen_strategy.pdf

[106] European Commission, “A European Green Deal,” *European Commission - European Commission*. https://ec.europa.eu/info/strategy/priorities-2019-2024/european-green-deal_en (accessed Jun. 14, 2022).

- [107] European Commission, “REPowerEU: affordable, secure and sustainable energy for Europe,” *European Commission - European Commission*, 2022. https://ec.europa.eu/info/strategy/priorities-2019-2024/european-green-deal/repowereu-affordable-secure-and-sustainable-energy-europe_en (accessed Jun. 09, 2022).
- [108] J. Jens, A. Wang, K. van der Leun, D. Peters, and M. Buseman, “Extending the European Hydrogen Backbone,” 2021. Accessed: Mar. 17, 2022. [Online]. Available: https://gasforclimate2050.eu/sdm_downloads/extending-the-european-hydrogen-backbone/
- [109] Council of the European Union, *Proposal for a REGULATION OF THE EUROPEAN PARLIAMENT AND OF THE COUNCIL on the deployment of alternative fuels infrastructure, and repealing Directive 2014/94/EU of the European Parliament and of the Council - General approach*. 2022. Accessed: Jun. 14, 2022. [Online]. Available: https://eur-lex.europa.eu/legal-content/EN/TXT/?uri=CONSIL:ST_9111_2022_INIT
- [110] European Commission, *Proposal for a REGULATION OF THE EUROPEAN PARLIAMENT AND OF THE COUNCIL on the deployment of alternative fuels infrastructure, and repealing Directive 2014/94/EU of the European Parliament and of the Council*. 2021. Accessed: Jun. 14, 2022. [Online]. Available: <https://eur-lex.europa.eu/legal-content/EN/TXT/?uri=CELEX:52021PC0559>
- [111] European Parliament, “Revision of the Directive on Deployment of Alternative Fuels Infrastructure,” *European Parliament*, 2022. <https://www.europarl.europa.eu/legislative-train/theme-a-european-green-deal/file-revision-of-the-directive-on-deployment-of-alternative-fuels-infrastructure> (accessed Jun. 14, 2022).
- [112] Federal Ministry for Economics Affairs and Climate Action, “The National Hydrogen Strategy,” 2020. <https://www.bmwk.de/Redaktion/EN/Publikationen/Energie/the-national-hydrogen-strategy.html> (accessed Jun. 14, 2022).
- [113] N. J. Kurmayer, “German government disavows blue hydrogen,” *www.euractiv.com*, Jan. 17, 2022. <https://www.euractiv.com/section/energy/news/german-government-disavows-blue-hydrogen/> (accessed Jun. 14, 2022).
- [114] Federal Ministry for Economics Affairs and Climate Action, “Germany and Norway sign joint statement on cooperation on hydrogen imports,” 2022. <https://www.bmwk.de/Redaktion/EN/Pressemitteilungen/2022/03/20220316-germany-and-norway-sign-joint-statement-on-cooperation-on-hydrogen-imports.html> (accessed Jun. 14, 2022).
- [115] Partenariat Énergétique Algérie-Allemagne, “The German-Algerian Energy Partnership,” *Partenariat Énergétique Algérie-Allemagne*. <https://www.energypartnership-algeria.org/home/> (accessed Jun. 14, 2022).
- [116] AHK Saudi-Arabien - Die Deutschen Auslandshandelskammer in Saudi Arabien, “Hydrogen,” *AHK Saudi-Arabien - Die Deutschen Auslandshandelskammer in Saudi Arabien*, 2021. <https://saudi-arabien.ahk.de/en/themes/hydrogen> (accessed Jun. 14, 2022).
- [117] Federal Ministry for Economics Affairs and Climate Action, “Declaration of Intent signed to establish German-Australian hydrogen alliance,” 2021. <https://www.bmwk.de/Redaktion/EN/Pressemitteilungen/2021/06/20210613-declaration-of-intent-signed-to-establish-german-australian-hydrogen-alliance.html> (accessed Jun. 12, 2022).
- [118] Energy Partnership Chile-Alemania, “Energy Partnership Chile-Alemania.” <https://www.energypartnership.cl/home/> (accessed Jun. 14, 2022).
- [119] Port of Rotterdam, “Import of hydrogen,” *Port of Rotterdam*. <https://www.portofrotterdam.com/en/port-future/energy-transition/ongoing-projects/hydrogen-rotterdam/import-of-hydrogen> (accessed Jun. 14, 2022).

- [120] Hamburg News, “Hamburg presents hydrogen import strategy,” *Hamburg News*, 2022. <https://hamburg-news.hamburg/en/innovation-science/hamburg-presents-hydrogen-import-strategy> (accessed Jun. 14, 2022).
- [121] République Française, *LOI n° 2015-992 du 17 août 2015 relative à la transition énergétique pour la croissance verte (1)*. 2015.
- [122] Ministère de la Transition Écologique et Solidaire, “Plan de déploiement de l’hydrogène pour la transition énergétique,” Ministère de la Transition Écologique et Solidaire, 2018. Accessed: Jul. 15, 2022. [Online]. Available: https://www.ecologie.gouv.fr/sites/default/files/Plan_deploiement_hydrogene.pdf
- [123] Ministère de l’Économie, des Finances et de la Souveraineté Industrielle et Numérique, “Présentation de la stratégie nationale pour le développement de l’hydrogène décarboné en France,” 2020. <https://www.economie.gouv.fr/presentation-strategie-nationale-developpement-hydrogene-decarbhone-france> (accessed Jul. 15, 2022).
- [124] Emmanuel Macron, “#France2030, objectif 2. Devenir le leader de l’hydrogène vert.,” *Twitter*, Oct. 12, 2021. <https://twitter.com/EmmanuelMacron/status/1447885273145266180> (accessed Jul. 15, 2022).
- [125] Ministerio para la Transición Ecológica y el Reto Demográfico, “Borrador del plan nacional integrado de energía y clima 2021-2030,” 2019. https://energy.ec.europa.eu/system/files/2019-02/spain_draftnecp_0.pdf (accessed Aug. 01, 2022).
- [126] Ministerio para la Transición Ecológica y el Reto Demográfico, “Hoja de ruta del hidrogeno,” 2020. https://energia.gob.es/es-es/Novedades/Documents/hoja_de_ruta_del_hidrogeno.pdf (accessed Aug. 01, 2022).
- [127] R. Strockl, “The Spanish Hydrogen Strategy,” *WFW*, Mar. 30, 2021. <https://www.wfw.com/articles/the-spanish-hydrogen-strategy/> (accessed Aug. 01, 2022).
- [128] Ministry of Climate and Environment, “The Norwegian Government’s hydrogen strategy,” *Government.no*, Jun. 03, 2020. <https://www.regjeringen.no/en/dokumenter/the-norwegian-governments-hydrogen-strategy/id2704860/> (accessed Aug. 01, 2022).
- [129] Northern Lights, “Northern Lights.” <https://norlights.com/what-we-do/> (accessed Aug. 01, 2022).
- [130] OPEC, “Algeria facts and figures.” https://www.opec.org/opec_web/en/about_us/146.htm (accessed Jun. 08, 2022).
- [131] Anna Ivanova, “Algeria’s energy min to devise hydrogen development strategy,” *Renewablesnow.com*, May 09, 2022. Accessed: Jun. 08, 2022. [Online]. Available: <https://renewablesnow.com/news/algerias-energy-min-to-devise-hydrogen-development-strategy-783843/>
- [132] GIZ, “Étude exploratoire sur le potentiel du Power-to-X (hydrogène vert) pour l’Algérie,” Deutsche Gesellschaft für Internationale Zusammenarbeit GmbH, 2021. Accessed: Jun. 08, 2022. [Online]. Available: https://www.energypartnership-algeria.org/fileadmin/user_upload/algeria/21_12_07_Hydrog%C3%A8ne_vert_en_Alg%C3%A9rie_-_Rapport_PE.pdf
- [133] ENI, “New agreement reached by SONATRACH and Eni to accelerate the development of gas projects and decarbonization via green hydrogen,” 2022. <https://www.eni.com/en-IT/media/press-release/2022/05/new-agreement-eni-sonatrach-gas-development-green-hydrogen-draghi-tebboune.html> (accessed Jun. 08, 2022).

- [134] H2 Bulletin, “Algeria’s Sonatrach and Eni to explore hydrogen production,” *H2 Bulletin*, Mar. 26, 2021. <https://www.h2bulletin.com/algerias-sonatrach-and-eni-to-explore-hydrogen-production/> (accessed Jun. 08, 2022).
- [135] Corporate Europe Observatory, “EU plans to import hydrogen from North Africa,” 2022. <https://corporateeurope.org/en/2022/05/eu-plans-import-hydrogen-north-africa> (accessed Jun. 08, 2022).
- [136] International Trade Administration, “Qatar – Hydrogen Supply Chain Opportunity in the Existing Liquefied Natural Gas (LNG) Economy.,” 2022. <https://www.trade.gov/market-intelligence/qatar-hydrogen-supply-chain-opportunity-existing-liquefied-natural-gas-lng> (accessed Jul. 19, 2022).
- [137] World Energy Council, “Working Paper - National Hydrogen Strategies,” 2021. https://www.worldenergy.org/assets/downloads/Working_Paper_-_National_Hydrogen_Strategies_-_September_2021.pdf (accessed Jul. 19, 2022).
- [138] S. Pekic, “Qatar and Germany to strengthen LNG and hydrogen cooperation,” *Offshore Energy*, May 23, 2022. <https://www.offshore-energy.biz/qatar-and-germany-to-strengthen-lng-and-hydrogen-cooperation/> (accessed Jul. 19, 2022).
- [139] Kingdom of Saudi Arabia, “Vision 2030.” <https://www.vision2030.gov.sa/> (accessed Jul. 19, 2022).
- [140] J. Nakano, “Saudi Arabia’s Hydrogen Industrial Strategy,” 2022. <https://www.csis.org/analysis/saudi-arabias-hydrogen-industrial-strategy> (accessed Jul. 19, 2022).
- [141] Reuters, “Saudi Arabia wants to be top supplier of hydrogen - energy minister,” 2021. <https://www.reuters.com/business/energy/saudi-arabia-wants-be-top-supplier-hydrogen-energy-minister-2021-10-24/> (accessed Jul. 19, 2022).
- [142] ACWA Power, “NEOM Green Hydrogen Project.” <https://www.acwapower.com/en/projects/neom-green-hydrogen-project/> (accessed Jul. 19, 2022).
- [143] Australian Government, “Australia’s National Hydrogen Strategy,” *Department of Industry, Science, Energy and Resources*, 2019. <https://www.industry.gov.au/data-and-publications/australias-national-hydrogen-strategy> (accessed Jun. 12, 2022).
- [144] S. Rees, P. Grubnik, L. Easton, and A. Feitz, “Australian Hydrogen Projects Dataset (March 2022).” Commonwealth of Australia (Geoscience Australia), 2022. doi: 10.26186/146425.
- [145] CSIRO, “HyResource,” *HyResource*. <https://research.csiro.au/hyresource/> (accessed Jun. 12, 2022).
- [146] bp, “Statistical Review of World Energy,” *bp global*, 2021. <https://www.bp.com/en/global/corporate/energy-economics/statistical-review-of-world-energy.html> (accessed Jun. 12, 2022).
- [147] Port of Rotterdam, “Tasmania and Port of Rotterdam Authority sign green hydrogen MOU,” *Port of Rotterdam*, 2021. <https://www.portofrotterdam.com/en/news-and-press-releases/tasmania-and-port-of-rotterdam-authority-sign-green-hydrogen-mou> (accessed Jun. 12, 2022).
- [148] Port of Rotterdam, “Western Australia and Port of Rotterdam to collaborate on renewable hydrogen,” *Port of Rotterdam*, 2021. <https://www.portofrotterdam.com/en/news-and-press-releases/western-australia-and-port-of-rotterdam-to-collaborate-on-renewable> (accessed Jun. 12, 2022).
- [149] Port of Rotterdam, “First exports of hydrogen from South Australia to Rotterdam feasible this decade,” *Port of Rotterdam*, 2021. <https://www.portofrotterdam.com/en/news-and-press-releases/first-exports-of-hydrogen-from-south-australia-to-rotterdam-feasible-this> (accessed Jun. 12, 2022).

- [150] E.On, “Fortescue Future Industries and E.ON Partner on journey to become europe’s largest green renewable hydrogen supplier and distributor,” 2022. <https://www.eon.com/en/about-us/media/press-release/2022/2022-03-29-fortescue-future-industries-and-eon-partnership.html> (accessed Jun. 12, 2022).
- [151] Ministerio de Energia, Gobierno de Chile, “National Green Hydrogen Strategy,” 2020. Accessed: Jun. 08, 2022. [Online]. Available: https://energia.gob.cl/sites/default/files/national_green_hydrogen_strategy_-_chile.pdf
- [152] CORFO, “Corfo adjudica propuestas de Hidrógeno Verde que atraerán inversiones por 1.000 millones de dólares,” *CORFO*, 2021. <https://www.corfo.cl> (accessed Jun. 08, 2022).
- [153] H. Liu and J. Ma, “A review of models and methods for hydrogen supply chain system planning,” *CSEE J. Power Energy Syst.*, pp. 1–12, 2020, doi: 10.17775/CSEEJPES.2020.02280.
- [154] W. Short, D. J. Packey, and T. Holt, “A manual for the economic evaluation of energy efficiency and renewable energy technologies,” National Renewable Energy Lab. (NREL), Golden, CO (United States), NREL/TP-462-5173, Mar. 1995. doi: 10.2172/35391.
- [155] K. Branker, M. J. M. Pathak, and J. M. Pearce, “A review of solar photovoltaic levelized cost of electricity,” *Renew. Sustain. Energy Rev.*, vol. 15, no. 9, pp. 4470–4482, Dec. 2011, doi: 10.1016/j.rser.2011.07.104.
- [156] Eurostat, “Electricity and heat statistics - Statistics Explained,” 2020. https://ec.europa.eu/eurostat/statistics-explained/index.php?title=Electricity_and_heat_statistics#Installed_electrical_capacity (accessed May 21, 2021).
- [157] European Central Bank, “Euro foreign exchange reference rates,” *European Central Bank*, Mar. 02, 2022. https://www.ecb.europa.eu/stats/policy_and_exchange_rates/euro_reference_exchange_rates/html/index.en.html (accessed Jun. 10, 2022).
- [158] Eurostat, “Harmonised Indices of Consumer Prices (HICP)” <https://ec.europa.eu/eurostat/web/hicp> (accessed Jun. 10, 2022).
- [159] J. Gräfström and R. Poudineh, “A critical assessment of learning curves for solar and wind power technologies,” *Oxford Institute for Energy Studies*, 2021. <https://www.oxfordenergy.org/publications/a-critical-assessment-of-learning-curves-for-solar-and-wind-power-technologies/> (accessed May 13, 2022).
- [160] A. Zauner, H. Böhm, D. Rosenfeld, R. Tichler, and S. Schirrmeister, “Analysis on future technology options and on techno-economic optimization,” Store&Go, Feb. 2019. Accessed: Apr. 01, 2022. [Online]. Available: https://www.storeandgo.info/fileadmin/downloads/deliverables_2019/20190801-STOREandGO-D7.7-EIL-Analysis_on_future_technology_options_and_on techno-economic_optimization.pdf
- [161] K. Schoots, F. Ferioli, G. J. Kramer, and B. C. C. van der Zwaan, “Learning curves for hydrogen production technology: An assessment of observed cost reductions,” *Int. J. Hydrog. Energy*, vol. 33, no. 11, pp. 2630–2645, Jun. 2008, doi: 10.1016/j.ijhydene.2008.03.011.
- [162] L. Bertuccioli, A. Chan, D. Hart, F. Lehner, B. Madden, and E. Standen, “Development of Water Electrolysis in the European Union,” 2014. <https://www.fch.europa.eu/node/783> (accessed Apr. 28, 2022).
- [163] Romiter Group, “100kg/h Stainless Steel Shell Electric Steam Boilers | Reliable Steam Boiler, Thermal Oil Heater Manufacture,” Jul. 14, 2014. <https://www.steam-generator.com/100kgh-stainless-steel-shell-electric-steam-boilers/> (accessed Jun. 01, 2022).

- [164] H. Böhm, S. Goers, and A. Zauner, “Estimating future costs of power-to-gas – a component-based approach for technological learning,” *Int. J. Hydrog. Energy*, vol. 44, no. 59, pp. 30789–30805, Nov. 2019, doi: 10.1016/j.ijhydene.2019.09.230.
- [165] G. Glenk and S. Reichelstein, “Economics of converting renewable power to hydrogen,” *Nat. Energy*, vol. 4, no. 3, Art. no. 3, Mar. 2019, doi: 10.1038/s41560-019-0326-1.
- [166] Guidehouse Insights, “Press Release | Global Capacity for Water Electrolysis Technologies Is Expected to Grow at a Compound Annual Growth Rate of 62% Through 2031,” 2022. <https://guidehouseinsights.com/news-and-views/global-capacity-for-water-electrolysis-technologies-is-expected-to-grow-at-a-compound-annual-growth?msclkid=8808ba3db66211ec8b7bac9ff9909db5> (accessed May 13, 2022).
- [167] International Energy Agency, “Global installed electrolyser capacity in 2020 and projects planned for commissioning, 2021-2026 – Charts – Data & Statistics,” *IEA*, 2021. <https://www.iea.org/data-and-statistics/charts/global-installed-electrolyser-capacity-in-2020-and-projects-planned-for-commissioning-2021-2026> (accessed Mar. 30, 2022).
- [168] European Commission and European Clean Hydrogen Alliance, “European Electrolyser Summit - Joint Declaration,” 2022. <https://ec.europa.eu/docsroom/documents/50014> (accessed Jun. 30, 2022).
- [169] Department for Business, Energy & Industrial Strategy, “Hydrogen production costs 2021,” p. 36, 2021.
- [170] E. Alvarado and A. C. Buitrago, “Prognosis of electricity price in Germany & France until 2030.,” KTH Royal Institute of Technology, 2022.
- [171] M. Ram, M. Child, A. Aghahosseini, D. Bogdanov, A. Lohrmann, and C. Breyer, “A comparative analysis of electricity generation costs from renewable, fossil fuel and nuclear sources in G20 countries for the period 2015-2030,” *J. Clean. Prod.*, vol. 199, pp. 687–704, Oct. 2018, doi: 10.1016/j.jclepro.2018.07.159.
- [172] IRENA, “Renewable Power Generation Costs in 2020,” */publications/2021/Jun/Renewable-Power-Costs-in-2020*, 2021. <https://www.irena.org/publications/2021/Jun/Renewable-Power-Costs-in-2020> (accessed Jun. 09, 2022).
- [173] J. Hernández-Moro and J. M. Martínez-Duart, “Analytical model for solar PV and CSP electricity costs: Present LCOE values and their future evolution,” *Renew. Sustain. Energy Rev.*, vol. 20, pp. 119–132, Apr. 2013, doi: 10.1016/j.rser.2012.11.082.
- [174] E. Williams, E. Hittinger, R. Carvalho, and R. Williams, “Wind power costs expected to decrease due to technological progress,” *Energy Policy*, vol. 106, pp. 427–435, Jul. 2017, doi: 10.1016/j.enpol.2017.03.032.
- [175] E. P. P. Soares-Ramos, L. de Oliveira-Assis, R. Sarrias-Mena, and L. M. Fernández-Ramírez, “Current status and future trends of offshore wind power in Europe,” *Energy*, vol. 202, p. 117787, Jul. 2020, doi: 10.1016/j.energy.2020.117787.
- [176] R. R. Beswick, A. M. Oliveira, and Y. Yan, “Does the Green Hydrogen Economy Have a Water Problem?,” *ACS Energy Lett.*, vol. 6, no. 9, pp. 3167–3169, Sep. 2021, doi: 10.1021/acsenergylett.1c01375.
- [177] Agora Energiewende and Frontier Economics, “The Future Cost of Electricity-Based Synthetic Fuels,” 2018. <https://www.agora-verkehrswende.de/en/publications/the-future-cost-of-electricity-based-synthetic-fuels/>, <https://www.agora-verkehrswende.de/en/publications/the-future-cost-of-electricity-based-synthetic-fuels/> (accessed May 14, 2022).
- [178] U. Caldera, D. Bogdanov, S. Afanasyeva, and C. Breyer, “Role of Seawater Desalination in the Management of an Integrated Water and 100% Renewable Energy Based Power Sector in Saudi Arabia,” *Water*, vol. 10, no. 1, Art. no. 1, Jan. 2018, doi: 10.3390/w10010003.

- [179] G. Maggio, G. Squadrito, and A. Nicita, “Hydrogen and medical oxygen by renewable energy based electrolysis: A green and economically viable route,” *Appl. Energy*, vol. 306, p. 117993, Jan. 2022, doi: 10.1016/j.apenergy.2021.117993.
- [180] A. O. Oni, K. Anaya, T. Giwa, G. Di Lullo, and A. Kumar, “Comparative assessment of blue hydrogen from steam methane reforming, autothermal reforming, and natural gas decomposition technologies for natural gas-producing regions,” *Energy Convers. Manag.*, vol. 254, p. 115245, Feb. 2022, doi: 10.1016/j.enconman.2022.115245.
- [181] B. Cotton, “Clean Hydrogen. Part 1: Hydrogen from Natural Gas Through Cost Effective CO₂ Capture,” *The Chemical Engineer*. <https://www.thechemicalengineer.com/features/clean-hydrogen-part-1-hydrogen-from-natural-gas-through-cost-effective-co2-capture/> (accessed Jun. 10, 2022).
- [182] Umwelt Bundesamt, *CO₂ Emission Factors for Fossil Fuels*. Umweltbundesamt, 2016. Accessed: May 15, 2022. [Online]. Available: <https://www.umweltbundesamt.de/publikationen/co2-emission-factors-for-fossil-fuels>
- [183] E. Smith, J. Morris, H. Kheshgi, G. Teletzke, H. Herzog, and S. Paltsev, “The cost of CO₂ transport and storage in global integrated assessment modeling,” *Int. J. Greenb. Gas Control*, vol. 109, p. 103367, Jul. 2021, doi: 10.1016/j.ijggc.2021.103367.
- [184] J. Jakobsen, S. Roussanaly, and R. Anantharaman, “A techno-economic case study of CO₂ capture, transport and storage chain from a cement plant in Norway,” *J. Clean. Prod.*, vol. 144, pp. 523–539, Feb. 2017, doi: 10.1016/j.jclepro.2016.12.120.
- [185] European Technology Platform for Zero Emission Fossil Fuel Power Plants, “The Costs of CO₂ Capture, Transport and Storage.” <https://www.globalccsinstitute.com/archive/hub/publications/17011/costs-co2-capture-transport-and-storage.pdf> (accessed Jun. 10, 2022).
- [186] T. Keipi, V. Hankalin, J. Nummelin, and R. Raiko, “Techno-economic analysis of four concepts for thermal decomposition of methane: Reduction of CO₂ emissions in natural gas combustion,” *Energy Convers. Manag.*, vol. 110, pp. 1–12, Feb. 2016, doi: 10.1016/j.enconman.2015.11.057.
- [187] Hubert JANNEL and Matthias TORQUET, “Deliverable 7.1-1 - Conceptual design of salt cavern and porous media underground storage site,” *Hystories*. <https://hystories.eu/publications-hystories/> (accessed Jul. 31, 2022).
- [188] A. Saraf, “Techno-economic Pricing model for Carbon Neutral Fuels as Seasonal Energy Storage,” KTH Royal Institute of Technology, 2021.
- [189] CoolProp, “Welcome to CoolProp — CoolProp 6.4.1 documentation.” <http://www.coolprop.org/index.html> (accessed Jul. 26, 2022).
- [190] I. H. Bell, J. Wronski, S. Quoilin, and V. Lemort, “Pure and Pseudo-pure Fluid Thermophysical Property Evaluation and the Open-Source Thermophysical Property Library CoolProp,” *Ind. Eng. Chem. Res.*, vol. 53, no. 6, pp. 2498–2508, Feb. 2014, doi: 10.1021/ie4033999.
- [191] Uniper, “Gas Storage Technology.” <https://www.uniper.energy/energy-storage-uniper/gas-storage-technology> (accessed Jul. 29, 2022).
- [192] W. A. Amos, “Costs of Storing and Transporting Hydrogen,” NREL/TP-570-25106, ON: DE00006574, 6574, Jan. 1999. doi: 10.2172/6574.
- [193] E. Tzimas, C. Filiou, S. D. Peteves, and J. B. Veyret, *Hydrogen storage: state-of-the-art and future perspective*. Netherlands: European Communities, 2003.

- [194] U.S. Department of Energy, “DOE Technical Targets for Hydrogen Delivery.” <https://www.energy.gov/eere/fuelcells/doe-technical-targets-hydrogen-delivery> (accessed Jul. 29, 2022).
- [195] A. M. Elberry, J. Thakur, A. Santasalo-Aarnio, and M. Larimi, “Large-scale compressed hydrogen storage as part of renewable electricity storage systems,” *Int. J. Hydrog. Energy*, vol. 46, no. 29, pp. 15671–15690, abril 2021, doi: 10.1016/j.ijhydene.2021.02.080.
- [196] S. Hawkins, “Technological Characterisation of Hydrogen Storage and Distribution Technologies,” p. 37, 2006.
- [197] J. B. Taylor, J. E. A. Alderson, K. M. Kalyanam, A. B. Lyle, and L. A. Phillips, “Technical and economic assessment of methods for the storage of large quantities of hydrogen,” *Int. J. Hydrog. Energy*, vol. 11, no. 1, pp. 5–22, Jan. 1986, doi: 10.1016/0360-3199(86)90104-7.
- [198] D. G. Caglayan *et al.*, “Technical potential of salt caverns for hydrogen storage in Europe,” *Int. J. Hydrog. Energy*, vol. 45, no. 11, pp. 6793–6805, Feb. 2020, doi: 10.1016/j.ijhydene.2019.12.161.
- [199] C. van Leeuwen and A. Zauner, “Innovative large-scale energy storage technologies and Power-to-Gas concepts after optimisation,” 2018. https://www.storeandgo.info/fileadmin/downloads/deliverables_2020/Update/20180424_STOREandGO_D8.3_RUG_accepted.pdf (accessed Jul. 26, 2022).
- [200] Engie, “H2 storage in salt caverns - Project HyPSTER in Étretz (FR),” 2021. <https://www.storengy.de/sites/default/files/mediateque/pdf/2021-11/HyPSTER%20EN.pdf> (accessed Jul. 29, 2022).
- [201] R. Folkson, *Alternative fuels and advanced vehicle technologies for improved environmental performance: Towards zero carbon transportation*. 2014, p. 760.
- [202] W. U. Notardonato, A. M. Swanger, J. E. Fesmire, K. M. Jumper, W. L. Johnson, and T. M. Tomsik, “Final test results for the ground operations demonstration unit for liquid hydrogen,” *Cryogenics*, vol. 88, pp. 147–155, Dec. 2017, doi: 10.1016/j.cryogenics.2017.10.008.
- [203] V. Pattabathula, N. Raghava, and D. Timbres, “Ammonia Storage Tanks,” *AmmoniaKnowHow*. <https://ammoniaknowhow.com/ammonia-storage-tanks/> (accessed Jul. 29, 2022).
- [204] R. E. Sanders, “9 - Accidents involving compressors, hoses, and pumps,” in *Chemical Process Safety (Fourth Edition)*, R. E. Sanders, Ed. Butterworth-Heinemann, 2015, pp. 235–267. doi: 10.1016/B978-0-12-801425-7.00009-1.
- [205] M. Stewart, “7 - Compressor fundamentals,” in *Surface Production Operations*, M. Stewart, Ed. Boston: Gulf Professional Publishing, 2019, pp. 457–525. doi: 10.1016/B978-0-12-809895-0.00007-7.
- [206] A. Lahnaoui, C. Wulf, H. Heinrichs, and D. Dalmazzone, “Optimizing hydrogen transportation system for mobility via compressed hydrogen trucks,” *Int. J. Hydrog. Energy*, vol. 44, no. 35, pp. 19302–19312, Jul. 2019, doi: 10.1016/j.ijhydene.2018.10.234.
- [207] U.S. Department of Energy, “H2A Hydrogen Delivery Infrastructure Analysis Models and Conventional Pathway Options Analysis Results - Interim Report,” *Energy.gov*, 2014. <https://www.energy.gov/eere/fuelcells/downloads/h2a-hydrogen-delivery-infrastructure-analysis-models-and-conventional> (accessed Jul. 30, 2022).
- [208] D. W. Green and R. H. Perry, *Perry’s Chemical Engineers’ Handbook, Eighth Edition*. McGraw-Hill Education, 2008. Accessed: Jul. 30, 2022. [Online]. Available: <https://www.accessengineeringlibrary.com/content/book/9780071422949>

- [209] M. Graf and O. Turkovska, “Costs and energy efficiency of long-distance hydrogen transport options,” 2021. <https://www.semanticscholar.org/paper/Costs-and-energy-efficiency-of-long-distance-Graf-Turkovska/f7390dd2726541274049ebfab4178ad64699514e> (accessed Jun. 10, 2022).
- [210] M. Aziz, “Liquid Hydrogen: A Review on Liquefaction, Storage, Transportation, and Safety,” *Energies*, vol. 14, no. 18, Art. no. 18, Jan. 2021, doi: 10.3390/en14185917.
- [211] D. Berstad, G. Skaugen, and Ø. Wilhelmsen, “Dissecting the exergy balance of a hydrogen liquefier: Analysis of a scaled-up claudie hydrogen liquefier with mixed refrigerant pre-cooling,” *Int. J. Hydrog. Energy*, vol. 46, no. 11, pp. 8014–8029, Feb. 2021, doi: 10.1016/j.ijhydene.2020.09.188.
- [212] U.S. Department of Energy, “Current status of hydrogen liquefaction costs,” 2019. Accessed: Jul. 30, 2022. [Online]. Available: https://www.hydrogen.energy.gov/pdfs/19001_hydrogen_liquefaction_costs.pdf
- [213] Air Liquide, “How is hydrogen stored?,” *Air Liquide Energies*, Jun. 16, 2017. <https://energies.airliquide.com/resources-planet-hydrogen/how-hydrogen-stored> (accessed Jul. 30, 2022).
- [214] J.-H. Yang, Y. Yoon, M. Ryu, S.-K. An, J. Shin, and C.-J. Lee, “Integrated hydrogen liquefaction process with steam methane reforming by using liquefied natural gas cooling system,” *Appl. Energy*, vol. 255, p. 113840, Dec. 2019, doi: 10.1016/j.apenergy.2019.113840.
- [215] J. Stang and P. Neksa, “Development of large-scale hydrogen liquefaction processes from 1898 to 2009,” *Int. J. Hydrog. Energy - INT J Hydrog. ENERGY*, vol. 35, pp. 4524–4533, May 2010, doi: 10.1016/j.ijhydene.2010.02.109.
- [216] S. Faramarzi, S. M. M. Nainiyan, M. Mafi, and R. Ghasemiasl, “A novel hydrogen liquefaction process based on LNG cold energy and mixed refrigerant cycle,” *Int. J. Refrig.*, vol. 131, pp. 263–274, Nov. 2021, doi: 10.1016/j.ijrefrig.2021.07.022.
- [217] S. Cho, J. Park, W. Noh, I. Lee, and I. Moon, “Developed hydrogen liquefaction process using liquefied natural gas cold energy: Design, energy optimization, and techno-economic feasibility,” *Int. J. Energy Res.*, vol. 45, no. 10, pp. 14745–14760, Aug. 2021, doi: 10.1002/er.6751.
- [218] K. K. Humphreys *et al.*, *Project and Cost Engineers’ Handbook*, 4^o edizione. Morgantown, W. Va.?: New York: CRC Press, 2004.
- [219] U. F. Cardella, “Large-scale hydrogen liquefaction,” p. 192, 2018.
- [220] International Energy Agency, “Technology Roadmap - Hydrogen and Fuel Cells,” *IEA*, 2015. <https://www.iea.org/reports/technology-roadmap-hydrogen-and-fuel-cells> (accessed Jul. 30, 2022).
- [221] M. Reuß, T. Grube, M. Robinius, and D. Stolten, “A hydrogen supply chain with spatial resolution: Comparative analysis of infrastructure technologies in Germany,” *Appl. Energy*, vol. 247, pp. 438–453, Aug. 2019, doi: 10.1016/j.apenergy.2019.04.064.
- [222] Britannica, “Haber-Bosch process | Definition, Conditions, Importance, & Facts.” <https://www.britannica.com/technology/Haber-Bosch-process> (accessed Jul. 30, 2022).
- [223] K. H. R. Rouwenhorst *et al.*, “Chapter 13 - Future Trends,” in *Techno-Economic Challenges of Green Ammonia as an Energy Vector*, A. Valera-Medina and R. Banares-Alcantara, Eds. Academic Press, 2021, pp. 303–319. doi: 10.1016/B978-0-12-820560-0.00013-8.
- [224] S. Giddey, S. P. S. Badwal, C. Munnings, and M. Dolan, “Ammonia as a Renewable Energy Transportation Media,” *ACS Publications*, Oct. 10, 2017. <https://pubs.acs.org/doi/pdf/10.1021/acssuschemeng.7b02219> (accessed Jul. 30, 2022).

- [225] M. B. Hocking, “11 - Ammonia, Nitric Acid and Their Derivatives,” in *Handbook of Chemical Technology and Pollution Control (Third Edition)*, M. B. Hocking, Ed. San Diego: Academic Press, 2005, pp. 321–364. doi: 10.1016/B978-012088796-5/50014-4.
- [226] J. R. Bartels, “A feasibility study of implementing an Ammonia Economy,” Master of Science, Iowa State University, Digital Repository, Ames, 2008. doi: 10.31274/etd-180810-1374.
- [227] C. Arnaiz del Pozo and S. Cloete, “Techno-economic assessment of blue and green ammonia as energy carriers in a low-carbon future,” *Energy Convers. Manag.*, vol. 255, p. 115312, Mar. 2022, doi: 10.1016/j.enconman.2022.115312.
- [228] D. Cheddie, “Ammonia as a Hydrogen Source for Fuel Cells: A Review,” IntechOpen, 2012. Accessed: Jul. 30, 2022. [Online]. Available: <https://www.intechopen.com/chapters/40233>
- [229] M. H. Hasan, T. Mahlia, Md. M. Rahman, I. M. Rizwanul Fattah, F. Handayani, and H. C. Ong, “A Comprehensive Review on the Recent Development of Ammonia as a Renewable Energy Carrier,” *Energies*, vol. 14, p. 3732, Jun. 2021, doi: 10.3390/en14133732.
- [230] J. G. Speight, “Chapter 15 - Hydrogen Production,” in *Heavy Oil Recovery and Upgrading*, J. G. Speight, Ed. Gulf Professional Publishing, 2019, pp. 657–697. doi: 10.1016/B978-0-12-813025-4.00015-5.
- [231] ENTSOG, “Transmission capacity and system development maps,” 2021. <https://www.entsog.eu/maps#transmission-capacity-map-2021> (accessed May 16, 2022).
- [232] Google, “Google Earth 9.159.0.0.” <https://earth.google.com/web/@0,0,0a,22251752.77375655d,35y,0h,0t,0r> (accessed May 16, 2022).
- [233] S. Bertoli, M. Goujon, and O. Santoni, “The CERDI-seadistance database,” Mar. 2016. Accessed: May 16, 2022. [Online]. Available: <https://halshs.archives-ouvertes.fr/halshs-01288748>
- [234] Searoutes, “Classic searoutes.” <https://classic.searoutes.com> (accessed May 16, 2022).
- [235] R. van Gerwen, M. Eijgelaar, and T. Bosma, “Hydrogen in the electricity value chain,” DNV GL, 2019. Accessed: Mar. 17, 2022. [Online]. Available: <https://www.dnv.com/Publications/hydrogen-in-the-electricity-value-chain-142956>
- [236] Z. Wan, Y. Tao, J. Shao, Y. Zhang, and H. You, “Ammonia as an effective hydrogen carrier and a clean fuel for solid oxide fuel cells,” *Energy Convers. Manag.*, vol. 228, p. 113729, Jan. 2021, doi: 10.1016/j.enconman.2020.113729.
- [237] TNO and smartport.nl, “Power-2-Fuel Cost Analysis,” 2020. Accessed: May 24, 2022. [Online]. Available: https://smartport.nl/wp-content/uploads/2020/09/Cost-Analysis-Power-2-Fuel_def_2020.pdf
- [238] Mahytec, “Datasheet - TANK, 500bar from 160L to 300L - High-pressure hydrogen storage,” 2021. https://www.mahytec.com/wp-content/uploads/2021/07/CL-DS7-Data-Sheet_500bar-EN.pdf (accessed Jun. 29, 2022).
- [239] Total Energies, “Prix de l’électricité : différences entre renouvelable et thermique,” *TotalEnergies*, 2018. <https://www.totalenergies.fr/particuliers/parlons-energie/dossiers-energie/comprendre-le-marche-de-l-energie/prix-de-l-electricite-differences-entre-renouvelable-et-thermique> (accessed Jun. 07, 2022).
- [240] HyPSTER, “HyPSTER | 1st demonstrator for H2 green storage.” <https://hypster-project.eu/> (accessed Jul. 26, 2022).

- [241] A. Reveillere and G. Hevin, “Future roles of Hydrogen in the energy transition and examples of operating and future Hydrogen storages,” p. 27, 2019.
- [242] Fraunhofer ISE, “Levelized Cost of Electricity - Renewable Energy Technologies,” *Fraunhofer Institute for Solar Energy Systems ISE*, 2021. <https://www.ise.fraunhofer.de/en/publications/studies/cost-of-electricity.html> (accessed Jun. 09, 2022).
- [243] Hans Böhm, Andreas Zauner, Sebastian Goers, Robert Tichler, and Pieter Kroon, “Deliverable 7.5 Innovative large-scale energy storage technologies and Power-to-Gas concepts after optimization, Report on experience curves and economies of scale, 2018,” *STORE&GO*. <https://www.storeandgo.info/publications/deliverables/> (accessed Jul. 30, 2022).
- [244] NREL, “StoreFAST: Storage Financial Analysis Scenario Tool.” <https://www.nrel.gov/storage/storefast.html> (accessed Jul. 30, 2022).
- [245] A. I. Gonzalez, T. Huld, F. Careri, F. Monforti-Ferrario, and A. Zucker, “EMHIRES dataset: Part II: Solar Power Generation: European Meteorological derived HIGH resolution RES generation time series for present and futures scenarios: Part II: PV generation using the PVGIS model,” *JRC Publications Repository*, May 24, 2017. <https://publications.jrc.ec.europa.eu/repository/handle/JRC106897> (accessed Jun. 09, 2022).
- [246] F. Dalla Longa *et al.*, “Wind potentials for EU and neighbouring countries: Input datasets for the JRC-EU-TIMES Model,” *JRC Publications Repository*, Mar. 26, 2018. <https://publications.jrc.ec.europa.eu/repository/handle/JRC109698> (accessed Jun. 09, 2022).
- [247] I. Staffell and S. Pfenninger, “Renewables.ninja,” *Renewables.ninja*. <https://www.renewables.ninja/> (accessed Jun. 09, 2022).
- [248] I. Staffell and S. Pfenninger, “Using bias-corrected reanalysis to simulate current and future wind power output,” *Energy*, vol. 114, pp. 1224–1239, Nov. 2016, doi: 10.1016/j.energy.2016.08.068.
- [249] S. Pfenninger and I. Staffell, “Long-term patterns of European PV output using 30 years of validated hourly reanalysis and satellite data,” *Energy*, vol. 114, pp. 1251–1265, Nov. 2016, doi: 10.1016/j.energy.2016.08.060.
- [250] International Energy Agency, “Macro drivers – World Energy Model – Analysis,” *IEA*. <https://www.iea.org/reports/world-energy-model/macro-drivers> (accessed Jun. 09, 2022).
- [251] Ship & Bunker, “Global 20 Ports Average Bunker Prices,” *Ship & Bunker*, 2022. <https://shipandbunker.com/prices/av/global/av-g20-global-20-ports-average> (accessed Jun. 09, 2022).
- [252] European Commission, “Weekly Oil Bulletin.” https://energy.ec.europa.eu/data-and-analysis/weekly-oil-bulletin_en (accessed Jun. 09, 2022).
- [253] H. Barthélémy, “Hydrogen storage – Industrial perspectives,” *Int. J. Hydrog. Energy*, vol. 37, no. 22, pp. 17364–17372, Nov. 2012, doi: 10.1016/j.ijhydene.2012.04.121.
- [254] Office of Energy Efficiency and Renewable Energy, “Hydrogen Tube Trailers,” *Energy.gov*. <https://www.energy.gov/eere/fuelcells/hydrogen-tube-trailers> (accessed Jul. 31, 2022).
- [255] Statista, “Europe: countries by area,” *Statista*, 2021. <https://www.statista.com/statistics/1277259/countries-europe-area/> (accessed Jun. 10, 2022).
- [256] International Energy Agency and Nuclear Energy Agency, “Projected Costs of Generating Electricity 2020 – Analysis,” *IEA*, 2020. <https://www.iea.org/reports/projected-costs-of-generating-electricity-2020> (accessed Jun. 10, 2022).

- [257] H. Böhm, A. Zauner, S. Goers, R. Tichler, and P. Kroon, “Report on experience curves and economies of scale,” Store&Go, Oct. 2018. Accessed: May 29, 2022. [Online]. Available: https://www.storeandgo.info/fileadmin/downloads/deliverables_2019/20190801-STOREandGO-D7.5-EIL-Report_on_experience_curves_and_economies_of_scale.pdf
- [258] Lazard, “Lazard’s Levelized Cost of Hydrogen analysis,” 2021. Accessed: Feb. 14, 2022. [Online]. Available: <https://www.lazard.com/media/451779/lazards-levelized-cost-of-hydrogen-analysis-vf.pdf>
- [259] BloombergNEF and The Business Council for Sustainable Energy, “2022 Sustainable Energy in America Factbook,” *BCSE*, 2022. <https://bcse.org/factbook/> (accessed Jul. 19, 2022).
- [260] Hinicio and Ludwig Bölkow Systemtechnik, “Power-to-gas. Short term and long term opportunities to leverage synergies between the electricity and transport sectors through power-to-hydrogen.,” 2016.
- [261] Enea Consulting, “The potential of power-to-gas,” 2016. <https://www.enea-consulting.com/en/publication/the-potential-of-power-to-gas/> (accessed Jul. 19, 2022).
- [262] J. L. L. C. C. Janssen, M. Weeda, R. J. Detz, and B. van der Zwaan, “Country-specific cost projections for renewable hydrogen production through off-grid electricity systems,” *Appl. Energy*, vol. 309, p. 118398, Mar. 2022, doi: 10.1016/j.apenergy.2021.118398.
- [263] E. Vartiainen *et al.*, “True Cost of Solar Hydrogen,” *Sol. RRL*, vol. 6, no. 5, p. 2100487, 2022, doi: 10.1002/solr.202100487.
- [264] Navigant, “Gas for Climate. The optimal role for gas in a net-zero emissions energy system,” 2019. Accessed: Jun. 15, 2022. [Online]. Available: <https://gasforclimate2050.eu/publications/>
- [265] F. I. Gallardo, A. Monforti Ferrario, M. Lamagna, E. Bocci, D. Astiaso Garcia, and T. E. Baeza-Jeria, “A Techno-Economic Analysis of solar hydrogen production by electrolysis in the north of Chile and the case of exportation from Atacama Desert to Japan,” *Int. J. Hydrog. Energy*, vol. 46, no. 26, pp. 13709–13728, Apr. 2021, doi: 10.1016/j.ijhydene.2020.07.050.
- [266] M. H. A. Khan *et al.*, “Designing optimal integrated electricity supply configurations for renewable hydrogen generation in Australia,” *iScience*, vol. 24, no. 6, Jun. 2021, doi: 10.1016/j.isci.2021.102539.

Appendix

Appendix I

RE locations and capacity factor

Table 60: RE locations and corresponding capacity factors.

Country	Location	Coordinates	RES	CF	Ref.
Germany	country average	-	Solar PV	10.2 %	[245]
			Onshore wind	44.0 %	[246]
			Offshore wind	24.0 %	
France	country average	-	Solar PV	13.4 %	[245]
			Onshore wind	42.0 %	[246]
			Offshore wind	27.0 %	[246]
Spain	country average	-	Solar PV	17.5 %	[245]
			Onshore wind	31.0 %	[246]
			Offshore wind	26.0 %	
Algeria	country average	-	Solar PV	21.0 %	[132]
			Onshore wind	30.0 %	
Saudi Arabia	Neom	28.15°, 34.75°	Solar PV	22.2 %	
			Onshore wind	35.6 %	
Australia	Western Australia	-27.65°, 114.24°	Solar PV	21.0 %	[247]–
			Onshore wind	46.3 %	[249]
Chile	Atacama Desert	-22.05°, -69.08°	Solar PV	25.2 %	
	Magallanes region	-52.48°, -70.94°	Onshore wind	63.0 %	

Appendix II

Graphical description of the Excel tool

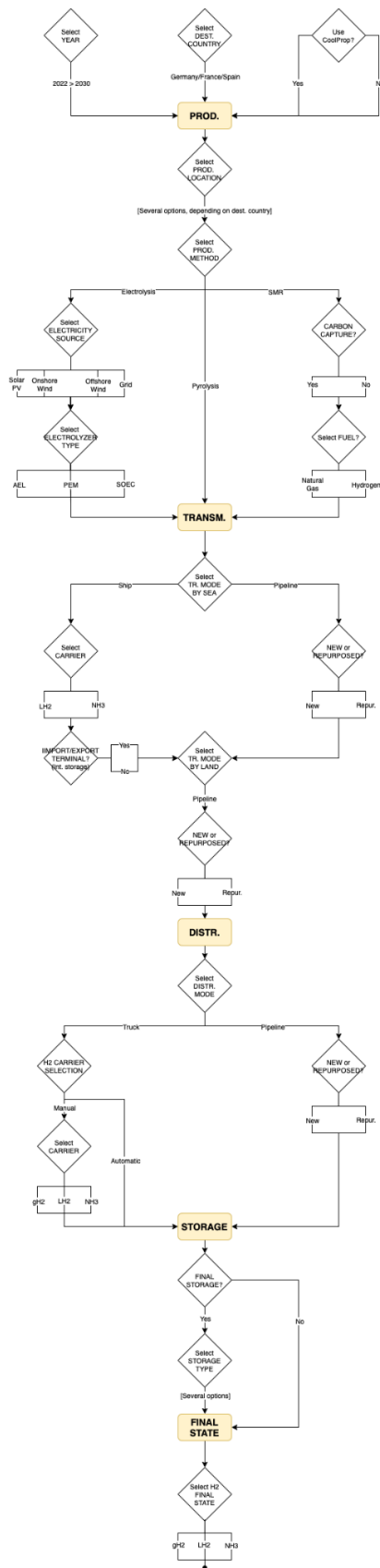


Figure 84: Graphical description of the Excel tool.

Appendix III

Commodity prices

Table 61: Projection of commodity prices until 2030.

Reference	[170]		Based on calculations from industrial partner. See Appendix IV for detailed methodology.				[250] AP scenario, advanced economies	Own assumption, based on [251]	Own assumption, based on [252]
Unit	[€/MWh _{el}]		[€/MWh _{ng,HHV}]				[€/tCO ₂]	[€/G]	[€/L]
Commodity	Electricity		Gas ²⁹	Gas (upstream costs)			CO ₂	HFO	Diesel
Country	Germany	France	Europe	Algeria	Norway	Qatar	Europe+Norway	Global	Global
2022	139	219	91.75	3.0	8.0	4.0	80.0	10.11	1.30
2023	139	219	74.43				82.7		
2024	118	176	56.80				85.4		
2025	106	148	44.40				88.1		
2026	97	108	32.93				90.7		
2027	97	99	20.53				93.4		
2028	99	98	28.68				96.1		
2029	103	96	28.45				98.8		
2030	107	95	28.25				101.5		
Long term	107	95	28.25				169.1		

In some cases (e.g., cash flow analysis), a commodity price is needed also beyond 2030. Given the high uncertainty, it is assumed that the value remains constant after 2030, unless stated otherwise.

²⁹ Retail price for large consumers

Appendix IV

Estimates for gas well upstream cost

Dr. Antonius Kies, 2022-08-05

To calculate the production cost of so-called "blue hydrogen" ³⁰ in potential export countries close to the coal mines, oil fields or gas fields, the upstream cost needs to be known. For this thesis fossil natural gas was chosen as example. The upstream costs are the sum of all capital and operational expenditures to find, develop, produce from and disassemble a gas field and its wells. The gas transport from the field, the companies' net income and the state's corporate and export taxes are by definition not included in the upstream cost.

1.1) Results

- Estimates for gas well upstream cost 2025 and later, for selected gas exporting countries.
- Lowest cost around 3 €₂₀₂₁/MWh_{HHV} for conventional onshore gas wells, here in Algeria.
- Highest cost. of ca. 12 €₂₀₂₁/MWh_{HHV} for deep water offshore wells, here in Mozambique.

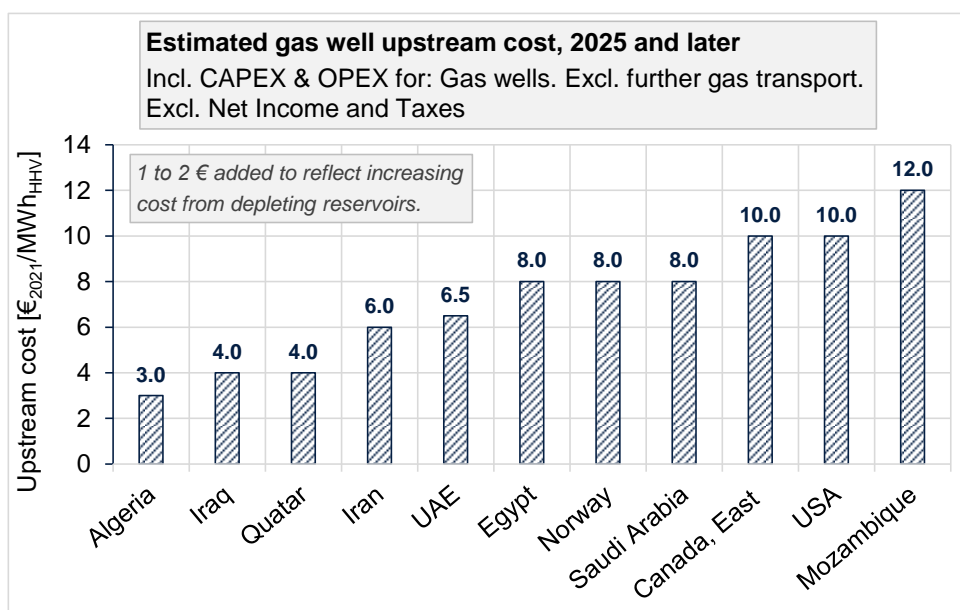


Figure 1: Gas well upstream cost, 2025 and later. For selected gas exporting countries.

³⁰ Hydrogen from fossil hydrocarbons with Carbon Capture and Storage (CCS).

Blue hydrogen can be produced from coal, crude oil and natural gas with multiple processes, e. g. steam reforming, autothermal reforming, partial oxidation, pyrolysis or gasification. The same processes are also applicable for biogenic solid, liquid or gaseous hydrocarbons like e. g. woodchips, vegetable oil or biomethane.

1.2) Definition of upstream cost

The upstream costs of a gas field are the Total Delivered Cost ³¹ for gas coming out of the wells. If a plant for blue hydrogen production would be built directly besides the gas field, the upstream cost plus short pipelines would be the feedstock cost for the hydrogen plant. Upstream costs are also called "Wellhead Breakeven" or "Full cycle breakeven" price or cost, and the split is shown in Table 1.

Table 1. Split of upstream cost (full cycle) for gas and oil wells [Kleinberg 2017, p. 73]

Full Cycle	Half Cycle	Lifting Cost	Operating Expense	Finding	Exploration Leasing Reservoir Delineation
				Development	Financing of Field Dev Engineering Regional Pipelines Roads & Infrastructure
	Financing of Well Dev Well Pad Construction Local Pipelines Well Construction <ul style="list-style-type: none"> ● Drill, Case, Cement ● Complete Reservoir Mgmt CAPEX <ul style="list-style-type: none"> ● Secondary Recovery ● Tertiary Recovery Workovers Refracture Decommissioning <ul style="list-style-type: none"> ● Plug & Abandon ● Site Restoration 				
Production	Lease Operating Expense <ul style="list-style-type: none"> ● Repair & Maintain ● Fuels & Power ● Labor Reservoir Mgmt OPEX <ul style="list-style-type: none"> ● Secondary Recovery ● Tertiary Recovery Royalties & Taxes Transport to Market Water & Waste Disposal General & Administrative				

In the same reference a comprehensive description of the cost components for gas and oil wells is given [Kleinberg 2017, p. 72-74].

³¹ **CAPEX.** Capital Expenditure to get the infrastructure in place: (Exploration cost to find the resources +) Planning cost & fees + Overnight cost to build all infrastructure + Other initial investment + Interest during construction period + Interest during depreciation period + Reserve fund for disassembly

OPEX. Operational Expenditure to produce something with the available infrastructure and deliver it: Raw material + Semi-finished products + Fuel cost + Labour cost + Rental & leasing cost + Repair & Maintenance (R&M) + Selling, General & Administrative Expense (SG&A) + Other backoffice + Other fix OPEX + Other variable OPEX + Transport cost + Waste disposal cost + Emission cost + Fees & Royalties.

OPEX is also called Short Run Marginal Cost (SRMC).

TDC. Total Delivered Cost: All CAPEX + All OPEX, to deliver a product to the customer.

TDC is also called Long Run Marginal Cost (LRMC).

Note: The entrepreneur's net income and the government's taxes are by definition not included in TDC.

It is: TDC + Net income + Taxes = Price.

1.3) Upstream cost for selected gas exporting countries

From literature the upstream cost for selected gas exporting countries were collected and converted to $\text{€}_{2021}/\text{MWh}_{\text{HHV}}$, i. e. referred to the gas' higher heating value. A security margin of 1 to 2 € was added to the found numbers, to reflect the increasing upstream cost with decreasing field productivity. The correction for inflation is shown in the data section 1.4), the diagram with the results above in Figure 1, and the list with the results and notes to the gas production conditions here in Table 2:

Table 2. Gas well upstream cost, 2025 and later. For selected gas exporting countries

Country	Upstream Costs	Gas well type	Reference
	$\text{€}_{2021}/\text{MWh}_{\text{HHV}}$	-	-
Algeria	3.0	Onshore, conventional gas. Depleting gas fields.	Möst 2009, p. 1514 Aissaoui 2013, p. 4
Canada, East	10.0	Onshore, shale gas, hydraulic fracturing	CERI 2018, p. 37
Egypt	8.0	Offshore, conventional gas	Ramboll 2017, p. 79
Iran	6.0	Offshore, conventional gas, shallow water (South Pars, to be developed)	Ramboll 2017, p. 79
Iraq	4.0	Onshore, conventional gas	Ramboll 2017, p. 79
Mozambique	12.0	Offshore, conventional gas, deep water	Timera 2017 USAID 2018, p. 68
Norway	8.0	Offshore, conventional gas, shallow water. Depleting gas fields.	Lochner 2009, p. 1524 Möst 2009, p. 1514 Betzuege 2010, p. 15
Quatar	4.0	Offshore, conventional gas, shallow water (North Field, already developed)	Ramboll 2017, p. 79 IEA 2017, p. 381 Qamar 2020, p. 6
Saudi Arabia	8.0	Onshore, shale gas, hydraulic fracturing	Ramboll 2017, p. 79
United Arab Emirates	6.5	Offshore, conventional gas, shallow water	Qamar 2020, p. 6 Timera 2017
USA	10.0	Onshore, shale gas, hydraulic fracturing	Cornot 2016, p. 29 IEA 2017, p. 373 Timera 2017

The upstream cost were found to be lowest at 3 $\text{€}_{2021}/\text{MWh}_{\text{HHV}}$ for onshore conventional gas wells (Algeria) to highest with 12 $\text{€}_{2021}/\text{MWh}_{\text{HHV}}$ for offshore conventional wells in deep water (Mozambique).

1.4) Supporting data

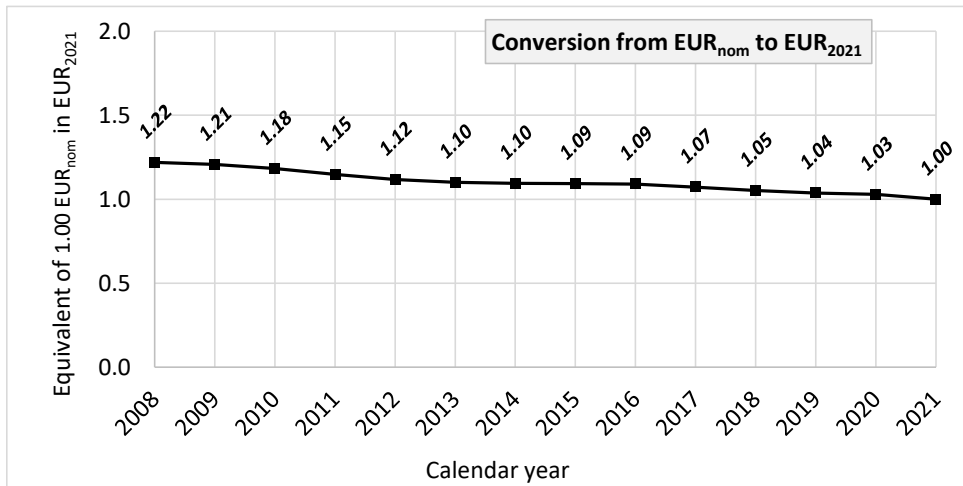


Figure 2. Correction for inflation: European Economic Area [Eurostat 220719]

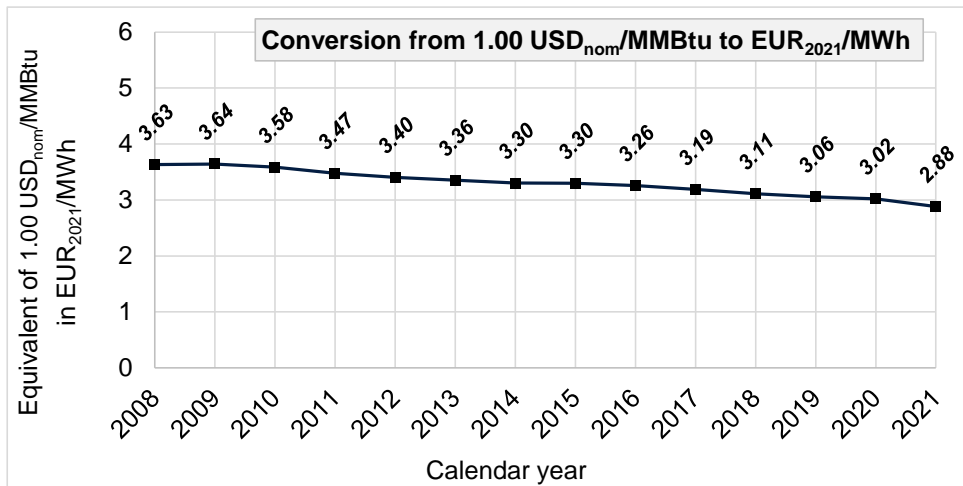


Figure 3. Correction for inflation: USA. [BLS 220711] [ECB 220728]

$$1 \text{ M M Btu} = 1'000 * 1'000 * 1'055 \text{ J}_{\text{HHV}} = 1.055 \text{ GJ}_{\text{HHV}} = 0.2931 \text{ MWh}_{\text{HHV}}$$

$$1 \text{ EUR}_{2021} = 1.183 \text{ USD}_{2021}$$

1.5) Abbreviations

CAPEX : Capital Expenditure

CCS : Carbon Capture and Storage

HHV : Higher Heating Value. Also called Gross Calorific Value

MMBtu : Million British Thermal Units, 1.055 GJ.

MWh : Mega Watt Hour, 3.6 GJ.

OPEX : Operational Expenditure

R&M : Repair & Maintenance

TDC : Total Delivered Cost. All CAPEX + OPEX to produce and deliver a product to a customer.

1.6) References

Aissaoui 2013. Algeria's Natural Gas Policy. APICORP Research, Economic Commentary, vol. 8, no. 7. Dammam: Arab Petroleum Investments Corporation, 2013-07.

<https://web.archive.org/web/20191105051036/http://www.apicorp-arabia.com/2013-economic-commentary>

Betzuege 2010. Model-based Analysis of Infrastructure Projects and Market Integration in Europe with Special Focus on Security of Supply Scenarios. Köln: Energiewirtschaftliches Institut, 2010-06-14.

<https://www.ceer.eu/documents/104400/-/-/2e03b430-3d68-5381-e875-fb34e04e9a34>

BLS 220711. Historical CPI-U, April 2022. Washington: U.S. Bureau of Labor Statistics, 2022-07-11.

<https://www.bls.gov/cpi/tables/supplemental-files/home.htm>, <https://www.bls.gov/cpi/tables/supplemental-files/historical-cpi-u-202206.pdf>. CPI-U: Consumer Price Index for All Urban Consumers

CERI 2018. Competitive Analysis of Canadian LNG. Study no. 172. Calgary: Canadian Energy Research Institute, 2018-07-17. <https://ceri.ca/studies/competitive-analysis-of-canadian-lng>

Cornot 2016. The US Natural Gas Exports. Paris: Institut Français des Relations Internationales (IFRI), 2016-06-30. ISBN 9782365676243. <https://www.ifri.org/en/publications/notes-de-lifri/us-natural-gas-exports-new-rules-european-gas-landscape>

ECB 220728. Euro foreign exchange reference rates / US dollar (USD). Frankfurt: European Central Bank, 2022-07-28. https://www.ecb.europa.eu/stats/policy_and_exchange_rates/euro_reference_exchange_rates/html/eurofxref-graph-usd.en.html.

EIA 2022. Natural Gas Gross Withdrawals and Production. Washington: U.S. Energy Information Administration, 2022-07-29. https://www.eia.gov/dnav/ng/ng_prod_sum_a_EPG0_FGW_mmcf_a.htm

Eurostat 220719. Harmonised index of consumer prices (HICP) / European Economic Area. Luxembourg: Eurostat 2022-07-19. https://ec.europa.eu/eurostat/databrowser/view/PRC_HICP_MIDX/default/table

IEA 2017. World Energy Outlook 2017. Paris: IEA, 2017-10. <https://iea.org/weo>

Note to p. 373: From 2016 to 2021, the accumulated US gas production ("gross withdrawals") was 6.4 tcm [EIA 2022].

Kleinberg 2017. Tight oil market dynamics: Benchmarks, breakeven points, and inelasticities. Energy Economics, vol. 70, pp. 70-83. ISSN 0140-9883. Amsterdam: Elsevier, 2017-11. <https://doi.org/10.1016/j.eneco.2017.11.018>

Lochner 2009. The development of natural gas supply costs to Europe. Energy Policy, vol. 37, iss. 4, pp. 1518–1528. ISSN 0301-4215. Amsterdam: Elsevier, 2009-01. <https://doi.org/10.1016/j.enpol.2008.12.012>

Möst 2009. Prospects of gas supply until 2020 in Europe and its relevance for the power sector in the context of emission trading. Energy, vol. 34, iss. 10, pp. 1510-1522. ISSN 0360-5442. Amsterdam: Elsevier, 2009-07. <https://doi.org/10.1016/j.energy.2009.06.045>

Qamar 2020. Hydrogen in the GCC. Dubai: Qamar Energy, 2020-11.

<https://www.rvo.nl/sites/default/files/2020/12/Hydrogen%20in%20the%20GCC.pdf>

Ramboll 2017. Pan Arab Regional Energy Trade. København: Ramboll, 2017-09.

<https://ppiaf.org/documents/5485/download>

Timera 2017. Where will the next wave of LNG supply come from? London: Timera Energy, 2017-10-30.

<https://timera-energy.com/where-will-the-next-wave-of-lng-supply-come-from/>

USAID 2018. Power Africa. Gas Roadmap for Southern Africa. Washington: US Agency for International Development, 2018-08-10. <https://www.usaid.gov/documents/1860/power-africa-gas-roadmap-southern-africa>

Appendix V

Geological storage, economic parameters

Table 62: Economic parameters for each type of geological reservoir.

Type of geological storage	Country	Cost base [M€]	Ref.	Size base [m ³]	Ref.	Pressure base geo. storage reservoir [bar]	Ref.	s.f.	Ref.	cush. gas%	Ref.
Geological - Depleted NG or Oil Reservoir	Germany	28.61 ; 375	[79]; [74, p. 1]	500000 ; 32797585	[79]; [74, p. 1]	N/D	[79]	1; 0.48	[192]; same as salt cavern	50%-60%; (Avg. 55%)	[73]
	France	28.61 ; 375	[79]; [74, p. 1]	500000 ; 32797585	[79]; [74, p. 1]	N/D	[79]	1; 0.48	[192]; same as salt cavern	50%-60%; (Avg. 55%)	[73]
	Spain	28.61 ; 375	[79]; [74, p. 1]	500000 ; 32797585	[79]; [74, p. 1]	N/D	[79]	1; 0.48	[192]; same as salt cavern	50%-60%; (Avg. 55%)	[73]
Geological – Salt Cavern	Germany	28.1; 81; (Avg. 54.55)	[74]; [49]	500000	[74]; [49]	60-180; (Avg. 120)	[74]	1; 0.48 ; 0.28	[192]; [244]; [188]	30%	[73]
	France	28.1; 81; (Avg. 54.55)	[74]; [49]	500000	[74]; [49]	60-180; (Avg. 120)	[74]	1; 0.48 ; 0.28	[192]; [244]; [188]	30%	[73]
	Spain	28.1; 81; (Avg. 54.55)	[74]; [49]	500000	[74]; [49]	60-180; (Avg. 120)	[74]	1; 0.48 ; 0.28	[192]; [244]; [188]	30%	[73]
Geological – Lined Rock Cavern	Germany	27 ; 173	[74]	40000 ; 320000	[74]	10-230; (Avg. 120)	[74]	1; 0.50; (Avg. 0.75)	[192]; [188]	18%; 18%; (Avg. 18%)	[74]
	France	27 ; 173	[74]	40000 ; 320000	[74]	10-230; (Avg. 120)	[74]	1; 0.50; (Avg. 0.75)	[192]; [188]	18%; 18%; (Avg. 18%)	[74]
	Spain	27 ; 173	[74]	40000 ; 320000	[74]	10-230; (Avg. 120)	[74]	1; 0.50; (Avg. 0.75)	[192]; [188]	18%; 18%; (Avg. 18%)	[74]
Geological Aquifer	Germany	-	-	-	-	-	-	1	[192]	50%;65%;80%; 50%; (Avg. 62%)	[74], [51], [73]
	France	-	-	-	-	-	-	1	[192]	50%;65%;80%; 50%; (Avg. 62%)	[74], [51], [73]
	Spain	-	-	-	-	-	-	1	[192]	50%;65%;80%; 50%; (Avg. 62%)	[74], [51], [73]

Note: The investment cost data for geological storage is only varying with the type of technology (not with the location). The model is built in such way that these values can be later updated when more data is available. The values in bold are the selected values introduced in the model. Due to lack of cost data for aquifers, this technology is intentionally left out from the present analysis. Aquifers are intentionally left out of the present analysis to enable a clear comparison between the technologies that are perceived to have the best technology development level for hydrogen storage.

The cushion gas percentage *cush. gas%* is equal to:

$$cush. gas\% = \frac{Cushion\ gas\ volume\ [m^3]}{Cushion\ gas\ volume\ [m^3] + Working\ gas\ volume\ [m^3]}$$

(163)

A more detailed calculation of the cost base investment for depleted NG or oil reservoirs is here reported:

Data:

$(LHV)_{H_2} = 33.33 \text{ kWh/kg}_{H_2}$

Cush. gas% (depleted NG reserv.) = 55%

Depleted gas field

Minimum Investment Cost (Min_{cost}): 280 EUR₂₀₁₉/MWh_{H₂ stored}

Maximum Investment Cost (Max_{cost}): 424 EUR₂₀₁₉/MWh_{H₂ stored}

Calculation:

$$\begin{cases} Min_{cost} = 280 \times \frac{33.33}{10^3} = 9.33 \text{ €/kg} \\ Max_{cost} = 424 \times \frac{33.33}{10^3} = 14.13 \text{ €/kg} \end{cases}$$

Considering an average size depleted gas reservoir with 500000 m³:

$$\begin{aligned} V_{total} &= V_{working \ gas} + V_{cush.gas} \Leftrightarrow \\ \Leftrightarrow 500000 \text{ [m}^3\text{]} &= V_{working \ gas} + 0.55 \times 500000 \text{ [m}^3\text{]} \Leftrightarrow \\ \Leftrightarrow V_{working \ gas} &= 225000 \text{ [m}^3\text{]} \end{aligned}$$

Hydrogen's density for the operating temperature and pressure of the depleted NG reservoir:

$$\begin{aligned} \rho(T = 35^\circ C, P = 150 \text{ bar}) &= 10.84 \text{ [kg/m}^3\text{]} \Leftrightarrow \\ \Leftrightarrow m &= 10.84 \times 225000 = 2439000 \text{ [kg]} \end{aligned}$$

Finally, it is possible to obtain the maximum and minimum CAPEX of the depleted gas field for a geometric volume of reservoir of 500000 m³:

$$\begin{cases} Min_{cost} = 2439000 \times 9.33 = 22.76 \text{ [M €]} \\ Max_{cost} = 2439000 \times 14.13 = 34.46 \text{ [M €]} \end{cases} \Rightarrow Avg_{cost} = 28.61 \text{ [M €]}$$

Appendix VI

Pressure and temperature for different applications

Table 63: Pressure and temperature for each type of applications.

Type of application	Inlet pressure [bar]	Ref.	Outlet pressure [bar]	Ref.	Inlet temperature [°C]	Ref.	
Compression of hydrogen to storage	Tank – Type I	<i>Dependent on the supply chain pathway chosen</i>	Considered pressure for hydrogen transportation by land	200-300; (Avg. 250)	[253]	25	[188]
	Tank – Type II	<i>Dependent on the supply chain pathway chosen</i>	Considered pressure for hydrogen transportation by land	250	Same as Type I	25	[188]
	Tank – Type III	<i>Dependent on the supply chain pathway chosen</i>	Considered pressure for hydrogen transportation by land	200-450; 700 (w/ some issues); (Avg. 325)	[253]	25	[188]
	Tank – Type IV	<i>Dependent on the supply chain pathway chosen</i>	Considered pressure for hydrogen transportation by land	200-1000; (Avg. 600)	[253]	25	[188]
	Geological - Depleted NG or Oil Reservoir	<i>Dependent on the supply chain pathway chosen</i>	Considered pressure for hydrogen transportation by land	15-285; (Avg. 150)	[62, p. 13]	35	[191]
	Geological – Salt Cavern	<i>Dependent on the supply chain pathway chosen</i>	Considered pressure for hydrogen transportation by land	35-210; (Avg. 122.5)	[62, p. 13]	35	[191]
	Geological – Lined Rock Cavern	<i>Dependent on the supply chain pathway chosen</i>	Considered pressure for hydrogen transportation by land	20-200; (Avg. 110)	[62, p. 13]	35	[191]
	Geological Aquifer	<i>Dependent on the supply chain pathway chosen</i>	Considered pressure for hydrogen transportation by land	30-315; (Avg. 172.5)	[62, p. 13]	35	[191]
Compression of hydrogen into trucks for transp.	Truck – 250 bar	<i>Dependent on the supply chain pathway chosen</i>	Linked in the model	250	[254]	32	[94]
Compression of hydrogen in pipeline	Pipeline inlet - transmission	<i>Dependent on the supply chain pathway chosen. Either equal to the pressure out of the production site or to the pressure required for transmission by sea</i>	Linked in the model	<i>Operating pressure at the inlet of the pipeline</i>	Linked in the model	32	[94]
	Pipeline inlet - distribution	<i>Dependent on the supply chain pathway chosen</i>	Linked in the model	<i>Operating pressure at the inlet of the pipeline</i>	Linked in the model	32	[94]
	Pipeline booster – transmission offshore	<i>Pressure in the pipeline after 700 km</i>	Linked in the model	<i>Operating pressure at the inlet of the pipeline</i>	Linked in the model	32	[94]
	Pipeline booster – transmission onshore	<i>Pressure in the pipeline after 700 km</i>	Linked in the model	<i>Operating pressure at the inlet of the pipeline</i>	Linked in the model	32	[94]
	Pipeline booster – distribution	<i>Pressure in the pipeline after 500 km</i>	Linked in the model	<i>Operating pressure at the inlet of the pipeline</i>	Linked in the model	32	[94]

Appendix VII

Transmission distances

Table 64: Transmission by ship, in km [233], [234].

Departure \ Arrival	Germany	France	Spain
Norway	605	1726	3151
Algeria	3174	864	449
Saudi Arabia	8294	3364	4805
Qatar	12830	8007	9408
Australia	18712	14354	15261
Chile	12512	14329	13258

Table 65: Transmission by offshore pipeline, in km [231], [232].

Departure \ Arrival	Germany	France	Spain
Norway	670	840	840
Algeria	155	210	210
Saudi Arabia	2000	-	-
Qatar	2000	-	-
Australia	-	-	-
Chile	-	-	-

Table 66: Transmission by onshore pipeline, in km [231], [232].

Departure \ Arrival	Germany	France	Spain
Norway	-	-	838
Algeria	2338	1350	547
Saudi Arabia	2140	-	-
Qatar	3940	-	-
Australia	-	-	-
Chile	-	-	-
Spain	1239	401	-

In the *Home* page of the tool, the user can select whether the arrival point is at the closest border/harbor or in the center of the country, with average distance from the border/harbor. The standard setting is the first option, therefore the values shown in Table 66 refer to the arrival border/harbor. If instead the user selects the second option, the tool automatically adds a section to the onshore pipeline. Its length is approximated to be equal to the radius of a circumference with the same area of the country, so it corresponds to 337 km for Germany, 419 km for France, and 401 km for Spain [255].

Appendix VIII

Comparison with literature data

Levelized cost of electricity (LCOE)

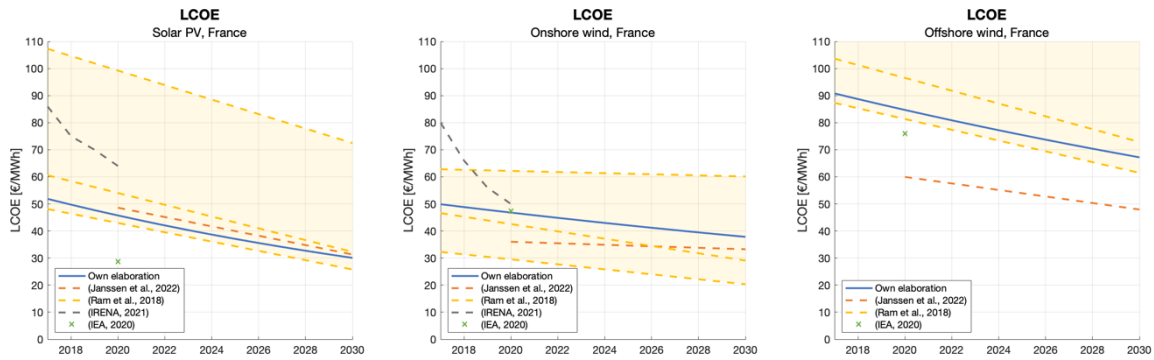


Figure 85: Comparison between own LCOE in France and values from the literature, for different RES [15], [171], [172], [256].

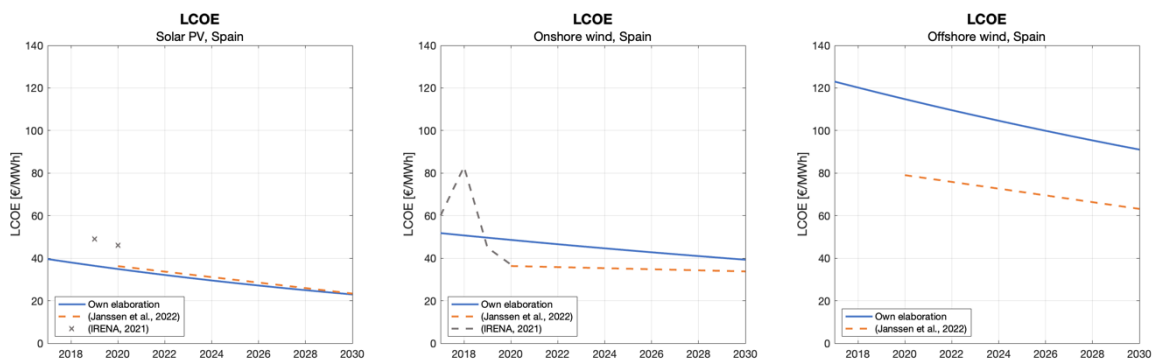


Figure 86: Comparison between own LCOE in Spain and values from the literature, for different RES [15], [172].

The comparison for Germany is presented in the main body of this work.

Electrolyzer CAPEX

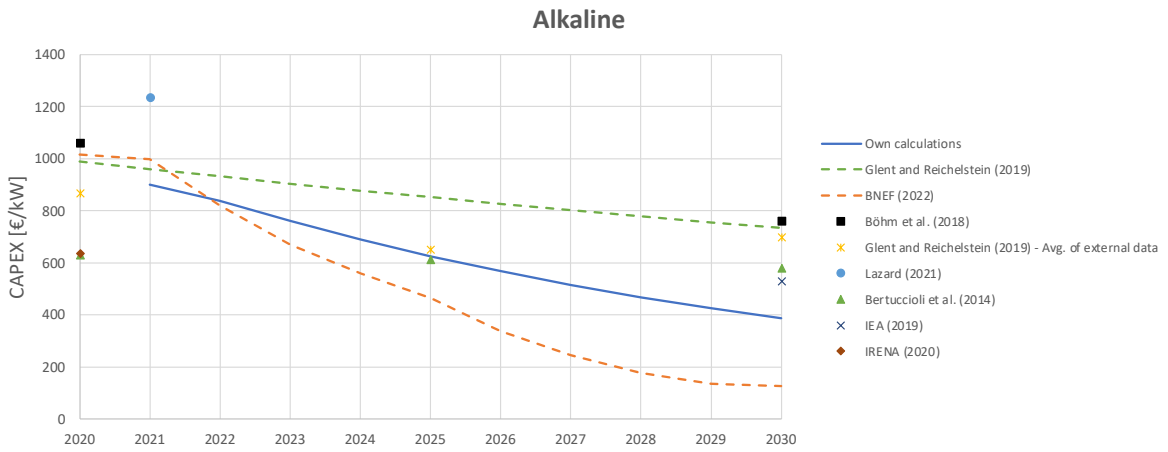


Figure 87: Comparison between own CAPEX projections for alkaline electrolyzer and values from the literature [3], [47], [162], [165], [257]–[259].

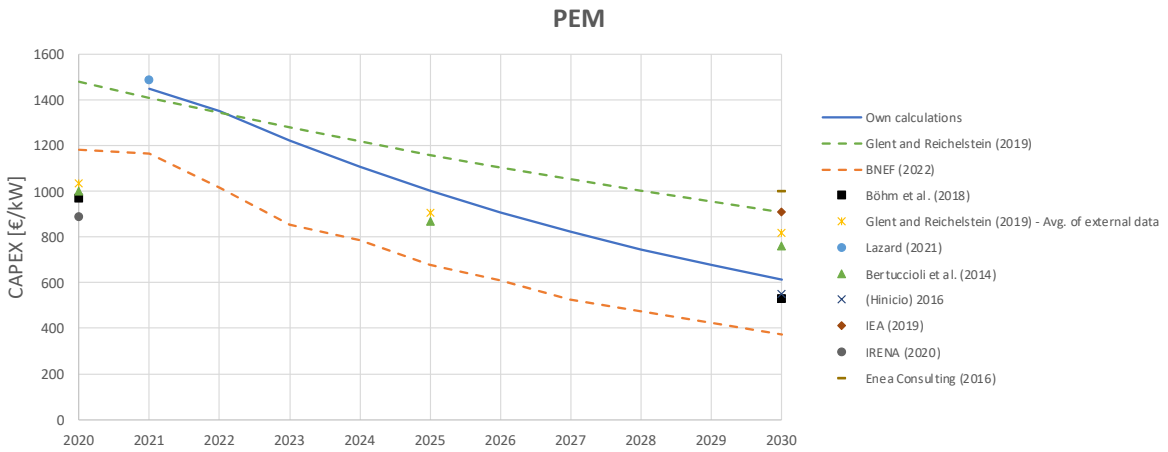


Figure 88: Comparison between own CAPEX projections for PEM electrolyzer and values from the literature [3], [47], [162], [165], [257]–[261].



Figure 89: Comparison between own CAPEX projections for PEM electrolyzer and values from the literature [3], [165], [257].

Levelized cost of hydrogen production (LCOH_p) – Electrolysis

The hydrogen production costs for electrolysis powered with different renewable electricity sources in different countries are compared in the following figures. The colors of the different lines indicate the typology of electricity: orange is solar PV, blue is onshore wind, dark gray is offshore wind, and green is green hydrogen with non-specified origin. In some figures, the line corresponding to the values from Brändle *et al.* [37] appears twice in the same chart. In these cases, the upper line is the baseline scenario and the lower one is the optimistic one. Where instead only one line is present, this always refers to the baseline scenario.

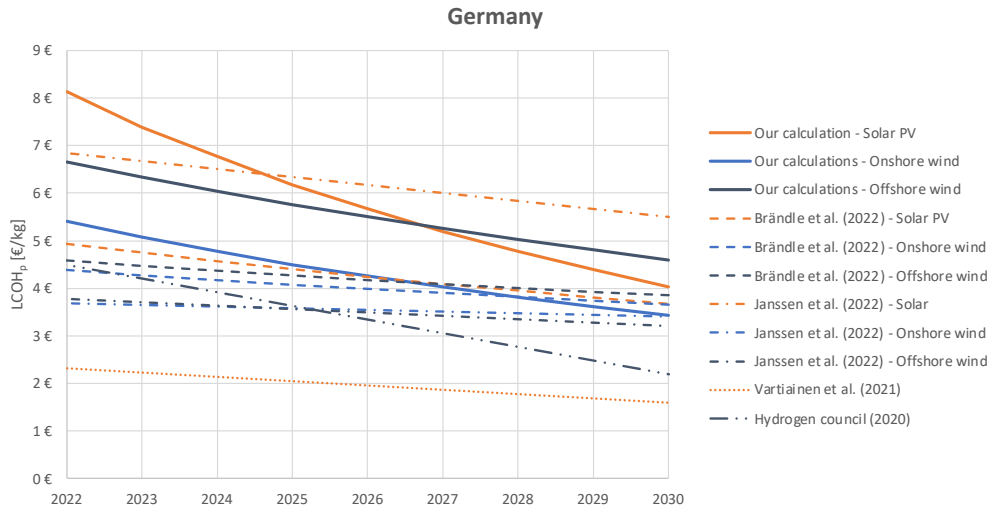


Figure 90: Comparison between own LCOH_p in Germany and values from the literature, for electrolysis and different RES [2], [37], [262], [263].

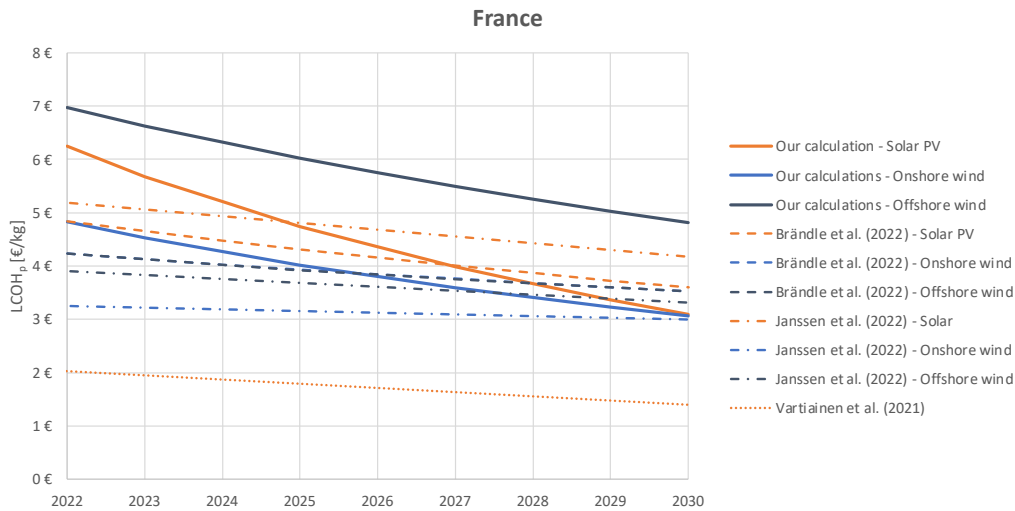


Figure 91: Comparison between own LCOH_p in France and values from the literature, for electrolysis and different RES [37], [262], [263].

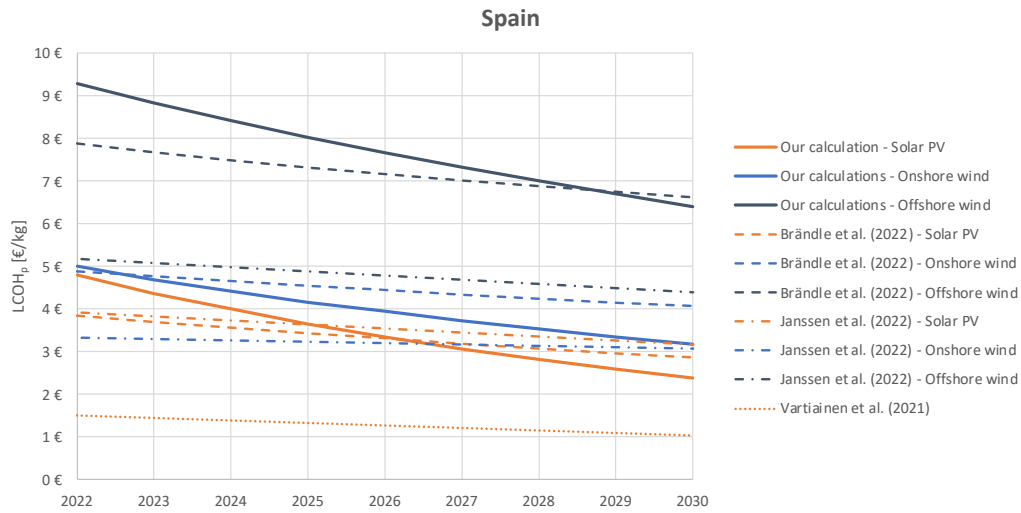


Figure 92: Comparison between own LCOH_p in Spain and values from the literature, for electrolysis and different RES [37], [262], [263].

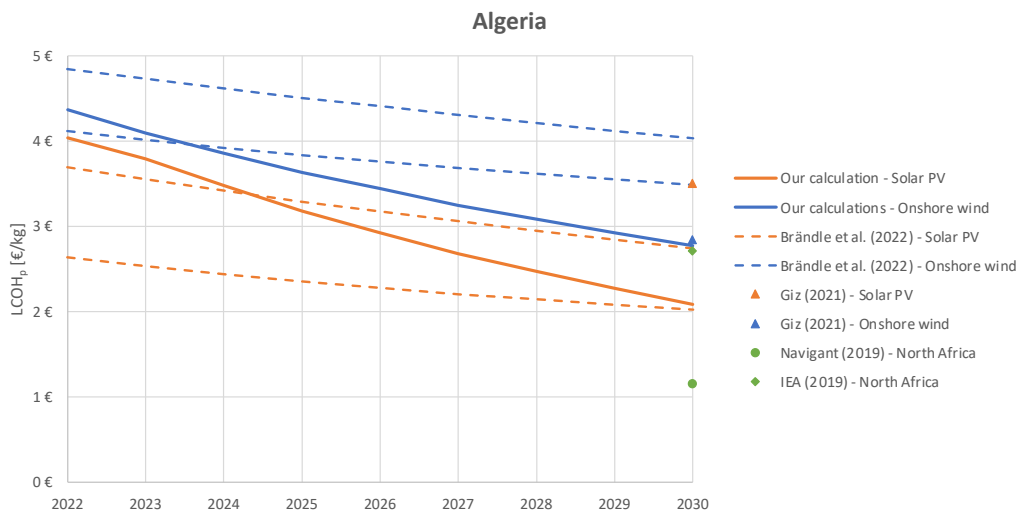


Figure 93: Comparison between own LCOH_p in Algeria and values from the literature, for electrolysis and different RES [3], [37], [132], [264].

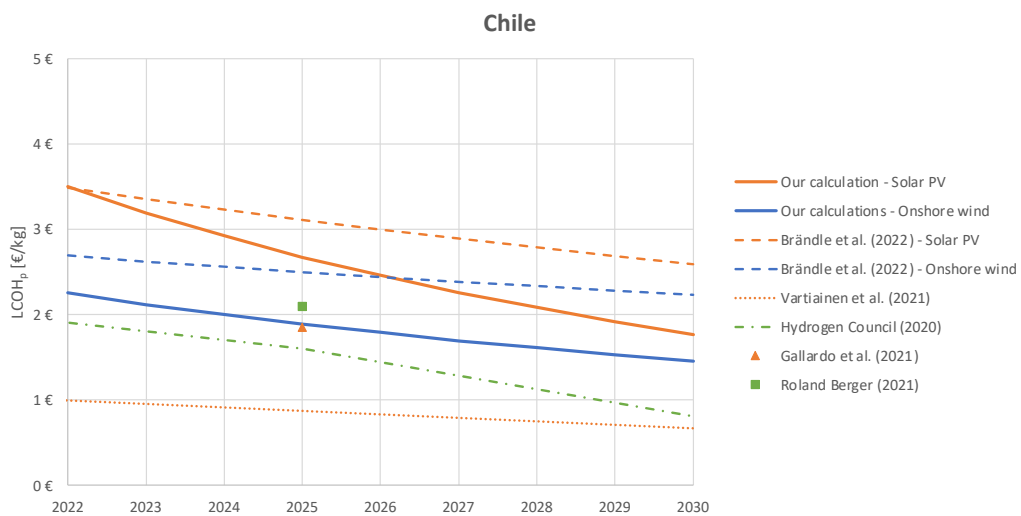


Figure 94: Comparison between own LCOH_p in Chile and values from the literature, for electrolysis and different RES [2], [37], [93], [263], [265].

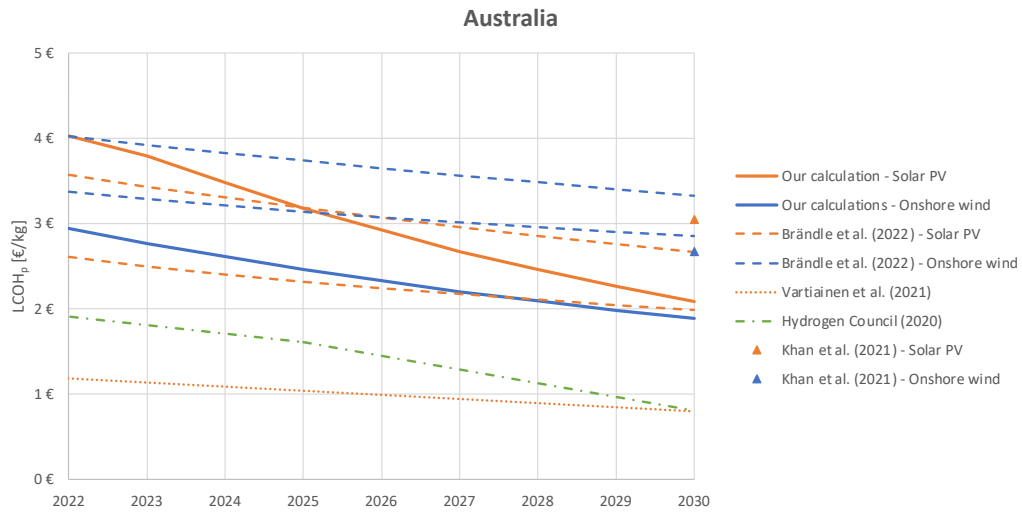


Figure 95: Comparison between own LCOH_p in Australia and values from the literature, for electrolysis and different RES [2], [37], [263], [266].

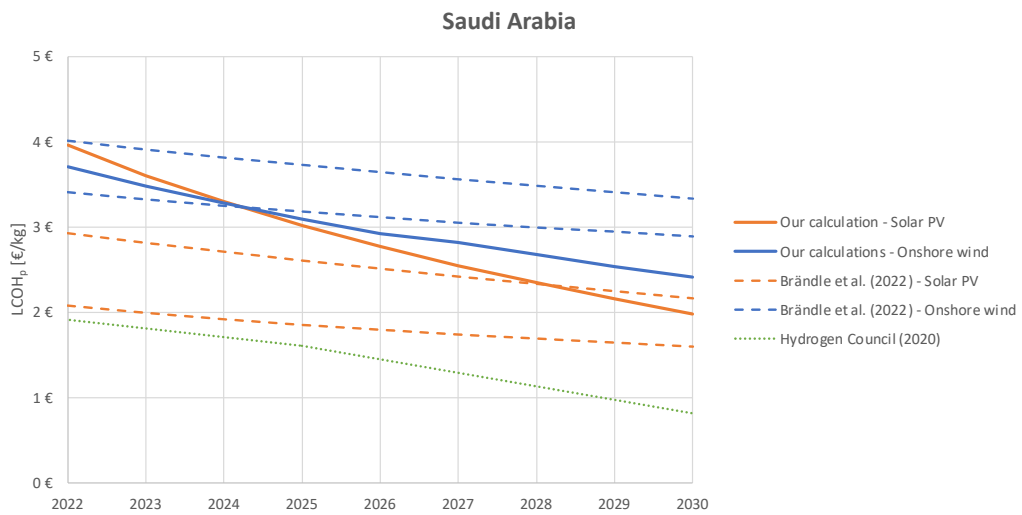


Figure 96: Comparison between own LCOH_p in Saudi Arabia and values from the literature, for electrolysis and different RES [2], [37].

